ПУБЛИКАЦИЈЕ АСТРОНОМСКОГ ДРУШТВА "РУЂЕР БОШКОВИЋ" Св. 15
PUBLICATIONS OF THE ASTRONOMICAL SOCIETY "RUDJER BOŠKOVIĆ" No. 15

PROCEEDINGS
OF THE IX BULGARIAN-SERBIAN ASTRONOMICAL CONFERENCE: ASTROINFORMATICS

Sofia, Bulgaria, July 2-4, 2014

Eds. Milcho K. Tsvetkov, Milan S. Dimitrijević, Ognyan Kounchev, Darko Jevremović and Katya Tsvetkova

BELGRADE, 2015

ПУБЛИКАЦИЈЕ АСТРОНОМСКОГ ДРУШТВА "РУЂЕР БОШКОВИЋ"
PUBLICATIONS OF THE ASTRONOMICAL SOCIETY "RUDJER BOŠKOVIĆ"
Св. 15 No. 15

PROCEEDINGS OF THE IX BULGARIAN-SERBIAN ASTRONOMICAL CONFERENCE: ASTROINFORMATICS

Sofia, Bulgaria, July 2-4, 2014

Eds. Milcho K. Tsvetkov, Milan S. Dimitrijević, Ognyan Kounchev, Darko Jevremović and Katya Tsvetkova

Б Е О Г Р А Д
2015

PUBL. ASTRON. SOC. "RUDJER BOŠKOVIĆ" No. 15, 1-207 BELGRADE, SEPTEMBER 2015

Under the auspices of
Bulgarian Academy of Sciences
Ministry of Education, Science and Technological Development of Serbia

ORGANIZERS:
Institute of Mathematics and Informatics of Bulgarian Academy of Sciences
Astronomical Observatory Belgrade, Serbia

Co-organizers:
Institute of Astronomy with National Astronomical Observatory, BAS
Department of Astronomy, Faculty of Physics, Sofia University "St. Kliment Ohridski"
Faculty of Mathematics and Department of Astronomy, University of Belgrade
Society of Astronomers of Serbia

Cover design: Tatjana Milovanov

Text arrangement by computer: Tatjana Milovanov

Financially supported by the Ministry of Education, Science and Technological Development of Serbia

ISBN 978-86-89035-06-3

Production: Solution+, Bulevar umetnosti 27, 11070 Beograd, in 100 copies

CONTENTS

Darko Jevremović
ASTROINFORMATICS IN SERBIA 7

Alexander A. Kolev
ASTROWEB ASTROINFORMATICS PROJECT AND COMPARISON OF THE WEB-GIS PROTOCOL STANDARDS 13

Milan S. Dimitrijević, Sylvie Sahal-Bréchot, Nicolas Moreau and Nabil Ben Nessib
STARK-B DATABASE FOR STARK BROADENING FOR ASTROPHYSICAL PLASMA ANALYSIS AND MODELLING 23

Katya Tsvetkova
UV CETI TYPE VARIABLE STARS PRESENTED IN THE GENERAL CATALOGUE OF VARIABLE STARS 29

Jovan Aleksić, Veljko Vujčić and Darko Jevremović
ALERT SIMULATOR - SYSTEM FOR SIMULATING DETECTION OF TRANSIENT EVENTS ON LSST 37

Nikolay Kirov, Milcho Tsvetkov and Katya Tsvetkova
WFPDB: SOFTWARE FOR TIME AND COORDINATES CONVERSIONS 43

Zoran Simić, Milan S. Dimitrijević and Luka Č. Popović
ATOMIC DATA AND STARK BROADENING OF Nb III 49

Damyan Kalaglarsky, Katya Tsvetkova and Milcho Tsvetkov
WFPDB: UPGRADING THE CATALOGUE OF WIDE-FIELD PLATE ARCHIVES AND RECENT DEVELOPMENT 55

Cristina Yubero, Maria Carmen García, Milan S. Dimitrijević, Antonio Sola and Antonio Gamero
ON THE DETERMINATION OF ELECTRON DENSITY IN NON-THERMAL PLASMAS USING BALMER SERIES HYDROGEN LINE 63

Alexandra M. Zubareva, Daria M. Kolesnikova, Kirill V. Sokolovsky, Sergei V. Antipin and Nikolai N. Samus
VARIABLE STARS NEAR β CAS DISCOVERED ON SCANNED PHOTOGRAPHIC PLATES AT THE STERNBERG ASTRONOMICAL INSTITUTE 67

Saša Simić and Luka Č. Popović
BROAD SPECTRAL LINE AND CONTINUUM VARIABILITIES IN QSO SPECTRA INDUCED BY MICROLENSING: METHODS OF COMPUTATION 75

Andjelka Kovačević, Luka Č. Popović, Alla I. Shapovalova, and Dragana Ilić
TIME SERIES ANALYSIS OF AGNs 83

Daniela Boneva
FLUCTUATIONS IN THE FLOW AND DEVELOPMENT OF FLARE-UPS IN COMPACT BINARY STARS 93

Zorica Cvetković, Slobodan Ninković, Rade Pavlović, Svetlana Boeva and Georgi Latev
DETERMINATION OF NATURE FOR ELEVEN DOUBLE STARS 99

Krasimira Yankova
BEHAVIOUR OF THE FLOW ON THE BOUNDARY IN THE SYSTEM DISK-CORONA 107

Momchil Dechev, Kostadinka Koleva, Peter Duchlev and Nikola Petrov
MULTI-WAVELENGTH OBSERVATIONS OF AN ERUPTIVE PROMINENCE ON 7 AUGUST 2010 117

Cyril Ron, Jan Vondrák and Yavor Chapanov
ATMOSPHERIC, OCEANIC AND GEOMAGNETIC EXCITATION OF NUTATION 127

Aleksandra Nina, Vladimir M. Čadež, Luka Č. Popović, Vladimir A. Srećković and Saša Simić
DIFFERENCES IN DETECTION OF D-REGION PERTURBATIONS INDUCED BY THE UV, X AND γ RADIATION FROM OUTER SPACE USING VLF SIGNALS 137

Boris Komitov, Momchil Dechev and Peter Duchlev
THE RELATION BETWEEN SOLAR PROTON FLARES AND THE BACKGROUND CONCENTRATIONS OF NITROGEN OXIDES IN THE TROPOSPHERE 149

Zlatko Majlinger, Zoran Simić and Milan S. Dimitrijević
ON THE STARK BROADENING OF Zr IV IN THE SPECTRA OF DB WHITE DWARFS 159

Goran Damljanović, Francois Taris, Georgi Latev and Milan Stojanović
OBSERVATIONS AT THE 60 cm ASV TELESCOPE AND THE LINK GAIA CRF - ICRF 165

Katya Tsvetkova, Milan S. Dimitrijević and Milcho Tsvetkov
THE MATHEMATICIAN AND THE ASTRONOMER SIMON MARIUS (1573 – 1624) 171

Nada Pejović, Saša Malkov, Nenad Mitić and Žarko Mijajlović
MILUTIN MILANKOVIĆ DIGITAL LEGACY 179

Milan S. Dimitrijević
SOCIETY OF ASTRONOMERS OF SERBIA 2012-2014 189

AUTHORS' INDEX 207

Proceedings of the IX Bulgarian-Serbian Astronomical Conference: Astroinformatics (IX BSACA) Sofia, Bulgaria, July 2-4, 2014,
Editors: M. K. Tsvetkov, M. S. Dimitrijević, O. Kounchev, D. Jevremović and K. Tsvetkova
Publ. Astron. Soc. "Rudjer Bošković" No 15, 2015, 7-12

ASTROINFORMATICS IN SERBIA

DARKO JEVREMOVIĆ

Astronomical Observatory, Volgina 7, 11060 Belgrade, Serbia
E-mail: darko@aob.rs

Abstract. I review some aspects of development of the astroinformatics in Serbia. Special attention is paid to the funding and educational challenges. As we recently joined the LSST project, we expect huge impact on Serbian science especially in the Big Data areas. Among others, our contribution will be in building simulator of alerts for the astronomical community and prototype of the CEP engine for analyzing data generated by the survey.

1. OVERVIEW OF ASTRONOMY IN SERBIA

There are two main institutions with significant number of astronomers in Serbia: Astronomical Observatory in Belgrade (AOB) and Department of Astronomy, Faculty of Mathematics, Belgrade University (DAFM). AOB employs about twenty researchers with PhD at different stages of their career and about fifteen PhD students. DAFM has about ten tenured/tenure track professors and about 15 Phd students. There are few astronomers at other institutions such as Institute of Physics Belgrade, Institute of Nuclear Sciences Vinča, Department of Physics University of Kragujevac, Department of Physics University of Niš, Department of Physics University of Novi Sad.

Funding of Astronomy (and generally science) in Serbia is grant based. Serbian Government currently funds the following eight projects with significant astronomical component:

- Astrophysical Spectroscopy of Extragalactic Objects (led by Luka Popović)
- Gravitation and the large scale structure of the Universe (Predrag Jovanović)
- Emission nebulae: structure and evolution (Dejan Uroević)
- Influence of collisions on astrophysical plasma spectra (Milan Dimitrijević, Zoran Simić)
- Stellar physics (Gojko Djurašević)
- Visible and Invisible Matter in Nearby Galaxies: Theory and Observations (Srdjan Samurović)
- Dynamics and kinematics of celestial bodies and systems (Zoran Knežević, Rade Pavlović)
- Astroinformatics: application of IT in astronomy and close fields (Darko Jevremović).

1. 1. INTERNATIONAL COLLABORATION

Astronomers from Serbia were and are involved in many internationally funded projects. The first European project we were involved was Virtual Atomic and Molecular Data Center VAMDC (Dubernet et al. 2010, Jevremović et al. 2009). More details in section 2.1.3.

Project BELISSIMA (BELgrade Initiative for Space Science, Instrumentation and Modeling in Astrophysics) started in 2010. It is funded by European Comission under the FP7 REGPOT schema. The BELISSIMA will be concluded in June 2015. Main goals are:

- Reinforcement of the scientific potential of AOB (and, therefore, Serbian astronomical and space sciences) through increase of both width and depth of its overall research activities, observational and theoretical, as a consequence of "brain gain". This will be operational on several levels, in both theoretical and observational aspects of envisioned future research activity.
- Purchase, installation and testing of new observing equipement (telescope "Milanković" with1.5 m-class mirror, to be installed on Astronomical Station Vidojevica
- Human potential, training and public outreach. Exchange of know-how and experience between EU research institutes and AOB. Training of AOB researchers in observational astronomy techniques and work towards establishing collaboration with other observatories in Europe and worldwide
- Popularization of Astronomy and Science

Stardust, the Asteroid and Space Debris Network, is an Advanced research network we participate in. One PhD student from Greece started his PhD thesis work at AOB in the September of the last year.

Astromundus is a master program in astrophysics. Five universities are involved - namelly Insbruck, Goettingen, Padova, Rome and Belgrade. Typically, 4-6 students attend classes in Belgrade during the fall semester of the second year of their course. Also, few students are doing their master thesis research in the final semester in Belgrade (either under our supervision or under joint supervision between two partners).

We actively participate in the following COST actions:

- MP0905 - Black Holes in a Violent Universe 24 March 2010 - 01 June 2014
- MP1104 — Polarization as a tool to study the Solar System and beyond — 21 November 2011 - 20 November 2015
- TD1308 Origins and evolution of life on Earth and in the Universe (ORIGINS) 15 May 2014 - 14 May 2018
- TD1403 Big data era in sky and Earth observations November 2014 - November 2018

There are four joint research projects of the Serbian Academy of Sciences and Arts and Bulgarian Academy of Sciences:

- OPTICAL SEARCH FOR SUPERNOVA REMNANTS AND HII REGIONS IN NEARBY GALAXIES (M81 AND IC342 GROUPS OF GALAXIES) DAFMBU & Institute of Astronomy with National Astronomical Observatory BAS project leaders Dr. Dejan Urošević & Dr. Nikola Petrov
- OBSERVATIONS OF ICRF RADIO-SOURCES VISIBLE IN OPTICAL DOMAIN AOB & Institute of Astronomy with National Astronomical Observa-

Figure 1: The home page of the Serbian Virtual Observatory.

tory, BAS (Dr. Goran Damljanović & Dr. Svetlana Boeva)

- INVESTIGATION OF VISUAL DOUBLE AND MULTIPLE STARS AOB & Institute of Astronomy with National Astronomical Observatory BAS (Dr. Zorica Cvetković & Dr. Svetlana Boeva)
- ASTROINFORMATICS: WAY TO FUTURE ASTRONOMY AOB & Institute of Mathematics and Informatics BAS (Dr. Darko Jevremović & Prof.Dr. Ognyan Kounchev)

2. ASTROINFORMATICS IN SERBIA

2. 1. TR13022/2008 AND III44002/2011

Small project TR13022/2008 "Serbian Virtual Observatory" was funded in years 2008-2010. This project was funded as technological developement project. The main goals of this project were digitization and publishing of old photo plates in Virtual Observatory, developement of BelData, Stark broadening database (it became STARK-B database), contribution to Darthmouth Stellar Evolution Database and collection of other Serbain data. Idea was that all these would be accessible at http://servo.aob.rs (Fig. 1).

Other goal was a developement of services as one point contact with VO world, as well as installation and testing software for accessing different astronomical and other databases.

From 2011 onwards, our activities in this field are supported through the interdisciplinary project III44002 Astroinformatics: "Application of IT in Astronomy and Close Fields". Apart from continuing of efforts of the SerVO project, the goal of the project is to develop new services. The main goals are as follows.

2. 1. 1. History

In historical part of the project we are focused at:

- Digitization of certain number of photo plates from the AOB archive in SerVO
- organisatioin of database and services according to VO standards
- Digitisation of important astronomical works
- Publications of GAS are digitized and electronically available at http/servo.aob.rs/eeditions

2. 1. 2. High Performance Computing

In the last few years there is shift in HPC by using new technologies ?such as Graphical Processor Units (GPU). Of course this leads to new set of problems and paradigms for efficient usage of GPU. Paralelisation of existing codes is very different from message passing interface (MPI) or OpenMP paralelization.

We joined the bandwagon in 2010 by obtaining system with 4 Tesla 1070 GPU units (every GPU 230 processors) through the grant from Alexander von Humboldt fondation. Towards the end of 2012 we obtained small server which consists of 12 nodes + master node. Each node comprises of 2x X5675 processor, 24 Gb memory, 2 Tb disk 2x M2090 Fermi GPU. Nodes are interconnected by Mellanox infiniband network. This system has theoretically $\sim 16 TFlops$ double precision power ($\sim 10 Tflops$ in practice).

The system is mainly used for the general stellar atmosphere code Phoenix runs. We did some adaptation and paralelisation using GPU (in collaboration with OU i Hamburg), mainly using GPU libs for solving matrix equations. Apart from that the system is used for N body simulations, SKIRTS a dusty 3D radiative transfer code in AGN's. For another project 40% of SDSS DR9 images are transfered. We expect the rest to be available to us in the next few months.

2. 1. 3. VAMDC

The VAMDC was supported by EU in the framework of the FP7 "Research Infrastructures - INFRA-2008-1.2.2 - Scientific Data Infrastructures" initiative. AOB was one of 15 partners in the consortium via Stark B database. We are actively involved in continuation of the project. We had and still have an active role in VAMDC - Consortium of Databases & Services Providers that has built a unified, secure, documented, flexible and interoperable e-science environment-based interface to its members atomic and molecular databases.

This project will in near future grow into Consortium of Atomic and Molecular databases very likely become European Research Infrastructure Consortium. Also we expect two new atomic and molecular databases to join the consortium.

2. 2. INVOLVEMENT IN LSST

LSST is an optical- near infrared survey of half the sky in six bands (ugrizy') town to r$\sim$ 27.5 (36 nJy) based on thousand visits over ten year period. The 8.2 m telescope will be situated at Cerro Pachon in Chile on the close to Gemini South and SOAR telescope. The first light is expected in the year 2019 and the full survey will start in 2022.

We expressed our interest in involvement in LSST project in 2009. Through grant III44002 we applied for funding and it was granted from the EIB loan In November of 2013 we formally signed the Memorandum of Understanding with LSST Corporation. We have, so far, possibility to engage up to four PI's and their students and postdocs. Our interest is in variable phenomena, variable stars, AGN variability, gravitational micro-lensing, SNR & Planetary nebulae, Small solar system bodies (orbits, elements...), development of astroinformatics and development of algorithms, software... At the moment we appointed two PI's Luka Popović in AGN collaboration and Darko Jevremović in Transients and Variable stars collaboration.

As part of our contribution to the project we are developing simulator of alerts. More details about the requirements and strategies are given in (Aleksić et al. 2014).

2. 3. TEACHING ASTROINFORMATICS AT DAMF

Since 2011/2012 academic year DAMF offers course with a major in astroinformatics. There are several problems with this course. In essence, one really shoudn't just mechanically glue the Computer Science and Astronomy classes because:

Computer science classes + **Astronomy classes** $\neq$ **Astroinformatics**!!!

Other problem is that there is no introduction nor space to follow newest developement in the very dynamic field astroinformatics. Third problem the course faces is lack of interested students. Namely, most of enrolled students are unsuccessful applicants in Computer Science course and after the first year they change their major accordingly. So, an opportunity to really change something in education of new generation of astronomers is missed.

2. 4. OTHER ACTIVITIES

Our group has two stations for collecting ionospheric radio data. We are in the phase of obtaining new stations (fund are awarded). For this system data are collected in Stanford, and our contribution is in definition of standards as well as reorganization of databases.

Recently we launched a new service for fitting of FeII lines in AGN. Basically if you provide a AGN spectrum, we calculate 'best fit' and return fitted spectrum as well as physical parameters using method from Kovačević et al. (2010). Service is accessible at http://servo.aob.rs/FeII_AGN/

3. CONCLUDING REMARKS

As seen from the above, Astroinformatics is an active and vibrant new research field in Serbia. We expect new opporunities to arise and that we put foundations for the next generation of astronomers to be able to do top level science in this exciting new field.

Acknowledgements

I am gratefull for the support from the Ministry of Education, Science and Technological Developement of Republic of Serbia through the grant No. III44002 Astroinformatics: Application of IT in Astronomy and Close Fields.

References

Aleksić, J., Vujčić, V., Jevremović, D.: 2014, Alert Simulator - A system for simulating detection of transient events on LSST, this volume.
Dubernet, M. L., Boudon, V., Culhane J. L. et al.: 2010, *JQSRT*, **111**, 2151.
Jevremović, D., Dimitrijević, M. S., Popović, L. Č. et al.: 2009, *New Astron. Rev.*, **53**, 222.
Kovačević, J., Popović, L. Č., Dimitrijević, M. S.: 2010, Analysis of Optical Fe II Emission in a Sample of Active Galactic Nucleus Spectra, *ApJS*, **189**, 15.

Proceedings of the IX Bulgarian-Serbian Astronomical Conference: Astroinformatics (IX BSACA) Sofia, Bulgaria, July 2-4, 2014,
Editors: M. K. Tsvetkov, M. S. Dimitrijević, O. Kounchev, D. Jevremović and K. Tsvetkova
Publ. Astron. Soc. "Rudjer Bošković" No 15, 2015, 13-21

ASTROWEB ASTROINFORMATICS PROJECT AND COMPARISON OF THE WEB-GIS PROTOCOL STANDARDS

ALEXANDER A. KOLEV

Defense Institute, Bulgarian MO
E-mail: sashokolev@abv.bg

Abstract. At this time finished AstroWeb project was implemented some advanced GIS (Geographical Information System) information techniques, based on the one of most commonly used WMS (Web Map Service) protocol. Like a WMS, Open Geospatial Consortium offers another WEB-GIS protocol, named WFS (Web Feature Service). AstroWeb Astroinformatics Project is a good starting point to produce scientific research of this two protocols effectiveness.

1. THE PROJECT ASTROINFORMATICS AND VIRTUAL OBSERVATORY ASTRO WEB

Astroinformatics, the new field for scientific research, arises as a result of applying modern information and communication technology in astronomy. Astroinformatics is an interdisciplinary area of science based on the achievements in data transfer and information services on the Internet.

Leading specialists in the fields of astronomy, math and informatics from various institutions of the Bulgarian Academy of Sciences (BAS), as well as other Bulgarian scientific institutions specialized in other close scientific areas have participated in the Astroinformatics project, which started a few years ago.

Among the goals of the project are building of a compatible interactive database with a web interface and insuring a web access to digitized astronomical data and imagery. Bulgarian scientist and specialists, in cooperation with international initiative are working on building a WFPDB, containing millions of professional astronomical photo-images. The complicated information structure of maintaining data in extraordinarily large volumes brings the need of creating an effective, easily accessed and user friendly informational system with an intuitive interface, easily used by professionals as well as amateur astronomers. Among the achieved goals of the project Astroinformatics is the software solution „Astroinformatics AstroWeb Virtual Observatory", shortly named AstroWEB (Kolev et al. 2012).

AstroWEB is build as to provide a natural and comfortable interface for visualizing and accessing data from the astronomical database WFPDB. The basis of the software solution AstroWEB are open-source software products for creating web-based GIS (Geographical Information System), maintained by the international organization OGC (Open Geospatial Consortium) (http://www.opengeospatial.org/standards). Application of the OGC standards covered in the present realization of AstroWEB, as well as in its future evolutions are discussed in this paper.

2. OGC STANDARDS AND CURRENT REALIZATION OF THE ASTROWEB PROJECT

The Open Geospatial Consortium is an international industrial association, containing hundreds of business organizations, government agencies and universities, all of which support the process of developing and publishing of standards for compatibility of spatial and geographical data and services, predominantly based on web information technology. These standards make possible the technological development of complex spatial databases and online services for visualization and analysis.

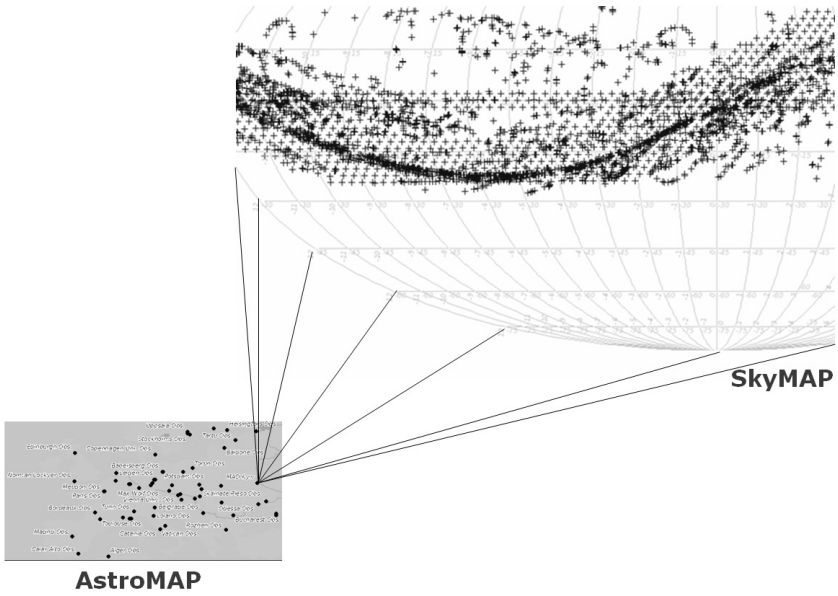

Figure 1: Basic functionality of AstroWEB.

Access to an archive of digitalized images is realized in the functionality of AstroWEB, as data can be accessed from the different observatories by pointing. The basic screen forms AstoMAP and SkyMAP execute this action as shown in Fig. 1. Both screen forms have WEB-GIS properties – scaling, panning, selection of objects, and are dynamically generated by OGC standards.

In the interest of AstroWeb software project are few OGS standards:

- **WMS** (Web Map Service). Provides operations in support of the creation and display of map-like raster data views of geographic information;
- **WFS** (Web Feature Service) Allows a client to retrieve geographic data encoded in GML text data format. The specification defines interfaces for data access and manipulation operations on geographic features and information behind a map image;
- **GML** (Geography Markup Language). Is an XML encoding for the transport and storage of geographic information, including both the geometry and properties (textual and numeric attribute data) of geographic features;
- **SLD** (Styled Layer Descriptor). Is an XML encoding that allows user-defined symbolization of geographic feature data. It allows the system to determine which features or layers are rendered with which colors or symbols.

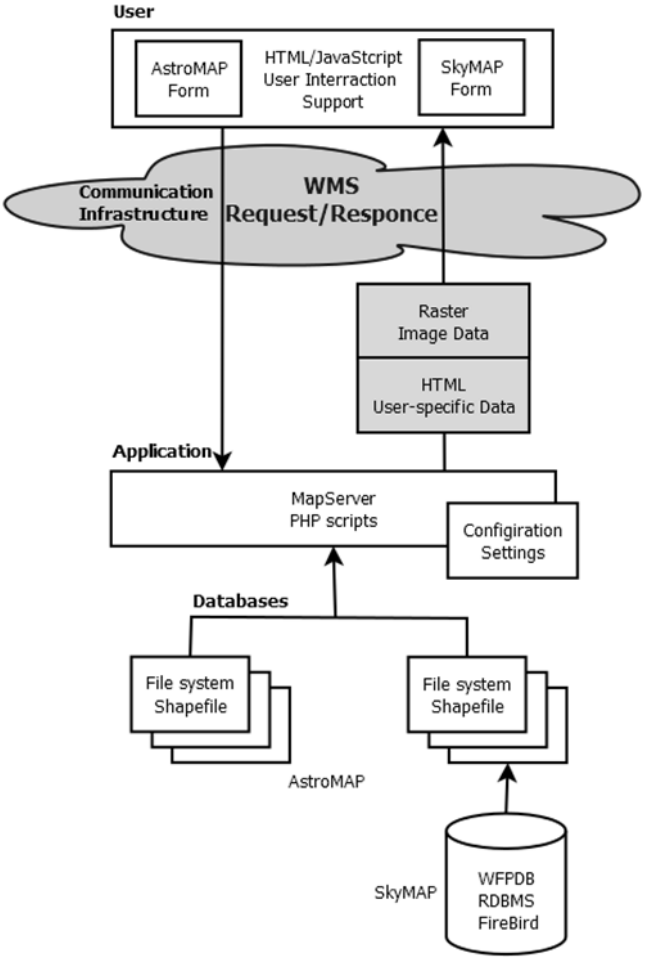

Figure 2: Current AstroWEB realization.

A dataflow diagram is presented in Fig. 2, which illustrates the principal sequence of working stages in AstroWEB.

The current realization of AstroWEB is built adhering to the principals of the WMS standard. The basic software is a FGS (Free GIS Suite http://maptools.org/fgs/), in which a server and client subsystems are included. The server subsystem is built with the MapServer software – a project of a OSCGeo (Open Source Geospatial Foundation http://www.osgeo.org/), in collaboration with OGC (OSGeo http://wiki.osgeo.org/wiki/Open_Geospatial_Consortium).

A dataflow diagram illustrating the principal working stages of the current AstroWEB realization is presented in Fig. 2.

For the needs of the current analysis, details of the basic structural programming modules are presented, which are: **databases, application, communication infrastructure and user layer**.

Databases: The functioning of AstroMAP in the sense of the WEB-GIS application as seen from the database is maintained by a few "shapefile" file structures. Maintenance of the AstroMAP is insured by geographical data in a few commonly based layers and an additional georeffered data layer for astronomical observatories. The functioning of SkyMAP also depends on a "shapefile" structure and provides an image of a selected digitalized archive of astronomical data. The used RDBMS (Relational Data Base Management System) is Firebird, with the information structure WFPDB. The intermediate georeffered data of the "shapefile" type is generated programmatically with WFPDB information;

Application: The most important component in the application layer is the MapServer module. In response to a user request, the MapServer module generates a requested image in a raster format, in addition to specific data in HTML format, which are visualized on a client web-browser, and together create an adequate user interface;

Communication infrastructure: An existing web infrastructure, or a local network with http protocol support. Driven by the user request, the server system generates a response containing graphical data of a raster type in accordance to the WMS standard for building a functioning WEB-GIS system and HTML structure for maintaining the user interface;

User: At the AstroWEB Virtual Observatory's end user disposal is a standard modern Operational Systems WEB browser. The user interface is created using HTML and JavaScript code. The user has WEB-GIS disposal – he is presented with a graphical navigation interface (pan&zoom) though the screen forms AstroMAP and SkyMAP. When selecting an astronomical observatory-type object, the form AstroMAP and a mediary form for digitally archiving list selections belonging to the selected observatory, together generate the relevant SkyMAP form with a graphical image of the requested archive. In the last form the available astronomical objects are visualized in their natural positions on the celestial plane, where the pictogram "filled square" signifies a digitized astro-object, and a "plus sign" signifies an object from the catalog which isn't yet

digitized. Selecting the "filled square" pictogram draws additional information about the digitized object and previews the digitized Wide Field Plate.

3. POSSIBLE REALIZATION WHEN APPLYING A WFS STANDARD

Fig. 3 represents a dataflow diagram which describes AstroWEB's software operation under the WFS standard. We'll note the main differences between it and the version using the WMS standard.

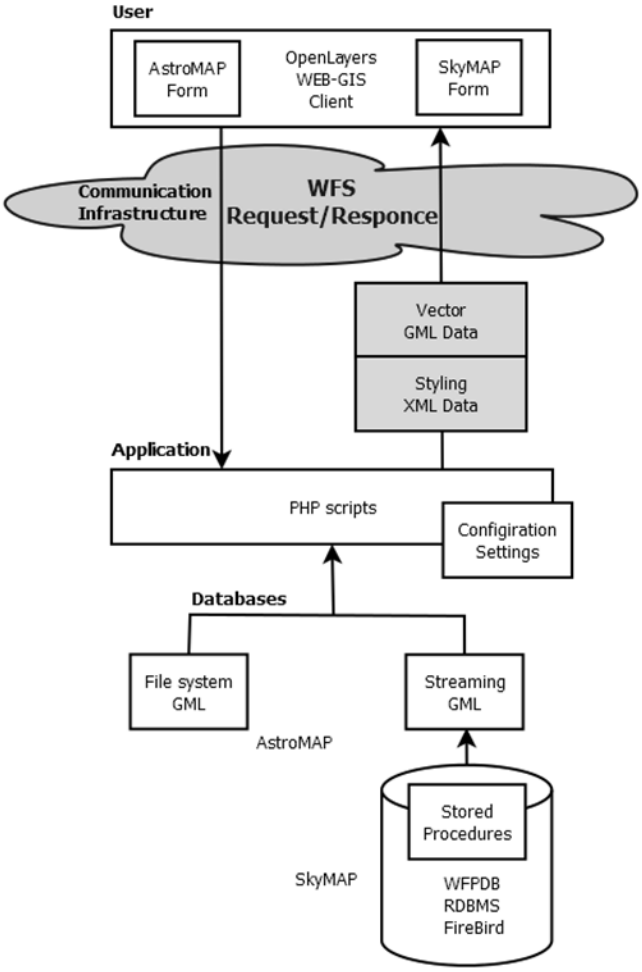

Figure 3: Possible AstroWEB realization.

Database: In addition to the aforementioned current realization, a "stored procedures" programming code is defined in the RDBMS Firebird. With it, the screen form AstroMAP uses georeferred data of a file type with a structure under the GML standard. The screen form SkyMAP uses data of the same type. When

processing a user request, the "stored procedures" generate GML data of a stream type that isn't saved as files on the file system;

Application: Consists of a server script which communicates with the RDBMS and processes user requests.

Communication infrastructure: In contrast to the aforementioned realization, here the response to the user request is in conjunction with the WFS standard's requirements for building WEB-GIS systems. The data sent to the user is vector georeferred data in GML format and graphic style data used for visualization in an SLD format;

User: Like in the previous case, the client module is a standard web browser. The WEB-GIS functionality of the screen forms AstroMAP and SkyMAP are maintained by the specialized client software OpenLayers. OpenLayers is an open-source product of OSGeo and insures the necessary functionality when presenting geographical data in different WEB-GIS standards. OpenLayers is a JavaScript object library that gets loaded on-line and works in the web browser.

As a principal difference between the two described approaches the author points out the application of the different WEB-GIS software environments. In the Fig. 2 realization, the main WEB-GIS software package is the product "MapServer", while the newly proposed realization insures WEB-GIS functionality whilst applying the OpenLayers software. This principal difference reflect in the organization of the database (RDBMS), the organization of the application layer, the type of geodata and the client subsystem's way of functioning.

In regards to the RDBMS, it starts overloading when the "stored procedures" are applied. Their purpose is to extract a subset of available georeferred data and generate the respective GML structure.

In regards to the application layer, the newly proposed realization does not require use of the MapServer system. There, the application layer is presented by a general-purpose script server language.

The main difference in the data type is that the current AstroWEB realization sends a raster image in response to the client's request, while the newly proposed variant sends the geodata in a GML text format.

In the newly proposed solution, the client subsystem (or user layer) is an object-oriented library of JavaScript classes. This library takes over the functions of rendering the georeferred image in the user's web browser.

Fig. 4 presents diagrams explaining the structure of the georeferred data in the case of using the WFS standard when generating a current image for the screen forms AstroMAP and SkyMAP. For this purpose, the outflow code (which is specially formatted as XML text for the GML and SLD structures) is processed via reverse-engineering. As the figure points out, the GML and SLD data for the two screen forms have some differences.

The main differences in the GML structure when building the AstroMAP and SkyMAP images are in the volume, naming and type of attribute data which the database presents as information to the user. Important attribute data for the

AstroWEB form are geographical coordinates, the screen name of the observatory and the outside key to the charts with supported digital archives for any given observatory. With the SkyMAP format, which pictures a digitalized archive of astronomical images, the important attribute data are the star coordinates of every digitalized object from any given catalogue, data about the observatory and astronomer who did the digitalizing, and a flag signifying the availability of a preview for the original image.

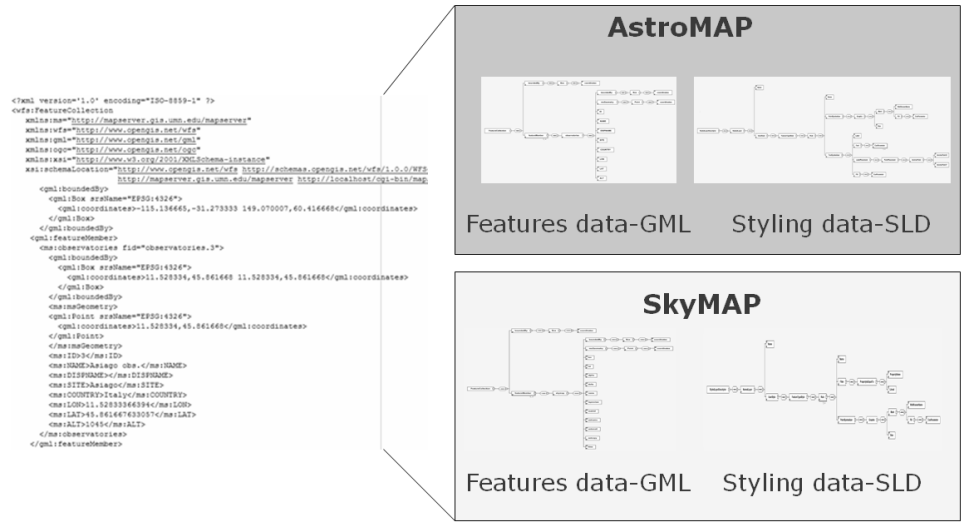

Figure 4: GML and SLD data on the basic screen forms.

The differences in the SLD structures for the two screen forms are more substantial. In the case of drawing the AstroMAP form, data for the color and shape of the point styled image of any given observatory and data on its relative position, color and font of the on-screen text for the observatory's name is supported. When drawing the SkyMAP form, a logical filter for the image is applied. Elements of the catalogue for the astronomical objects, for which the preview availability flag is raised, are visualized with the "filled square" form, which has a set size and color. The rest, for which a preview is not available, are visualized as a "plus sign", also with a set size and color.

4. CONDUCTION OF A SOFTWARE EXPERIMENT, RESULTS AND CONCLUSIONS

After the structural analysis of AstroWEB's modifications when migrating from the WMS to the WFS standard, the question of what advantages does the end user gain after this system upgrade remains open. To answer this question, the author elects to conduct a simplified software experiment, the goal of which is to determine the response times of the application layer and respectively the server

subsystem, whilst separately using both WMS and WFS standards when visualizing the AstroMAP screen form. In the first case, the time in which a raster image generates in .png format is taken into account, and in the second case - a GML data structure in XML text format for a few hundred dots of the WFODB database with astronomical observatories is observed.

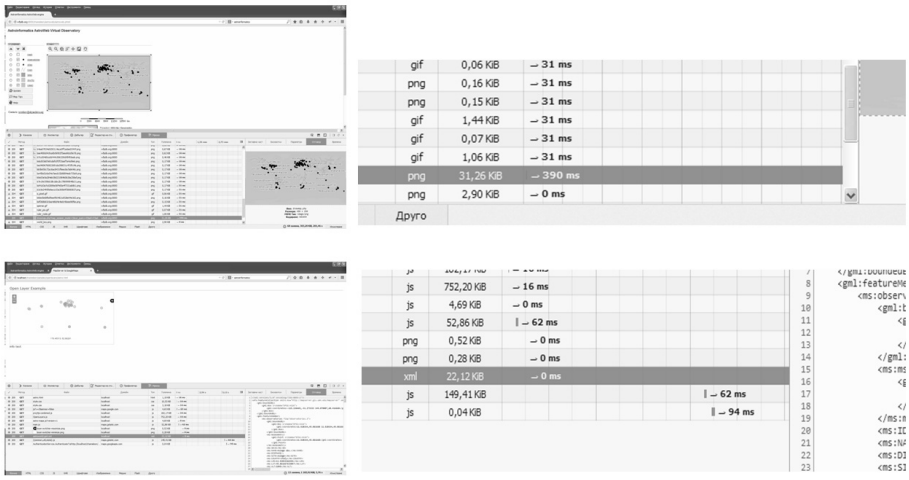

Figure 5: In the case of WMS and WFS standards response times.

Fig. 5 shows functional AstroWEB screens with a visualized AstroMAP form (up), using raster data in a WMS standard and an experimentally created form for visualizing the same set of data, but using vector data in an WFS standard (down). The server subsystem's reaction times are shown on the right. To determine the reaction times in question, Firefox 30.0's Web Developer Web Console Network Analyzer was used. A simple comparison of the reaction times shows that in the conditions of the WMS standard, the raster image is generated for about 390 ms, while under the WFS standard conditions, the vector data for rendering an image to the client is generated for less than a millisecond.

In light of the expected positive results on increasing the productivity of the application layer, and thus the server subsystem, let's look at the possible difficulties that could arise when converting from the WMS to the WFS standard of geodata in relation to the AstroWEB project. As seen in Fig. 3, the GML and SLD files of XML text format are expected to generate whilst applying the "stored procedures" of RDBMS Firebird. This process of generation could provisionally be divided into two phases – executing a spatial request for selecting a subset of data, and the creation of a GML structure. The current version of Firebird doesn't include built-in software tools that could aid either phase. In contrast, both the PostGIS of RDBMS PostGres and SpatialDataTypes of Microsoft SQL Server (versions post-2008) add-ons possess built-in mechanisms for processing spatial query data and generating GML data. That is why, in the interest of a seamless

transition to an WFS standard for the AstroWEB project (especially concerning the SkyMAP module, in which the archives of astroimagery contain hundreds of thousands of units), applying an appropriate spatial data system for the indexing, as well as finding an efficient approach to creating text GML vector georeferral data are of paramount importance.

Acknowledgments

This work is supported by a grant of the Bulgarian National Science Foundation, Ministry of Education and Science, under number DO-02-275.

References

Kolev, Al., Tsvetkov, M., Dimov, D., Kalaglarsky, D.: 2012, Astroweb – A Graphical Representation Of An Astronomical WFPDB Database Using A Web-Based Open Source Geographical Information System, *Serdica J. Computing* **6**, 101–112 #2.

Links

FGS Linux Installer, http://maptools.org/fgs/, accessed may 2014 #4;

OGC® Standards and Supporting Documents, http://www.opengeospatial.org/standards, accessed may 2014 #3.

OSGeo, http://wiki.osgeo.org/wiki/Open_Geospatial_Consortium, accessed may 2014 #6.

OSGeo, http://www.osgeo.org/, accessed may 2014 #5.

Proceedings of the IX Bulgarian-Serbian Astronomical Conference: Astroinformatics (IX BSACA) Sofia, Bulgaria, July 2-4, 2014,
Editors: M. K. Tsvetkov, M. S. Dimitrijević, O. Kounchev, D. Jevremović and K. Tsvetkova
Publ. Astron. Soc. "Rudjer Bošković" No 15, 2015, 23-28

STARK-B DATABASE FOR STARK BROADENING FOR ASTROPHYSICAL PLASMA ANALYSIS AND MODELLING

MILAN S. DIMITRIJEVIĆ[1,2], SYLVIE SAHAL-BRÉCHOT[2], NICOLAS MOREAU[2] and NABIL BEN NESSIB[3]

[1]Astronomical Obsevatory, Volgina 7, 11060 Belgrade, Serbia
[2] Laboratoire d'Étude du Rayonnement et de la Matière en Astrophysique (LERMA), Observatoire de Paris, UMR CNRS 8112, UPMC, Bâtiment Evry Schatzman, 5 Place Jules Janssen, F-92195 Meudon Cedex, France
[3]Department of Physics & Astronomy, College of Science, King Saud University, P. O. Box 2455, Riyadh, 11451Saudi Arabia
E-mail: mdimitrijevic@aob.rs, sylvie.sahal-brechot@obspm.fr, nicolas.moreau@obspm.fr, nbennessib@KSU.EDU.SA

Abstract. The creation and development of STARK-B database (http://stark-b.obspm.fr) is a collaborative project between the "Laboratoire d'Étude du Rayonnement et de la matière en Astrophysique" (LERMA) of the Paris Observatory and CNRS, and the Astronomical Observatory of Belgrade (AOB). Database contains widths and shifts of isolated lines of atoms and ions due to electron and ion impacts (Stark broadening parameters) determined theoretically in more than 150 papers by Dimitrijević, Sahal-Bréchot, and colleagues, and published in international journals. Here we present the state of advancement as well as our programme of its further development. Applications of Stark broadening parameters from STARK-B are also discussed. This database enters in Virtual Atomic and Molecular Data Center (VAMDC – http://www.vamdc.eu).

1. INTRODUCTION

Stark broadening of spectral lines arises when an atom or an ion which emits or absorbs radiation in a gas or in a plasma, is perturbed by interactions with charged particles of the medium. Theoretical and experimental investigations in this research field were stimulated by needs for such data in Astrophysics, for laboratory plasma diagnostics, different applications in Physics (e.g. laser produced plasmas, inertial fusion plasmas…), and also by the needs in industrial plasmas (discharge lighting, laser welding and piercing of metals...). Due to the developments of space born spectroscopy the accuracy of observations in astrophysics is constantly increasing, as well as the number of atomic data

including Stark broadening parameters, needed for the interpretation and analysis of obtained spectra. The development of new generations of powerful computers also enabled sophysticated investigations needing a large number of atomic data as well as their production on a large scale. Consequently, the possibility to access such atomic data via on line databases becomes essential.

Already about thirty years, two of us (MSD-SSB) have operated at a large scale the computer code created by Sahal-Bréchot (1969a, 1969b) and later update and optimized several times (see the review of updates in Sahal-Bréchot et al. 2014), for example: Sahal-Bréchot (1974) for complex atoms, Fleurier et al. (1977) for the inclusion of Feshbach resonances in the elastic ion-electron cross-sections, Dimitrijević and Sahal-Bréchot (1984) and further papers, and Mahmoudi et al. (2008) for transitions arising from very complex configurations. The code is based on the impact semiclassical-perturbation theory (SCP) for isolated spectral lines of neutral and ionized atoms broadened and shifted by collisions with electrons and ions, and gives Stark broadening parameters, spectral line widths and shifts. It was used to calculate results published in more than 150 papers so that the need of creation of an on-line database appeared.

Thus, the database STARK-B (formerly called BELDATA) was initiated in the Astronomical Observatory of Belgrade (AOB), and then a collaborative project between AOB and LERMA was born and led to the present database. A history of BELDATA can be followed in Popović et al. (1999a,b), Milovanović et al. (2000a,b), Dimitrijević et al. (2003) and Dimitrijević and popović (2006).

Actualy, the STARK B database, is on-line in free access, since the end of 2008 (http://stark-b.obspm.fr Sahal-Bréchot et al. 2012). It is currently maintained and developed at Paris Observatory and now contains the Stark broadening parameters, obtained by using the SCP theory and code, from all our papers. We note that there is a link to the Serbian Virtual Observatory (SerVO, http://servo.aob.rs/~darko) at AOB, where latter, a mirror site is planned. STARK-B is also a database included in VAMDC (Virtual Atomic and Molecular Data Centre), an FP7 European project "Research Infrastructures" which has been created in summer 2009 for 3.5 years, in order to create an interoperable e-infrastructure for search and exchange of atomic and molecular data (Dubernet et al. 2011, Rixon et al. 2011 - http://www.vamdc.eu, and http://portal.vamdc.eu).

Here, the STARK-B database is presented and described as well as the plans for its future development.

2. THE STARK-B DATABASE

On the homepage of STARK-B database, proposed menus are "Introduction", "Data Description", "Access to the Data", "Updates" and "Contact". In "Introduction" are described methods used for Stark broadening parameter calculations and different approximations. "Data Description" describes the tabulated data. "Access to the Data" offers a graphical interface which enables to click on the desired element in the Mendeleev periodic table and after this on the

needed ionization degree. Stark broadening parameters are present for elements in yellow cells, with symbols enhanced by boldface, while for elements in other cells, with the lighter color, there is no data. After choosing the element and ionization stage, the visitor should choose the colliding perturber(s), the perturber density, the transition(s) and the plasma temperature(s). It is possible also to search a domain of wavelengths instead of transitions. Finally, a table containing the Stark full widths at half maximum of intensity and shifts appears. Before the Table is an instruction how to cite the STARK-B, as well as the bibliographic references for the data in the Table, which are linked to the publications via the SAO/NASA ADS Physics Abstract Service (http://www.adsabs.harvard.edu/) and/or within DOI, if available. The Stark broadening parameters, widths and shifts, can be obtained as an ASCII table or in format adapted for Virtual Observatories - VOTable format (XML format).

STARK-B displays Stark line widths W and shifts d for a set of temperatures and densities and for electrons and different ions as perturbers. The accuracy of the Stark line widths varies from about 15-20 percent to 35 percent, and in some cases up to 50 percent which depends on the degree of excitation of the upper level, on the completeness of the set of perturbing energy levels, and on the quality of the used atomic structure.

The temperature and density range covered by the tables depends on the ionization degree of the considered ion. The temperatures vary from several thousands for neutral atoms to several millions of Kelvin for highly charged ions. The electron or ion densities vary from 10^{12} (case of stellar atmospheres) to several 10^{22} cm^{-3} (some white dwarfs, subphotospheric layers and some laboratory and fusion plasmas). For the densities lower than the lowest density in the tables, the data can be obtained through a linear extrapolation. At high densities some data are not provided since the impact approximation is not more valid; an asterisk, instead of the data, indicates this. An asterisk preceding the data, denotes that the impact approximation reaches its limit of validity, i.e. when the product of density and typical collisional volume is larger than 0.1 and smaller or equal to 0.5.

With the increase of the density, when the Stark width becomes comparable to the separation between the perturbing energy levels and the initial or final level, the isolated line approximation becomes invalid. The limit of validity of this approximation is indicated in the database by a parameter C defined in Dimitrijević and Sahal-Bréchot (1984) and in following papers. For a perturber density N lower than the limiting value N_{lim} (cm^{-3}) = C/W, the line can be treated as isolated even if a weak forbidden component due to the failure of this approximation remains in the wing.

The definition of configurations, terms and levels follow the VAMDC standards, in order to allow interoperability with other atomic databases. The wavelengths (Å units) in the tables are in majority calculated from the energy levels used as input data. So, they are most often different from the measured ones

and for the identification of lines it is better to use the configurations, terms and levels.

Actually (1st of July 2014) in the STARK-B are Stark broadening parameters obtained by using the SCP method for 79 transitions of He, 61 Li, 29 Li II, 19 Be, 30 Be II, 27 Be III, 1 B II, 12 B III, 148 C II, 1 C III, 90 C IV, 25 C V, 1 N, 7 N II, 2 N III, 1 N IV, 30 N V, 4 O I, 12 O II, 5 O III, 5 O IV, 19 O V, 30 O VI, 14 O VII, 8 F I, 5 F II, 5 F III, 2 F V, 2 F VI, 10 F VII, 25 Ne I, 22 Ne II, 5 Ne III, 2 Ne IV, 26 Ne V, 20 Ne VIII, 62 Na, 8 Na IX, 57 Na X, 270 Mg, 66 Mg II, 18 Mg XI, 25 Al, 23 Al III, 7 Al XI, 3 Si, 19 Si II, 39 Si IV, 16 Si V, 15 Si VI, 4 Si XI, 9 Si XII, 61 Si XIII, 114 P IV, 51 P V, 6 S III, 1 S IV, 34 S V, 21 S VI,2 Cl, 10 Cl VII, 18 Ar, 2 Ar II, 9 Ar VIII, 32 Ar III, 51 K, 4 K VIII, 30 K IX, 189 Ca, 28 Ca II, 8 Ca V, 4 Ca IX, 48 Ca X, 10 Sc III, 4 Sc X, 10 Sc XI,10 Ti IV, 4 Ti XI, 27 Ti XII, 26 V V, 33 V XIII, 9 Cr I, 7 Cr II, 6 Mn II, 3 Fe II, 2 Ni II, 9 Cu I, 32 Zn, 18 Ga, 11 Ge, 3 Ge IV, 16 Se, 4 Br, 11 Kr, 1 Kr II, 6 Kr VIII, 24 Rb, 33 Sr, 32 Y III, 3 Pd, 48 Ag, 70 Cd, 1 Cd II, 18 In II, 20 In III, 4 Te, 4 I, 14 Ba, 64 Ba II, 6 Au, 7 Hg II, 2 Tl III and 2 Pb IV.

Under the menu "Updates" is the description of newly added data with the date of importation as well as the date of the first importation and the importation of the modification for revised data are given. Additionally, for enquiries or user support, at the end is the menu "Contact" enabling to send an e-mail with questions to the any of four authors of this article.

3. FURTHER DEVELOPMENT OF STARK-B

The stage one of the STARK-B database was the inclusion of all our SCP results. The beginning of the stage two was the development and implementation of the formulae enabling to fit the tabulated data with temperature. In order to do this, we have derived (Sahal-Bréchot et al., 2011) a simple and accurate fitting formula based on a least-square method:

$$\log (W) = a_0 + a_1 \log (T) + a_2 \log (T)^2,$$
$$d/W = b_0 + b_1 \log (T) + b_2 \log (T)^2.$$

Consequently, in STARK-B, under each table with Stark broadening parameters, a table with coefficients a_0 , a_1, a_2 and b_0 , b_1, b_2, enabling fitting with the temperature using above equations, is added.

We will develop and implement also, the fitting formulae as functions of perturber densities in order to make easier the use of data on high densities.

Within the STARK-B second stage, we also begin to implement Stark broadening data obtained with the Modified semiempirical method (MSE) (Dimitrijević and Konjević 1980; Dimitrijević and Kršljanin 1986, Dimitrijević and Popović 2001). We use this method when the needed atomic data set is not sufficiently complete to perform an adequate semiclassical perturbation

calculation. Stark line widths and in some cases also shifts of spectral lines of the following emitters have been calculated up to now:

Ag II, Al III, Al V, Ar II, Ar III, Ar IV, As II, As III, Au II, B III, B IV, Ba II, Be III, Bi II, Bi III, Br II, C III, C IV, C V, Ca II, Cd II, Cl III, Cl IV, Cl VI, Co II, Cu III, Cu IV, Eu II, Eu III, F III, F V, F VI, Fe II, Ga II, Ga III, Ge III, Ge IV, I II, Kr II, Kr III, La II, La III, Mg II, Mg III, Mg IV, Mn II, N II, N III, N IV, N VI, Na III, Na VI, Nb III, Nd II, Ne III, Ne IV, Ne V, Ne VI, O II, O III, O IV, O V, P III, P IV, P VI, Pt II, Ra II, S II, S III, S IV, Sb II, Sc II, Se III, Si II, Si III, Si IV, Si V, Si VI,
Sn III, Sr II, Sr III, Ti II, Ti III, V II, V III, V IV, Xe II, Y II, Zn II, Zn III, and Zr II.

Up to 1st of July 2014, MSE data for the following emitters have been implemented:

Al V, P VI, Cl IV, Cl VI, Ar IV, Mn III, Co III, Ga III, Ge III, Ge IV, Cd III and Ra II.

Plans for other future developments are: implementation of our quantum-mechanical results in STARK-B. Also, the development of additional fittings along a spectral series, for charge of the ion collider along isoelectronic sequences, and for homologous ions in order to enable to estimate by interpolation and extrapolation the data that are missing in STARK-B database. We will also implement little applets for fitting along temperatures, along a spectral series, charge of the ion collider along isoelectronic sequences, homologous ions… in order to enable the obtaining of data that are missing in the database.

STARK-B database is devoted to modelling and spectroscopic diagnostics of stellar atmospheres and envelopes, as well as for laboratory plasmas, laser equipment and technological plasmas investigations and will be useful for a number of topics in astrophysics, physics and technology.

Acknowledgments

The support of Ministry of Education, Science and Technological Development of Republic of Serbia through projects 176002 and III44022 is acknowledged.

References

Dimitrijević, M. S., Konjević, N.: 1980, *JQSRT*, **24**, 451.
Dimitrijević, M. S., Kršljanin, V.: 1986, *A&A*, **165**, 269.
Dimitrijević, M. S., Popović, L. Č.: 2001, *J. Appl. Spectr*., **68,** 893.
Dimitrijević, M. S., Popović, L. Č.: 2006, in Virtual Observatory; Plate Content Digitization, Archive Mining, Image Sequence Processing, eds. M. Tsvetkov, V. Golev, F. Murtagh, R. Molina, Heron Press Science Series, Sofia, 115.

Dimitrijević, M. S., Popović, L. Č., Bon, E., Bajčeta, V., Jovanović, P., Milovanović, N.: 2003, *Publ. Astron. Obs. Belgrade,* **75,** 129.
Dimitrijević, M. S., Sahal-Bréchot, S.: 1984, *JQSRT,* **31,** 301.
Dubernet, M.L., Boudon, V., et al.: 2010, *JQSRT,* **111,** 2151, http://www.vamdc.eu/.
Fleurier, C., Sahal-Bréchot, S., Chapelle, J.: 1977, *JQSRT,* **17,** 595.
Mahmoudi, W. F., Ben Nessib, N., Sahal-Bréchot, S.: 2008, *EPJD,* **47,** 7.
Milovanović, N., Popović, L. Č., Dimitrijević, M. S.: 2000a, *Publ. Astron. Obs. Belgrade,* **68,** 117.
Milovanović, N., Popović, L. Č., Dimitrijević, M. S.: 2000b, *Baltic Astron.*, **9,** 595.
Popović, L. Č., Dimitrijević, M. S., Milovanović, N., Trajković, N.: 1999a, *Publ. Astron. Obs. Belgrade,* **65,** 225.
Popović, L. Č., Dimitrijević, M. S., Milovanović, N., Trajković, N.: 1999b, *J. Res. Phys.*, **28,** 307.
Rixon, G., Dubernet, M. L., et al.: 2011, 7th International Conference on Atomic and Molecular Data and their Applications -ICAMDATA-2010, *AIP Conf. Proc.,* **1344,** 107.
Sahal-Bréchot, S.: 1969a, *A&A,* **1,** 91.
Sahal-Bréchot, S.: 1969b, *A&A,* **2,** 322.
Sahal-Bréchot, S.: 1974, *A&A,* **35,** 321.
Sahal-Bréchot, S., Dimitrijević, M.S., Ben Nessib, N.: 2011, *Baltic Astronomy*, **20**, 523.
Sahal-Bréchot, S., Dimitrijević, M.S., Ben Nessib, N.: 2014, *Atoms*, **2**, 225.
Sahal-Bréchot, S., Dimitrijević, M. S., Moreau, N.: 2012, *STARK-B database, [online]. Available:* http://stark-b.obspm.fr *[Jul 8, 2014]. Observatory of Paris, LERMA and Astronomical Observatory of Belgrad*e.

Proceedings of the IX Bulgarian-Serbian Astronomical Conference: Astroinformatics (IX BSACA) Sofia, Bulgaria, July 2-4, 2014,
Editors: M. K. Tsvetkov, M. S. Dimitrijević, O. Kounchev, D. Jevremović and K. Tsvetkova
Publ. Astron. Soc. "Rudjer Bošković" No 15, 2015, 29-35

UV CETI TYPE VARIABLE STARS PRESENTED IN THE GENERAL CATALOGUE OF VARIABLE STARS

KATYA TSVETKOVA

Institute of Mathematics and Informatics, Bulgarian Academy of Sciences
E-mail: katya@skyarchive.org

Abstract. We present the place and the status of UV Ceti type variable stars in the General Catalogue of Variable Stars (GCVS4, edition April 2013) having in view the improved typological classification, which is accepted in the already prepared GCVS4.2 edition. The improved classification is based on the understanding of the major astrophysical reasons for variability. The distribution statistics is done on the basis of the data from the GCVS4 and addition of data from the 80thName List of Variable Stars - altogether 47 966 variable stars with determined type of variability.

The class of the eruptive variable stars includes variables showing irregular or semi-regular brightness variations as a consequence of violent processes and flares occurring in their chromospheres and coronae and accompanied by shell events or mass outflow as stellar winds and/or by interaction with the surrounding interstellar matter. In this class the type of the UV Ceti stars is referred together with the types of Irregular variables (Herbig Ae/Be stars; T Tau type stars - classical and weak-line ones, connected with diffuse nebulae, or RW Aurigae type stars without such connection); FU Orionis type; YY Orionis type; Yellow massive evolved hypergiants with Rho Cas as aprototype); S Doradus type variables - giants and supergiants with high mass loss and occasional larger eruptions (with subtypes η Car and P Cyg, connected with diffuse nebulae and surrounding by expanding envelopes); R Coronae Borealis variables (prototype R CrB), which are simultaneously eruptive and pulsating variables, showing brightness fading suddenly for months to years; Wolf–Rayet variables with binary interactions and rotating gas clumps around the star; Gamma Cassiopeiae fast-rotating Be spectral type variables with formation of equatorial rings or disks; proto-planetary objects; as well as L dwarfs with causes of variability not quite clear yet.

The statistics shows that the eruptive stars are the most common class of variable stars after pulsating and eclipsing classes on the base of their total number. About 60% of all eruptive stars are considered as irregular variables with not completely clear origin of light variations and spectral types and that is why being rather inhomogeneous group of objects. The type of UV Ceti flare stars designated as UV (for flare stars from the solar vicinity) and UVN types variables (flare stars in stellar clusters and associations) are the next ones (30%), and only 10% are the other eruptive variable stars – with designations GCAS+Be, SDor, WR, and RCB.

1. INTRODUCTION

Borne (2013) describes Astroinformatics as a fourth paradigm of astronomical research, after the observation, theory, and computation/modeling. Astroinformatics as data oriented astronomy includes a lot of disciplines as data-intensive computing, astrostatistics, data mining, knowledge extraction, information visualization, information retrieval methods, semantic science presented by semantic data integration, sky-based and catalog-based indexing techniques, consensus semantic annotation tags, astronomical classification taxonomies, astronomical concept ontologies (see Borne, 2010). The significant role of the semantic science is defined by the benefit of the semantic search and indexing in the shared astronomical data and in the academic literature, as well as by the possibility to increase the level of connectivity between them.

In order to support the classification and semantic enrichment of the scholarly literature, where a certain search is conducted, the International Virtual Observatory Alliance (IVOA) Semantics Working Group pleads for usage of standard keywords in the field of astronomy and astrophysics. The idea is to transform the list of keywords into an IVOA standard vocabulary. As a result appeared the Unified Astronomy Thesaurus (http://astrothesaurus.org.), which is intended to provide a formal language that can be used to describe the entire concept field and thus to stimulate the development of astronomical resources. One of the suggested keyword by the IVOA Semantics Working Group is "star: flare". Under the term "*Flare*" a lot of variable stars showing flares with different origin can be found – the red dwarf flare UV Ceti stars from the Solar neighborhood, the flare stars in the open stellar clusters and associations, BY Draconis stars, FU Orionis stars, R Coronae Borealis variables, RS Canum Venaticorum variables, i.e. the concept of flare star is not clear and needs a defining.

In order to define the term *Flare Star* here we consider the flare stars designated in the General Catalogue of Variable Stars (GCVS, Samus et al. 2013) as of types UV and UVN, respectively located in the Solar neighborhood, and in the open stellar clusters and associations. The reason for putting together both types of flare stars is their common physical nature of the observed flares. The prototype is the UV Ceti star, which is the only star (up to the moment) having a dedicated monument in Toronto (Canada) since 1982 presenting a bronze V-shaped center piece with a big orb in the middle situated in a fountain with a sitting area around as was the idea of the sculptor Andrew Posa. The sculptor inspiration obviously comes from the fact that the classical flare stars of the UV Ceti type around the Sun form a physical system - several nearby red dwarf stars including the nearest stellar neighbor of the Sun – Proxima (at distance of 1.3 pc), are flare stars (together with CN Leo at 2.4 pc, UV Cet at 2.7 pc, V1216 Sgr at 2.9 pc), etc.

2. CLASS OF THE ERUPTIVE VARIABLE STARS IN GCVS

According to the typological classification of the variable stars in GCVS (**http://cdsarc.u-strasbg.fr/afoev/var/etypo.htx**) the class of the eruptive variable stars includes variables showing irregular or semi-regular brightness variations as a consequence of violent processes and flares occurring in their chromospheres and coronae, and accompanied by shell events or mass outflow as stellar winds and/or by interaction with the surrounding interstellar matter. The class includes the following separated types of variable stars: UV Ceti stars; Irregular variables (Herbig Ae/Be stars; T Tau type stars - classical and weak-line ones, connected with diffuse nebulae, or RW Aurigae type stars without such connection; FU Orionis type; YY Orionis type; Yellow massive evolved hypergiants with Rho Cas as aprototype); S Doradus type variables - giants and supergiants with high mass loss and occasional larger eruptions (with subtypes η Car and P Cyg, connected with diffuse nebulae and surrounding by expanding envelopes); R Coronae Borealis variables (prototype R CrB), which are simultaneously eruptive and pulsating variables, showing brightness fading suddenly for months to years; Wolf–Rayet variables with binary interactions and rotating gas clumps around the star; Gamma Cassiopeiae fast-rotating Be spectral type variables with formation of equatorial rings or disks; proto-planetary objects; as well as L dwarfs with causes of variability not quite clear yet.

In 1958 at the X General Assembly of the International Astronomical Union (IAU) especially accepted a terminology for eruptive variables of UV Ceti type, which is adopted in GCVS. UV Ceti type stars were ranked as a special type of eruptive variables with UV Cet as a prototype of the flare stars from the solar neighbourhood and the best-known flare star.

The UV Ceti type stars are designated as “UV” in the GCVS in order to distinguish them from the flaring Orion variables designated as “UVN”. In addition to being related to nebulae and their location in stellar clusters and associations, UVN variables are normally characterized by being of earlier spectral types (Ke-Me), and having greater luminosity, with slower development of flares and greater amplitudes reaching up to 9.0 magnitudes in U photometric band - e.g. at V341 Tau, V515 Per, SV Ori, etc. according to the Flare Star Database (Tsvetkova et al. 1995, 1996).

According to the typological classification of GCVS the variable dwarf stars of M spectral class have unpredictable flare activity expressing itself with sudden increases in brightness across the spectrum with quit various amplitudes, reaching the maximum brightness for seconds or a few minutes and returning to their quiescent brightness in several more minutes to hours. They are located in the solar neighbourhood and the common belief is that their flares are analogous to the solar flares but far more energetic and intensive. The cause of the flares is the sudden release of magnetic energy in the photosphere of the star, expressing itself as a spike in brightness, i.e. a flare.

The observed differences between UV and UVN variable stars are due to the difference in ages. Except the increased luminosity during the flare, high energy particles are released such as x-rays and gamma rays. Still in the beginning of the discovery and the investigation of flare stars the idea that these flares may be similar to the solar flares is evinced.

The common physical nature of UV and UVN variables obviously is the cause that in the improved typological classification based on understanding the major astrophysical reasons for variability and accepted in the already prepared GCVS4.2 edition (Samus 2006, http://www.sai.msu.su/gcvs/future/classif.htm), these two types of eruptive variables are merged in one with designation UV.

Some basic characteristics derived from investigations of flare stars applying different methods for observations (optical, spectral, polarimetric, ultraviolet, infrared and radio) of the flares and their random characters, are:

- The relative number of flare stars among all red dwarfs increases at lower luminosities.
- The flare stars are formed in a system from certain luminosity, and this limiting luminosity decreases with increasing age of the system.
- Their evolutionary status gives a plausible scenario how the most numerous stars in the Galaxy – the red dwarf stars - are evolved passing through the stage of flare activity.

3. FLARE STARS STATISTICS

The distribution statistics is on the base of standardization of the object types used in the GCVS, which refers to a categorization of the nature of astronomical sources. At http://www.sai.msu.su/gcvs/gcvs/iii/vartype.txt one can find a distribution statistics of designated variable stars according to their types of variability on the base of the GCVS volumes I-III and the 67th – 79th Name Lists of Variable Stars (NLVS). What has to be done is to add the information for the variable stars from the 80th NLVS. Table 1 presents our sources of information for the total number of designated variable stars - the GCVS edition (Feb. 12, 2009) and the 80th NLVS with its three parts, published in Information Bulletin of Variable Stars (IBVS).

In the following updated versions of the GCVS4 (edition from March 2014 which is uploaded on April 9, 2014, as well as the last one from September 25, 2014, Samus et al. 2014) the total number of designated variable stars is 47968 (or with two stars more than is calculated in Table 1). There is some discrepancy in the total number of variable stars – 47811, quoted in the Introductory of GCVS at http://www.sai.msu.su/gcvs/gcvs/intro.htm and the downloaded GCVS4. The downloaded catalogue contains exactly 47968 variable stars. The difference of 155 variable stars obviously is due of not updated number of stars in the introductory notes of GCVS, but even if there is another reason this difference presents 0.3% from the total number of variable stars and can be neglected for the statistics needs.

Table 1. Statistics sources

Source	Date of source publishing	Number of variable stars
GCVS4	2009, February 12	41638
80th NLVS:		
IBVS 5969	2011, January 31	2036
IBVS 6008	2011, December 21	2159
IBVS 6052	2013, April 5	2133
	Total Number of Variable Stars:	47966

Searching for the latest GCVS edition one can find at http://www.sai.msu.su/groups/cluster/gcvs/gcvs/GCVS5/, the designation "GCVS5", which may cause some misunderstanding. Practically this is a part of the GCVS, which takes into account the new data accumulated since the GCVS4 edition for only three southern constellations: Aquila, Caelum and Camelopardalis.

Following the criteria of the GCVS4 for attachment to certain class of variability given in http://www.sai.msu.su/gcvs/gcvs/iii/vartype.txt, as well as the improved typological classification at http://www.sai.msu.su/gcvs/future/classif.htm), we performed a distribution statistics on the basis of the presented in Table 1 sources. All variable stars are referred to the classes of Pulsating, Eruptive, Rotating, Cataclysmic, Eclipsing, X-ray sources and Other Symbols variable stars.

To Other Symbols are referred also a group of the variable stars designated in GCVS with symbol * which stands for unique variable stars outside the range of the given classifications and representing either short stages of transition from one variability type to another or the earliest and latest evolutionary stages of these types, or they are insufficiently studied members of future new types of variables. Their number is 95. Another group of variable stars which we included in Other Symbols is the group of variable stars without any assigned type of variability – their number is 564. Fig. 1 presents the distribution of all 47966 variable stars according to their class of variability. This distribution among the classes of variable stars shows that the class of the eruptive variable stars according to their number follows the classes of the pulsating and eclipsing variables. In Fig. 2 the distribution of the number of stars from a certain type of variables constituting the class of eruptive variables with total number of 5383 stars is shown. Inside the class of eruptive variables about 60% of all eruptive stars (with total number 5383) are considered as irregular variables with not completely clear origin of light variations and spectral types and that is why being rather inhomogeneous group of objects. The type of UV Ceti flare stars designated as UV (for flare stars from the solar vicinity) and UVN types variables (flare stars in stellar clusters and associations) with total number 1608, are the next ones (30%). About 10% are the other eruptive variable stars – with designations GCAS+Be, SDor, WR, and RCB.

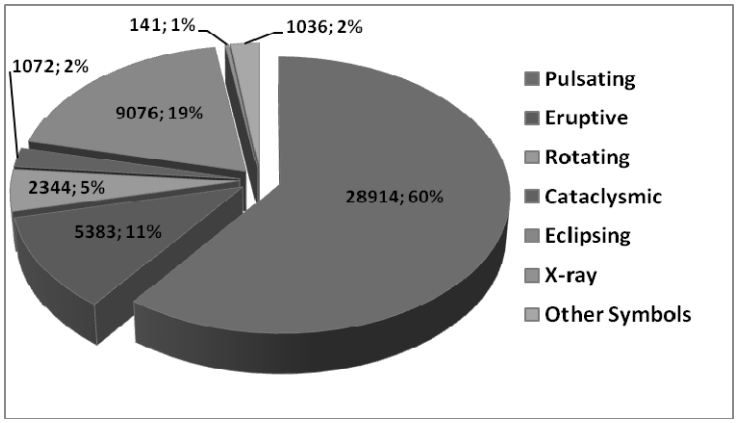

Figure 1: Distribution of 47966 variable stars according to their class of variability.

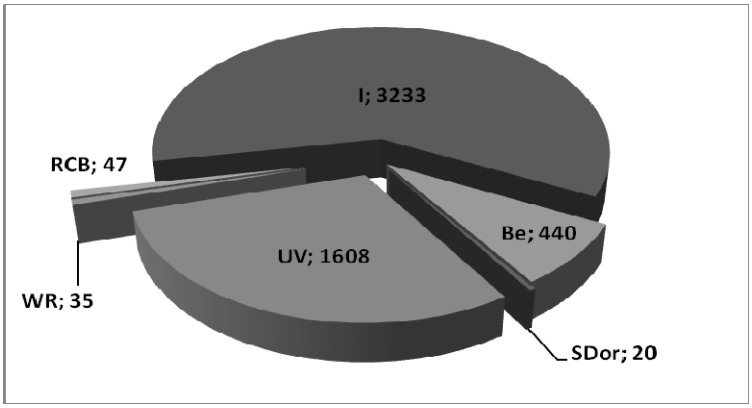

Figure 2: Distribution of the number of variable stars from a certain type inside the class of eruptive variables.

4. CONCLUSIONS

The need of defining the term *Flare Star* initiated the present work on the distribution statistics of the UV Ceti type variable stars presented in GCVS4 edition.

More than 11% of all known variable stars belong to the class of eruptive variable stars, whose number is 5383, and which have different nature of the physical processes, leading to irregular/semi-regular brightness variations or sudden eruptions. The considered types of eruptive variable stars UV and UVN, which are united in the proposed improved typological classification of variable

stars in one type – UV, are well defined type – 30%, having in view that the group of the irregular variables, which are 60%, are not homogeneous group - with not completely clear origin of light variations and spectral types. These 30% of all known eruptive stars are evidence that the flare activity is a common characteristic of all red dwarf stars, whose evolution scenario follows the scheme: T Tau type stars - Flare stars - Main Sequence stars. The number of flare stars among all red dwarfs increases at lower luminosities, which is proved also by the present light-curve data from the *Kepler* Space Observatory by applying a Bayesian method for detecting stellar flares (Pitkin et al. 2014).

An attempt to build a digital data library providing interlinking of original data about the UVN flare stars and their recorded flares on photographic plates (from the Wide-Field Plate Database, http://wfpdb.org) with scholarly literature (especially with Information Bulletin on Variable Stars, http://www.konkoly.hu/IBVS/IBVS.html) was made in Holl et al. (2006).

References

Borne, K.: 2010, *Journal of Earth Science Informatics*, **3**, 5-17.

Borne, K.: 2013, in *Planets, Stars and Stellar Systems*, T. D. Oswalt, H. E. Bond (Eds.), Springer, Netherlands, 403-443.

Holl, A., Kalaglarsky, D., Tsvetkov, M., Tsvetkova, K., Stavrev, K.: 2006, in Virtual Observatory, Plate Content Digitization, Archive Mining, Image Sequence Processing, Eds. M. Tsvetkov, V. Golev, F. Murtagh, R. Molina, Heron Press Science Series, Sofia, 374-378.

Pitkin, M., Williams, D., Fletcher, L., Grant, S. D. T.: 2014, *MNRAS* **445**, 3, 2268-2284.

Samus, N. N.: 2006, IAU XXVI General Assembly, Prague, August 9, 2006, in "The draft classification for new GCVS versions".

Samus, N. N., Goranskij, V. P., Durlevich, O. V., Kazarovets, E. V., Kireeva, N. N., Pastukhova, E. N., Zharova A. V.: 2013, *General Catalogue of Variable Stars.*

Samus, N. N., Goranskij, V. P., Durlevich, O. V., Kazarovets, E. V., Kireeva, N. N., Pastukhova, E. N., Zharova, A. V.: 2014, GCVS 4, http://www.sai.msu.su/gcvs/gcvs/iii/iii.dat, edition uploaded on April 9, 2014.

Tsvetkova, K. P., Tsvetkov, M. K., Stavrev, K. Y.: 1995, *Lecture Notes in Physics*, 454, Eds. J. Greiner, H. W. Duerbeck, R. E. Gershberg, Springer, p. 121.

Tsvetkova, K. P., Tsvetkov, M. K., Stavrev, K. Y.: 1996, *Proceedings of the Second Astronomical Conference of the Hellenic Astronomical Society*, Thessaloniki, Eds. M. E. Contadakis, J. D. Hadjidemetriou, L. N. Mavridis, J. H. Seiradakis, p. 146.

Proceedings of the IX Bulgarian-Serbian Astronomical Conference: Astroinformatics (IX BSACA) Sofia, Bulgaria, July 2-4, 2014,
Editors: M. K. Tsvetkov, M. S. Dimitrijević, O. Kounchev, D. Jevremović and K. Tsvetkova
Publ. Astron. Soc. "Rudjer Bošković" No 15, 2015, 37-41

ALERT SIMULATOR - A SYSTEM FOR SIMULATING DETECTION OF TRANSIENT EVENTS ON LSST

JOVAN ALEKSIĆ[1,2], VELJKO VUJČIĆ[2] and DARKO JEVREMOVIĆ[2]

[1] *Faculty of Mathematics, University of Belgrade, Serbia*
[2] *Astronomical Observatory Belgrade, Serbia*
E-mail: jaleksic@aob.rs

Abstract. Large Synoptic Survey Telescope will be a large ground-based telescope system which will provide sky survey in unsurpassed details. One of the modules will be time-domain astronomy and detection of transient events.

In order to properly design the system, a simulation framework is required to optimize algorithms to large data volumes and frequent events. The Serbian contribution to the project is the Alert Simulator, a system which will simulate detection of transient events. Main use of AlertSim will be to test the performance of event brokers/CEP engines and their ability to detect and identify transients as well as various failures or exceptional/extreme modes of operation.

1. INTRODUCTION

Large Synoptic Survey Telescope (LSST) will be a large, ground-based, optical telescope that will obtain images over half the sky every few nights (Ivezić et al. 2008). It will contain an 8.4 m primary mirror, 3.2 Gigapixel camera and will operate in six bands (u,g,r,i,z and y). After 10-years survey period, it is expected that total amount of about 100 PB of data will be collected.

2. TRANSIENT EVENTS AND ALERTS

2.1 LSST data products

LSST data products will mostly consist of catalogs and images (Jurić et al. 2013). Since they will be used for different purposes, there will be three main categories of data products. **Level 1** products are intended to detect time-domain events. These data are the product of continuous observations (nightly) followed by analysis of difference images. Variable and moving objects are the result of L1 data products. **Level 2** products are generated as part of a Data Release. These

data are the product of yearly observations, followed by analysis of direct images. Catalogs and images are the result of L2 data products. **Level 3** products will be generated by users, using LSST software and/or hardware. Various user-created data will be available that not belong to automatically generated L1 and L2 products (Jurić et al. 2013, Conolly et al. 2013).

2.2 Transient events

A transient astronomical event is the event where the image of observed object changes in time, usually in short time period. Roughly, they can be classified as variable objects, where flux changes are detected and moving objects, where position changes are detected.

Variable objects (Flux changes)	Moving objects (Position changes)
Variable stars Eclipsing binaries Transits of extrasolar planets Galaxies AGN Bursts (optical)	Planets Asteroids Comets Trans-Neptunian objects

2.3 Transient alert

A Transient Alert is a notification of the detection and characterization of a moving or variable object. Very simple procedure can be described as follows. A visit image is acquired from the telescope. A template image presents what should be seen. Visit image is compared against the template image, and if the difference exists, the alert is raised. This explanation is very simplified. Actually, each of these steps consist several other subprocedures, but the core idea is as described.

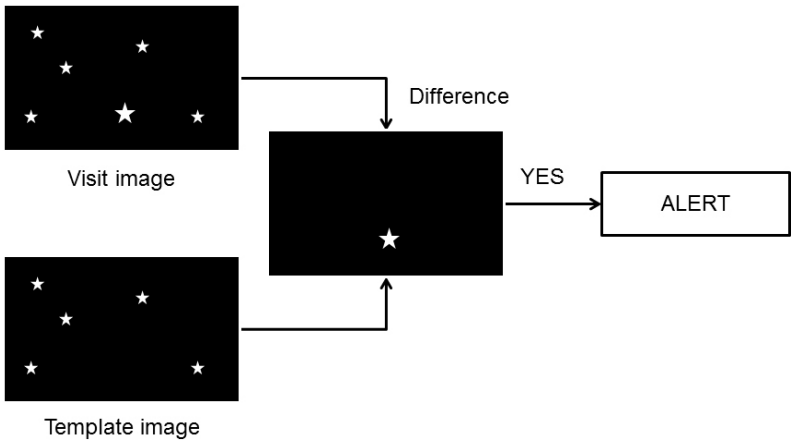

Figure 1: Basic procedure.

A transient alert is a piece of information containing characterization of the object. Each alert contains several data:

- alert ID
- timestamp
- level1 database ID
- Science data
  - position
  - flux, size, and shape
  - light curves in all bands (up to a year; stretch: all)
  - variability characterization (e.g., low-order light-curve moments, probability the object is variable)
- cut-outs centered on the object (template, difference image)

In addition, alerts will have the following properties:

- Alerts will be available world-wide within 1 min of visit acquisition. This is the result of fast image processing as well as distributing procedures.
- The rate of generating alerts is expected to be quite high, about 10 M per night or about 10 k per visit. This assumption is included in design of Alert Simulator process.
- The format should be easy to read and process by variety of systems. The most appropriate format is XML, or even better VOEvent (XML record with defined structure, used to describe events in astronomy)

3. SIMULATOR

LSST will produce several millions alerts per night. Such amount of data requires particular approach of handling it. One of such approaches is filtering, a set of algorithms for analysing incoming alerts and to reduce their number to most relevant ones. In early design stage, useful tools are simulations, to test the performance well in advance of first light. Alert Simulator will be a software package whose main purpose will be to simulate input that is expected to encounter in operation mode, and then to test the behaviour of the system. In this way, the proper respond and performance will be predicted, so appropriate design can be made.

3.1 Requirements

In order to accomplish the tasks, this software package has to meet the following requirements (Jevremović et al. 2014):

- to generate realistic streams of alerts at data rates that are expected in operational mode
- to simulate various failures or exceptional/extreme cases that might occur:

  - large numbers of fake/spurious detections
  - unusually large numbers of detections simulating observations of high-density fields
  - disruptions in the event stream, which may occur due to forced termination of difference image processing
  - corruptions of the event stream, which may occur due to hardware or software errors
  - network connectivity interruptions
- to provide facilities to ease troubleshooting. This will be achieved through logging and packet inspection (VO Event is structured information, so it can be processed easily).
- to be configurable, automated, and capable of keeping provenance information
- to follow standards and conventions. The package will be written in accordance with standards, conventions, and development processes defined in LSST documents. Some examples are that it will be written in Python programming language and the format will most probably be VOEvent.
- to be developed in coordination with group. Alert Simulator will be just one part of the large software system. There are several groups working on simulations (photon, operations, catalog, image simulations), so Alert Simulator will be developed in cooperation with them to ensure integration and interoperability with other parts of the system.

3.2 Goals and benefits

The main goal of simulator is to evaluate whether the properties of as-delivered components are sufficient. It will also evaluate how design modifications or optimizations impact the overall science performance of the system. Finally, it will verify that the algorithms used in the processing the LSST data are capable of characterizing the astrometric, photometric, and morphological properties of sources at the level of fidelity described in the SRD) (Conolly et al. 2013).

In addition, it will reduce LSST Operations cost by (Jevremović et al. 2014):

- Delivering functionality early, that is currently planned to be developed in Operations
- Reducing the need for help desk and technical support personnel by automating the validation/troubleshooting activities and increasing this aspect of staff productivity.
- Further reducing potential down-time and troubleshooting personnel costs by providing the capability for full characterization of the behaviour of connected public brokers in the full suite of exceptional/extreme operation modes that may occur in Operations, but are unlikely to occur with real data in Commissioning.

4. CONCLUSIONS

Alert Simulator will provide predictions of system behaviour and its performance in case when frequent events are expected. This will allow to design the system appropriately and optimize algorithms before the first light, so the overall cost will be reduced.

Acknowledgments

This work is supported by a grant of the Ministry for Education and Science of Republic of Serbia through the project III 44002. ”Astroinformatics: Application of IT in Astronomy and Close Fields”.

References

Connolly, Andrew et al.Č 2013, *Requirements for the LSST Simulation Framework*.

Ivezić et al.: 2008, *LSST: from Science Drivers to Reference Design and Anticipated Data Products*, arXiv:0805.2366 [astro-ph].

Jevremović, D., Vujčić, V., Malović, M., Aleksić, J., Popović, L.: 2014, AlertSim - Serbian contribution to LSST, Proceedings of XIII International Symposium Infoteh, Jahorina, ISBN 978-99955-763-3-2, 414-418.

Jurić, M. et al.: 2013, *LSST Data Products Definition Document*, LSE-163.

Proceedings of the IX Bulgarian-Serbian Astronomical Conference: Astroinformatics (IX BSACA) Sofia, Bulgaria, July 2-4, 2014,
Editors: M. K. Tsvetkov, M. S. Dimitrijević, O. Kounchev, D. Jevremović and K. Tsvetkova
Publ. Astron. Soc. "Rudjer Bošković" No 15, 2015, 43-48

WFPDB: SOFTWARE FOR TIME AND COORDINATES CONVERSIONS

NIKOLAY KIROV[1,2], MILCHO TSVETKOV[2] and KATYA TSVETKOVA[2]

[1]*New Bulgarian University*
E-mail: nkirov@nbu.bg
[2]*Institute of Mathematics and Informatics, Bulgarian Academy of Sciences*
E-mail: nkirov@math.bas.bg, milcho.tsvetkov@gmail.com,
katya.tsvetkova09@gmail.com

Abstract. The article consists of a detailed description of two software tools for time and coordinates conversions. The digitization of astronomical photographic plates has to start with collection of data for the plates. Wide Field Plate Database (WFPDB) is the most popular WEB-based database that contains data for more than 600 thousand plates. To add new data in WFPDB, it has to obey the requirements of content and data structure. The time of observation is UT and the coordinates are in J2000. The presented software can convert the time from the Local Sidereal Time or Local Time to Universal Time, and the equatorial coordinates from any equinox to J2000. The input and output files of the programs are in data format of WFPDB.

1. INTRODUCTION

The technology for digitization of astronomical photographic plates assumes that the data for digitized plates is already collected (see Kirov et. al (2012a,b), Tsvetkov et al. (2012)). Wide-Field Plate Database (WFPDB – `www.skyarchive.org` or `wfpdb.org`) is WEB-based database that contains data for more than 600 thousand astronomical photographic plates. Over two million and half plates are identified and collected in this database. The database structure is shown in Figure 1.

To add new plates in WFPDB, the data has to obey the requirements of content and data structure for WFPDB. The time of observation has to be Universal Time (UT) and the coordinates have to be J2000 (the currently used standard equinox). The software can convert the time from Local Sidereal Time (LST) or Local Time (LT) to UT; the equatorial coordinates (RA and DEC) from any equinox to J2000.

The input and output files are in data format of WFPDB.

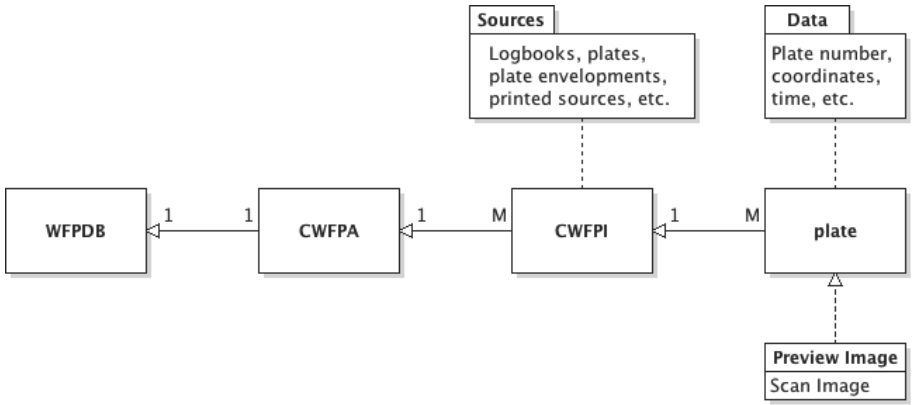

Figure 1: Main elements of WFPDB.

2. WIDE-FIELD PLATE DATABASE

The Catalogue of Wide-Field Plate Archives (CWFPA – `wfpdb.org/catalogue.html`) contains data for plate archives – the set of plates which are obtained with one instrument. The instrument means one telescope or camera at one place for observation (location). In the actual version 7.0 (February 2014) of CWFPA 495 archive descriptions are collected (Kalaglarski et al. 2014). The following example represents one line from the catalogue table containing the data for the archive with identifier ROB033.

```
ROB033 CdC Astrograph Brussels Belgium Royal Obs.Belgium Brussels Obs. Uccle
Belgium 12 1 04 21.5 50 47.9 105 0.33 3.43 60 Ast 2.6 1908 1950 1160 T T.Pauwels
```

Table 1 explains some fields of the example.

Table 1. Part of the content of the Catalogue of Wide-Field Plate Archives

No	Description	Format	Example
1a	Instrument Identifier (observatory code and instrument aperture)	`[LLLDDD]`	`ROB033`
1b	Original Name of the Instrument	text	`CdC Astrograph`
2-3	Location of the Archive	text	`Brussels Belgium`
8	Time Zone (main)	hours	`1`
9	Observatory Longitude	deg min	`04 21.5`
10	Observatory Latitude	deg min	`50 47.9`

Remark: `L` denotes a capital letter; `D` denotes a digit.

The Catalogue of Wide-Field Plate Indexes (CWFPI) contains data for plates. The following fields store data for the plates: the coordinates of the plate center, the date and time of the observation, object name and type, method of observation, duration of exposures, type of emulsion, the size of the plate, the quality of the plate, the name of the observer, etc.

All the data are distributed in 6 plain text files with names: maindata, quality, observer, availability, digitization and notes. For the instrument `ROB033` they are: `ROB033maindata.txt`, `ROB033quality.txt`, `ROB033observer.txt`, etc.

The example below represents a line form the file `ROB033maindata.txt` containing the data about plates obtained by the instrument with the identifier `ROB033`.

Example: `ROB033 000008 233256+333308 19081019214619`

Some important field from maindata file are given in the Table 2.

Table 2. Part of maindata file

Positions		Description	Format	Example	
1-6	6	Instrument Identifier	`[LLLDDD]`	`ROB033`	
7	1	Suffix	`[ ]` or `[L]`		
8-13	6	Plate Number	`[DDDDDD]`	`000008`	8
14	1	Suffix for Duplicates	`[ ]` or `[L]`		
15-20	6	Right Ascension (RA)	`[hhmmss]`	`233256`	$23^{\mathrm{h}}32^{\mathrm{m}}56^{\mathrm{s}}$
21-27	6	Declination (DEC)	`[±ggmmss]`	`+333308`	+33°33'8"
28	1	Missing Data	`[ ]` or `M`		
29-36	8	Date	`[yyyymmdd]`	`19081019`	19.10.1908
37-42	6	Time	`[hhmmss]`	`214619`	21:46:19
43	1	Missing Data	`[ ]` or `M`		

Remark: `L` denotes a capital letter; `D` denotes a digit.

3. SOURCES AND CONVERSIONS

The data for plates are collected from various sources: telescope logbooks, photographic plates, plate envelopes, printed sources (books, plates' copies, etc.). The most important data are the coordinates of the plate center and the time of observation. Usually in the sources the time is given as LST or LT. `timetool` software transforms the time from LST or LT or local Daylight Saving Time (DST) to UT. The coordinates originally are given in Besselian Equinoxes (BE: B1875.0, B1900.0, B1925.0 and B1950.0) or in the Time of Observation (TO). `epochtool` software transforms equatorial coordinates (RA and DEC) from arbitrary equinox to J2000.

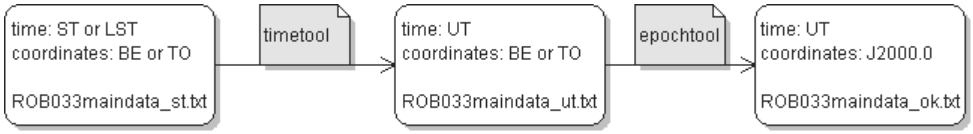

Figure 2: The conversion diagram.

4. TIMETOOL

For time conversion we use the approximation given in Aoki et al. (1982) – (12), (13):

$$T_U = \frac{J - 2451545}{36524}$$

$$G = 24110.54841 + 8640184.812866 T_U + 0.093104 T_U^2 - 6.2 \times 10^{-6} T_U^3$$

$$U = L - \frac{G}{3600} - \frac{O}{15}$$

where J denotes Julian day, G – Greenwich Mean Sidereal Time, L – Local Sidereal Time, O – Observatory Latitude, U – Universal Time.

Input files for `timetool` are:

- config file: `timetool.cfg`;
- summer time file (optional): `<instrument name>.dst`;
- data file: `<dir><instrunent name>maindata_st.txt`;
- catalog file: `<dir>Cat<version>.txt`.

The configuration file `timetool.cfg` for the example is:

```
2
ROB033
Cat7.0
0
../../astroinformatics/data/
```

Time Zones and Daylight Saving Dates for a given location can be found in `www.timeanddate.com/time/change/`. Table 3 presents a part of summer time file `BAL080.dst` (Baldone Schmidt, Riga).

Table 3. Part of summer time file `BAL080.dst` (Baldone Schmidt, Riga)

```
1987-03-29 03:00:00 1987-09-27 02:59:59 3 4 UTC+4h MSD
1988-03-27 03:00:00 1988-09-25 02:59:59 3 4 UTC+4h MSD
1989-03-26 03:00:00 1989-09-24 02:59:59 3 3 UTC+3h EEST
1989-09-24 03:00:00 1989-12-31 23:59:59 3 2 UTC+2h EET
1990-03-25 03:00:00 1990-09-30 02:59:59 2 3 UTC+3h EEST
```

The data for plates are contained in the file `<instrunent name>maindata_st.txt` where the time is LST or LT and the coordinates are in arbitrary time epoch.

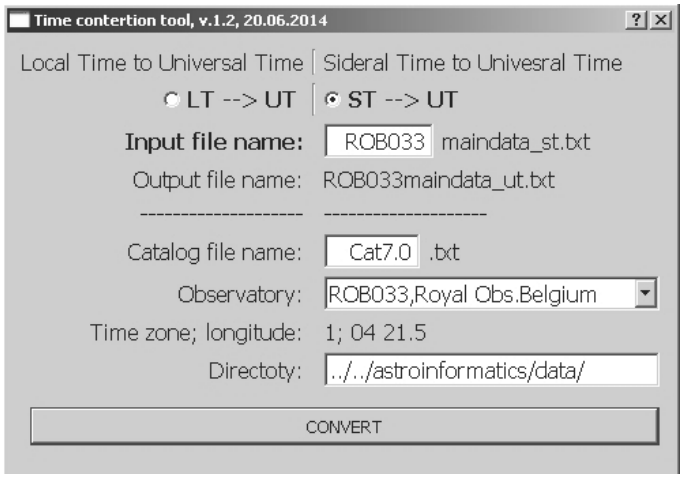

Figure 3: The user interface of `timetool`.

Output files for `timetool` are:
- config file: `timetool.cfg`;
- data file: `<dir><instrument name>maindata_ut.txt`.

5. Epochtool

The formulas for epoch transformations can be found in `idlastro.gsfc.nasa.gov/ftp/pro/astro/premat.pro`.

Input files for `epochtool` are:
- config file: `epochtool.cfg`
- data file: `<dir><instrunent name>maindata_ut.txt`

The configuration file `epochtool.cfg` for the example is:

```
0 0 0 1 0 0
ROB033
../../astroinformatics/data/
```

The data for plates are contained in the file `<instrunent name>maindata_ut.txt` where the time is UT and the coordinates are in arbitrary time epoch.

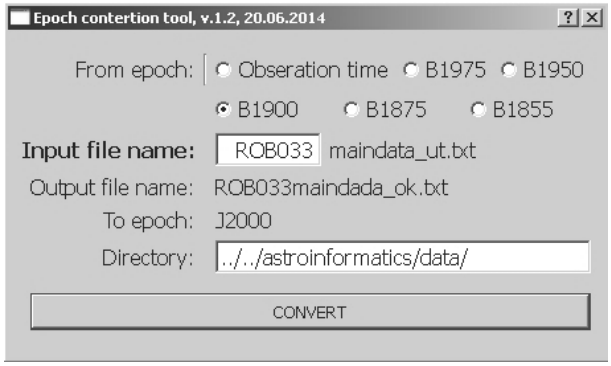

Figure 4: The user interface of `epochtool`.

Output files for `epochtool` are:
- config file: `epochtool.cfg`
- data file: `<dir><instrunent name>maindata_ok.txt`

The data for plates are contained in the file `<instrunent name>maindata_ut.txt` where the time is UT and the coordinates are in J2000. Now the metadata file is ready and it can be added as a new archve to WFPDB.

6. CONCLUSIONS

Two software tools for time and coordinates conversions suitable for needs of WFPDB are presented. For our example – for the plate No 8 from the archive with identifier ROB033 we have:

- original data in ST, B1900.0
  `ROB033 000008 232800+330000 19081019235400`
- converted data in UT, J2000.0
  `ROB033 000008 233256+333308 19081019214619`

The software is written in C++ using Qt – cross-platform application and UI development framework (`qt.digia.com`). The software tools are publicly available in GitHub and open source. The links are: `github.com/nkirov/timetool` and `github.com/nkirov/epochtool`.

References

Aoki, S., Kinoshita, H., Guinot, B., Kaplan, G. H., McCarthy, D. D., Seidelmann, P. K.: 1982, The New Definition of Universal Time, *Astron. Astrophysics*, **105**, 359-361.

Kalaglarsky, D., Tsvetkova, K., Tsvetkov, M.: 2014, WFPDB: Import of Catalogue of Wide-Field Plate Archives v7.0 and Recent Development, Proceedings of the IX Serbian-Bulgarian Astronomical Conference (IX SBAC), Sofia, Bulgaria, July 2-4, 2014, Editors: M. S. Dimitrijević and M. K. Tsvetkov, *Publ. Astron. Soc. "Rudjer Bošković"*, in this issue.

Kirov, N., Tsvetkov, M., Tsvetkova, K.: 2012a, Software Tools for Digitization of Astronomical Photographic Plates, *Serdica Journal of Computing*, **6**(1), 67-76.

Kirov, N., Tsvetkov, M., Tsvetkova, K.: 2012b, Technology for digitization of astronomical photographic plates, Proceedings of the 8th Annual International Conference on Computer Science and Education in Computer Science, Boston, USA, 5-8 July 2012, Publ. New Bulgarian Uiniversity, 109-114.

Tsvetkov, M., Tsvetkova, K., Kirov, N.: 2012, Technology for scanning of astronomical photographic plates, *Serdica Journal of Computing*, **6**(1), 77-88.

Proceedings of the IX Bulgarian-Serbian Astronomical Conference: Astroinformatics (IX BSACA) Sofia, Bulgaria, July 2-4, 2014,
Editors: M. K. Tsvetkov, M. S. Dimitrijević, O. Kounchev, D. Jevremović and K. Tsvetkova
Publ. Astron. Soc. "Rudjer Bošković" No 15, 2015, 49-54

ATOMIC DATA AND STARK BROADENING OF Nb III

ZORAN SIMIĆ, MILAN S. DIMITRIJEVIĆ and LUKA Č. POPOVIĆ

Astronomical Observatory, Volgina 7, 11060 Belgrade, Serbia
E-mail: zsimic@aob.rs, mdimitrijevic@aob.rs, lpopovic@aob.rs

Abstract. We have calculated the electron-impact widths for 15 doubly charged Nb ion lines by using the modified semiempirical method. Here, a part of preliminary results has been presented and discussed. Using the obtained results, we considered the influence of the electron-impact mechanism on line shapes in spectra of chemically peculiar stars and white dwarfs.

1. INTRODUCTION

Atomic data for Rare Earth Elements (REE) are needed in astrophysics for example in order to solve the problems like the relative abundance of r- and s-process elements in metal-poor stars with enhanced neutron-capture abundances, but also for analysis, modelling and research of stellar atmospheres. We will determine and provide here data on broadening of Nb III spectral lines by impacts with electrons, i.e, Stark broadening data. Such data are particularly of interest for white dwarfs, but also for A-type stars and other hot stars, especially the chemically peculiar ones, since Nb is present in stellar atmospheres. Consequently, using the the modified semiempirical approach - MSE (Dimitrijević and Konjević, 1980), tested several times for complex spectra (see e.g. Popović and Dimitrijević, 1996a,b, 1997), we have determined the electron-impac (Stark) full width at half maximum intensity (FWHM) of 15 Nb III spectral lines from $4d^2$ (^{3}F)5s - $4d^2$ (^{3}F)5p transitions.

The complete results and their analysis, as well as the details of calculations will be given in Simić et al. (2014) and here only the basic information and examples of obtained results are given.

The obtained results will be used also for the research of Stark broadening and its importance for plasma conditions in atmospheres of A type stars and DB white dwarfs.

2. THEORY

In order to determine the electron-impact line widths of Nb III lines, we have used the modified semiempirical (MSE) approach (Dimitrijević and Konjević, 1980), since for this ion, there is no a sufficient number of known atomic energy levels allowing more

sophysticated semiclassical perturbation (SCP) calculations (Sahal-Bréchot, 1969a,b). Namely, in comparison with SCP, a considerably smaller number of atomic data is needed for MSE method. Within the MSE approach the electron-impact (Stark) full width (FHWM) of an isolated line for an ionized emitter is given as:

$$w_{MSE} = N\frac{4\pi}{3c}\frac{\hbar^2}{m^2}\Big(\frac{2m}{\pi kT}\Big)^{1/2}\frac{\lambda^2}{\sqrt{3}}\cdot\{\sum_{\ell_i\pm1}\sum_{L_{i'}J_{i'}}\vec{\Re}^2_{\ell_i,\ell_i\pm1}\widetilde{g}(x_{\ell_i,\ell_i\pm1})+$$

$$\sum_{\ell_f\pm1}\sum_{L_{f'}J_{f'}}\vec{\Re}^2_{\ell_f,\ell_f\pm1}\widetilde{g}(x_{\ell_f,\ell_f\pm1})+\Big(\sum_{i'}\vec{\Re}^2_{ii'}\Big)_{\Delta n\neq0}g(x_{n_i,n_i+1})+$$

$$\Big(\sum_{f'}\vec{\Re}^2_{ff'}\Big)_{\Delta n\neq0}g(x_{n_f,n_f+1})\}. \tag{1}$$

In the above equations, the initial level is denoted with i, the final one with f, $\vec{\Re}^2_{\ell_k,\ell_{k'}}$, $k=i,f$ is the square of the matrix element, and

$$\Big(\sum_{k'}\vec{\Re}^2_{kk'}\Big)_{\Delta n\neq0}=(\frac{3n^*_k}{2Z})^2\frac{1}{9}(n^{*2}_k+3\ell^2_k+3\ell_k+11), \tag{2}$$

(in Coulomb approximation).

In Eq. (1)

$$x_{l_k,l_{k'}}=\frac{E}{\Delta E_{l_k,l_{k'}}},k=i,f$$

where $E=\frac{3}{2}kT$ is the electron kinetic energy and $\Delta E_{l_k,l_{k'}}=|E_{l_k}-E_{l_{k'}}|$ is the energy difference between levels l_k and l_k ±1 (k=i, f),

$$x_{n_k,n_k+1}\approx\frac{E}{\Delta E_{n_k,n_k+1}},$$

where for $\Delta n\neq0$ the energy difference between energy leves with n_k and n_k+1, $\Delta E_{n_k,n_k+1}$, is estimated as $\Delta E_{n_k,n_k+1}\approx 2Z^2E_H/n^{*3}_k$. $n^*_k=[E_HZ^2/(E_{ion}-E_k)]^{1/2}$ is the effective principal quantum number, Z is the residual ionic charge, for example Z=1 for neutral atoms and E_{ion} is the appropriate spectral series limit.

With N and T are denoted electron density and temperature, respectively, while $g(x)$ (Griem, 1968) and $\widetilde{g}(x)$ (Dimitrijević and Konjević, 1980) are Gaunt factors for width, for $\Delta n\neq0$ and $\Delta n=0$, respectively.

The needed atomic energy levels for Nb III, have been taken from Gayazov (1998). In the Nb III spectrum configuration mixing is present. If we want to include in calculations terms which are a mixture of different configurations, we can represent them as a mixture with K_1 part of the leading configuration and K_2 of the second one, where $K_1+K_2=1$, and then, we can use the expression:

$$\vec{\Re}^2_{j,j'},=K_1\vec{\Re}^2_{\alpha,\alpha'}+K_2\vec{\Re}^2_{\beta,\beta'}$$

where α,α' denote the energy level corresponding to the leading configuration, and its perturbing levels, and β,β' is the same for the second configuration (Dimitrijević and Popović, 1993).

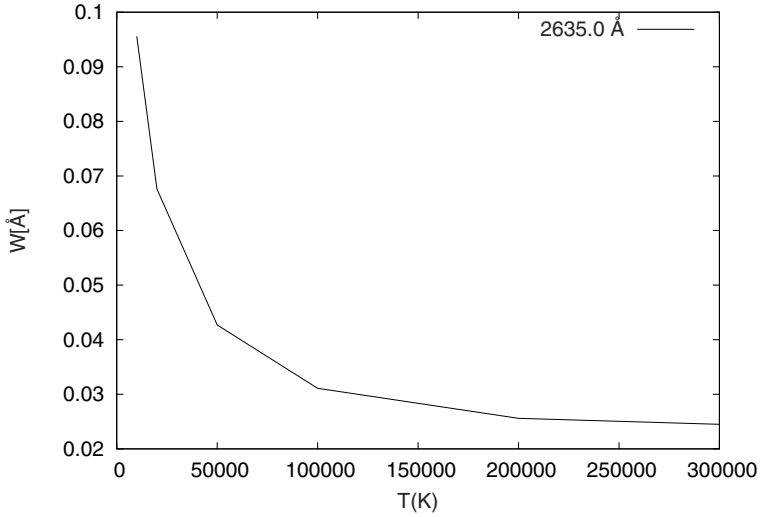

Figure 1: Stark widths for Nb III spectral line $4d^2$ (^{3}F) 5s $^4F_{5/2}$ - $4d^2$ (^{3}F) 5p $^4G^o_{5/2}$ (λ=2635.0 Å), as a function of temperature.

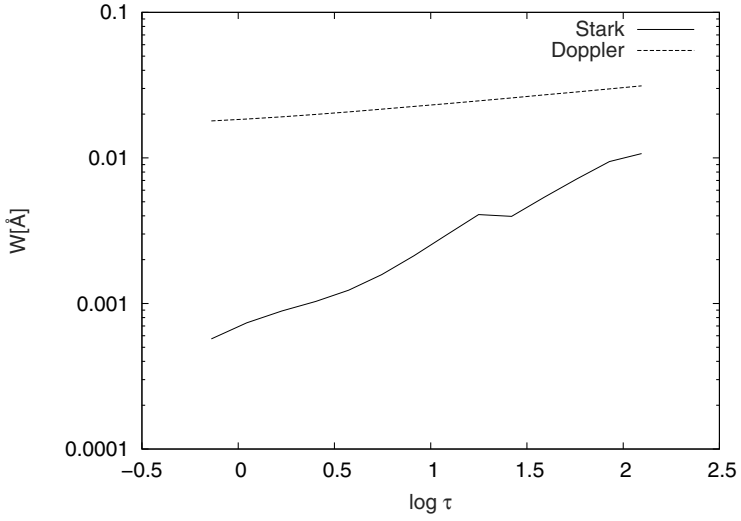

Figure 2: Thermal Doppler and Stark widths for Nb III spectral line $4d^2$ (^{3}F) 5s $^4F_{5/2}$ - $4d^2$ (^{3}F) 5p $^4G^o_{5/2}$ (λ=2635.0 Å), for an A type star atmosphere model with T_{eff} = 10,000 K and log g = 4.5, as a function of the Rosseland optical depth.

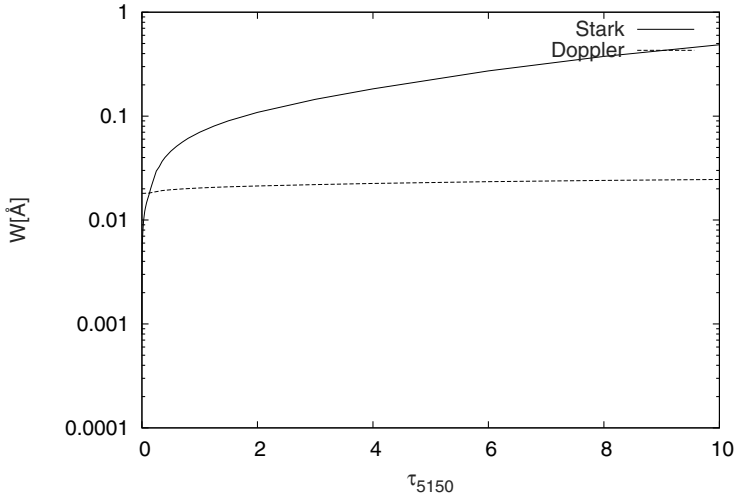

Figure 3: Thermal Doppler and Stark widths for Nb III spectral line $4d^2$ (^{3}F) 5s $^4F_{5/2}$ - $4d^2$ (^{3}F) 5p $^4G^o_{5/2}$ (λ=2635.0 Å) for a DB white dwarf atmosphere model with T_{eff} = 15,000 K and log g = 8, as a function of optical depth τ_{5150}.

3. RESULTS AND DISCUSSION

We have analyzed the Nb III spectrum and selected all spectral lines from 5s-5p transition array where the MSE method (Dimitrijević and Konjević, 1980) is applicable, and, if the configuration mixing is present, where the leading terms of initial and final energy level contribute at least 80 per cent to the corresponding term. With such constraints, 15 lines from $4d^2$ (^{3}F) 5s - $4d^2$ (^{3}G)5p have been choosen and their Stark widths determined.

In Table 1, is shown a sample of our results for Stark full width for six Nb III lines. The data are given for an electron density of 10^{17} cm^{-3} and temperatures from 10,000 up to 300,000 K. The complete results, more detailed description of calculations and the corredsponding discussion will be given in Simić et al. (2014). Here is shown in Fig. 1 the behavour of Stark width with temperature for 2635 Å line.

In Figs. 2 and 3, are compared Stark and Doppler widths for atmospheres of A-type stars and white dwarfs respectively, for Nb III line 5s $^4F_{5/2}$ - 5p $^4G^o_{5/2}$ (λ=2635.0 Å).

For A type stars, we used a model atmosphere with T_{eff} = 10,000 K and log g = 4.5 (Kuruczs, 1979), and for DB white dwarfs a model with T_{eff} = 15,000 K and log g = 8 (Wickramasinghe, 1972). We note that for the DB white dwarfs, the prechosen optical depth points at the standard wavelength λ_s=5150 Å(τ_{5150}) are used in (Wickramasinghe, 1972), as well as in our Fig. 3, because of this. This is different from the A type star model (Kuruczs, 1979), where the Rosseland optical depth scale (τ_{Ross}) has been taken, as well as for our Fig. 2. From Figs. 2 and 3 one can see that in the considered DB white dwarf atmosphere thermal Doppler broadening has much less importance in comparison with the Stark broadening mechanism than in A-type stellar atmospheres.

We can see that especially for white dwarf atmosphere analysis, the obtained Nb III Stark broadening data will be of interest.

Table 1: This table presents Nb III electron-impact broadening parameters (full width at half maximum W) for $4d^2$ (^{3}F) 5s - $4d^2$ (^{3}F) 5p transitions obtained by the modified semiempirical method (Dimitrijević and Konjević, 1980) for a perturber density of 10^{17} cm^{-3} and temperatures from 10,000 up to 300,000 K.This a sample of six lines and the complete results will be published in Simić et al. (2014).

Transition	T(K)	W(Å)	Transition	T(K)	W(Å)
	10000.	0.929-01		10000.	0.858-01
	20000.	0.657-01		20000.	0.607-01
$^4F_{3/2}$ - $^4G^o_{5/2}$	50000.	0.415-01	$^4F_{9/2}$ - $^4F^o_{7/2}$	50000.	0.384-01
2599.7 Å	100000.	0.302-01	2469.5 Å	100000.	0.278-01
	200000.	0.249-01		200000.	0.228-01
	300000.	0.238-01		300000.	0.219-01
	10000.	0.736-01		10000.	0.823-01
	20000.	0.521-01		20000.	0.582-01
$^4F_{3/2}$ - $^4D^o_{1/2}$	50000.	0.329-01	$^4F_{9/2}$ - $^4F^o_{9/2}$	50000.	0.368-01
2274.6 Å	100000.	0.238-01	2414.7 Å	100000.	0.267-01
	200000.	0.195-01		200000.	0.218-01
	300000.	0.188-01		300000.	0.210-01
	10000.	0.988-01		10000.	0.956-01
	20000.	0.698-01		20000.	0.676-01
$^4F_{9/2}$ - $^4G^o_{7/2}$	50000.	0.442-01	$^4F_{5/2}$ - $^4G^o_{5/2}$	50000.	0.427-01
2657.3 Å	100000.	0.321-01	2635.0 Å	100000.	0.311-01
	200000.	0.264-01		200000.	0.256-01
	300000.	0.253-01		300000.	0.245-01

References

Dimitrijević, M. S., Konjević, N.: 1980, Stark widths of doubly- and triply-ionized atom lines, *JQSRT*, **24**, 451.

Dimitrijević, M. S., Popović, L. Č.: 1993, Stark Broadening of B III Lines of Astrophysical Interest, *A&AS*, **101**, 583.

Gayazov, R. R., Ryabtsev, A. N., Churilov, S. S.: 1998, Spectrum of Doubly Ionized Niobium (Nb III), *Physica Scripta*, **57**, 45.

Griem, H. R.: 1968, Semiempirical Formulas for the Electron-Impact Widths and Shifts of Isolated Ion Lines in Plasmas *Phys. Rev.*, **165**, 258.

Kuruczs, R. L.: 1979, Model atmospheres for G, F, A, B and O stars. *ApJS*, **40**, 1.

Popović, L. Č., Dimitrijević, M. S.: 1996a, Stark broadening of heavy ion lines: As II, Br II, Sb II and I II, *Physica Scripta*, **53**, 325.

Popović, L. Č., Dimitrijević, M. S.: 1996b, Stark broadening of Xe II lines, *A&AS*, **116**, 359.

Popović, L. Č., Dimitrijević, M. S.: 1997, The modified semiempirical approach for complex spectra, In: The Physics of Ionized Gas, eds. Vujičić, B., Djurović, S., Purić, J., Institute of Physics, Novi Sad, p. 477.

Sahal-Bréchot, S.: 1969a, Impact theory of the broadening and shift of spectral lines due to electrons and ions in a plasma, *A&A*, **1**, 91.

Sahal-Bréchot, S.: 1969b, Impact theory of the broadening and shift of spectral lines due to electrons and ions in a plasma (continued), *A&A*, **2**, 322.
Wickramasinghe, D. T.: 1972, *Mem. R. Astron. Soc.*, **76**, 129.
Simić, Z., Dimitrijević, M. S., Popović, L. Č.: 2014, *Advances in Space Research*, **54**, 1231.

Proceedings of the IX Bulgarian-Serbian Astronomical Conference: Astroinformatics (IX BSACA) Sofia, Bulgaria, July 2-4, 2014,
Editors: M. K. Tsvetkov, M. S. Dimitrijević, O. Kounchev, D. Jevremović and K. Tsvetkova
Publ. Astron. Soc. "Rudjer Bošković" No 15, 2015, 55-62

WFPDB: UPGRADING THE CATALOGUE OF WIDE-FIELD PLATE ARCHIVES AND RECENT DEVELOPMENT

DAMYAN KALAGLARSKY, KATYA TSVETKOVA
and MILCHO TSVETKOV

Institute of Mathematics and Informatics, Bulgarian Academy of Sciences
Acad. Georgi Bonchev Str., Block 8, Sofia 1113, Bulgaria
E-mail: damyan@skyarchive.org, katya@skyarchive.org,
tsvetkov@skyarchive.org

Abstract. We consider the new upgrade of the Catalogue of Wide-Field Plate Archives (CWFPAs, http://wfpdb.org/catalogue.html) and its actual version 7.0 (February 2014). The increase of the number of wide-field plate archives and the new information, which has to be included, is the reason for adding new codes for plate archive observatory and storage, in order to constitute the unique archive identifier (see http://wfpdb.org/data/NotesCat7.txt). The work on importing the aforementioned catalogue is described, as well as some recent development and features of the Wide-Field Plate Database online access system (WFPDB, http://www.wfpdb.org/search).

1. INTRODUCTION

The Wide-Field Plate Database (WFPDB, http://www.wfpdb.org, Tsvetkov et al. 1997, Tsvetkov 2006) aims usage of the old astronomical photographic plates. The selection of worthy observations is dependent on the quantity and quality of the available plate metadata. In Fig. 1 the WFPDB meta-model is presented. This article focuses only on development regarding archive descriptions, which are represented in the upper part of the diagram. The first established standards of plate metadata were given in the ReadMe file (http://cdsarc.u-strasbg.fr/viz-bin/ Cat?VI/90) of the WFPDB (Tsvetkov et al. 1997) which can be found through the Catalog VI/90 Selection Page in the Strasbourg Astronomical Data Center. The WFPDB development has required improvement of the accepted formats as standards for plate/archive description, which one can find in Tsvetkova and Tsvetkov (2013). The increase in number of wide-field plate archives, as well as the new defining information about the archives and their storage put the condition for better archive description in order

to constitute the unique archive identifier. This topic is a subject of the present article.

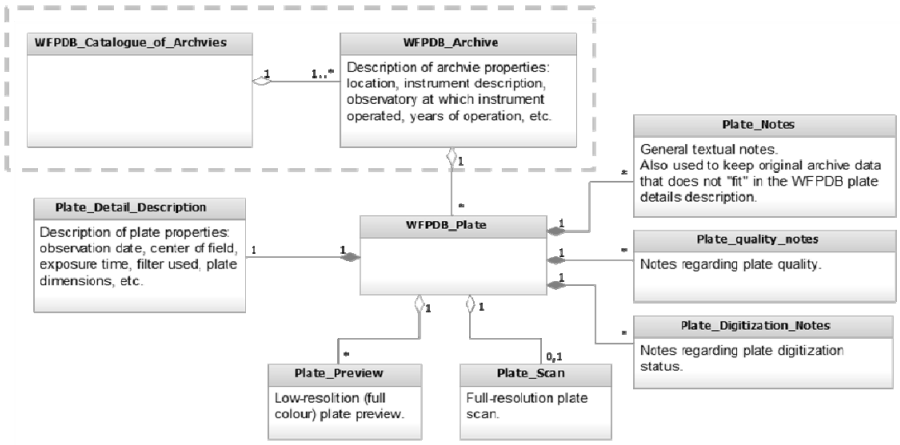

Figure 1: WFPDB meta-model.

2. CATALOGUE OF THE WIDE-FIELD PLATE ARCHIVES

Every wide-field plate archive is considered as a unit in the CWFPAs (Tsvetkova and Tsvetkov 2006, 2008) if the astronomical photographic plates, which this archive contains, are:

- obtained by a single instrument (telescope or camera) at a definite location (observatory);
- stored currently at a single location.

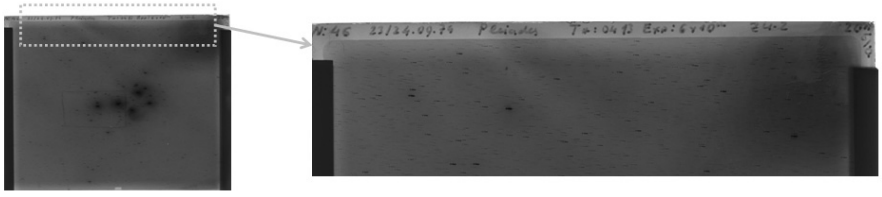

Figure 2: Written plate data on the plate emulsion**.**

From informatics point of view the CWFPAs represents description of archive attributes (archive meta-data) in a defined format/schema. In Fig. 2 a sample of plate with hand-written information on the emulsion is presented together with its enlarged part with the text. The text contains data about the plate number, date of observation, object observed, beginning of exposure, exposure duration, and used plate emulsion.

2.1. DATA IN CWFPAs

The upgraded version of the CWFPAs currently contains description of **495** archives from **163** observatories. The catalogue description and its upgraded version from February 2014 are available at http://www.wfpdb.org/catalogue.html. The observatory geographical location can be visualized by AstroWeb – an application which presents graphically the data of the CWFPAs version 2011. Fig. 3 presents the map of observatories with plate archives from AstroWeb (http://wfpdb.org:8000/chameleon/astroweb/astroweb.phtml). AstroWeb also ensures fast and easy access to the digitalized plate information (Kolev et al. 2012).

Figure 3: Distribution of the observatories possessing plate archives and presented by AstroWeb.

.

2.2. PLATE ARCHIVE ATTRIBUTES

Byte-by-byte description of the archive attributes in the WFPDB format can be found in Tsvetkova and Tsvetkov (2013). This description includes: WFPDB observatory identifier; Instrument aperture; Suffix to the instrument identifier; Location of the plate archive, town (site); Location of the plate archive, country; Observatory, name; Observatory, site; Observatory, country; Marsden's number; Time zone, sign; Time zone; Observatory longitude, sign; Observatory longitude, deg; Observatory longitude, arcmin; Observatory latitude, sign; Observatory latitude, deg; Observatory latitude, arcmin; Observatory altitude; Multiplicity of telescope cameras; Sign 'x'; Clear aperture of the telescope; Diameter of telescope mirror; Focal length of the telescope; Plate scale; Instrument type; Field angular

dimension; Year of beginning of telescope operation; Year of end of telescope operation; [F] Indication 'F' for 'film; Number of direct plates; Uncertainty of the number of plates; Plate catalog form (direct plates); Number of objective prism plates; Uncertainty of the number of plates; Plate catalog form (for objective prism plates); Code for archive quality; Astronomer in charge.

2.3. ARCHIVE ATTRIBUTES CHANGES

The WFPDB instrument identifier, which is equal of the archive identifier, is composed by <observatory name><instrument aperture><suffix>, e.g. HAR020A. The number of the wide-field plate archives continues (although slowly) to increase. The information concerning the plate receiving and storage becomes more and more accurate. This is the reason for adding new codes for plate archive observatory and storage. The additional **Archive Code** is needed when some of the plates of one archive are stored in different observatories. The additional **Site Code** is needed when the instrument operated at different locations. These additional codes complement the WFPDB archive identifier on the way to make it a unique archive identifier.

In order to support the WFPDB identifier change, described above, corresponding enhancements have been introduced to the CWFPAs. Version 7.0 of the CWFPAs contains two additional columns - sub-column "Archive Code" (coded as 1, 2, 3 ...) in column "Location of the Archive" and "Site Code" (coded as a, b, c...) in column "Observatory". The addition of these sub-columns is a result of the need of unique archive identifier in the cases:

- Certain plate archive was made with certain instrument in one observatory, but part of its plates is stored also in another observatory, e.g. the plate archives having Instrument identifier "HAR025" made with 10" Metcalf Triplet of the Harvard Observatory when the telescope was located in Harvard–Boyden Station, South Africa (Observatory code: 74) and now stored as separated archives in Cambridge (USA) are mentioned with archive code (1), Sonneberg (Germany) - mentioned with archive code (2), in Hamburg (Germany) - with archive code (3), and Bamberg (Germany) - with archive code (4);
- Certain plate archive was made with certain instrument moved during the certain time period in another observatory, e.g. the plate archives having Instrument identifier "HAR025" made with 10" Metcalf Triplet of the Harvard Observatory are coded with Site Code "a" in the case of telescope operation in Cambridge (USA), with Site Code "b" when the telescope was moved to Harvard–Boyden Station in Arequipa (Peru), with "c" - for the time period of operation of the instrument in Harvard-Chuquicamata Station (Chile), with "d" - in Harvard-San Jose Station (Peru), and with "e" - in Harvard–Boyden Station in Bloemfontein (South Africa);

- Certain plate archive made with one certain instrument and stored in one certain observatory/institution but by different astronomers in charge, e.g. the plate archives having Instrument identifier "NAV155" are coded as Side Code "1" for 1650 plates stored in Washington DC (USA) by C. Dahn, and Side Code "2" for 50000 plates taken in the period 1976-1996 for which astronomer in charge is B. Mason.

Below are listed the changes made in the CWFPAs version 7.0. The mentioned archives were “separate archives” only because the difference in the time interval of plate obtaining. Now in the last CWFPAs version the “separate archives” are unified:

1) V**ersion 7.0 of CWFPAs:** CAT033 archive.

Previous CWFPAs versions: There were three CAT033 sub-archives in dependence of the time interval:

Period	Number of Obtained Plates
1894-1932	1600
1956-1964	100
1985-1992	100

2) V**ersion 7.0 of CWFPAs:** HAR020A archive made when the telescope operated in Harvard Observatory (Observatory code: 802).

Previous CWFPAs versions: There were three HAR020A sub-archives in dependence of the time interval:

Period	Number of Obtained Plates	Plate Serial Number
1885-1888	3186	1-3186
1906-1907	16	37264-37280
1914-1915	86	45182-45268

3) V**ersion 7.0 of CWFPAs:** HAR020A archive made when the telescope had been moved to Harvard–Boyden Station in Arequipa (Peru) with Observatory Code: 800.

Previous CWFPAs versions: There were three HAR020A sub-archives in dependence of the time interval:

Period	Number of Obtained Plates	Plate Serial Number
1891-1905	31417	5846-37263
1907-1914	7900	37281-45181
1915-1923	8485	45269-53754

4) V**ersion 7.0 of CWFPAs:** HAR020A archive made when the telescope had been moved to Harvard–Boyden Station in Bloemfontein (South Africa) with Observatory Code: 74.

Previous CWFPAs versions: There were two sub-archives as follows:

Period	Number of Obtained Plates	Plate Serial Number
1930-1954	23109	53755-76864
1959-1959	314	

5) V**ersion 7.0 of CWFPAs:** HAR020B archive made when the telescope had operated in Harvard Observatory (Observatory code: 802).
Previous CWFPAs versions: There were two sub-archives:

Period	Number of Obtained Plates
1889-1934	52663
1934-1946	6423

(6) V**ersion 7.0 of CWFPAs:** HAR025 archive made when the telescope operated in Harvard–Boyden Station in Arequipa (Peru) with Observatory Code: 800.
Previous CWFPAs versions: There were two sub-archives:

Period	Number of Obtained Plates	Plate Serial Number
1918-1923	5705	2514-8219
1924-1924	558	8419-8973
1925-1925	929	8993-9922

(7) V**ersion 7.0 of CWFPAs:** HAR081 archive made when the telescope operated in Harvard–Boyden Station in Bloemfontein (South Africa) with Observatory Code: 74.
Previous CWFPAs versions: There were two sub-archives:

Period	Number of Obtained Plates
1950-1955	2100
1956-1963	3898

(8) V**ersion 7.0 of CWFPAs:** LOW012A archive made when the telescope operated in Lowell Observatory, Flagstaff (USA) with Observatory Code: 690.
Previous CWFPAs versions: There were two sub-archives:

Period	Number of Obtained Plates
1905-1907	100
1911-1916	1100

2.4 IMPORT OF CWFPAs TO THE ONLINE SYSTEM

The import of the new upgraded version of the CWFPAs is done via a custom tool to the Database Management System (DBMS). The representation of the CWFPAs in the online system comprises:

- The list of all WFPDB archives (http:/wfpdb.org/search/search.cgi?service=listofarchives&type=all).
- The list of archives with (at least some) plates already included in the WFPDB (http:/wfpdb.org/search/search.cgi?service=listofarchives&type=active).
- Details for an individual archive (available via links).

3. RECENT DEVELOPMENT IN THE WFPDB ONLINE ACCESS SYSTEM

The recent development in the WFPDB online access system includes the interoperability with AstroWeb – an application which presents graphically the data of the CWFPAs, as well as ensures fast and easy access to the digitalized plate information (Kolev et al. 2012). AstroWeb uses the same exact data-set as the WFPDB search system.

Another development is the Time Histogram of Observations (for the period of observations) for every plate archive included in the WFPDB (built on-the-fly) and presented in Fig. 4.

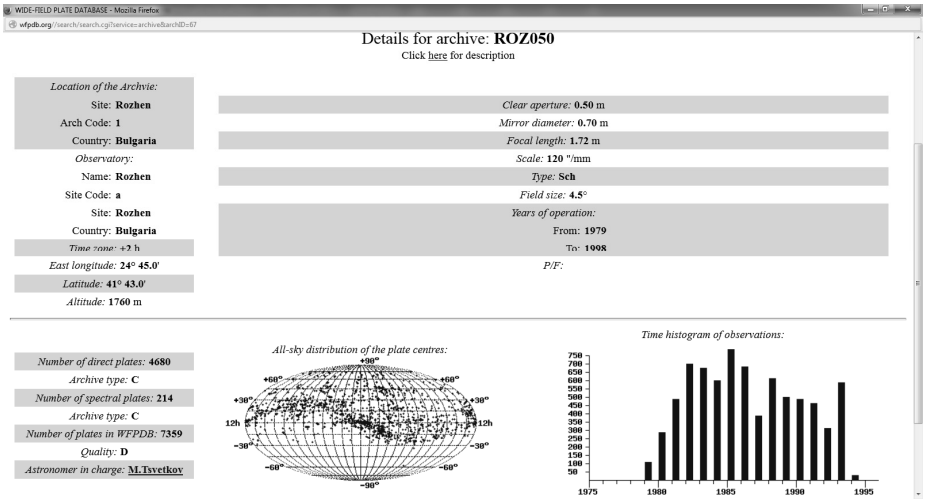

Figure 4: Details for archive ROZ050 including the time histogram of observations, which can be found in the WFPDB site.

References

Kolev, A., Tsvetkov, M., Dimov, D., Kalaglarsky, D.: 2012, *Serdica J. Computing* **6** , 89–100.

Tsvetkov, M. K., Stavrev, K. Y., Tsvetkova, K. P., Mutafov, A. S., Semkov, E. H.: 1997, Standardized description of the catalogue ReadMe (http://cdsarc.u-strasbg.fr/viz-bin/Cat?VI/90.

Tsvetkov, M.: 2006, Wide-Field Plate Database: a Decade of Development, In: Virtual Observatory: Plate Content Digitization, Archive Mining and Image Sequence, Processing, iAstro workshop, Sofia, Bulgaria, Eds. M. Tsvetkov, F. Murtagh, R. Molina.

Tsvetkova, K., Tsvetkov, M.: 2006, In: Virtual Observatory, Plate Content Digitization, Archive Mining, Image Sequence Processing, Eds. M. Tsvetkov, V. Golev, F. Murtagh, R. Molina, Heron Press Science Series, Sofia, 45-53.

Tsvetkova, K., Tsvetkov, M.: 2008, VizieR Online Data Catalog: VI/126.

Tsvetkova, K., Tsvetkov, M.: 2013, Proceedings of VIII BSAC, Leskovac, Serbia, May 8-12, 2012, Eds. M. S. Dimitrijević and M. K. Tsvetkov, *Publ. Astron. Soc. "Rudjer Bošković"*, **12**, 349-357.

Proceedings of the IX Bulgarian-Serbian Astronomical Conference: Astroinformatics (IX BSACA) Sofia, Bulgaria, July 2-4, 2014,
Editors: M. K. Tsvetkov, M. S. Dimitrijević, O. Kounchev, D. Jevremović and K. Tsvetkova
Publ. Astron. Soc. "Rudjer Bošković" No 15, 2015, 63-66

ON THE DETERMINATION OF ELECTRON DENSITY IN NON-THERMAL PLASMAS USING BALMER SERIES HYDROGEN LINES

CRISTINA YUBERO[1], MARIA CARMEN GARCÍA[1],
MILAN S. DIMITRIJEVIC[2], ANTONIO SOLA[1]
and ANTONIO GAMERO[1]

[1]*Grupo de Física de Plasmas: Diagnosis, Modelos y Aplicaciones (FQM-136)*
Edificio A. Einstein (C-2), Campus de Rabanales. Universidad de Córdoba,
14071 Córdoba, Spain
[2]*Astronomical Observatory, Volgina 7, 11060 Belgrade, Serbia.*
E-mail: f62yusec@uco.es, mdimitrijevic@aob.rs

Abstract. A new Optical Emission Spectroscopy method for measuring of electron density of non-thermal plasmas, based on the difference of Lorentzian broadenings of $H_{\square}$ and $H_{\square}$, two Balmer series hydrogen lines, valid for electron densities in 10^{14} cm^{-3} order and above, is presented. For the application of this method, there is no need to know the gas temperature and the van der Waals contribution to the Lorentzian part of the line profile. This method is applied for the determination of the electron density in an argon microwave-induced plasma at atmospheric pressure. The obtained results are compared with results obtained with other diagnostic methods.

1. INTRODUCTION

Non-thermal plasmas, also called non-equilibrium or cold plasmas, are characterized by a large difference in the electron temperature relative to those of the ions and neutrals (gas temperature). For the determination of electron density (n_e) of such plasmas, sustained at atmospheric pressure (Griem, 1974), optical emission spectroscopy methods, based on the analysis of Balmer series hydrogen lines, are commonly used if the gas temperature (T_g) is low But since in such conditions van der Waals broadening, depending on T_g becomes important, contributing non-negligibly to the Lorentzian part, in order to determine the electron density, we should know the value of T_g.

We present here a method to determine electron density of such plasmas without the necessity to know the value of T_g, with the help of Lorentzian widths

of H_α and H_β. This method can be applied for plasmas with electron density of the order of 10^{14} cm^{-3} or higher, namely above the so called fine structure limit (Konjević et al., 2012). It is tested here and compared with the results obtained using other diagnostic methods on an argon microwave plasma at atmospheric pressure.

2. THE METHOD

Different broadening mechanisms contribute to the shapes of spectral emitted by plasmas at pressures higher than 100 Torr. The line profiles generated by the *van der Waals broadening* (due to collisions of emitter with neutral atoms) have a Lorentzian form, while *Doppler broadening* (due to the thermal movement of emitters) and *instrumental broadening* (due to the device used for the spectrum registration) results in line shapes with a Gaussian form. *Stark broadening,* due to collisions of the emitter with charged particles, may deviate from a simple Lorentz form in the case of H_α and H_β lines, due to fine structure and quasistatic ion broadening, but for electron densities of the order of 10^{14} -10^{15} cm^{-3}, these line profiles can be approximated to a Lorentz function (Konjević et al., 2012). Consequently, their experimental profiles can be aproximated by a Voigt function resulting from the convolution of a Gaussian and Lorentzian profiles.

For an argon plasma at atmospheric pressure with a typical electron density n_e of $5\cdot10^{14}$ (cm^{-3}) and gas temperature T_g around 2000 K, the full width at half maximum (FWHM) of the Lorentzian profile for H_α and H_β lines, w_L, could be written as

$$w_L^{H_\alpha}(T_e, n_e, T_g, \mu_r) = w_S^{H_\alpha}(T_e, n_e, \mu_r) + w_W^{H_\alpha}(T_g) \tag{1}$$

$$w_L^{H_\beta}(T_e, n_e, T_g, \mu_r) = w_S^{H_\beta}(T_e, n_e, \mu_r) + w_W^{H_\beta}(T_g) \tag{2}$$

where w_s and w_w are FWHM due to Stark and van der Waals broadening, respectively, T_e is the plasma electron temperature and μ_r a fictitious reduced mass of the pair H-pertubed atom. In order to avoid the necessity to know the value of the gas temperature needed for the subtraction of the van the Waals contribution, if we want to obtain the electron density, we propose here an alternative method which uses the fact that H_α and H_β lines have very similar values of van der Waals widths. We demonstrated in Yubero et al. (2014) that for a typical gas temperature of 1000 K, the difference between van der Waals widths of these two lines is less than 5 %. Consequently, we can assume that the difference between the H_β and H_α Lorentzian widths not depends on the van der Waals broadening, and write:

$$\begin{aligned} w_L^{H_\beta}(T_e, n_e, T_g, \boldsymbol{\mu}_r) - w_L^{H_\alpha}(T_e, n_e, T_g, \boldsymbol{\mu}_r) &= w_S^{H_\beta}(T_e, n_e, \boldsymbol{\mu}_r) - w_S^{H_\alpha}(T_e, n_e, \boldsymbol{\mu}_r) + R(T_g) \\ &\approx f(T_e, n_e, \boldsymbol{\mu}_r) \end{aligned} \tag{3}$$

Gigosos et al. (2003) proposed the Computer Simulatiom (CS) method for the calculation of Stark broadened profiles and performed the corresponding

calculations for H_α and H_β lines, which enabled to us to obtain the corresponding value of $\left(w_S^{H_\beta} - w_S^{H_\alpha}\right)$ for several values of electron density, electron temperature and fictitious reduced mass. In Yubero et al. (2014), is found that the dependence of $\left(w_S^{H_\beta} - w_S^{H_\alpha}\right)$ on T_e and fictitious reduced mass for electron densities in the range between 10^{14} and 10^{16} cm^{-3} is weak, so that for this electron density range Eq. 3 becomes:

$$w_L^{H_\beta}(T_e, n_e, T_g, \mu_r) - w_L^{H_\alpha}(T_e, n_e, T_g, \mu_r) \approx f(n_e) \tag{4}$$

Moreover, the theoretical relationship between $\left(w_L^{H_\beta} - w_L^{H_\alpha}\right)$ and n_e can be approximated with a simple expression

$$n_e(\cdot 10^{14}\,\mathrm{cm}^{-3}) \approx 185\left(w_L^{H_\beta} - w_L^{H\alpha}\right)^{3/2} \tag{5}$$

$$n_e(\cdot 10^{14}\,\mathrm{cm}^{-3}) \approx 168\left(w_L^{H_\beta} - w_L^{H\alpha}\right)^{3/2} \tag{6}$$

where w are in nm.

Equations (5) and (6) are valid for an electron temperature range between 5000-15000 K, and give possibility for an easy and quick calculatio of the electron density, without necessity to know the gas temperature.

3. ELECTRON DENSITY OF A MICROWAVE PLASMA AT ATMOSPHERIC PRESSURE

In order to test this method we used it for the determination of electron density in an argon microwave (2.45 GHz) induced plasma at atmospheric pressure generated inside a quartz tube, using a *surfaguide* device (Moisan et al., 1998). The experimental set-up and experiment is described in detail in Yubero et al. (2014).

The electron density was determined in two ways, using the proposed method (Eq. 5) and the results for Stark broadening of H_α and H_β obtained by Gigosos et al. (2003). The values of n_e obtained with both methods are quite similar. All details are given in Yubero et al. (2014).

In order to test the adequacy of the used deconvolution procedure, the Lorentzian widths of H_α and H_β line profiles were also determined by fixing the Gaussian part (for a value of T_g = 1380 ± 120 K, typical in the plasmas studied) of the Voigt function as suggested in Konjevic et al. (2012), and significant differences were not found.

In Yubero et al. (2014) is shown that present results are in good agreement with those obtained using CS model for H_α and H_β lines (Garcia et al., 2004), extracting from the total Lorentzian contribution the van der Waals contribution (for T_g = 1380 ± 120 K).

Aknowledgements

The authors wish to acknowledge to *Física de Plasmas: Diagnosis, Modelos y Aplicaciones (FQM 136)* research group for their funding and technical support, as well as to the support through projects 176002 and III44002 of Ministry of Education and Science of Republic of Serbia.

References

García, M. C., Yubero, C., Calzada, M. D., Martínez-Jiménez, M. P.: 2004, Spectroscopic characterization of two different microwave (2.45 GHz) induced argon plasmas at atmospheric pressure, *Appl. Spectrosc.,* **59,** 519-528.

Gigosos, M. A., González, M. A., Cardeñoso, V.: 2003, Computer simulated Balmer-alpha, -beta and –gamma Stark line profiles for non-equilibrium plasmas diagnostics, *Spectrochim. Acta* Part B, **58,** 1489-1504.

Griem, H. R.: 1974, *Spectral Line Broadening by Plasmas*, Academia Press, New York.

Konjević, N., Ivković, M., Sakan, N.: 2012, Hydrogen Balmer lines for low electron number density plasma diagnostics, *Spectrochim. Acta* B, **76,** 16-26.

Moisan, M., Etermandi, E., Rostaing, J. C. : 1998, Fr. Pat. Specif. 2, 762.

Yubero, C., Garcia, M.C., Dimitrijević, M. S., Sola, A., Gamero, A.: 2015, Measuring the electron density in non-thermal plasmas from the difference of Lorentzian widths of two Balmer series hydrogen lines, *Spectrochim. Acta B*, **107**, 164-169.

Proceedings of the IX Bulgarian-Serbian Astronomical Conference: Astroinformatics (IX BSACA) Sofia, Bulgaria, July 2-4, 2014,
Editors: M. K. Tsvetkov, M. S. Dimitrijević, O. Kounchev, D. Jevremović and K. Tsvetkova
Publ. Astron. Soc. "Rudjer Bošković" No 15, 2015, 67-74

VARIABLE STARS NEAR β CAS DISCOVERED ON SCANNED PHOTOGRAPHIC PLATES AT THE STERNBERG ASTRONOMICAL INSTITUTE

ALEXANDRA M. ZUBAREVA[1, 2], DARIA M. KOLESNIKOVA[1],
KIRILL V. SOKOLOVSKY[3,1], SERGEI V. ANTIPIN[2,1]
and NIKOLAI N. SAMUS[1,2]

[1]*Institute of Astronomy of Russian Academy of Sciences, Moscow, Russia*
[2]*Sternberg Astronomical institute of Lomonosov Moscow State University, Moscow, Russia*
[3]*Astro Space Center of Lebedev Physical Institute, Moscow, Russia*
E-mail: zubareva.alex@gmail.com

Abstract. We present results of searching for variable stars in the field of β Cassiopeiae on digitized photographic plates of the Sternberg Astronomical Institute's plate stacks. The negative astronomical plates of 30 x 30 cm size (that corresponds to 10° x 10° field of view) were obtained with the 40 cm astrograph in 1940–90s. We have discovered and investigated 1011 new variable stars and found 263 previously known variable stars. New variables include 682 eclipsing binaries of different subtypes, 5 BY Draconis stars, 5 classical Cepheids and 4 Cepheids of the Galaxy's spherical component, 3 δ Scuti stars, 15 high-amplitude δ Scuti stars (HADS), 33 RR Lyrae stars, 1 RS CVn star, 44 semi-regular red variables, 207 irregular variables (65 yellow or white stars and 142 red stars of LB type), and 12 variable stars that need confirmation and more careful study with CCD. Some of discovered stars initially were marked as suspected, for now more than 20 of them have accurate elements derived from our CCD-photometry. We considered only about 400 plates of interest from the 22500 pieces collection. So the amount of the variables "hidden" in the Sternberg Astronomical Institute's plate stacks is enormous.

1. INTRODUCTION

Astronomers in Moscow started regular photographic observations of the sky for variable-star studies in 1895. Several different telescopes were used to take direct sky plates for astrometry and for astrophysics. The Moscow plate archive now contains more than 60 000 direct photographs and objective-prism plates taken in Moscow and at other sites in Russia. The most important part of the Moscow plate collection are direct sky photographs acquired in 1948–1996 with a

40-cm astrograph. This instrument was ordered by Prof. Cuno Hoffmeister for Sonneberg Observatory (Germany) and first installed there in 1938. 1658 plates from this telescope, taken in 1938–1945, are kept in Sonneberg. In 1945, the telescope was taken to the Soviet Union as a part of the World War II reparations. It was initially installed in Simeiz (Crimea), then brought to Kuchino near Moscow, and in 1958 became the first instrument of the Crimean Laboratory of the Sternberg Institute in Nauchny, Crimea. The total number of plates taken with the 40-cm astrograph after 1948 is about 22 500. A single attempt of direct comparison between Sonneberg and Crimean plates of the 40-cm astrograph at a blink comparator was undertaken in 1980s (Samus, 1983).

The field of view of the 40-cm astrograph is $10^{\circ}\times10^{\circ}$, on 30×30 cm plates (the focal length is 1600 mm). The typical exposure time for the variable-star fields was 45 minutes. The limiting magnitude of good-quality plates is about 17.5 in B-band. The instrument was mainly used for variable-star studies, including search for new variables. For some fields, rich series of plates exist (about 500 plates). For variable stars that can be found in several fields, sometimes as many as 1000 photographic plates are available. Plates are kept in good conditions, most plates, initially of excellent quality, are still perfect.

Guaranteed conservation of the vast amounts of information contained in the plate collection and its use by means of modern methods of image processing require digitization of plate archives. This work started in Moscow, in 2004, after the purchase of two Creo EverSmart Supreme II scanners.

Most plates from the 40-cm astrograph were taken for variable-star studies. We continue this work using digital images obtained in the process of scanning the Moscow collection plates. From 2006 to 2014 we discovered 595 new variable objects (mostly variable stars, but also extragalactic objects) on scans of some selected star fields (Sokolovsky 2006, Manannikov et al. 2006, Kolesnikova et al. 2007a,b, 2008, 2010, Sokolovsky et al. 2014). We introduced preliminary designations for variable stars discovered in this program with the prefix MDV (Moscow Digital Variable).

2. SCANNING AND REDUCTION OF IMAGES

B Cassiopeiae field ($00^{h}09^{m}.2$, $\delta = +59°09'$, J2000) was photographed with the 40-cm astrograph in 1964–1994, a total of 391 plates were acquired. The description of the scanning and reduction techniques used is given by Kolesnikova et al. (2008, 2010). We present a summary for our techniques. The software controlling the scanner provides a digital RGB image in TIFF format. We converted the resulting images to the FITS format, used in astronomical applications, using a code we specially developed, tiff2fits (ftp://scan.sai.msu.ru/pub/software/tiff2fits/). In this process, we kept only the green channel of the original TIFF image, chosen empirically.

Photometric properties of a plate vary considerably across the field of view due to aberrations in the astrograph, air mass differences, and possible inhomogeneity

of the emulsion layer and the chemical processes used when developing the plate. To avoid difficulties with the photometric calibration and facilitate the astrometric reduction, we subdivided the digital images into a number of subfields, each about 0.5 square degrees in size. These subfields were reduced completely independently, and the results were merged at the last stage.

Some of the plates were taken with offsets relative to the central star of β Cas, and the shifts between plates can reach 1◦ or more. To ensure that the subfields of different plates of the series correspond to the same regions on the sky, these subfields were not introduced relative to the plate center, but instead relative to the pixel coordinates of a reference star, chosen so that it was present on all plates of the series.

We reduced each set of photographs, divided into subfields, using the VaST (http://scan.sai.msu.ru/vast) software package that we developed earlier (Sokolovsky and Lebedev 2005), which incorporates the SExtractor package (Bertin and Arnouts 1996). We use SExtractor to detect stars in our images, and determine their pixel coordinates and instrumental magnitudes. A star's brightness was measured using a round aperture, whose size was selected according to the apparent sizes of the stars in the image. VaST launches SExtractor for the reduction of each digitized image, cross-identifies stars measured on different plates, and enables absolute calibrations of photometric and astrometric images.

To identify the stars found in an image with stars in the reference image, the VaST code derives a linear transformation between the systems of pixel coordinates for the two images.

We then related the magnitude scale for the identified image to the instrumental scale of the reference image. For more information see Sokolovsky et al. (2014).

In the last reduction stage, we refered the pixel coordinates of the reference-image stars to the equatorial stellar coordinates in the USNO-B1.0 catalog (Monet et al. 2003) and performed an absolute calibration of the magnitude scale. We used the Astrometry.net (http://astrometry.net/) software (Hogg et al. 2008, Lang et al. 2010) for the astrometric reduction of our reference images.

The resulting light curves are characterized by an rms error of 0.05–0.15 mag for stars in the 13.5–16.5 mag range.

3. SEARCH FOR VARIABLE STARS

Our semi-automated variable-star search techniques are described in detail in Kolesnikova et al. (2008). The stages of the search include: (i) deriving a relationship between a star's brightness and the rms deviation between its instrumental magnitude and the magnitude on the reference plate, (ii) identifying objects with possible brightness variations, and (iii) verifying the significance of periodic or aperiodic variations for the suspected objects. The last stage was a final selection of variable stars in a non-automatic mode, which consisted of a visual inspection of the light curves.

We verified that the detected variable stars were new variables using the database of the General Catalogue of Variable Stars (Samus et al. 2007-2014), the VSX International Variable Star Index (http://www.aavso.org/vsx/) maintained by the American Association of Variable Star Observers, and the SIMBAD database (http://simbad.u-strasbg.fr/simbad/).

4. RESULTS

After revision of our list of discoveries in summer of 2014 we have 1011 new variable stars and 263 previously known variables mentioned in the General Catalog of Variable Star (GCVS) or other lists. New variables include 682 eclipsing binaries (345 Algol type binaries, 124 β Lyrae type stars and 213 W Ursa Majoris type stars), 5 BY Draconis stars, 5 classical Cepheids and 4 Cepheids of the Galaxy's spherical component, 3 δ Scuti stars, 15 high-amplitude δ Scuti stars (HADS), 33 RR Lyrae stars, 1 RS CVn star, 44 semi-regular red variables, 207 irregular variables (65 yellow or white stars and 142 red stars of LB type), and 12 variable stars that need confirmation and more careful study with CCD. The results are preliminary. Some of discovered stars initially were marked as suspected, for now more than 20 of them have accurate elements derived from our CCD-photometry.

Some examples of phased light curves are presented in Figures 1, 2 and 3.

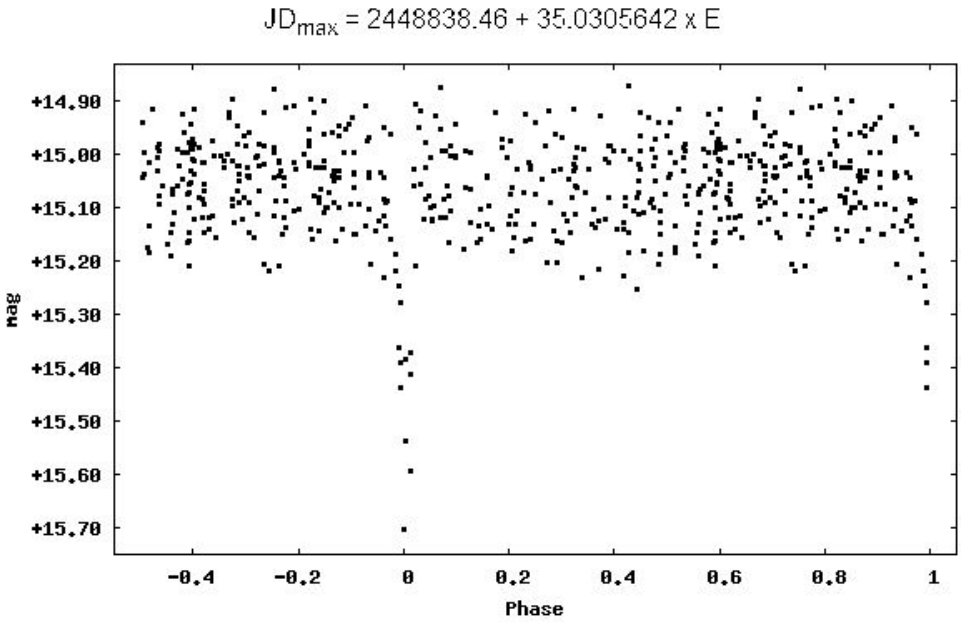

Figure 1: USNO-B1.0 1473-0013593, eclipsing binary of Algol type.

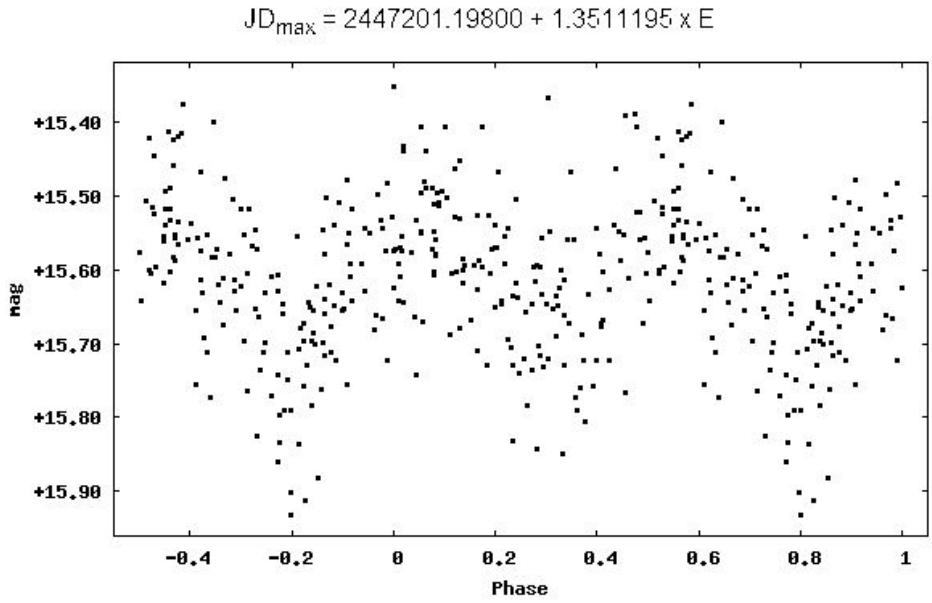

Figure 2: USNO-B1.0 1493-0392901, eclipsing binary of β Lyrae type.

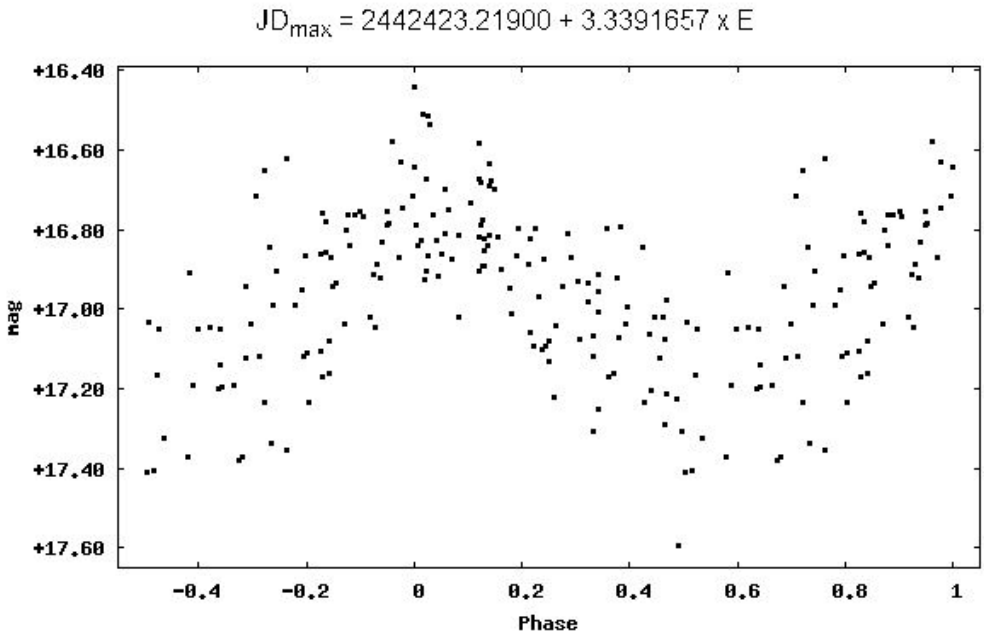

Figure 3: USNO-B1.0 1507-0011340, δ Cephei type star.

The field of β Cas has 100 square degrees which is less than 0.25 per cent of the overall sky area. We discovered 15 HADS variables here. Additionally we have two δ Scuti type stars with amplitudes of $0^m.3$ and more from GCVS. Simple extrapolation gives an expected number of HADS for all sky of more than 5000. Still, before our discoveries made with Moscow plate archive the total number of δ Scuti stars with amplitudes no less than $0^m.2$ in the GCVS was 121 only.

In the course of our study we found a bimodal HADS USNO-B1.0 1491-0020709. The star shows periods of P0 = $0^d.185785$ and P1=$0^d.244527$. The case itself is not outstanding for stars of this type in time of high time resolution CCD-photometry. But the discovery is made using photographic images with exposures of 45 minutes. Periodograms and light curves are given in Figures 4 and 5.

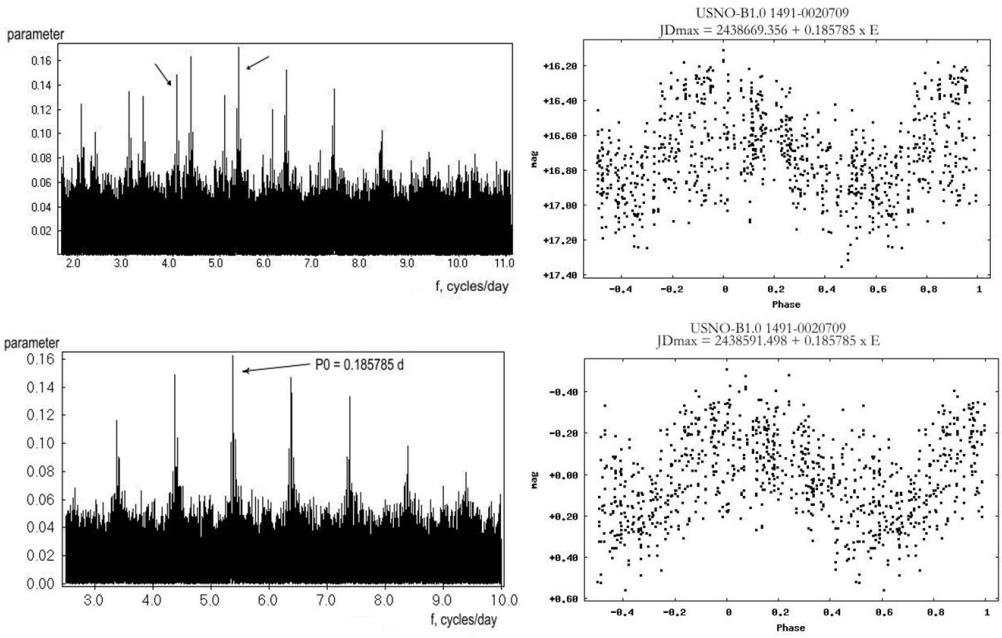

Figure 4: Periodograms (left) and phased curves (right) for USNO-B1.0 1491-0020709. The higher panel shows data for P0 = $0^d.185785$. The lower panel shows data after subtraction of P1 = $0^d.244527$.

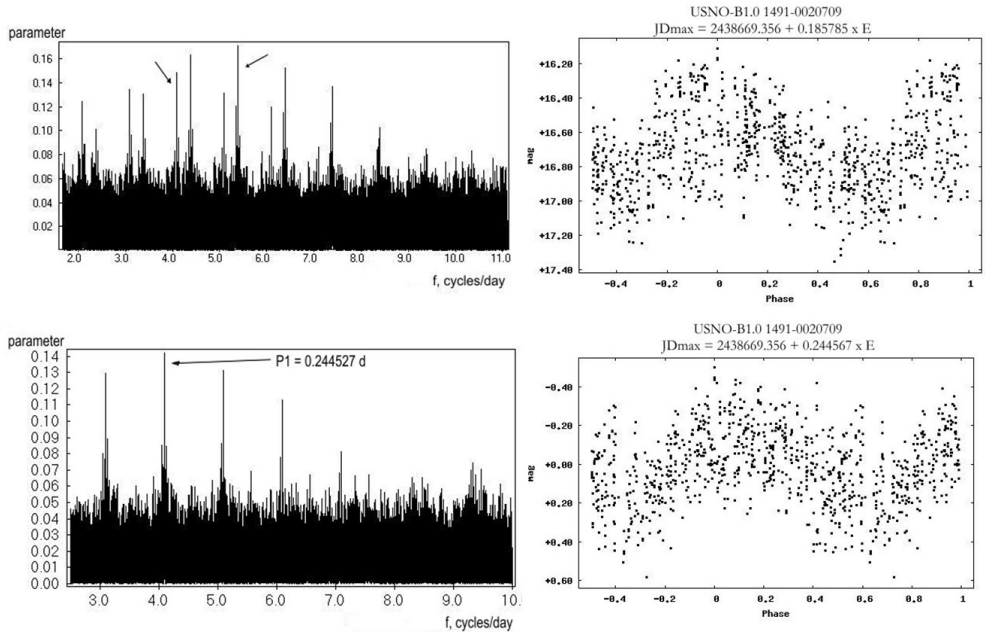

Figure 5: Periodograms (left) and phased curves (right) for USNO-B1.0 1491-0020709. The higher panel shows data for P0 = 0^d.185785. The lower panel shows data after subtraction of P0 = 0^d.185785.

5. CONCLUSIONS AND PERSPECTIVES

We have developed semi-automated techniques to digitize plates of the Moscow collection, search for variable stars on digital images and perform photographic photometry. We work to improve them and to fully automatize the process. The Sternberg Astronomical Institute's plate stacks have a lot of star fields, so we are going to continue collecting and investigating digital images of the photographic plates.

This study resulted in the discovery and investigation of 1011 new variable stars of different types. After a while we plan to publish a new part of the MDV list for β Cas field.

Acknowledgements

The authors are grateful to D. Nasonov, S. Nazarov, and especially to A. Lebedev for their contribution to the development of the VaST software package. This research has made use of the SIMBAD database, operated at CDS, Strasbourg, France, the International Variable Star Index VSX (American Association of Variable-Star Observers, USA), and the Astrometry.net Internet facility. This work was partially supported by the Russian Foundation for Basic Research (project no. 13-02-00664).

References

Bertin, E., Arnouts, S.: 1996, *Astron. Astrophys. Suppl. Ser.* **117**, 393.
Hogg, D. W., et al.: 2008, *ASP Conf. Ser.* **394**, 27.
Kolesnikova, D. M., et al.: 2007a, *Perem. Zvezdy Suppl.* **7**, 3.
Kolesnikova, D. M., et al.: 2007b, *Perem. Zvezdy Suppl*. **7**, 24.
Kolesnikova, D. M., et al.: 2008, *Acta Astron.* **58**, 279.
Kolesnikova, D. M., et al.: 2010, *Astron. Rep*. **54**, 1000.
Lang, D., et al, 2010, *Astron. J.* **139**, 1782.
Manannikov, A. L., et al.: 2006, *Perem. Zvezdy Suppl.* **6**, 34.
Monet, D. G., et al.: 2003, *Astron. J.* **125**, 984.
Samus, N. N.: 1983, *Mitt. Verand. Sterne* **9**, 87.
Samus, N. N., et al.: 2007-2014, General Catalogue of Variable Stars, B/gcvs (Centre de Donnees Astronomiques de Strasbourg.
Sokolovsky, K. V.: 2006, *Perem. Zvezdy. Suppl.* **6**, 18.
Sokolovsky, K. V. et al.: 2014, *Astron. Rep.* **58**, No. 5, 319.
Sokolovsky, K. V., Lebedev, A. A.: 2005, in Proceedings of the 12th Young Scientists' Conference on Astronomy and Space Physics, Kyiv, Ukraine, April 19–23, Ed. by A. Simon and A. Golovin, Univ. Press, Kyiv, p. 79.

Proceedings of the IX Bulgarian-Serbian Astronomical Conference: Astroinformatics (IX BSACA) Sofia, Bulgaria, July 2-4, 2014,
Editors: M. K. Tsvetkov, M. S. Dimitrijević, O. Kounchev, D. Jevremović and K. Tsvetkova
Publ. Astron. Soc. "Rudjer Bošković" No 15, 2015, 75-82

BROAD SPECTRAL LINE AND CONTINUUM VARIABILITIES IN QSO SPECTRA INDUCED BY MICROLENSING:METHODS OF COMPUTATION

SAŠA SIMIĆ[1] and LUKA Č. POPOVIĆ[2]

[1]*Faculty of Science, Department of Physics, University of Kragujevac*
E-mail: ssimic@kg.ac.rs
[2]*Astronomical Observatory Belgrade, Serbia*
E-mail: lpopovic@aob.rs

Abstract. We present methods and algorithms for computation of magnification maps and images of source in the case of microlensed QSO. The source (QSO) is assumed to be complex, that emits the continuum from an accretion disk and H_β broad line from the Broad Line Region (BLR). Accretion disk is assumed to be a standard, geometrically thin, optically thick, while BLR region is uniformly distributed around the disk with much larger diameter. Here we present the computational methodology for calculation of variability of H_β line during the crossing. This computation can be easily applied to the more complicated objects, like AGNs with binary black hole system. We present the results of spectral line variability during the full rotational period for binary system.

1. INTRODUCTION

Deflection of light while passing close to the massive astronomical objects is old and well established problem. In short, photons of light while crossing a certain distance follow the geodesics of space-time which are curved in the close vicinity of a massive object. The amount of deviation from straight line directly depends on the distribution of the interacting mass. This view has been considered exactly by Einstein in his work on General theory of Relativity, producing the rather simple solution, for deflection angle in case of a point like source and lens:

$$\alpha = \frac{4GM}{c^2 R}, \tag{1}$$

where R is the impact parameter, M mass of the lens and G and c are gravitational and light speed constant. In a simple case scenario, of point source and one perfectly spherical deflector (see Fig. 1), it is easy to compute paths of the light rays and deflection angle, by using the Eq. 1.

However, in other more realistic cases which for example include lens containing a number of randomly distributed deflector objects (usually the stars) or extended

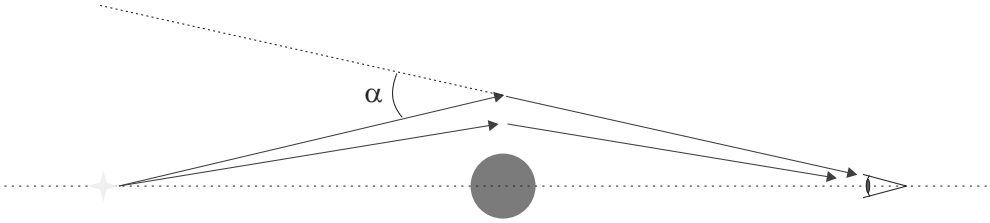

Figure 1: The point-like source presented at left side (yellow colored star) and deflector as a point-like massive object in the middle (red circle). Observer detect the deflected radiation.

instead of the point like source, those computations are rather complicated and more computer time consuming. In those cases one must implement suitable algorithms for computing the trajectories of light rays from all parts of the source, which are deflected by the complex lens structure, toward the observer.

In the case of a point like source those algorithms are discussed in details by Paczynski (1986), Kayser, et al. (1986), Schneider and Weiss (1986, 1987), and for the case of extended source by Treyer and Wambsganss (2004). They have used ray shooting technique to determine the path of light rays and in case of Treyer and Wambsganss (2004), convolution for computing the light curves of magnified sources. On the basis of their work we have applied these methods on the complex extended source with specific Spectral Energy Distribution (SED) and appropriate spectral lines. We have also avoid to use convolution for computing the light curves of source, but instead sum all contribution of particular pixels in the total emission output.

In the Chapters §2 and §3 we presented the computational model used together with our modifications, and in the Chapter §4 we present the results.

2. METHODS OF COMPUTATION

To calculate the microlensing of a distante source one needs to follow the rays of light from each part of the source toward the lens and observer plane. This is called ray-tracing method and it is highly computational demanding, since all possible paths of light rays have to be followed. On the other hand if we assume that observer can see only rays which fall in it's point, than the overall number of followed light-rays can be significantly reduced. This as a result substantially reduce the needed computational time. Therefore, we follow the rays of light in opposite direction, from the observer point toward the lens plane and further on the source plane (see Fig. 2). This is called the ray shooting method.

As one can see in Fig. 2 light rays are directed from the observer point uniformly toward the lens plane, where a certain number of point-like Solar mass deflectors are uniformly distributed. They produce a cumulative effect on the passing rays which can be accounted by computing the overall gravitational potential and consequently lensing potential. Knowing the lensing potential it is easy to compute deflection angle for particular light ray and further more a point in the source plane where this light ray will fall. For a great number of light rays shooted from the observer and deflected

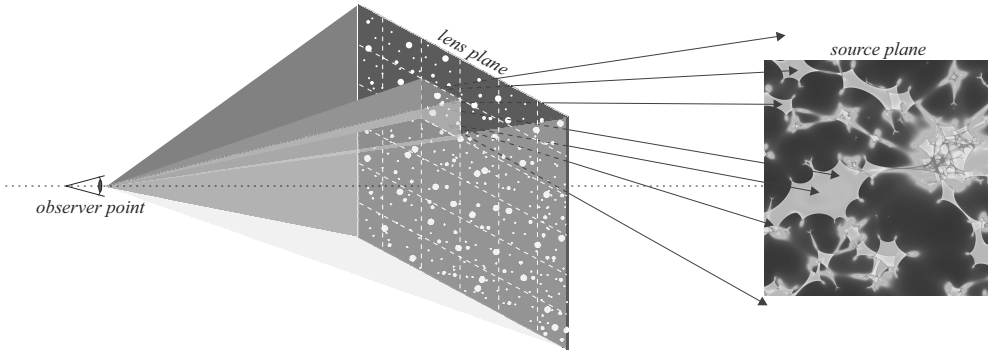

Figure 2: Scheme of ray shooting mehtod (see text).

by lens a collection in the source plane will be created, so called the magnification map. It presents a distribution of light rays deflected by lens, over the pixel map created in the source plane, which can be seen by the observer (see Fig. 2). When a light ray falls on the particular pixel in the source plane then it is accounted by summing with rest of the rays fallen on the same pixel. For better presentation we use rainbow color coding system, which means that for those pixels who collect more light rays, the lighter color is used, usually yellow or red, but if the number of fallen rays is lower, than color coding is green or blue.

Magnification map alone, does not present a source of light and can not be seen by an observer. Rather it gives a distribution of the amount of magnification each pixel can impose on fictional source itself. If we place the extend source on the same grid where magnification map is spread, then their superposition is calculated by multiplying the magnification of particular pixel with the intensity generated by the source at the position of pixel. At the end the result is achieved when we trace back magnified light rays toward the grid in the lens plane in order to create lensed image of the source.

Practical work with this method regards, first to divide the lens plane into segments (as shown on the Figure 1), then to compute the gravitational and lensing potential for each cell. In the source plane we construct a matrix of pixels which collect the light rays deflected by lens. Depending on the source dimension, usually we choose that source matrix has dimension of 2000 by 2000 pixels, dimension of the lens plane is about 10 times higher, and number of lens segments is mostly 256 or 512 pixels. Also, for constructing the source image in the lens plane we setup a matrix with same dimensions as for the source.

3. PARAMETERS OF SOURCE AND LENS

To apply described method we consider the complex source and lens. Here we will consider as a source an Active Galactic Nucleus (AGN) that has wavelength dependent structure. This practically means that different parts have emission in different spectral bands, i.e. a wavelength dependent emission of different regions are present in AGNs (see e.g. Popović et al. 2012). It is widely accepted that the majority

of radiation is coming from the accelerated material spiraling down toward the black hole in a form of an accretion disc. The radiation from the disc is mostly thermalized from outer regions R_{out} to the center, with slight exception at inner radius, i.e. very close to the black hole, where Compton upscattering due to the high mass accretion could have a significant role (see Done et al. 2012, Popović and Simić, 2014, Simić and Popović, 2014a). The disc inclination can be changed, but in the most simulations we assumed a face-on disc orientation.

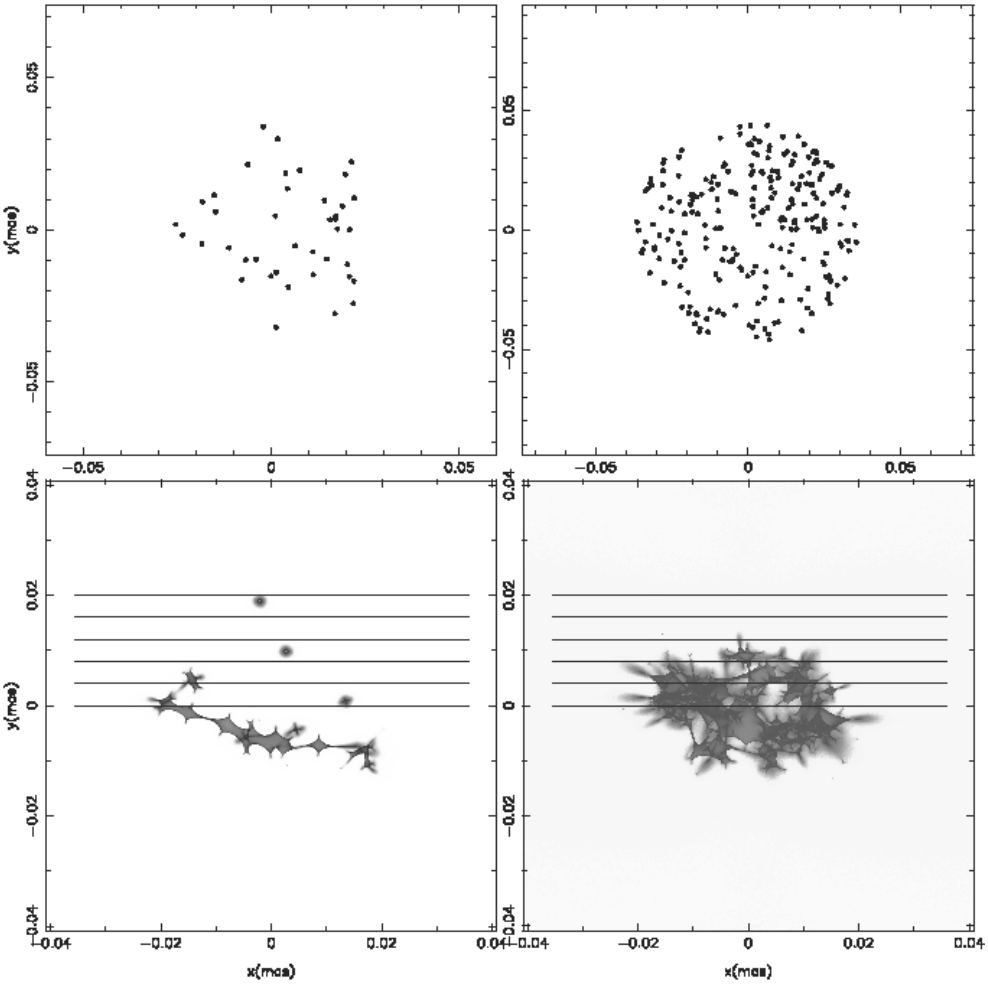

Figure 3: Upper panels show a random star distribution in the lens plane, a) case of $n_{lens} = 40$ (left panels) and b) case for $n_{lens} = 240$ (right panels). In the bottom panels we give the appropriate magnification map in the source plane for specified n_{lens}, respectively. Horizontal parallel solid lines present the paths of the source for which we calculated magnification light curves and variability of the photo-center positions. These plots are given for a standard lens system with $z_d = 0.5$ and $z_s = 2.0$ (Popović and Simić, 2014).

The lens has been assumed to have a circular shape, containing N_s stars of Solar masses ranging from 40 to 240 in this particular case, see Figure 3. We also assumed that lens and source are placed at the cosmological distances, with $z_d = 0.5$ and $z_s = 2.0$ (standard lens). We are confident that such carefully chosen lens reflects good enough condition for the gravitational bound systems. Any more massive and densely populated lens will act as one compact object with known influence on the distant source.

4. RESULTS

By using ray shooting method we are able to investigate effects of microlens on the observed AGN source. In the first place we present the lens with appropriate magnification maps and images of AGN perturbed by microlensing of a diffuse massive structure. In Figure 3 one can see the distribution of stars in the lens for two discussed cases, together with their respectfull magnification maps. As it is expected in case of higher populated lenses more caustics are distributed in the magnification maps. This case then have similar influence as one compact lens with similar mass. For lower populated lenses the perturbation of source light curve has more iregular impact with highly expressed peaks.

In the Figure 4 we can see that depending on the number of stars in the lens, image can become more or less deviated. In both cases we consider uniform distribution of stars in the lens as presented in the Figure 2. It is well known that AGN have particular SED which significantly depends on wavelengths, we compute the images in four different spectral bands. In both cases of lens population, we can see that images in lower energy bands are bigger then in higher energy bands.

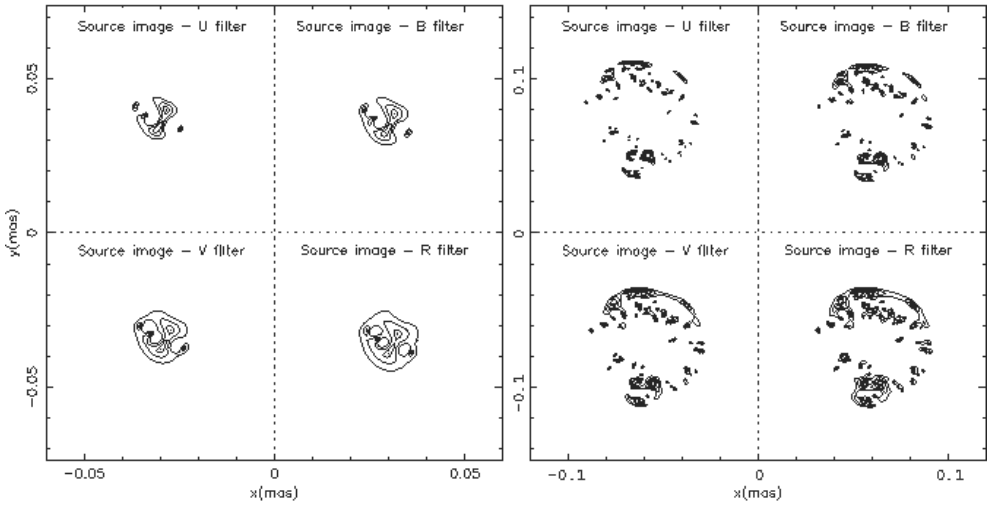

Figure 4: Images of source in four different energy channels U[332-398 nm], B[398-492 nm], V[507-595 nm] and R[589-727 nm]. Lens for this case is presented in Figure 3. Left four panels present the image for the case of $n_{lens} = 40$, while four on the right side are for the $n_{lens} = 240$ stars, with $z_d = 0.5$ and $z_s = 2.0$.

Additionally, by knowing the emission distribution over pixels of the AGN image, we compute light curve variations induced by crossing of lens over an AGN source, for both cases of lens population, see Fig. 5.

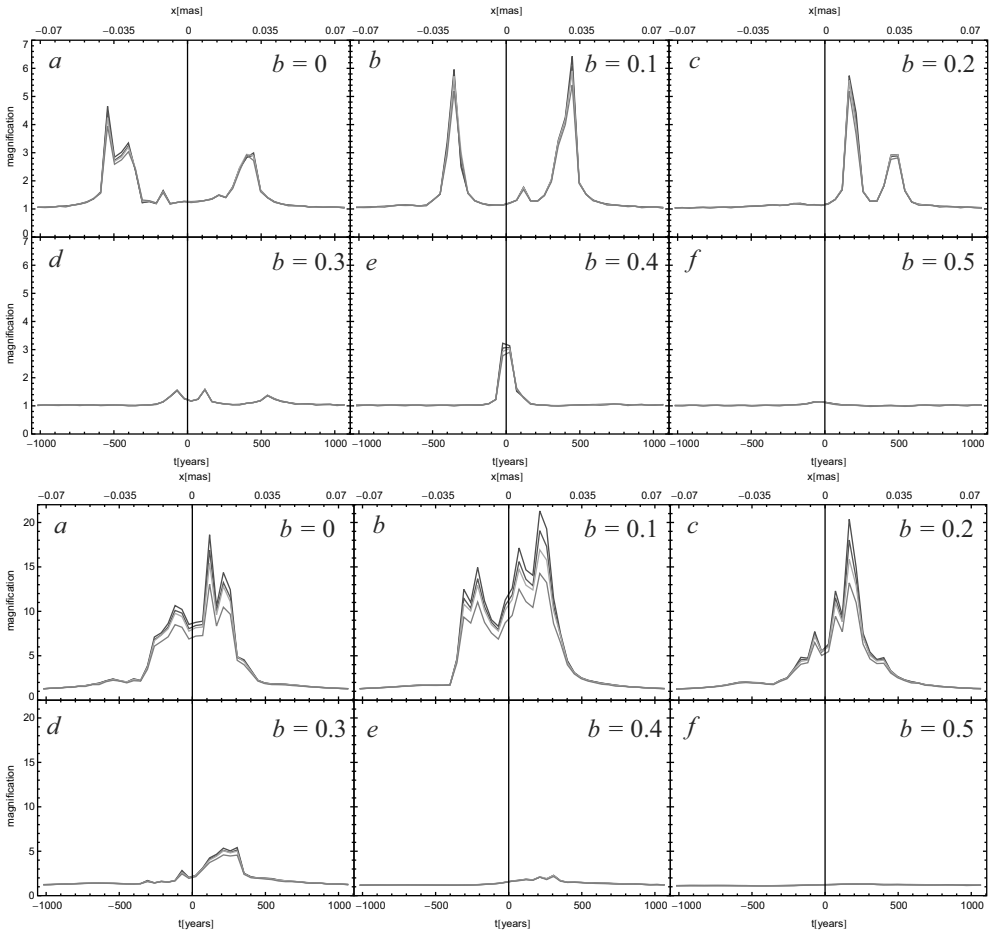

Figure 5: Magnification variability of a source image during the overcrossing event. Lens is populated with 40 and 240 Solar mass stars distributed uniformly in the circular area. In panels from a) to f) (upper and lower image) impact parameter b changes from 0 towards maximum value equal to the half of the half height of source map. Trajectories are presented as in the Figure 4.

We shell point out here that one peak in light curves presents a variation caused by a single caustic in the map (caused by a group of stars), with relative variation as much as 5 to 7 times. On the contrary, in the second case (Fig. 5), with a more massive lens (240 stars) we have the proportionally higher relative magnification of the order of 20 times, caused by an action of a bulk of overlapping caustics which gradually decreases with an increase of parameter b. For the last two cases e) and f)

in Fig. 5 the magnification is neglected. Such behavior suggests that the lens acts as a compact object with the mass equal to the sum of masses of all stars in the cluster. In both cases relative deviations per observed energy channels is at maximum for the moment of the highest magnification with the maximum in the U channel and decreased for another channels.

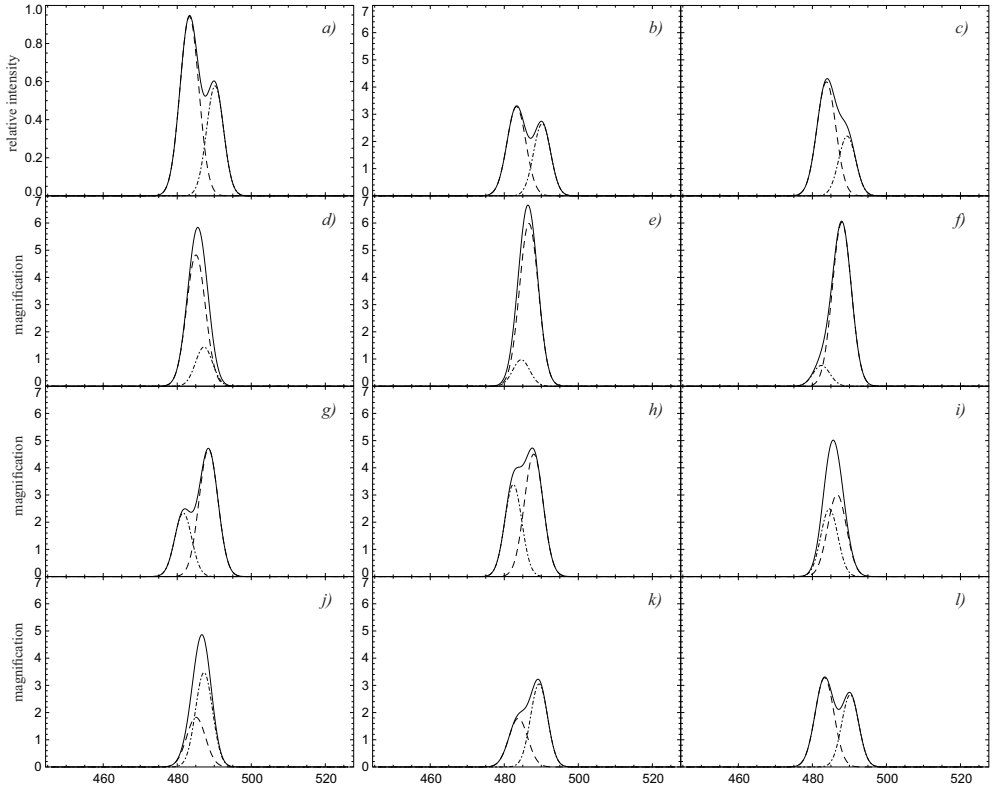

Figure 6: H_β spectral line from the binary system of super massive binary black holes, influenced by microlens during the full rotation. First image a) is without microlens with unit magnification. Dashed and dotted lines presents H_β spectral line for particular binary component, while full line presents their superposition.

In the case of a super massive binary black hole system (SMBBH) we have applied the presented method for computing the magnification maps and images (Simić and Popović, 2014a, in preparation). As most interesting we present the variability induced by microlens action on the H_β spectral line, during the full rotation of the system (see Fig. 6). It is very interesting to note that microlens can magnify or demagnify component lines, which has significant influence in composite line profile. One can see that magnification of both lines can be as high as 7 times in comparision with unlensed system.

5. CONCLUSION

In this paper we have presented the methodology used for computation of microlens influence on the distant source, particulary the AGNs. We have showed that the ray shooting algorithm is more efficient than the ray tracing method. We have presented a method and apply it in the case of a complex source (AGN) and taking a complex lens (massive diffusive object).

We found that presented method can be applied for a vast number of different cases. What is important to express is that applied method allow us to exactly follow each of the possible light rays emitted from the source and precisely determine deflection induced by lens. We additionally upgrade method by introducing the spectral stratification of particular pixels contained in source. This allows to study even spectral behavior of source under the microlensing influence.

Acknowledgments

This work is a part of the project (176001) *Astrophysical Spectroscopy of Extragalactic Objects*, supported by the Ministry of Science and Technological Development of Serbia.

References

Done C., Davis, S.W., Jin, C, Blaes, O., Ward, M.: 2012, Intristic disc emission and the soft X-ray excess in active galactic nuclei, *MNRAS*, **420**, 1848.

Kayser, R., Refsdal, S., Stabell, R.: 1986, Astrophysical applications of gravitational microlensing, *A&A*, **166**, 36.

Paczynski, B.: 1986, Gravitational microlensing at large optical depth, *ApJ*, **301**, 503.

Popović, L. Č., Jovanović, P., Stalevski, M., Anton, S., Andrei, A. H., Kovačević, J., Baes, M.: 2012, Photocentric variability of quasars caused by variation in their innner structure: consequence for Gaia measurements, *A&A*, **538A**, 107.

Popović, L. Č., Simić, S.: 2013, Spectro-photometric variability of quasars, caused by lensing of diffuse massive substructure: consequence on flux anomaly and precise astrometric measurements, *MNRAS*, **432**, 848.

Simić, S. & Popović, L. Č.: 2014, Broad spectral line and continuum variabilities in QSO spectra induced by microlensing of diffusive massive substructure, *ASR*, **54**, 1439.

Simić, S. & Popović, L. Č.: 2014a, in preparation.

Schneider, P. & Weiss, A.: 1986, The two-point-mass lens: detailed investigation of a special asymmetric gravitational lens, *A&A*, **164**, 237.

Schneider, P. & Weiss, A.: 1987, A gravitational lens origin for AGN-variability? Consequence of micro-lensing, *A&A*, **171**, 49.

Treyer, M. & Wambsganss, J.: 2004, Astrometric microlensing of quasars. Dependence on surface mass density and external shear, *A&A*, **416**, 19.

Proceedings of the IX Bulgarian-Serbian Astronomical Conference: Astroinformatics (IX BSACA) Sofia, Bulgaria, July 2-4, 2014,
Editors: M. K. Tsvetkov, M. S. Dimitrijević, O. Kounchev, D. Jevremović and K. Tsvetkova
Publ. Astron. Soc. "Rudjer Bošković" No 15, 2015, 83-91

TIME SERIES ANALYSIS OF AGNs

ANDJELKA KOVAČEVIĆ[1], LUKA Č. POPOVIĆ[2], ALLA I. SHAPOVALOVA[3] and DRAGANA ILIĆ[1]

[1] *Department of astronomy, Faculty of Mathematics*
University of Belgrade, Serbia
E-mail: andjelka@matf.bg.ac.rs, dilic@matf.bg.ac.rs
[2] *Astronomical Observatory Belgrade, Serbia*
E-mail: lpopovic@aob.bg.ac.rs
[3] *Special Astrophysical Observatory of the Russian AS, Russia*
E-mail: ashap@sao.ru

Abstract. In the context of information and astroinformatics, we present results of time series analysis of some of well known type 1 Active Galactic Nuclei.

1. INTRODUCTION

Sixty years have been passed since Cygnus A was optical identified (Baade & Minkowski, 1954) as an extra-galactic source and the first powerful active galactic nucleus (AGN). Since then, powerful AGNs have been identified across the electromagnetic spectrum and in galaxies inhabiting both the local Universe up to z$\sim$7 (Mortlock et al., 2011). Non-stellar character of AGNs has been widely accepted, since their spectra indicate a non-thermal source. The AGN's spectral energy density is consistent over most frequencies so it is too broad to originate from a radiating blackbody such as star.

To achieve extremely large observed luminosities ($> 10^{48}$ erg s^{-1}), AGN energy source must be $\sim$100 times more efficient than nuclear fusion. Up to now, the release of gravitational potential energy from the accretion of material onto a supermassive black hole ($M > 10^6 M_\odot$) is the only known mechanism able to explain the observations (Lynden-Bell, 1969). Matter falling onto the black hole that possesses angular momentum could be accreted onto a disk, radiating energy from both frictional heating of layers of the accretion disk, or from the release of gravitational potential energy. Some of the material could be accelerated to relativistic speeds and ejected perpendicular to the accretion disk, forming the jets of radio-loud AGN. The exact mechanisms are still not known.

The classification tree of AGNs is obscured, since the distinctive characteristics of various sources mainly reflect historical differences in advances of technology of their discovery. Soon after the discovery of quasars (the most luminous AGNs) it

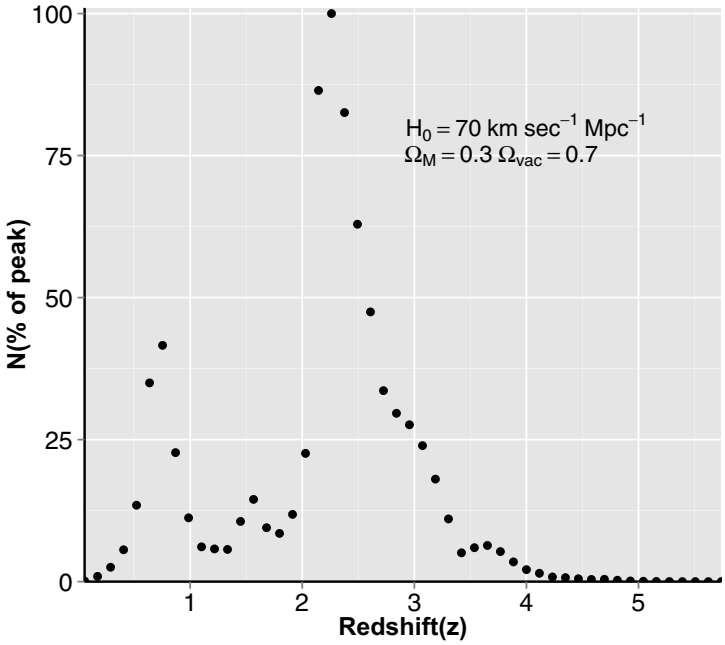

Figure 1: The SDSS-DR9 Quasar Catalog (DR9Q): Relative number of quasars (N- as a fraction of the peak value) per comoving volume element as a function of redshift z. Comoving volume element is calculated using astCalc procedure, the input cosmological parameters are given in the legend.

was evident that their space density reached peak at redshift $z \sim 2.3 - 2.5$ or at a look-back time of 78% of the age of the Universe (Fig. 1).

As emphasized by Bekenstein (2004), the General relativity sharpened the definition of black hole into a region of space rendered causally irrelevant to all its environment by gravity in the sense that no signal, by light, massive particles or whatever, can convey *information* about its nature and state to regions outside it. Using parallels with thermodynamics and information, where a black hole can be seen as a storage facility to hide information, Bekenstein (1973) proposed that the surface area of a black hole serves as a measure of its entropy, and it was refined by Hawking (1975). This relationship for an uncharged, non-rotating black hole is

$$S = \frac{kA}{4L_P^2} \tag{1}$$

where S is the entropy of black hole, A is the area of the event horizon of black hole, the k is Boltzmann constant and $L_P = \sqrt{\frac{G}{\hbar c^3}}$ is Planck length. If the Boltzmann constant is omitted the entropy has dimensionless form. While the surface area of the horizon of a black hole, measures the entropy of the black hole, the entropy is a

measure of information I (or information loss),

$$S = k \log_2 I \tag{2}$$

So the Bekenstein-Hawking formula (BHF, (1)) relates the total information content of a region of space to the area of the surface encompassing that volume. Soon, Bekenstein (1981) sought to generalize his result by postulating that the information content of any physical system can never be larger one quarter of the area of its encompassing surface. Following this attempt, Gerard 't Hooft (1993) and Susskind (1995) suggested the so-called holographic principle, according to which the information content of the entire universe is captured by an enveloping surface that surrounds it. Beside this, the principle was generlized that the total information content of a region of space cannot exceed one quarter of the surface area that confines it.

Hence, the entropy or potential information that can be extracted from a configuration of matter within a volume is strictly limited by the extension of its bounding surface, whereas its ontological determination requires a higher degree of actual information. This defines how much information can be contained in a specified region of space, or conversely, the maximum amount of information required to perfectly describe a given physical system down to the quantum level. One can attribute this quantity to the data store (or the thermodynamic microstates) and call it amount of data in the system.

Here, we will recapitulate some of our results of AGNs time series investigations in the context of profound notion of information and astroinformatics as a new discipline. The detailed description of objects, data and statistical methods are given in Kovačević et al. 2014, unless otherwise specified.

This work is organized as follows: some preliminaries on relation between information and black hole mass is examined in the section *Information and black hole mass*; in the section *Discussion* we estimate entropy density of objects with masses similar to Arp 102B and 3C 390.3, as well as entropy of Arp 102B and 3C 390.3 itself. Also we demonstrate that probability structure function (PSF) of ZDCF curves of Arp 102B, 3C 390.3, NGC 5548 and NGC 4051 assigned these objects to different clusters. The section *Conclusion* summarizes our results.

2. INFORAMTION AND BLACK HOLE MASS

Until the mid-twentieth century, the dominant paradigm in both science and technology was that of energy- the laws of physics had been developed to understand the nature of energy and how it could be transformed and used. In the mid-twentieth century, began a new revolution of technology of information processing and computation.

Hartley (1928) was the first who turns the notion of information into scientific concept by means of making information measurable. The unit of information (the bit), is actually a pure -dimensionless number. Due to this, the information must be invariant to coordinate transformations (while the mass, velocity, diameters are not such invariants). Those entities-invariants of coordinate transformations are of great interest in natural sciences.

In the natural sciences the constants of physical laws have the certain number of bits defined by their values. On the other hand, we are facing many processes which change with time- and they are actually information flow (Harmuth, 1982). For example, in order for a planet in our solar system to follow its orbit, it must constantly receive information about the ratio mass-distance $\frac{m}{\vec{r}}$, varying with time, of all the other bodies. Also, some particle in an experiment would not be able to follow the path through the modern instruments without the transfer of information about electromagnetic field. In the first case, it was used the metric field while in the second case, the electromagnetic field was used to explain the transfer of information.

Information is physical, this statement of Landauer (1996) has two complementary interpretations. First, information is registered and processed by physical systems. Second, all physical systems register and process information.

In principle, every physical process can be described in terms of interactions between particles that produce binary answers: yes or no, here or there, etc. Thus natural laws, governing the interactions and rearrangements of the constituents of the physical universe are perceived as the flipping of binary digits, as in a digital computer.

If one chooses to regard the universe as performing a computation, most of the elementary operations in that computation consists of protons, neutrons (and their constituent quarks and gluons), electrons and photons moving from place to place and interacting with each other according to the basic laws of physics. In other words, to the extent that most of the universe is performing a computation, it is computing its own dynamical evolution. We have already mentioned the link between physics and information established in BHF. For a spherically symmetrical black hole, Penrose (1989) suggested this surface area turns out to be proportional to the square of the mass of the black hole, and found that the entropy (information) of a black hole is proportional to the square of its mass

$$S = \frac{2\pi k G M^2}{\hbar c \ln 2} \tag{3}$$

where k is Boltzmann's constant, c is the speed of light, G is Newton's gravitational constant, and $\hbar$ is Planck's constant over 2π.

Almost parallel with this theoretical investigations, the methods for black hole mass determination has been developed.

Using dynamical methods to derive BH masses of AGNs have not been generally feasible, since AGNs are very distant objects and so bright that outshine the "test objects". Instead, their the most striking characteristics of rapid variability in all accessible energy bands is used.

Cherepashchuk and Lyutyi (1973) discovered time delay effect. The time delay ($\tau_{BLR} = R_{BLR}/c$) between the changes in the optical-ultraviolet continuum produced in the compact accretion disk and the emisiion line from the further broad line region (BLR) gas clouds is measured by spectroscopic monitoring. In order to determine BH masses in AGNs, a well accepted working hypothesis is that the gravitational field of a central object controls the motion of gas near the nucleus (Dibai 1984). So the mass of a black hole can be estimated with $M_{BH} \sim \frac{R_{BLR}V^2}{G}$ under assumption that the gas around a black hole is virialized. The V is the characteristic velocity of BLR

gas at distance R_{BLR} from the center of a AGN (Peterson and Wandel 1999) and G is the gravitational constant.

Once having the estimate of the black hole mass, we are able to calculate the information content of such object.

3. DISCUSSION

3. 1. ARP 102B AND 3C 390.3: SMBH MASSES AND ENTROPY

Using recent measurements of the supermassive black hole (SMBH) mass function, Egan and Lineweaver (2010) found that SMBHs (particularly around $10^9 M_\odot$) are the largest contributor to the entropy of the observable universe, contributing at least an order of magnitude more entropy than previously estimated. So, the SMBH mass determination of AGNs has significant importance of estimating the total entropy budget of the whole Universe.

In Table 1, we present results of time series investigations of 2 type 1 AGNs out of 4 such objects used in our analysis. For these two objects, we were able to determine SMBH masses in their centers. Using these values, we estimated the number density of objects per Mpc^3 per logarithmic mass interval (i. e. the values of SMBH mass function) with masses similar to Arp 102B and 3C 390.3 as well as entropy density of such objects.

We use three parametric Shechter function

$$\frac{dn}{d\log_{10} M} = \phi_* \left(\frac{M}{M_*}\right)^{\alpha+1} \exp\left(1 - \frac{M}{M_*}\right) \tag{4}$$

from (Graham et al. (2007), and Egan and Lineweaver (2010) as a model of SMBH mass function in observable Universe (see Fig. 2 the left panel). Expected contribution of objects with masses similar to Arp 102B (point 1 on the left panel) is greater than contribution of objects with masses similar to 3C 390.3 (point 2 on the left panel).

The SMBH entropy density Egan and Lineweaver (2010)) is related to SMBH mass function as follows:

$$entden = \frac{4\pi G k}{c\hbar} \int M^2 \frac{dn}{d\log_{10}(M)} d\log_{10}(M) \tag{5}$$

The entropy density is depicted at right panel of Figure 2. The primary contributors of entropy density are objects around $10^9 M_\odot$. The contributions of objects with masses similar to Arp 102B (point 1 on the right panel) is slightly smaller than contributions of objects with masses similar to 3C 390.3 (point 2 on the right panel). Their uncertainties are obtained varying Arp 102B and 3C 390.3 (Table 1) SMBH masses with $0.1 \times 10^8 M_\odot$ and $0.1 \times 10^9 M_\odot$, respectively. Arp 102B SMBH mass gives more accurate entropy density prediction than 3C 390.3 SMBH mass. It means that model used for Arp 102B is better matching the theoretical SMBH entropy density.

Also, using Penrose formula (3), we calculated the entropies of Arp 102B and 3C 390.3 (the last column of Table 1). Assuming that single SMBHs inhabit almost all of the 10^{11} galactic cores in the visible Universe, and that the information content

of such object is 1.7×10^{95} (average value of information content of our two object), we could obtain that total entropy contribution of SMBHs, in visible universe, is 1.7×10^{106}. These result is three order of magnitudes larger than predicted by Egan and Lineweaver (2010). The reason for the difference is that we used the average value ($1.1 \times 10^9 M_\odot$) of our two SMBH masses, while Egan and Lineweaver (2010), used mass function which peak is about $10^8 M_\odot$. This emphasize need of more accurate SMBH mass determination, in order to obtain much better estimate of SMBH mass function and better estimate of SMBH contribution to the over all entropy of the Universe. The increase of entropy of Universe has not yet been limited (e.g. by mentioned holographic bound), so this is the reason that dissipative processes are going on and that life exist.

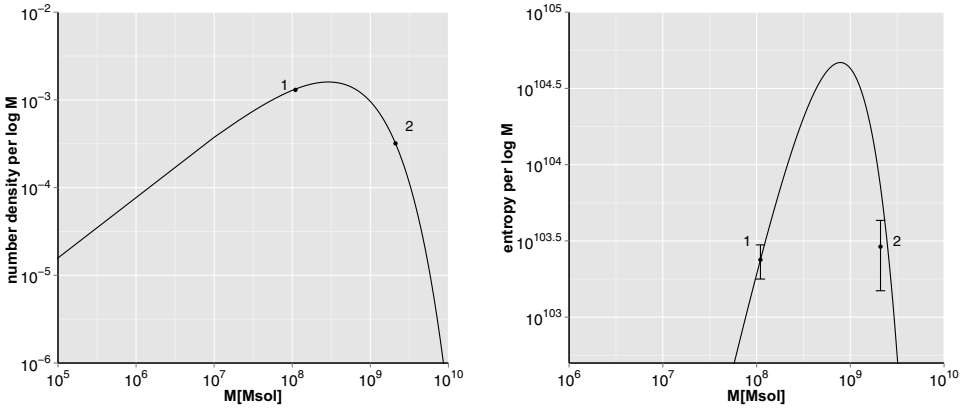

Figure 2: Left panel: SMBH mass function from Graham et al (2007) and Egan and Lineweaver (2010): the number of supermassive black holes per Mpc^3 per logarithmic mass interval. Ordinate of points 1 (0.0013) and 2 (0.000319) are values of SMBH mass function at our estimated masses of Arp 102B and 3C 390.3 respectively. Right panel: the mass distribution of SMBH entropies. Ordinate of points 1 and 2 are entropies densities of objects with masses similar to Arp 102B and 3C 390.3 (see Table 1).

Table 1: Arp 102B and 3C 390.3: time lag measurements and derived SMBH masses. The column ED: entropy density of objects with masses similar to Arp 102B and 3C 390.3. The colum E: entropies of SMBH of Arp102 B and 3C 390.3

Object	Continuum waveband (in Å)	Line	τ (days)	Method used	SMBH Mass $M_\odot$	ED	E
Arp 102B	cnt 6356-6406	Hα	$15^{24}_{-13.8}$,$24^{27.5}_{18.8}$	ZDCF,SPEAR	1.1×10^8 Shapovalova et al. (2013)	$(2.378 \pm 0.6) \times 10^{103}$	9.22×10^{92}
	cnt 5200-5250	Hβ	$23^{64}_{-20.9}$,48^{57}_{37}	ZDCF,SPEAR			
3C 390.3	cnt 5369-5399	Hα	$24^{99.8}_{-10.5}$,44^{49}_{-35}	ZDCF,SPEAR	2.1×10^9 Shapovalova et al. (2001)	$(7.15 \pm 1.4) \times 10^{103}$	3.4×10^{95}
	cnt 5369-5399	Hβ	95^{27}_{-48},77^{79}_{-75}	ZDCF,SPEAR			

3. 2. AN EXAMPLE OF CLUSTERING AGNS

Estimation of black hole masses could be done by time series analysis methods. There are a number of characterizing statistics based on the differences of all possible pairs of data points in a time series, e.g. different kind of cross correlation function (see Kovacevic at al (2014)). They have been frequently used since the time sampling of astronomical time series is often relatively sparse.

Usually, we compute a set of ~ 66 parameters and statistical measures for any of our objects, forming feature vectors in the parameter space of statistical measures. In such a way, our sparse heterogeneous light curves are translated into much more homogenized feature vectors in the statistical parameter space. Since, the classification is a primary feature of astronomical research, one can expect that using this statistical space could provide more insights in this problem.

As we mentioned earlier, the AGNs have obscured classification. Even the ZDCF curves are similar among different objects. As an example, the visualization of ZDCF analysis of 4 type 1 AGNs are given in Fig. 3.

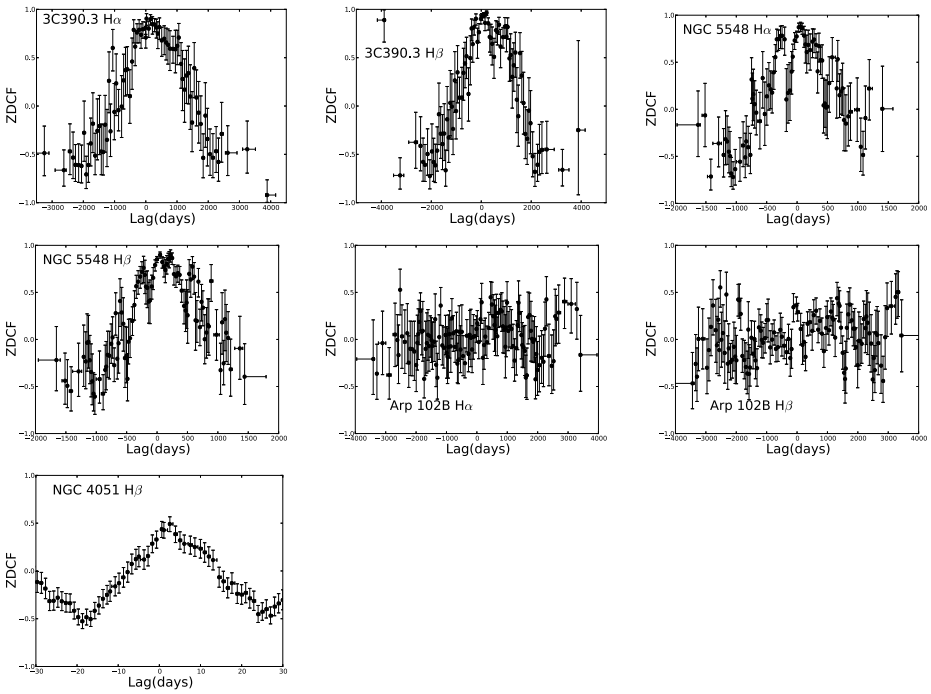

Figure 3: The ZDCF analysis: object and emission line denoted on each plot. The horizontal and vertical error bars correspond to 1σ uncertainties for a normal distribution.

We calculated 2D histograms of given ZDCF curves (see Fig. 4). These histograms can be viewed as probabilistic structure functions (PSF) of given ZDCF curves. According their shape, it is clear that 3C 390.3 and NGC 5548 have similar PSF of

ZDCF curves, while Arp 102b and NGC 4051 have distinctive PSF . The measure of a similiarity and divergence between the class PSF of ZDCF curves of objects should be tested on larger sets of simulated curves. If it is approved, this could be efficient method for clustering objects.

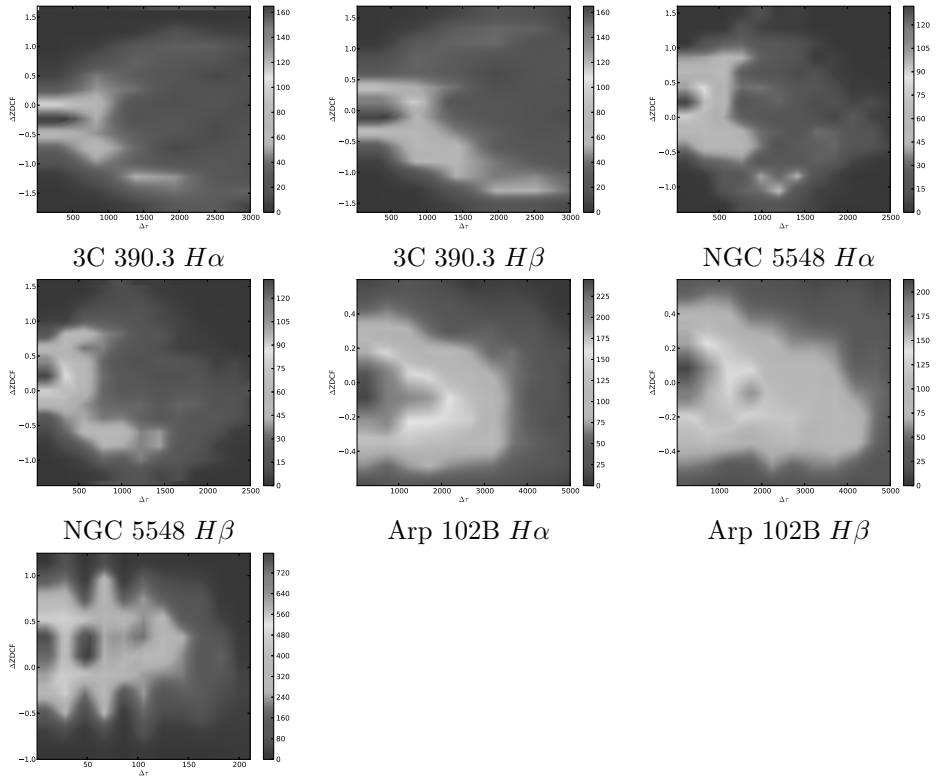

3C 390.3 $H\alpha$ | 3C 390.3 $H\beta$ | NGC 5548 $H\alpha$

NGC 5548 $H\beta$ | Arp 102B $H\alpha$ | Arp 102B $H\beta$

NGC 4051 $H\beta$

Figure 4: 'Heatmaps' of ZDCF and lags of the object and emission line denoted below each panel. Colorbar indicates number of pairs (lag, ZDCF), the largest number of pairs are indicated by red color. Aspect ratio of each heatmap is different due to its dependance on the range of lags and ZDCF coefficients.

4. CONCLUSION

Here we present entropy density of SMBH with masses similar to our mass-estimates of Arp 102B and 3C 390.3. Entropy density based on Arp 102B mass is closer to theoretical entropy density curve than value based on 3C 390.3. This suggests that model of Arp 102B is better suited to theoretical entropy density than the 3C 390.3 model.

Also we calculate individual entropy content of Arp 102B and 3C 390.3 using Penrose formula and give prediction of entropy of the observable universe assuming the mean value of Arp 102B and 3C 390.3 masses. Obtained value is about 3 orders of magnitude higher than value obtained by Egen and Lineweaver (2010). The major

dimension of astronomical research is the assignment of objects to classes, which is particularly accelerated with the development of astroinformatics. We demonstrate the utilization of features of statistical parameter space for clustering of 4 type 1 AGNs by means of PSF.

Acknowledgments

This work was supported by the Ministry of Education and Science of Republic of Serbia through the project Astrophysical Spectroscopy of Extragalactic Objects (176001) and RFBR (grants N1202-01237a, 1202- 00857a) (Russia) and CONACYT research grants 39560, 54480, and 151494 (Mexico). We would like to thank Organizers of 9 BSACA for financial support provided by project Astroinformatics: a way to future astronomy.

References

Baade, W., Minkowski, R.: 1954, Identification of the Radio Sources in Cassiopeia, Cygnus A, and Puppis A, *ApJ*, **119**, 206.

Bekenstein, J. D.: 1973, Black holes and entropy, *Phys. Rev. D*, **7**, 2333.

Bekenstein, J. D.: 1981, Universal upper bound on the entropy-to-energy ratio for bounded systems, *Phys. Rev. D*, **23**, 287.

Bekenstein, J. D.: 2004, Black holes and information theory, *Contemporary Physics*, **45**, 31.

Hawking, S.: 1975, Particle creation by black holes, *Comm. Math. Phys.*, **3**, 199.

Dibai, E. A.: 1984, Parameters of Non-Stationary Galactic Nuclei as a Fuction of Critical Luminosity, *Astron. Zh.*, **61**, 209.

Egan, C. A., Lineweaver, C. H.: 2010, A larger estimate of the entropy of the Universe, *ApJ*, **710**, 1825.

Graham, A. W., Driver, S. P., Allen, P. D., Liske, J.: 2007, The Millennium Galaxy Catalogue: the local supermassive black hole mass function in early and late-type galaxies, *MNRAS*, **378**, 198.

Harmuth, H. F.: 1982, Information theory applied to space-time physics, World Scientifc Publishing Co.

Hartley, R. V. L.: 1928, Transmission of Information, *Bell System Technical Journal*, **7**, 535.

Kovačević , A., Popović , L. Č., Shapovalova, A. I., Ilić, D., Burenkov, A. N., Chavushyan, V.: 2014, Time series analysis of active galactic nuclei: The case of Arp 102B, 3C 390.3, NGC 5548 and NGC 4051, *ASR*, **54**, 1414.

Landauer, R.: 1996, The physical nature of information, *Physics Letters A*, **217**, 188.

Lynden-Bell, D.: 1969, Galactic nuclei as collapsed old quasars, *Nature*, **223**, 690.

Mortlock, D. J., Warren, S. J., Venemans, B. P., Patel, M., Hewett, P. C. et al.: 2011, A luminous quasar at a redshift of z = 7.085, *Nature*, **474**, 616.

Peterson, B., Wandel, A.: 1999, Keplerian Motion of Broad-Line Region Gas as Evidence for Supermassive Black Holes in Active Galactic Nuclei, *ApJ*, **521**, L95.

Shapovalova, A. I., Burenkov, A. N., Carrasco, L., Chavushyan, V. H. et al.: 2001, Intermediate resolution H spectroscopy and photometric monitoring of 3C 390.3. I. Further evidence of a nuclear accretion disk, *A&A*, **376**, 775.

Shapovalova, A. I., Popović, L. Č., Burenkov, A. N., Chavushyan, V. H., Ilić, D., Kollatschny, W., et al.: 2013, Spectral optical monitoring of a double-peaked emission line AGN Arp 102B: I. Variability of spectral lines and continuum, *A&A*, **559**, A10, 1.

Susskind, L.: 1995, The World as a Hologram, *J. Math. Phys. (NY)*, **36**, 6377.

Susskind, L.: 2008, My Battle with Stephen Hawking to Make the World Safe for Quantum Mechanics, Little, Brown and Company, New York, USA.

't Hooft, G.: 1993, Dimensional Reduction in Quantum Gravity, in *Salanfestschrift*, edited by A. Alo, J. Ellis, S. Randjbar-Debi, http://arxiv.org/pdf/gr-qc/9310026.pdf

Proceedings of the IX Bulgarian-Serbian Astronomical Conference: Astroinformatics (IX BSACA) Sofia, Bulgaria, July 2-4, 2014,
Editors: M. K. Tsvetkov, M. S. Dimitrijević, O. Kounchev, D. Jevremović and K. Tsvetkova
Publ. Astron. Soc. "Rudjer Bošković" No 15, 2015, 93-97

FLUCTUATIONS IN THE FLOW AND DEVELOPMENT OF FLARE-UPS IN COMPACT BINARY STARS

DANIELA BONEVA

Space Research and Technology Institute, Bulgarian Academy of Sciences
E-mail: danvasan@space.bas.bg

Abstract. We study the relationship between the disc's structural transformations and the burst activity, which has an effect on the light curve shape's behavior. We present several methods for investigation of flare-up events in accreting compact binaries. The theoretical modeling explains the physical properties of flow unstable processes. It shows gas-dynamical mechanisms that are considered to be the most operative for the occurrence of flares in the binary star configuration. It is pointed to the changes in mass transfer rate that could also trigger bursts activity. We analyze the observational results of quasi-periodic variability in the luminosity of white dwarf binary stars systems.

1. INTRODUCTION

Disturbances of the disc structure due to periodic movement of the dense formations, as well as due to stream - pattern interaction, can result in low amplitude oscillations manifesting as irregular variations on the light curve. Note also that the casual low-magnitude variations on the light curve (flickering) can also be a consequence of the presence of the density formation in the disc. Brush (1992) has studied mechanisms generating the flickering. He proposes four possible mechanisms responsible for the observed variations in brightness: unstable mass transfer from the L1 point and interaction with the disc edge; dissipation of magnetic loops; turbulences in the accretion disc and unstable mass accretion onto the white dwarf. Bisikalo et al. (2001) have proposed a model that explains the variations of uneclipsed parts of light curves correlated with the presence of spiral shocks. Their observations correspond to results in variations to the theoretical one. In Boneva et. al (2009) and Kononov et al. (2008) we have showed the relation between the flow's elements dynamics and the active state of SS Cyg. According to study of Zamanov et al. (2010), more of the flickering's engines are all related to the accretion process: (i) the bright spot (the region of impact of the stream of transferred matter from the mass donor star on the accretion disc); (ii) the boundary layer (between the innermost accretion disc and the white dwarf surface); (iii) inside the accretion disc itself.

In the current survey, we investigate the relationship between the disc's flow fluctuations and the burst activity, which has an effect on the light curve shape's behavior. We study the mechanisms that cause the accretion rate to be sufficiently increased and then to realize the transition from a quiescent to an active state. The results reveal the accumulation of mass that could be transferred to the surface of the white dwarf from the secondary star through an accretion disc, as well as the structure transformations, accompanied with the flow patterns formation which could trigger outbursts. We analyze the observational results of quasi-periodic variability in the luminosity of white dwarf binary stars systems. We discuss the possibility of applying the polarization modeling into the study of brighten-up events in dwarf nova stars.

2. MODELING AND METHODS

When material reaches the compact object surface through the disc, it must pass through a violent transition region. We establish a part of disc's configuration around the primary (white dwarf) star after the mass transfer being started. When investigating close components, it is necessary to include physical essence of the flow dynamics response to the interaction processes.

Further, we use as a base the model of outburst in SS Cyg, presented in Kononov et al. (2008) and Boneva et al. (2009). Here, we apply the same consequence of the proposed physical model of the bursts appearing. We modify the stage of instability processes in the disc flow adding different types of instability behavior.

Based on the observations, we suggest the following scenario for the development of an outburst. At some time, an instability and the resulting flow fluctuations develop in the disc, leading to a considerable increase in the efficiency of angular momentum transport and an increase in the rate at which matter is accreted onto the white dwarf. The growing intensity of the radiation from the white dwarf inevitably results in heating of the nearest parts of the accretion disc, and hence to an increase in the thickness of inner parts of the disc.

The gas between the toroidal shell and the accretor experiences strong heating that leads to its expansion. However, the expansion cannot be isotropic, since it is restricted in the equatorial plane by the accretor surface and the inner surface of the toroidal shell, whereas expansion orthogonal to the disc's surface is impeded only by the accretor's gravitational field. The increased velocity of the heated gas will probably be comparable to the local sound speed, which is insufficient to form a collimated jet. The expanding gas can have a low angular velocity, and is prevented from falling on the star primarily by the gas-pressure gradient rather than by the centrifugal force. This enables the gas to leave the toroidal shell and form an expanding spherical shell around the accretor. The increased size of this shell can explain the stronger emission during the development of the outburst.

We employ with the next most applicable methods. Gas-dynamical numerical calculations include the "finite-difference scheme – high order", "Roe solver". We construct a "box-framed scheme" to apply it into the modeling (Boneva and Filipov 2012). Then, we make the calculations inside of the box, or frame with different measurement. This gives the possibility to configure the scheme for each problem in limited regions of all disc's areas.

We use the Doppler Tomography techniques to construct the true cart of image of the obtained data and then to derive the radiation intensity distribution in the system's velocity space, making it possible to determine the parameters of the main flow elements in which energy is released.

According to the study of many authors, the bursts and high rate of emission cause the changes in polarization state. Our interpretation of the problem shows that the polarization degree values grow during the flare-ups.

3. INDICATIONS OF FLOW'S FLUCTUATIONS AND FLARE-UPS

3.1. Density fluctuations

In the result of tidal interaction in binary star stars between out-flow from the donor star and the accretion flow, the flow changes its basic parameters values. The disturbances in the flow and mass tidal interaction give rise to the fluctuations in velocity and density. The physical essence of the flow dynamics responses to the interaction processes in binary. The disturbed flow's conditions can provoke periodic or quasi-periodic oscillations, giving rise to the light curve variations. Since the density decreases with increasing radius, approaching to the outer edge, the observed luminosities must be correlated with the distance from the inner Lagrange point L_1. In this way, the amplitude of light curve variations should be approximately corresponding to the density contrast. We have obtained the density distribution along the line connecting the centers of binary components for three runs with different orbital periods. Figure 1 shows this distribution:

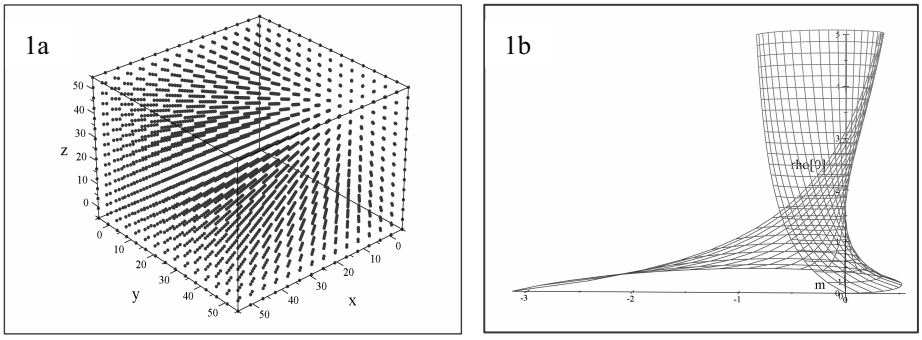

Figure 1: (a) Gradient of the density distribution in the field of calculation. It is seen the higher density areas, in the meaning of values heaping, modeled in the 3D box – framed scheme. (b) Increasing values of the density fluctuations in the disturbed mass transfer area.

We have detected the flow density fluctuations in the several type of accreting binaries, such as CV stars, Be/X stars (Kaygorodov et al. 2013), symbiotic binaries. The accretion rate is in a correlation with the level of mass transfer,

which depends on density. The high accretion rate here could give rise to the X-ray luminosity and stronger emission.

3.2. Wave - patterns formation and the Disc's shape

It is clear from the previous subsection that the variations of velocity and density have significant impact on the flow's behavior. By applying the gas-dynamical numerical methods and following the conditions of Klahr Bodenheimer (2003) we have simulated the presence of two-dimensional vortical-wave patterns in the disc's flow. They are considered to be an effective mechanism of angular momentum transport (Barranco and Marcus 2005). The development of vortices is more frequently observed along the outer sides, close to the disc's edges. According to the model above, when this kind of wave patterns leave the disc zone, they could crumble and merge into the matter of the curcumdisc hallo, influenced by the conditions of low density there. It follows from the results of that the density of outer regions of the accretion disc drops substantially during an outburst.

Analysis of the resulting Doppler tomograms shows that the flow structure changed appreciably during the observed outburst, compared to its structure in the quiescent state (Boneva et al. 2009). The most important difference in the flow is a change in the shape of the accretion disc, from nearly circular in the quiescent state to significantly elliptical in the active state. The asymmetrical shape of the disc's projection indicates the existence of heated material in the "bow shock" area, which can be caused by the spiral density formation. Figure 2 shows the position of vortical patterns on the disc's plane and the superposition of the flow structure elements.

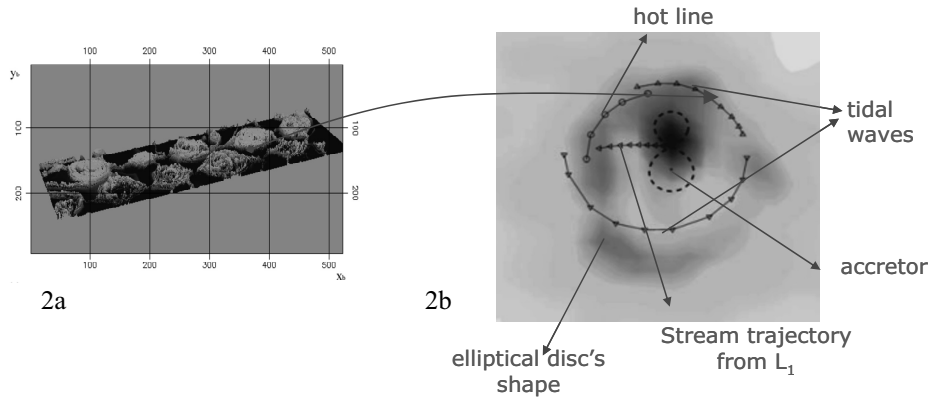

Figure 2: Vortical-like wave patterns may propagate throughout the disc, along the outer sides (a) (Boneva and Filipov 2013). The flow structure during the outburst: A result from the Doppler tomogram with superposed flow elements inferred from the numerical simulations (b) (Boneva et al. 2009).

.

4. CONCLUSION

In this survey, we present our modeling on the disc's flow morphology and its effect over the binaries' brightness variability. The model is developed on the base of increasing density and local areas with growing matter saturation. We have analyzed the flow structures during the outbursts and we indicate flow's fluctuations have been growing up in the mass transfer area. Our recent study also points to the long-lived wave patterns formation, which come rising by the tidal interaction in close binaries.

The casual low-magnitude variations on the light curve can also be a consequence of the presence of the vortical-like patterns in the disc structure.

Acknowledgments

Part of this work is supported by the Scientific Cooperation between Space Research and Technology Institute - Bulgarian Academy of Sciences and Institute of Astronomy – Russian Academy of Sciences.

References

Barranco, J. A. Marcus, P. S.: 2005, *ApJ*, **623**, 1157.

Bisikalo, D. V., Boyarchuk, A. A., Kaigorodov, P. V., Kuznetsov, O. A.: 2003, *Astron. Rep*. **47**, 809.

Boneva, D., Filipov, L.: 2013, Distribution of patterns and flow dynamics in accreting white dwarfs, *ASPCS*, **469**, 359-365.

Boneva, D., Filipov, L.: 2012, Density distribution configuration and development of vortical patterns in accreting close binary star system, http://adsabs.harvard.edu/abs/2012arXiv1210.2767B.

Boneva, D., Kaigorodov, P. V., Bisikalo, D. V., Kononov, D. A.: 2009, *Astron. Rep.,* **53**, 11, 1004–1012, http://adsabs.harvard.edu/abs/2009ARep...53.1004B.

Bruch, A.: 1992, *A&A* **266**, 237.

Klahr, H., Bodenheimer, P.: 2003, *ApJ*, **582**, 869-892.

Kyagarodov, P. V., Bisikalo, D. V., Kononov, D. A., Boneva, D. V.: 2013, *AIPC*, **1551**, 46-52.

Kononov, D. A., Kaigorodov, P. V., Bisikalo, D. V., Boyarchuk, A. A., Agafonov, M. I., Sharova, O. I., Sytov, A. Yu., Boneva, D. V.: 2008, *Astron. Rep.*, **85**, 10, 927-939, http://adsabs.harvard.edu/abs/2008ARep...52..835K.

Zamanov, R. K., Boeva, S., Bachev, R., Bode, M. F., Dimitrov, D., Stoyanov, K. A., Gomboc, A., Tsvetkova, S. V., Slavcheva-Mihova, L., Spasov, B., Koleva, K., Mihov, B.: 2010, *MNRAS*, **404**, 381.

Proceedings of the IX Bulgarian-Serbian Astronomical Conference: Astroinformatics (IX BSACA) Sofia, Bulgaria, July 2-4, 2014,
Editors: M. K. Tsvetkov, M. S. Dimitrijević, O. Kounchev, D. Jevremović and K. Tsvetkova
Publ. Astron. Soc. "Rudjer Bošković" No 15, 2015, 99-106

DETERMINATION OF NATURE FOR ELEVEN DOUBLE STARS

ZORICA CVETKOVIĆ[1], SLOBODAN NINKOVIĆ[1], RADE PAVLOVIĆ[1], SVETLANA BOEVA[2] and GEORGI LATEV[2]

[1] *Astronomical Observatory, Volgina 7, 11060 Belgrade, Serbia*
E-mail: zorica@aob.rs, sninkovic@aob.rs, rpavlovic@aob.rs
[2] *Institute of Astronomy and National Astronomical Observatory Rozhen, Bulgarian Academy of Sciences, 72 Tsarighradsko Shousse Blvd., 1784 Sofia, Bulgaria*
E-mail: sboeva@astro.bas.bg, glatev@astro.bas.bg

Abstract. We determined the linear solutions for eleven double stars by using the relative coordinates among which there are those obtained from our CCD frames, taken at NAO Rozhen and AS Vidojevica. Also, we applied existing criteria for establishing the nature of these double stars. The criteria are mostly based on some fundamental properties, such as the energy-conservation law, Kepler's third law, etc, which should be obeyed by bound pairs. Our analysis shows that all eleven double stars are most likely not gravitationally bound, i.e. they are optical pairs.

1. INTRODUCTION

The study of double stars makes possible more accurate determinations of masses and distances, as well as a better understanding of stellar formation and evolution. Systematic observations of these objects have been carried out for about 200 years. The results of measurements have been collected and the corresponding database is kept by the United States Naval Observatory. The Washington Double Star Catalog (WDS)[1] contains the data for more than 117000 pairs, components of double or multiple stars. Out of this number almost 90% pairs have been observed less than 10 times. Only for a small number of pairs, about 2100, the orbital elements have been calculated, i.e. a Keplerian motion has been confirmed. Their orbital elements can be found in the Sixth Catalog of Orbits of Visual Binary Stars.[2] In the case of more than 1200 pairs there are linear solutions given in the Catalog of Rectilinear Elements.[3] In the case of such pairs there are, in principle, three possibilities: to be gravitationally bound, but with large orbital periods, to be kinematically similar (say, common-proper-motion pairs) and to be mere optical pairs. For the purpose of

[1] http://www.usno.navy.mil/USNO/astrometry/optical-IR-prod/wds/WDS
[2] http://www.usno.navy.mil/USNO/astrometry/optical-IR-prod/wds/orb6
[3] http://www.usno.navy.mil/USNO/astrometry/optical-IR-prod/wds/lin1

establishing which of the three possibilities is the true one observations covering long time intervals or detailed analysis of their data are needed.

From 2004 till now a group of astronomers from the Belgrade Observatory have regularly stayed at the National Astronomical Observatory Rozhen (NAOR) in Bulgaria and taken frames of visual double and multiple stars. Series of observations of these stars at the NAOR have been made with a CCD camera attached to their 2-m telescope. The observations have been performed with the CCD camera VersArray: 1300B. More details can be found at website.[4] The results of observations have been published in Pavlović et al. (2005), Cvetković et al. (2006), Cvetković et al. (2007), Cvetković et al. (2010), Cvetković et al. (2011) and Pavlović et al. (2013).

During the summer of 2011 the first observations of celestial bodies from the new Astronomical Station on the mountain of Vidojevica (ASV) took place. More details can be found at website.[5] Series of observations of double and multiple stars at the ASV have been made with a CCD camera attached to the 60-cm telescope. For these series we used either SBIG ST-10ME or Apogee Alta U42 CCD cameras.

The basic characteristics of all three used cameras are given in Pavlović et al. (2013).

2. RESULTS

We calculated first linear solutions for eleven pairs for which the measurements show a linear trend: WDS 00057+4549 = STT 547 AC, WDS 00057+4549 = STT 547 AD, WDS 00057+4549 = STT 547 AE, WDS 00057+4549 = POP 217 AP, WDS 00121+5337 = CHR 1 AC, WDS 00251+1824 = HJ 621, WDS 03342+4837 = BU 787 AB, WDS 06092+6424 = MLB 259, WDS 07106+1543 = J 703, WDS 19289+3515 = POP 34 AC and WDS 23581+2840 = HJ 995. Except CHR 1 AC, for the calculation of other pairs we used the measuring results from our CCD frames obtained at NAOR and ASV. The linear solutions for pairs STT 547 AC, STT 547 AD, STT 547 AE, POP 217 AP and MLB 259 have been previously published in (Pavlović at al. 2013). The linear solutions for pairs HJ 621, BU 787 AB and HJ 995 have been previously published in (Cvetković at al. 2011). For the other three pairs CHR 1 AC, J 703 and POP 34 AC, the linear solutions are given in this paper for the first time.

In Figure 1 linear fits for eleven pairs are presented. In the lower right (or left) corner the arrow indicates the sense of the motion for the secondaries with respect to the primary (brighter star). The linear solutions for these pairs have been determined from a set of measurements also including our ones from the frames obtained at NAOR and/or ASV. Our measurements are indicated by filled circles in Figure 1.

The linear elements (equinox J2000) are listed in Table 1. The pair designation is given in Column 1, whereas Columns 2-8 show the linear elements: X_0 and Y_0 (coordinates of point with the closest relative separation, in arcseconds), X_A and Y_A (components of velocity of relative motion of the secondary for one year, in arcseconds), T_0 (epoch of the closest passage, in fractional Besselian year), ρ_0 (the closest relative separation, in arcseconds), θ_0 (position angle of the closest passage, in degrees). The velocity V of relative motion of the secondary is given in Column 9. The relative proper motion μ_{rel} is given in the final column.

[4] http://www.nao-rozhen.org/telescopes/fr_en.htm
[5] http://belissima.aob.rs/

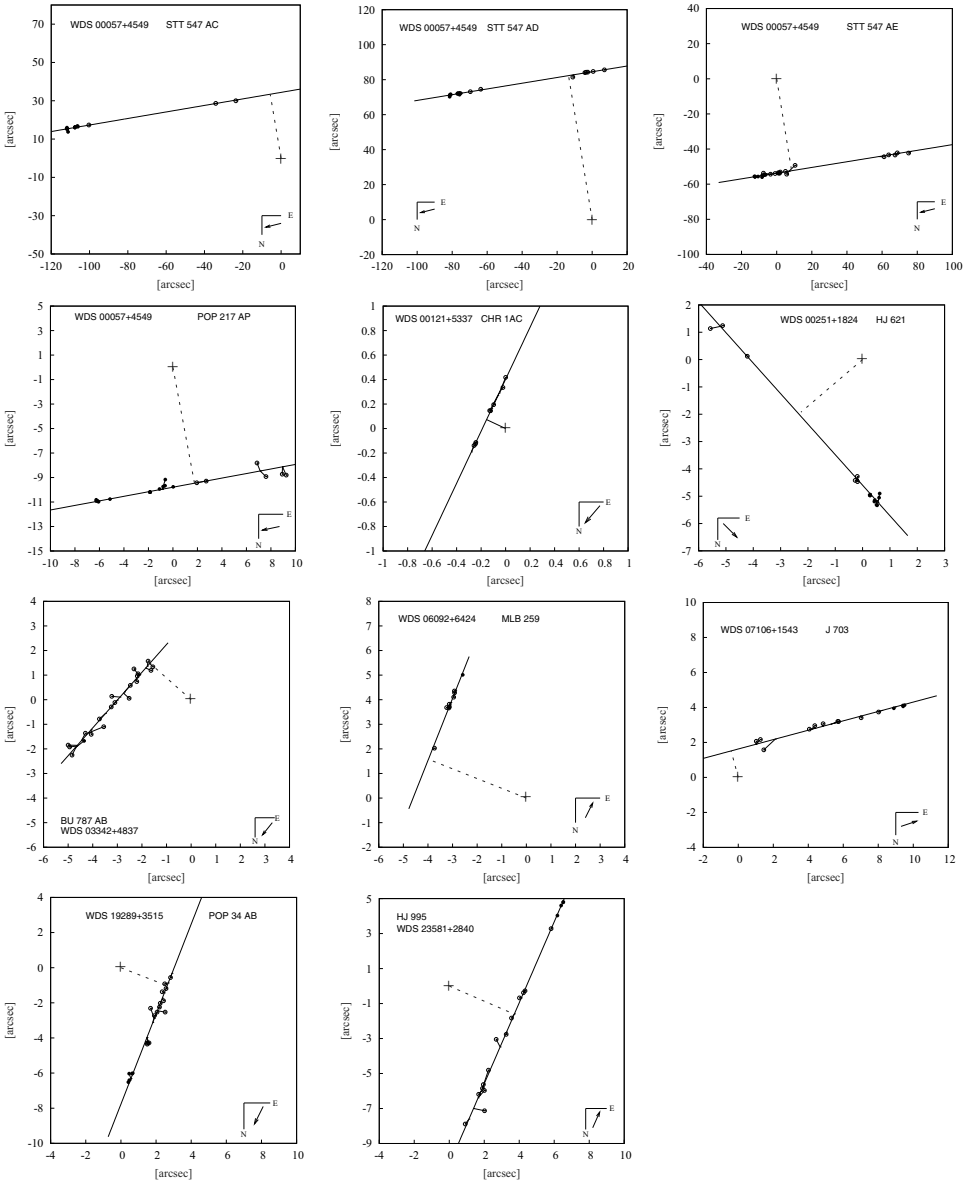

Figure 1: Linear fits for eleven pairs: the arrow at the lower right corner indicates the direction of relative motion of the secondary; the dashed perpendicular line from the linear fit to the origin indicates the closest relative separation. The micrometric observations and photographic measurements are represented by open circles and our CCD measurements are denoted by filled circles.

Our aim is to establish nature of these eleven pairs, i.e. whether they are gravitationally bound or they are mutually very distant in space so that only their projections are close in the field of view.

Table 1: Linear elements, relative velocity and relative proper motion of the eleven double stars.

Pair	X_0 [$''$]	X_A [$''$/yr]	Y_0 [$''$]	Y_A [$''$/yr]	T_0 [yr]	ρ_0 [$''$]	θ_0 [$^\circ$]	V [$''$/yr]	μ_{rel} [$''$/yr]
STT 547 AC	-5.6938	-0.8863	33.4055	-0.1511	1892.05	33.89	189.7	0.899	0.900
STT 547 AD	-13.4829	-0.8802	82.3063	-0.1442	1934.84	83.40	189.3	0.892	0.897
STT 547 AE	8.4875	-0.8836	-52.3353	-0.1433	1988.03	53.02	9.2	0.895	0.887
POP 217 AP	1.7603	-0.8897	-9.4639	-0.1655	2002.88	9.63	10.5	0.905	0.900
CHR 1 AC	-0.1553	-0.0129	0.0731	-0.0274	1991.93	0.17	244.8	0.030	0.040
HJ 621	-2.2541	0.0475	-1.9247	-0.0556	1954.07	2.96	0.1	0.011	0.011
BU 787 AB	-1.6755	-0.0235	1.4820	-0.0266	1881.37	2.24	228.5	0.035	0.037
MLB 259	-3.9808	0.0133	1.5769	0.0335	1910.18	4.28	248.4	0.036	0.055
J 703	-0.4066	0.0840	1.5165	0.0225	1895.17	1.57	195.0	0.087	0.046
POP 34 AB	2.6319	-0.0557	-1.0271	-0.1428	1974.75	2.82	68.7	0.153	0.154
HJ 995	3.7184	0.0434	-1.6069	0.1004	1948.56	4.05	66.6	0.109	0.037

Table 2: Magnitudes, spectral type, components of proper motion and parallax of the eleven pairs.

Pair	m_A	m_B	Sp	$\mu_{\alpha A}\cos\delta$ [$''$/yr]	$\mu_{\delta A}$ [$''$/yr]	$\mu_{\alpha B}\cos\delta$ [$''$/yr]	$\mu_{\delta B}$ [$''$/yr]	π [mas]
STT 547 AC	8.98	12.79	K6	+0.88748	−0.15202	0.	0.	88.44
STT 547 AD	8.98	12.51	K6	+0.88748	−0.15202	+0.003	+0.000	88.44
STT 547 AE	8.98	11.75	K6	+0.88748	−0.15202	+0.012	−0.008	88.44
POP 217 AP	8.98	13.40	K6	+0.88748	−0.15202	0.	0.	88.44
CHR 1 AC	7.25	.	A7Vn-F2V	+0.03846	−0.01120	0.	0.	8.34
HJ 621	10.2	11.4		0.	0.	−0.011	−0.001	-
BU 787 AB	7.38	11.9	B9.5V	+0.01884	−0.03217	0.	0.	3.83
MLB 259	12.1	13.0		+0.005	+0.018	−0.015	−0.033	-
J 703	10.43	12.4		+0.009	−0.017	−0.023	+0.016	-
POP 34 AB	10.63	13.6		+0.072	−0.137	0.001	0.	-
HJ 995	8.80	11.3	K0	−0.021	−0.030	0.	0.	-

To us of interest are X_A and Y_A - the components of the velocity of the secondary with respect to the primary (Table 1) which are used to calculate the velocities V of relative motion.

The basic parameters for our pairs are listed in Table 2. The pair designation is given in Column 1, the apparent magnitudes of the primary m_A and secondary m_B are given in Columns 2 and 3 and the spectral type Sp is given in Column 4. The proper motion in right ascension $\mu_\alpha \cos\delta$ and the proper motion in declination μ_δ are given in Columns 5 and 6 (for the primary A) and in Columns 7 and 8 (for the secondary B). The parallax π is given in the final column. For six pairs the parallax and components proper motion are given in the Hipparcos catalog. The other five pairs do not have parallax and the components of proper motion are given in the WDS catalog.

We can calculate the relative proper motion μ_{rel} for the pairs following this formula

$$\mu_{rel} = \sqrt{(\mu_{\alpha A}\cos\delta - \mu_{\alpha B}\cos\delta)^2 + (\mu_{\delta A} - \mu_{\delta B})^2}\ . \qquad (1)$$

Than, we can compare the proper motion μ_{rel} with the values of the velocity V for all eleven components in linear solutions. An agreement between them is argument in favor that pairs are not gravitationally bound, but they are mutually very distant in space so that only their projections are close in the field of view. As can be seen in Table 1, the values of V and μ_{rel} are in excellent agreement for eight pairs. In the

remaining three pairs there is a disagreement and the reason for that may be unreliably determined components of proper motion for the primary and/or secondary. Also, as can be seen in Table 2, there are no proper motion in right ascension $\mu_\alpha \cos\delta$ and declination μ_δ for all components of the pairs.

3. DETERMINING THE NATURE OF STAR PAIRS

In the consideration of the nature of star pairs we used the minimum separation ρ_0 (Table 1) and the basic parameters given in Table 2.

Four considered pairs, *STT 547 AC, STT 547 AD, STT 547 AE* and *POP 217 AP*, belong to a multiple system registered in ADS - Aitken Double Stars catalogue (Aitken 1932) - as ADS 48. The detailed analysis of the system ADS 48 is given in the paper Cvetković et al. (2012).

CHR 1AC: If for the brighter star one applied the absolute magnitude M_v=2.3 mag, expected on the basis of the spectral type (Gray 2005), the corresponding distance (extinction neglected) would be 98 pc, whereas the given parallax yields 120 pc. From these spectral types the masses are 1.93 and 1.56 solar masses, for the brighter and fainter component, respectively (Gray 2005). Besides, the distance of the brighter component combined with the proper motion yields tangential velocity of almost 23 km s^{-1}, a typical thin-disc star. If the two stars were at 120 pc from the Sun, the minimum separation (0.172 arcseconds) would correspond to 20.64 au. This is a lower limit for the mutual distance only. A semimajor axis of the order of 10^2 au with this total mass would result in a period of a few centuries. Such result is not unexpected for binaries, which means that this pair may be bound. The other well known dynamical criteria (Dommanget 1955a, 1955b; Sinachopoulos and Mouzourakis 1992) lead to a similar conclusion. The reason is the very small minimum separation used in this calculation, but the measurements show a very rapid increase of separation and they fit a straight line very well (Figure 1). Besides, all dynamical criteria apply the same distance for both components, but this can be valid only if they are bound.

HJ 621: Since the parallax is not known for either star, the distance(s) will be estimated from the given data. It is probable that these two stars belong to the thin disc and they are G K dwarfs (main sequence). Let their absolute magnitudes be, say, 5.6 and 6.8. Then the distance would be 83 pc. The proper motion of the brighter star is practically zero, for the fainter one it is small and, with this distance, it would result in a tangential velocity of 4.3 km s^{-1}. This value is rather small, so due to small proper motions these two stars are expected to be significantly farther from the Sun. Nevertheless, it is hard to believe that they are intrinsically very luminous. If they were two A main-sequence stars, the distance to them would be 794 pc, with corresponding masses of 2.34 and 2.04. This distance would agree with their small proper motions (also, note that the parallax is unknown). However, the minimum separation of almost $3''$ at this distance would yield 2353 au. A distance of about 3000 au at the periastron is really too large and even two rather massive stars (supposed total of 4.38 solar masses) could not keep them bound. The probability that this pair is bound seems to be very low. Due to small proper motions the heliocentric distances of these stars may be comparable, but far from to be the same, very likely their mutual distance is of the order of 10^2 pc.

BU 787 AB: From the available data the distance to the brighter star can be calculated, i.e. estimated, in three different ways: from the parallax, by using photometry and by assuming a "reasonable" value for its tangential velocity. The results are: 261 pc, 238 pc (absolute visual magnitude 0.5 mag according to Gray (2005), extinction neglected) and 283 pc (50 km s^{-1}). Thus the distance to this star seems reliable enough. Therefore, it remains to examine if such a distance is acceptable for the fainter star. The fainter star is significantly less bright, by 4.52 mag (Table 2). Thus, at the same distance this must be a G star (G5 - Gray (2005)). The total mass would be: 2.5+1.05=3.55 solar masses. At the given distance (260 pc) the minimum separation results in about 580 au. If these two stars were bound, then their periastron distance would be at least some 700-800 au. Due to this, for an eccentricity of 0.5, one would have a period of about 30 thousand years, a value extremely improbable. In other words, though it is difficult to find strong arguments that the distance found for the brighter star is unacceptable for the fainter one, most likely this pair is not bound and also, the real distance between the stars is rather large.

MLB 259: No parallax value is at our disposal, it is possible to assume a distance value valid for both stars and examine the consequences. Any such value will yield the values for the absolute magnitudes, masses, tangential velocities and finally, via minimum separation, the corresponding distance in projection. This procedure must converge, but if the convergence occurs for a very small distance to the Sun, then such system is likely to be unrealistic. It is difficult to accept a system composed by two substellar objects at, say, 5 pc from the Sun, which both have almost zero heliocentric tangential velocities. These two stars may be bound, but provided that they are at less than 10 pc from the Sun and with tangential velocities almost zero for both. A similar result (13 pc) is obtained by applying Dommanget's criterion. The conclusion is clear, it is highly improbable that this star pair forms a binary. If these stars were really so close to the Sun, at least for one of them there would exist the trigonometric parallax.

J 703: The same procedure is applied as for the preceding pair. The convergence occurs between 10 pc and 20 pc. The application of Dommanget's criterion yields 25 pc as the maximum distance for which they are still bound. For the same reason as in the preceding case this pair is regarded as very improbable to be bound.

POP 34 AB: Since the distance is not available, it can be estimated based on photometry and also tangential velocity of the the brighter star. If the fainter star still belongs to type K (K8), the distance would be 136 pc and tangential velocity of brighter star about 100 km s^{-1}. Perhaps it is closer to the Sun, or it is a thick-disc star. If the former is correct, the fainter component would have to be a low luminosity object, which seems to be against the same distance (Δm about 3 mag). If a distance over 100 pc is realistic for the brighter component, then due to the minimum separation a semimajor axis of the order of 1000 au would be obtained. With assumed masses one would have a period of $\sim 10^4$ years. This pair does not seem to be bound.

HJ 995: If assumed to belong to both main sequence and thin disc, the brighter component would be at a distance of 36.3 pc and tangential velocity of 6.3 km s^{-1}. The same distance applied to the fainter component, if it also is a main-sequence star, according to Gray 2005, yields an absolute magnitude of 8.5 (K8-9); the cor-

responding total mass would be 0.9+0.5=1.4 solar masses. The projected distance for the minimum separation, which corresponds to the assumed heliocentric distance is 147 au. Here one finds no strong arguments against the same distance for both stars. However, the smallest possible periastron distance exceeds 100 au. Therefore, for a not too high eccentricity (say 0.5) a semimajor axis of a few hundreds au is expected. This, combined with the mass values, yields a period of about 12,500 years. A situation similar to the preceding one, very probably not bound.

4. CONCLUSION

The relative coordinates obtained from our CCD frames for the pairs, except for CHR 1 AC, are used in the calculation of linear fits.

There is a good agreement between the relative velocity V obtained from our linear fits and relative proper motion μ_{rel} for almost all pairs. This fact is in favour that these pairs are optical (not gravitationally bound).

This conclusion is strengthened by applying dynamical criteria based on well-known laws (Kepler's third law, energy conservation, etc.).

Acknowledgments

The authors from the Astronomical Observatory in Belgrade gratefully acknowledge the observing grant support from the Institute of Astronomy and Rozhen National Astronomical Observatory, Bulgarian Academy of Sciences. This research has been supported by the Ministry of Education, Science and Technological Development of the Republic of Serbia (Project No 176011 "Dynamics and kinematics of celestial bodies and systems").

References

Aitken, R. G.: 1932, New General Catalogue of Double Stars (Carnegie Inst. Washington, Publ. 417) (ADS).

Cvetković, Z., Novaković, B., Strigachev, A. and Popović, G. M.: 2006, CCD measurements of double and multiple stars at NAO Rozhen. II., *Serb. Astron. J.*, **172**, 53.

Cvetković, Z., Pavlović, R., Strigachev, A., Novaković, B. and Popović, G. M.: 2007, CCD measurements of double and multiple stars at NAO Rozhen. III., *Serb. Astron. J.*, **174**, 83.

Cvetković, Z., Pavlović, R. and Boeva, S.: 2010, CCD measurements of double and multiple stars at NAO Rozhen. IV., *Serb. Astron. J.*, **180**, 103.

Cvetković, Z., Pavlović, R., Damljanović, G. and Boeva, S.: 2011, CCD measurements of double and multiple stars at NAO Rozhen. Orbits and linear fits of 5 pairs, *AJ*, **142**, 73.

Cvetković, Z., Pavlović, R., Ninković, S. and Stojanović, M.: 2012, System ADS 48: Visual binary or multiple system, *AJ*, **144**, 80.

Dommanget, J.: 1955a, Critére de Non-Périodicité du Mouvement Relatie D'un Couple Stellaire Visuel, *Bulletin Astronomique*, **20**, 1.

Dommanget, J.: 1955b, Limites Rationnelles D'un Catalogue D'étoiles Doubles Visuelles *Bulletin Astronomique*, **20**, 183.

Gray, D. F.: 2005, The Observation and Analysis of Stellar Photospheres, (Cambridge: Cambridge Univ. Press).

Pavlović, R., Cvetković, Z., Olević, D., Strigachev, A., Popović, G. M. and Novaković, B.: 2005, CCD measurements of double and multiple stars at NAO Rozhen, *Serb. Astron. J.*, **171**, 49.

Pavlović, R., Cvetković, Z., Boeva, S., Vince, O., and Stojanović, M,: 2013, CCD measurements of double and multiple stars at NAO Rozhen and ASV in 2011. Five linear solutions, *AJ*, **146**, 52.

Sinachopoulos, D. and Mouzourakis, P.: 1992, Searching for optical visual double stars, *Complementary Approaches to Double and Multiple Star Research, ASP Conference Series*, **32**, IAU Colloquium 135, H.A. McAlister and W.I. Hartkopf, Eds., 252.

Proceedings of the IX Bulgarian-Serbian Astronomical Conference: Astroinformatics (IX BSACA) Sofia, Bulgaria, July 2-4, 2014,
Editors: M. K. Tsvetkov, M. S. Dimitrijević, O. Kounchev, D. Jevremović and K. Tsvetkova
Publ. Astron. Soc. "Rudjer Bošković" No 15, 2015, 107-115

BEHAVIOUR OF THE FLOW ON THE BOUNDARY IN THE SYSTEM DISK-CORONA

KRASIMIRA YANKOVA

Space Research and Technology Institute, Bulgarian Academy of Sciences
E-mail: f7@space.bas.bg

Abstract. Evolution on the boundary in the system disk-corona has been considered. We present the main set of boundary distributions of the basic features of the flow. Also, the influence of the structure on stream in the primary component (the hot advection accretion disk), over the arising on the secondary component and, respectively, the development of the corona, have been analyzed.

1. INTRODUCTION

In series of articles we develop one model connected with interaction of field and plasma in the accretion disc. In earlier we presented global model for the radial structure of disk (Iankova, 2009; Yankova and Filipov, 2010; Yankova and Filipov, 2011), and model for the local structure (Yankova 2012b; Yankova and Filipov, 2010; Yankova and Filipov, 2011), as an adaptation of the model for the conditions of emerging corona (Yankova, 2012a; Yankova, 2013). We present in this work the behaviour of the boundary between an accretion disk and emerging corona.

2. MODEL

Model is based on the fundamental equations of the magneto-hydrodynamics of fluids. The basic equations of MHD of accretion - disk flow are: the continuity equation (Eq. 2.1), equation of motion (Eq. 2.2), equation of the magnetic induction (Eq. 2.3), equation of heat balance (Eq. 2.4) and equation of state (2.5).

$$\frac{\partial \rho}{\partial t} + \nabla .(\rho v) = 0 \qquad \nabla . v = 0 \qquad \nabla . B = 0 \tag{2.1}$$

$$\frac{\partial v}{\partial t} + v . \nabla v = -\frac{1}{\rho} \nabla p - \nabla \Phi + (\frac{B}{4\pi\rho} . \nabla) B + \vartheta \ \nabla^2 v \tag{2.2}$$

$$\frac{\partial B}{\partial t} = \nabla \times (v \times B) + \eta \nabla^2 B \qquad \eta = \frac{c^2}{4\pi\sigma} \tag{2.3}$$

$$\rho T \frac{\partial S}{\partial t} - \frac{\dot{M}}{2\pi r} T \frac{\partial S}{\partial r} = Q^+ - Q^- + Q_{mag} \tag{2.4}$$

$$p = p_r + p_g + p_m \tag{2.5}$$

Here v =(v_r, rΩ, v_z) is velocity of flux; ρ - mass density; B =(B_r, B_φ, B_z) - magnetic field; Φ - gravitational potential; p -pressure; $\vartheta = \alpha v_s H$ - kinematical viscosity; $\eta = \alpha_m v_s H$ - magnetic viscosity; α- viscosity coefficient; α_m- magnetic viscosity coefficient; v_s- sound velocity; H-half thickness of the disc; σ - magnetic turbulent conductivity ; T- temperature; S - entropy; $\dot{M}$ - accretion rate; Q_{adv} - advective term; Q^+ - viscosity dissipation; Q_{mag} - magnetic dissipation; Q^- - radiative cooling; p_r – radiative pressure; p_g – gas pressure; p_m – magnetic pressure.

3. BOUNDARY DISTRIBUTIONS

In this paper we use the results from theoretical 3D-model of the disk, as obtained in Iankova (2005); Yankova (2012c), for description of the processes on the boundary and to get the *correct boundary distributions* Eq. (3.1-3.8):

$$f_1(x,H) = \frac{c_1 + c_3}{(1 - c_{12} - c_{14})^4 x^{212}} \left[1 - (x - x_g)\right] + 1 \tag{3.1}$$

$$f_2(x,H) = (9c_{z10} + 2)(1 - c_{12} - c_{14})(x - 1) + 1 \tag{3.2}$$

$$f_3(x,H)=\frac{c_6}{2}(1-c_{12}-c_{14})^4(x^2-1)x^4+\frac{c_{z7}}{3}(1-c_{12}-c_{14})^2(x^3-1)x^2+$$
$$+\frac{c_5}{4}(1-c_{12}-c_{14})^2(x^2-1)+(c_1+c_3)\left(\frac{1-c_5(1-c_{12}-c_{14})^2}{2(1-c_{12}-c_{14})^2x^{12}}\right)(x-x_g-1)+1 \quad (3.3)$$

$$f_5(x,H)=\frac{1+c_4}{3}(1-c_{12}-c_{14})\left(\frac{1}{x^2}-x\right)+1 \quad (3.4)$$

$$f_6(x,H)=(1-c_{12}-c_{14})^{-2}\left[\begin{array}{ll}3\dfrac{2+\alpha c_{z10}}{4c_8x^{17/2}}(x-x_g-1)+ & \dfrac{\alpha c_{10}}{c_8x^{13/2}}\dfrac{1}{(x-x_g)^2}\\ -\dfrac{2ac_{z10}-1}{c_8x^{15/2}}\dfrac{1}{(x-x_g)}+ & \dfrac{\alpha c_{z10}-1}{c_8x^2}\end{array}\right]-$$
$$-\frac{c_1(1-c_{12}-c_{14})^{-4}}{c_8}\left(\frac{1}{x^8(x-x_8)}-\frac{1}{x^4}\right)+\frac{c_{z9}}{3c_8}\left(\frac{1}{x^3}-1\right)+ \quad (3.5)$$
$$+(1-c_{12}-c_{14})^2\frac{1}{2}\left(\frac{1}{x^2}-x^2\right)$$

(3.6)

$$f_7(x,H)=-(1-c_{12}-c_{14})^{-1}\left[\frac{c_3}{c_1}+\frac{c_3}{2c_1c_4}\right]\left(\frac{1}{x^{12}(x-x_g)}-\frac{1}{x}\right)-$$
$$-\frac{c_3(1-c_{12}-c_{14})^{-1}}{c_4c_1}\left(\frac{x^{12}}{(x-x_g)^2}-\frac{1}{x}\right)-\frac{c_{17}(1-c_{12}-c_{14})^{-3}}{c_1}\left(\frac{1}{x^3}-\frac{1}{x^{32}(x-x_g)}\right)+$$
$$+\frac{5+20c_{z10}}{c_1}(1-c_{12}-c_{14})\left(\frac{1}{x}-x\right)-\frac{4c_{z6}}{c_1}\left(\frac{1}{x}-1\right)$$

$$f_8(x,H)=\left(-\frac{c_4+1}{k_0}-\frac{2c_4}{c_{z6}}\right)(x-1)+\frac{(c_1+c_3)}{c_{z6}(1-c_{12}-c_{14})^2x^{12}}(x-x_g-1)-$$
$$-\frac{k_0^2+2}{2k_0(1-c_{12}-c_{14})^2}\left(1-\frac{1}{x^2}\right)+\frac{c_{z5}}{c_{z6}(1-c_{12}-c_{14})^2}\left(\frac{1}{x}-\frac{1}{x^2}\right)+ \quad (3.7)$$
$$+\frac{1+c_4}{(1-c_{12}-c_{14})}\left(1-\frac{1}{x}\right)$$

(3.8)

$$f_9(x,H) = \frac{c_{z3}}{\left(x - x_g\right)} - \frac{c_{z2}(1 - x^{-2})}{2(1 - c_{12} - c_{14})^2} - \frac{c_{z4}(1 - c_{12} - c_{14})^2}{3}(x^3 - 1)x^2 - c_{Z3} + 1$$

Here $f_1(x,H)$, $f_2(x,H)$, $f_3(x,H)$, $f_5(x,H)$, $f_6(x,H)$, $f_7(x,H)$, $f_8(x,H)$, $f_9(x,H)$, are respectively the dimensionless functions of the boundary distributions on the parameters ρ, $\boldsymbol{v}_r$, $\boldsymbol{v}_s$, $\boldsymbol{B}_r$, $\boldsymbol{B}_\varphi$, $\boldsymbol{v}_z$ of the flow, and the coefficients of meeting ω, k_φ, of the boundary in the system disk-corona. The c_i *and* c_{zi} are dimensionless combinations of parameter values at the outer edge of the disc F_{i0} (given in Appendix).

4. RESULTS

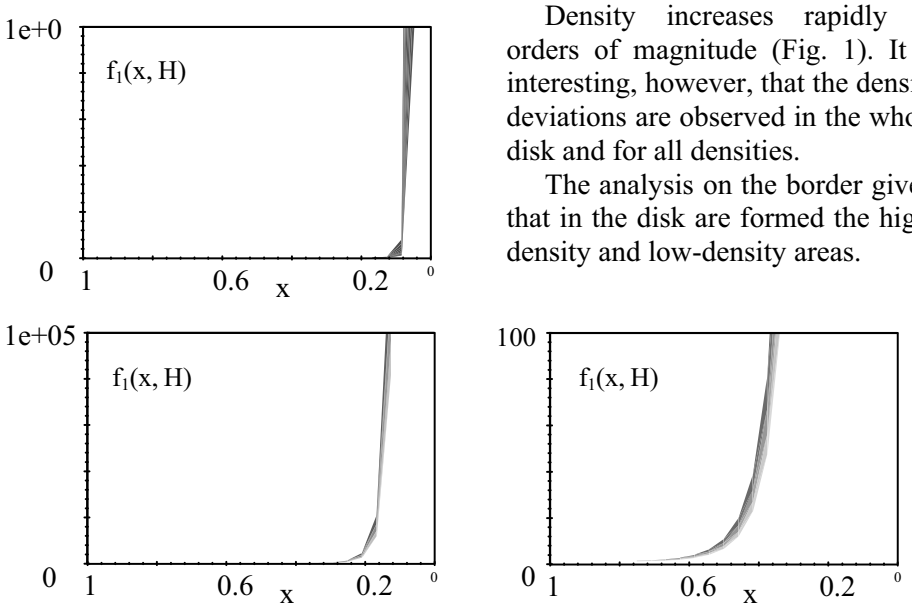

Density increases rapidly in orders of magnitude (Fig. 1). It is interesting, however, that the density deviations are observed in the whole disk and for all densities.

The analysis on the border gives, that in the disk are formed the high-density and low-density areas.

Figure 1: Vertical boundary distributions of the function of the equatorial density.

Equatorial density shows two types of contours. The low-density contours are closed rings. And the high-density contours are open-helices, which follow the angle of the tidal helix (Fig. 2). This can be easily supposed and explained by amenable, movable boundary distributions of the sound and the magneto-sonic speeds (Fig. 3c, d). Mutability of these boundary distributions is caused by the overall interaction between the parameters and the influence of the non-linear effects over them.

These two types of velocities are the most sensitive to the energy exchange and energy distribution in the disk. The mobile maximum and minimum, respectively, create multiple contours of increasing. This behaviour, combined with existing and fast growing magnetic field (Fig. 4) ensure the emergence of compacted regions genetically unrelated to the helices. These are precisely the advective rings that provide heating function of the pad at the base of the corona.

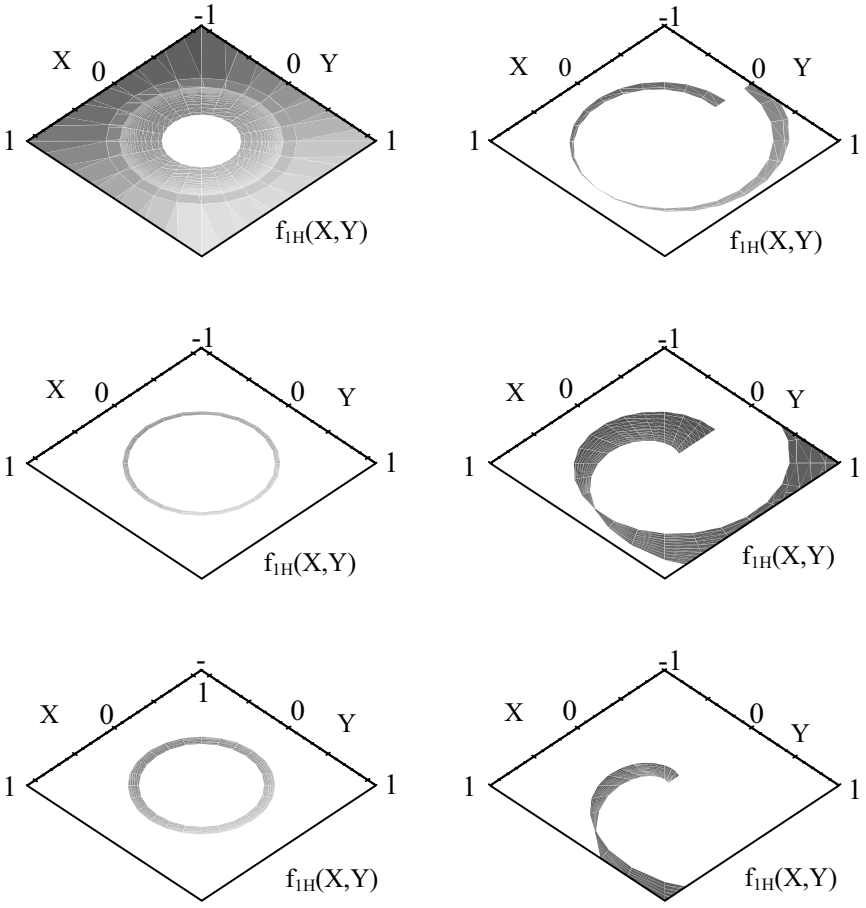

Figure 2: Cylindrical boundary contours of the function of the equatorial density.

The radial and the vertical velocities show typical behaviour along the border (Fig. 3a, b).

Contours of the increase of the radial field (Fig. 5) are not continuous, however, maintains a certain axisymmetry. On one hand, this confirms the presence of the compact regions and on the other, talks about the energy exchange between the components of the field.

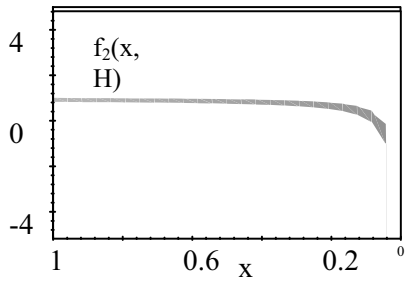

(a) Distribution of the radial velocity.

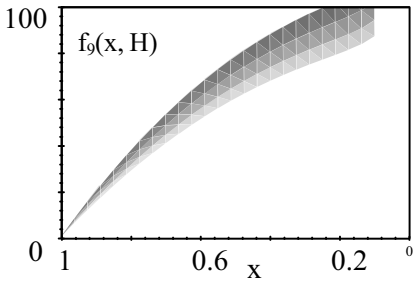

(b) Distribution of the vertical velocity.

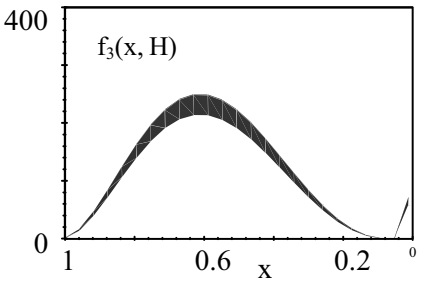

(c) Distribution of the sound velocity.

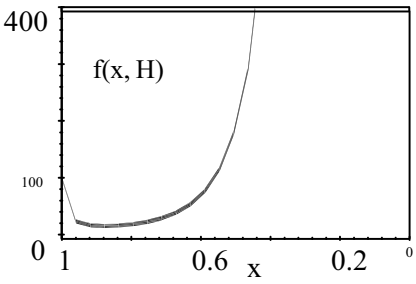

(d) Distribution of the magneto-sonic velocities.

Figure 3: Vertical boundary distributions of the functions of the velocities.

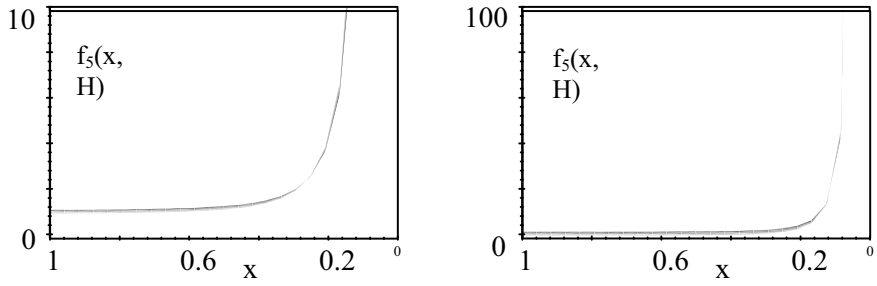

Distributions of the contours of the radial magnetic field.

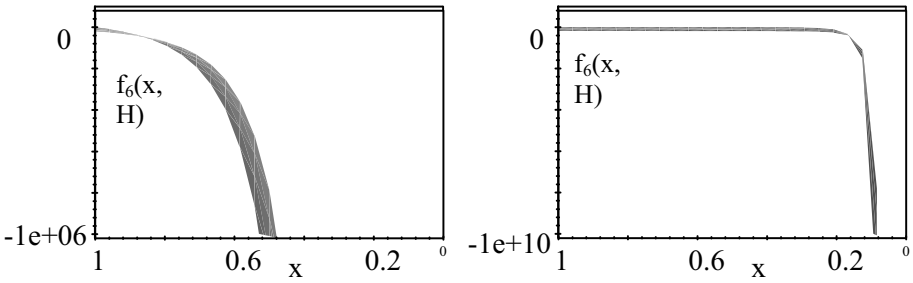

Distributions of the contours of the azimuthal magnetic field.

Figure 4: Vertical boundary distributions of the functions of the magnetic fields.

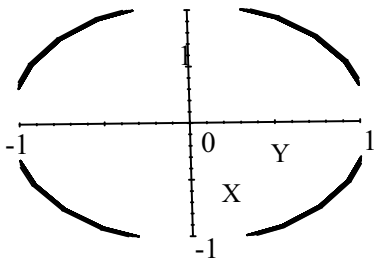

Figure 5: Cylindrical boundary contours of the function of the radial magnetic field.

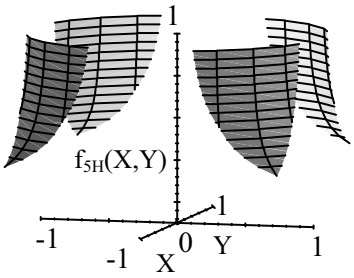

Cylindrical distributions of the boundary function of the radial magnetic field.

5. CONCLUSION

Vertical structure allows correcting the initial distributions $f_i(x, H)$ for the fluid on the boundary disc-corona $f_4(x)$. (On the lower limit of corona such conditions obtained from 2D-structure: $f_i(x, 0)= f_i(x)$ are not suitable because of averaging over z). It complements the 2D-model quality by unfolding descriptive possibilities of the global model as a whole.

Correction is especially important because on the boundary manifest themselves the effects of the warming into the pad:

Tightening of advective rings leads the energy in the form of heat, to the center of the disk. Negative entropy leads to a new state by irreversible conversion and arises corona. The warming into the pad is the major factor that supports the disk's wind and does not allow corona to attenuate (convective coronas shows a cyclic attenuation).

The effect is reinforced by behaviours of the floating extremums of the magneto-sonic and of the sound velocities. They create the necessary environment of the magnetic field to transfer energy between its components - thus creating a permanent instability in the plasma and condition to the self-induction of advection in disk.

These results will allow us in the future when we use the model for real object, to estimate the life cycle of radiative corona that shows such a disc. Also to determine the extent to which the primary component exerts influence on the development of the coronal component of the system.

References

Iankova, Kr. D.: 2005, SSTRI-BAN, SES 2005 proceedings, 30-36.

Iankova, Kr. D.: 2007, 5th Bulgarian-Serbian Conference (V BSCASS): "Astronomy and Space Science", Heron Press Ltd. Science series, pp 326-29. http://aquila.skyarchive.org/5_BSCASS/create/presentations/Iankova.pdf

Iankova, Kr. D.: 2009, Proc. VI Serbian-Bulgarian Astronomical Conference, *Publ. Astr. Soc. "Rudjer Bošković",* **9**, 327-333. http://aquila.skyarchive.org/6_SBAC/pdfs/31.pdf

Yankova, Kr. D.: 2012a, SSTRI-BAN, SENS 2011 proceedings, 73-78. http://www.space.bas.bg/SES2011/Sp-Ph-9.pdf

Yankova, Kr. D.: 2012b, *Publications of the Astronomical Society "Rudjer Boskovic",* **11**, 375-383. http://adsabs.harvard.edu/abs/2012PASRB..11..375Y

Yankova, Kr. D.: 2012c, JUBILEE INTERNATIONAL CONGRESS: SCIENCE, EDUCATION, TECHNOLOGIES "40 YEARS BULGARIA – SPACE COUNTRY ", proceedings, Tom 1, 152-158.

Yankova, Kr. D.: 2013, Proceedings of the VIII Serbian-Bulgarian Astronomical Conference (VIII SBAC), *Publ. Astron. Soc. "Rudjer Bošković",* **12**, 375-381. http://wfpdb.org/ftp/8_SBAC_D1/pdfs/34.pdf

Yankova, Kr., Filipov, L.: 2010, SSTRI-BAN, SENS 2009 proceedings, 370-375.

Yankova, Kr., Filipov, L.: 2011, SSTRI-BAN, SENS 2010 proceedings, 389-394.

APPENDIX

In the table are presented the dimensionless constants in the boundary distributions of the leading parameters of the flow Eq. (3.1-3.8). They were obtained in the process of solving 2D- and 3D-structures of the model on the disk Eq. (3.1-3.8).

$c_1 = \frac{r_0 \omega_0}{v_{r0}}$	$c_2 = \frac{9 v_{s0} H_0}{v_{r0} r_0}$	$c_3 = \frac{\Omega_0 r_0 k_{\phi 0}}{v_{r0}}$
$c_4 = \frac{k_{\phi 0} B_{\phi 0}}{B_{r0}}$	$c_5 = \frac{v_{r0}^2}{v_{s0}^2}$	$c_6 = \frac{k_{\phi 0} B_{\phi 0} B_{r0}}{8 \pi \rho_0 v_{s0}^2}$
$c_7 = \frac{B_{z0} B_{r0} r_0}{8 \pi \rho_0 H_0 v_{s0}^2}$	$c_8 = \frac{B_{r0} B_{\phi 0}}{4 \pi \rho_0 r_0 \Omega_0 v_{r0}}$	$c_9 = \frac{B_{z0} B_{\phi 0}}{4 \pi \rho_0 H_0 \Omega_0 v_{r0}}$
$c_{10} = \frac{v_{s0} H_0}{v_{r0} r_0}$	$c_{11} = \frac{2 v_{s0} r_0}{v_{r0} H_0}$	$c_{12} = \frac{2 \rho_0 v_{s0}^2}{3 B_{z0} B_{r0}}$
$c_{13} = c_{10} k_{\phi 0}$ $c_{16} = c_{10} k_{\phi 0}^2$	$c_{14} = \frac{2 \rho_0 r_0^2 \Omega_0^2}{3 B_{z0} B_{r0}}$	$c_{15} = \frac{r_0 B_{z0}}{H_0 B_{r0}}$
$c_{17} = \frac{\Omega_0 r_0^2 B_{z0}}{v_{r0} H_0 B_{\phi 0}}$	$c_{z1} = \frac{v_{z0}}{v_{r0}}$	$c_{z2} = \frac{v_{s0}^2}{v_{r0} v_{z0}}$
$c_{z3} = \frac{\Omega_0^2 r_0^2}{v_{r0} v_{z0}}$	$c_{z4} = \frac{3 B_{z0} B_{r0}}{4 \pi \rho_0 v_{r0} v_{z0}}$	$c_{z5} = \frac{B_{z0}}{B_{r0}}$
$c_{z6} = c_{z10} k_{\phi 0}$	$c_{z7} = \frac{B_{z0} B_{r0}}{8 \pi \rho_0 v_{s0}^2}$	$c_{z9} = \frac{B_{z0} B_{\phi 0}}{4 \pi \rho_0 v_{r0} \Omega_0 r_0}$
$c_{z10} = \frac{v_{s0}}{v_{r0}}$	$c_{z16} = \frac{k_{\phi 0} v_{s0} B_{r0}}{v_{r0} B_{\phi 0}}$	$c_{z17} = \frac{\Omega_0 r_0 B_{z0}}{v_{r0} B_{\phi 0}}$

The constants here are dimensionless combinations of initial values of the leading parameters on the outer edge of the disk: r_0- outer radius; v_{r0} is the initial radial velocity of flux; Ω_0- initial angular velocity; v_{z0}- initial vertical velocity; v_{s0}- initial sound velocity; H_0- initial half thickness of the disc; ρ_0 – initial equatorial mass density; B_{r0} $B_{\varphi 0}$ B_{z0} – components magnetic field; ω_0- and $k_{\varphi 0}$- the coefficients of meeting, too.

Proceedings of the IX Bulgarian-Serbian Astronomical Conference: Astroinformatics (IX BSACA) Sofia, Bulgaria, July 2-4, 2014,
Editors: M. K. Tsvetkov, M. S. Dimitrijević, O. Kounchev, D. Jevremović and K. Tsvetkova
Publ. Astron. Soc. "Rudjer Bošković" No 15, 2015, 117-126

MULTI-WAVELENGTH OBSERVATIONS OF AN ERUPTIVE PROMINENCE ON 7 AUGUST 2010

MOMCHIL DECHEV, KOSTADINKA KOLEVA, PETER DUCHLEV and NIKOLA PETROV

Institute of Astronomy, Bulgarian Academy of Sciences
E-mail: mdechev@astro.bas.bg, koleva@astro.bas.bg, duchlev@astro.bas.bg

Abstract. We aim to investigate the morphology and kinematic evolution of a helically-twisted quiescent prominence. The kinematic pattern during the main stages of prominence eruption were studied, using data from both ground-based and space born observatories. The prominence environment and related activity was also considered.

1. INTRODUCTION

The observations show that the eruptive phenomena, such as prominence/filament eruptions, coronal mass ejections (CMEs) and flares are often physically related to each other by the same magnetic flux rope (MFR) occurring in the solar atmosphere (e.g., Gilbert et al. 2000; Gopalswamy et al. 2003; Schrijver et al. 2008; Filippov and Koutchmy 2008). This relation is better expressed between eruptive prominences (EPs) and CMEs. Being one of the earliest known forms of mass ejections from the Sun, EPs started to receive attention in the late 1800s (see Tandberg-Hanssen 1995). Coronagraph observations reveal that CMEs generally have a three-part structure: a bright leading front, a dark cavity, and an inner bright core (e.g. Illing and Hundhausen 1983; Chen et al. 2011). The cavity is usually believed to be a helical flux rope (e.g., Gibson et al. 2006; Riley et al. 2008) and the bright core is thought to be cool prominence/filament matter that is suspended in magnetic dips of a flux rope configuration (e.g., Guo et al. 2010; Jing et al. 2010).

The aforementioned specific physical relationship between EPs and CMEs suggests that the study of the EPs can provide critical clues not only to the prominence activity, but also to the physics of CMEs. Moreover, their study has indicated that the triggering mechanism is related to an unstable MFR (Rubio da Costa et al. 2012 for a review). The observations indicate that the temporal evolution of these phenomena and especially the role played by prominence activation and eruption can be significantly different from event to event (e.g. Sterling and Moore 2005; Wang et al. 2007; Liu et al. 2009; Zuccarello et al. 2009). Therefore, a detailed examination of the kinematic patterns of EP and its triggering mechanism may advance our ability to predict the launch of CME, will the CME be fast or slow etc. Such prediction is

one of the most important subjects in the field of space weather, because the ejections of CMEs from the Sun lead to a significant disturbance of the magnetosphere and affect human technologies and life.

Erupting prominences/filaments are sometimes observed to undergo a rotation about the vertical direction as they rise (e.g. Kliem et al. 2012; Su and van Ballegooijen 2013; Yan et al. 2014 for reviews). Several types of rotating motion of the EP MFR were found out. Rotating magnetic structures driven by underlying photospheric vortex flows were observed by several authors (e.g. Zhang et al. 2011; Wedemeyer - Böhm et al. 2012; Yan et al. 2013). The rotation about the vertical direction and non-radial motion of solar filaments were often observed during their eruptions (e.g. Ji et al. 2003; Green et al. 2007; Jiang et al. 2009; Liu and Alexander 2009; Thompson 2011; Bi et al. 2013). This filament rotation is interpreted as a conversion of twist into writhe in a kink-unstable flux rope. Therefore, MHD helical-kink instability is often taken to be the primary trigger of these eruptions (Fan and Gibson 2007; Török et al. 2010; Kliem et al. 2012). The prominence-related rotation phenomenon was named as giant tornadoes, which were recently concerned due to high-quality observational data of SDO (Li et al. 2012; Su et al. 2012; Wedemeyer et al. 2013; Panesar et al. 2013).

Magnetic reconnection with the ambient field can also cause filament rotation during eruption (Cohen et al. 2010; Thompson 2011). The aforementioned filament rotations should be distinguished from the rotation of the filament around its own axis, namely the "roll effect" (Martin 2003; Panasenco et al. 2011), i.e., the top of the prominence spine gradually bends to one side of the spine during the rise of the filament. This sideways rolling creates twist of opposite sign in the two prominence legs as the prominence continues to rise.

In this paper, we address these issues in analyzing the multi-wavelength observations of an eruptive prominence on 7 August 2010, which showed strong rotational motions during the eruption. We treat an EP and the associated CME as different parts of a flux rope with specific assumed geometrical relationships among the EP, CME, and flux rope. Multi-wavelength observations allow us to investigate the behavior of features of the EP MFR kinematic and geometrical evolution, which helps address whether and in what conditions the eruption of the prominence plays an active role in CME occurrence.

2. OBSERVATIONAL DATA

The eruptive prominence (EP) occurred on the southwestern limb at a mean PA of 255 deg – S15W90 in a quiet Sun region.The observations of the EP on 7 August 2010 used in the present study include the following observations and data.

1. Limb H_α line-center (6563 Å, 1.8 Å bandpass) images by the coronagraph in the National Astronomical Observatory (NAO) - Rozhen, Bulgaria. The resolution of the H-alpha filtergrams is about 2". The images were obtained with a digital camera CANON EOS 350D (8 Mpx). The registered images, at maximal camera resolution, have size of 3456 x 2304 px and one pixel have size of 6.4 x 6.4 μm. The observations of the EP were made between 4:55 UT and 12:47 UT. For this period we have 82 frames. Unfortunately only 21 frames were usable in the time interval 5:05 UT –

12:02 UT. This gives us a bad average cadence of 20 min per frame. The cadence does not allow deriving well kinematic parameters of the eruption and can be used only for illustrative purposes (Fig. 1).

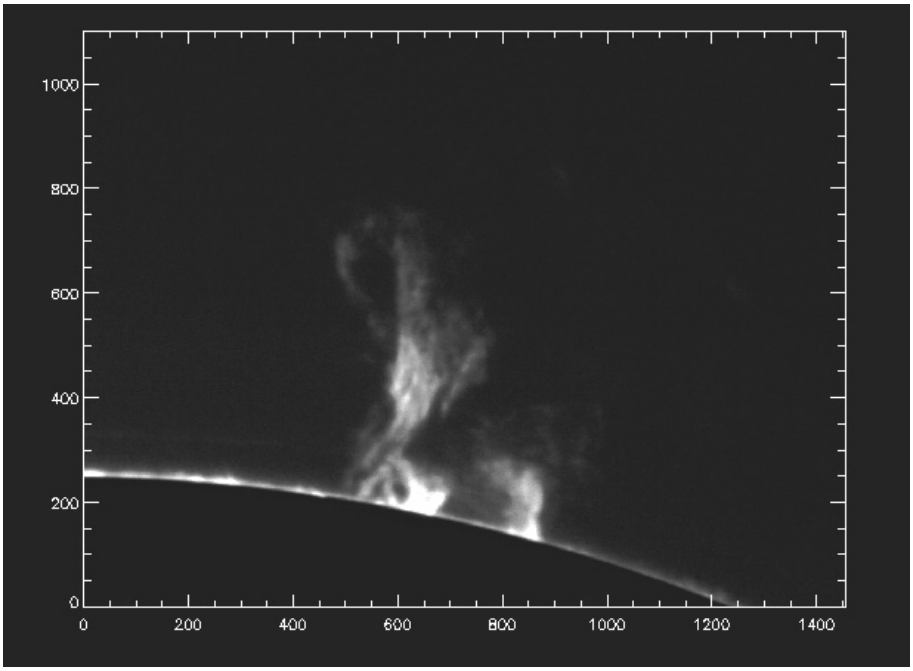

Figure 1: H-alpha image of EP observed at National Astronomical Observatory – Rozhen on 07 August 2010.

2. Full-disk EUV 304 Å high-resolution observations from Solar Dynamics Observatory (SDO: Pesnell et al. 2012)/Atmospheric Imaging Assembly (AIA: Lemen et al. 2012) that provide the opportunity to study the detailed morphological changes in the EP MFR during the development of the EP rotational motion.

3. LASCO C2 white-light coronagraph data (Brueckner et al. 1998) of the Solar and Heliospheric Observatory (SOHO: Brueckner et al. 1995) that cover the range 2-6 solar radii were available for the associated CME.

4. The Extreme-Ultraviolet imager (EUVI: Howard et al. 2008) imaging package onboard the Solar-Terrestrial Relations Observatory (STEREO: Kaiser et al. 2008) also observed this eruption. STEREO-A (Ahead) viewed this event as filament eruption on the solar disk. The separation angle between the twin STEREO spacecraft was about 171°.

2. 1. H-ALPHA

The eruptive prominence (EP) was observed on the southwestern limb at a mean PA of 255 deg – S15W90 in a quiet Sun region. The prominence was observed in National Astronomical observatory – Rozhen by a 15-cm coronagraph with H-alpha filter (1.8 Å bandpass). The resolution of the H-alpha filtergrams is about 2". The images were

obtained with adigital camera CANON EOS 350D (8 Mpx). The registered images, at maximal camera resolution, have size of 3456 x 2304 px and one pixel have size of 6.4 x 6.4 μm.

The observations of the EP were made between 4:55 UT and 12:47 UT. For this period we have 82 frames. Unfortunately only 21 frames were usable in the time interval 5:05 UT – 12:02 UT. This gives us a bad average cadence of 20 min per frame. The cadence does not allow to derive well kinematic parameters of the eruption and can be used only for illustrative purposes (Fig. 1).

2. 2. SDO - AIA

To trace and study the development of the eruption we used the data from SDO (Solar Dynamic Observatory) mission.

SDO mission is part of NASA's Living With a Star (LWS) Program, a program designed to understand the causes of solar variability and its impacts on Earth (http://sdo.gsfc.nasa.gov). SDO supports three scientific experiments:

- Atmospheric Imaging Assembly (AIA);
- EUV Variability Experiment (EVE);
- Helioseismic and Magnetic Imager (HMI);

Each of these experiments performs several measurements, witch show us how and why the Sun varies. The AIA images the solar sphere in multiple wavelengths. Data includes images of the Sun in 10 wavelengths every 10 seconds.

The AIA consists of seven Extreme Ultra-Violet (EUV) and three Ultra-Violet (UV) channels, which provide an unprecedented view of the solar corona with an average cadence of ∼12 s. The AIA image field-of-view reaches 1.3 solar radii with a spatial resolution of ∼1.5". We used level 1 reduced data, i.e. with the dark current removed and the flat-field correction applied. The images were further processed using the standard SolarSoftware procedures.

For the present study we used images (Fig. 2) taken with 1 min cadence in the He II 304 Å and 193 Å passband of AIA/SDO (Lemen et al.,2011). In 193 Å wavelength eruption is not visible and we selected the 304 Å wavelength to work with.

One can see that 304 Å data started 07:30 UT and at ended at 10:59 UT, so a part of the eruption development is not presented.

We also analyzed observations from the Extreme Ultraviolet Imager (EUVI) onboard STEREO Ahead (A) spacecraft. EUVI has a field-of-view of $1.7R_{\odot}$ and observes in four spectral channels (He II 304 Å, Fe IX/X 171 Å, Fe XII 195 Å and Fe XIV 284 Å) that cover the 0.1 to 20 MK temperature range (Wuelser et al., 2004). The EUVI detector has 2048×2048 pixels^2 size and a pixel size of 1.6".

We used images in the He II 304 Å channel with an average cadence of 10 minutes, taken between 07:06 and 12:56 UT.

The separation angle between the two STEREO spacecrafts (A and B) at the time of observation was 150.541 deg.

Images obtained by the Large Angle and Spectrometric Coronagraph (LASCO)/C2 onboard SOHO, whose field-of-view extends from 2 to 6 solar radii (Brueckner, 1995) were also analyzed.

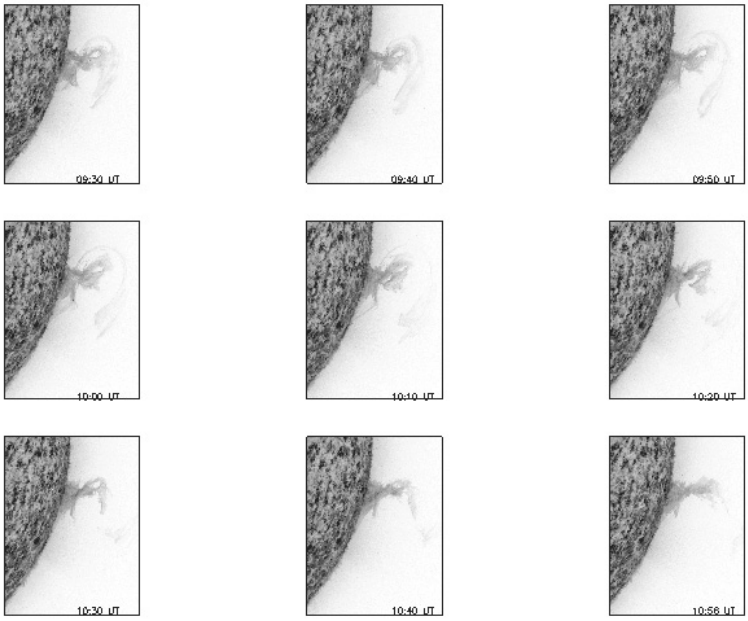

Figure 2: AIA data prominence eruption sequence EP, observed on 07 August 2010 at 304 A. Courtesy of NASA/SDO and the AIA, EVE, and HMI science teams.

3. KINEMATICS

The prominence eruption evolved as a two height-expanding helically twisted magnetic flux ropes with both legs anchored in the quiet Sun region. The main prominence flux ropes was composed of thin magnetic tubes filled with prominence plasma. In the early stages of the eruption the prominence appears to be very dense and one cannot still distinguish any fine structure. During the eruption the prominence body rise and untwist and its small-scale structure becomes visible.

We determined the height of the main prominence flux ropes as well as the height of the projection of the cross point between its legs (Fig. 3). The prominence height was determined as the height of the main axis of the prominence above the visible limb as observed in the He II 304 Å channel of the AIA/SDO images (Fig. 2).

As one can see in the height time diagram (Fig. 4), from 07:31 to 10:59 UT the height of the top prominence loop increase from 180 Mm to 270 Mm with mean velocity of about 8.84 km/s. The velocity was derived with error of $\pm 0.34\ km/s$ from the linear fit of the height-time diagram.

After 10:59 UT the top of the prominence loop quits the AIA FOV During this raising any lift off of the prominence material in to the space was not observed. The prominence eruption was accompanied by a significant untwisting of the main prominence flux ropes.

The height of the bottom prominence loop was measured from 08:30 UT to 10:59 UT. The height-time profile for this part of the prominence body shows similar

behavior as the top loop. The height increase from 190 to 225 Mm with a velocity of about 3.4 km/s (derived with error of ±0.41 km/s).

As regards the projection of the crossing-point of prominence body, it does not change its position during the eruption (Fig. 4).

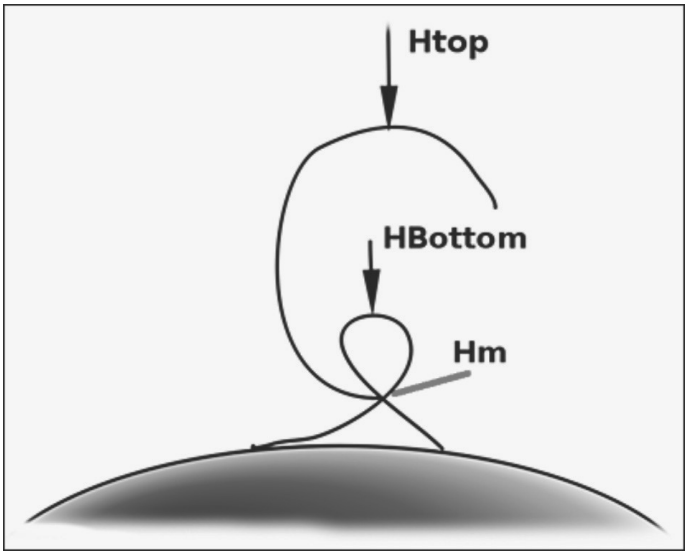

Figure 3: Simple sketch of prominence eruption.

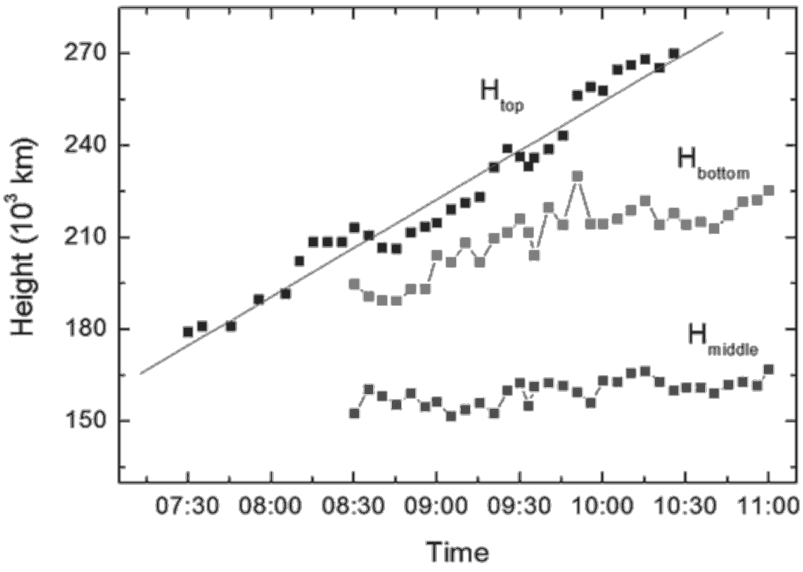

Figure 4: Height-time diagram of the prominence eruption.

4. DISCUSSION

The prominence eruption more often is a result of some kind of instability. A clear sign for magnetohydrodynamic (MHD) instability is the development of helical shape in the course of the eruption (Rust and LaBonte 2005). The Magnetic Flux Rope (MFR) becomes kink-instable when the twist exceeds a critical value of 2π (Hood and Priest 1981, Török and Kleim 2005).

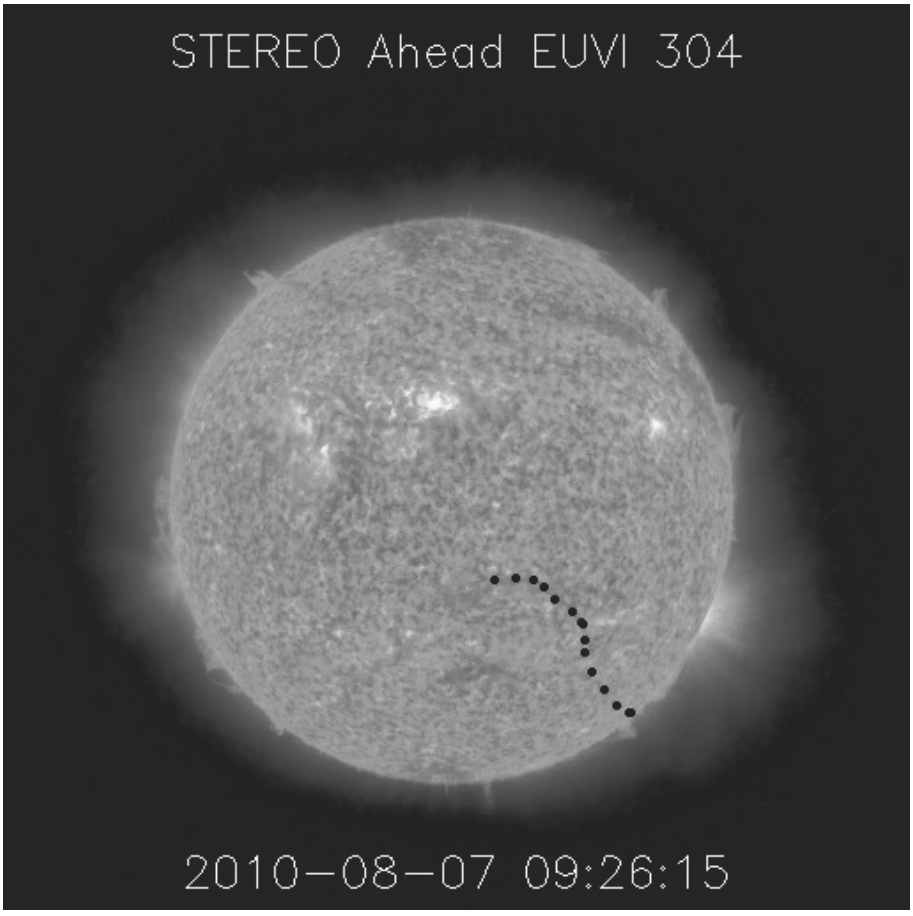

Figure 5: STEREO A/EUVI 304 Å image with traced filament that is the source of the EP on 7 August 2010.

Kink instability was suggested as the trigger of prominence eruption by Sakurai (1976) and later by Török and Kleim (2005) and Fan (2005).

It is difficult to prove observationally the kink instability as a main trigger of prominence destabilization because the helicity can force a flux rope to writhe without any instability occurring (Gilbert et al. 2007 and references therein).

In our case it is well seen on Fig. 1 the helical shape twist of the erupting prominence. So, it is probable that the eruption is due to kink instability. The trigger for development of such instability may be a new emerging flux below the prominence MFR or a propagating disturbance outside the MFR.

There is no sign of new emerging flux in our case, moreover as we see in Fig. 4 the middle point does not change its heights as it should does if an emerging flux push the PMS from below. On the other hand looking at STEREO A/EUVI 304 Å images we can trace the geometrical evolution of the associated filament (Fig. 5) that is the source of the EP at the limb.

The geometrical pattern of the filament and its evolution presented in Figure 6 reveal several specific features of the filament eruption, which throw light on the intricate picture of the EP at the limb.

1. Two neighbor filament segments are undergone eruption. They are located in the eastern part of the filament traced in Figure 5. Therefore, there are two erupted MFRs corresponding of the two filament segments in the event on 7 August 2010.

2. As can see in Figure 6, the MFR of the western segment is located above a part of the eastern one. So, the western MFR correspond to the top one presented in Figure 3, while the eastern MFR correspond to the bottom one in Figure 3.

3. The western MFR erupts more rapidly than the eastern one. At 10:46 UT, when western MFR show well visible kinked loop (Figure 6, central frame), the eastern MFR shows visible rising.

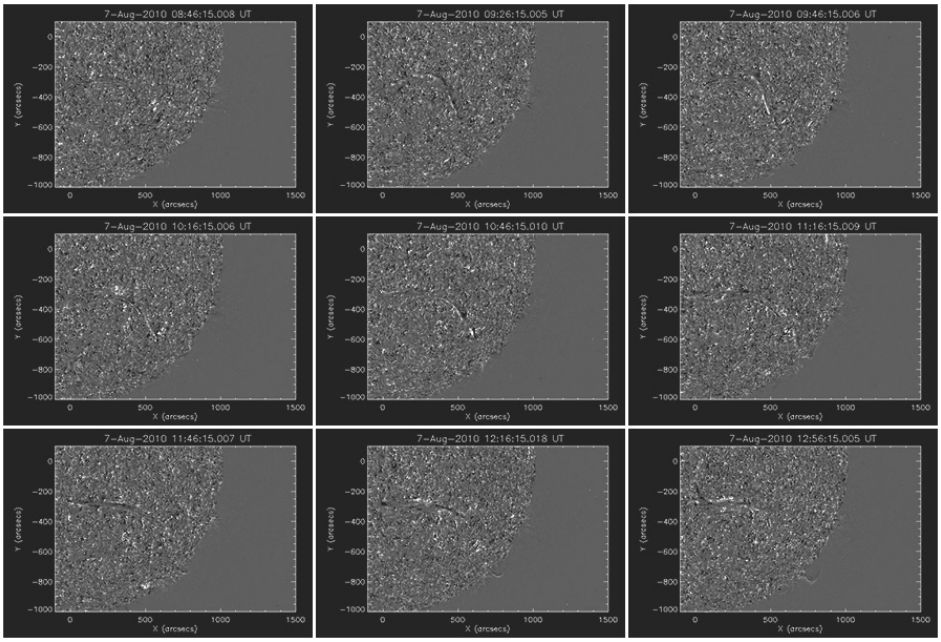

Figure 6: A sample of cropped STEREO A/EUVI 304 Å images showing the evolution of the filament eruption between 09:46 and 12:56 UT.

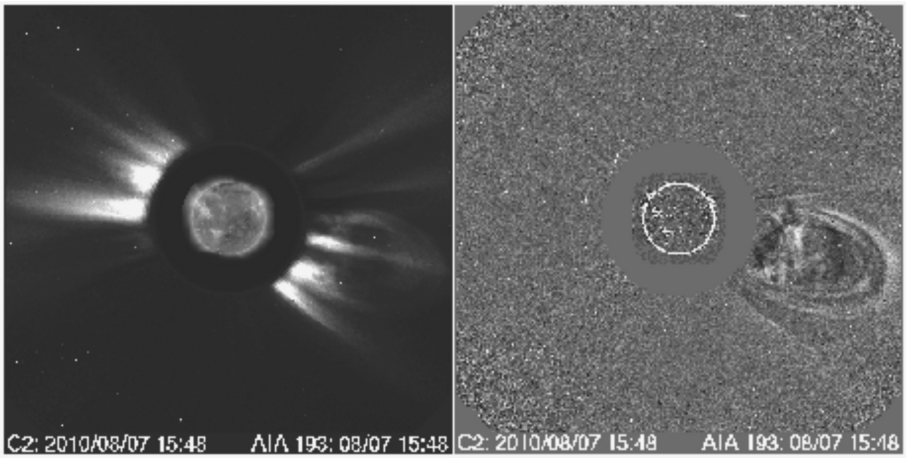

Figure 7: The associated CME, which was registered by LASCO/C2 coronagraph on board on SOHO.

4. At 12:56 UT, when the top of western MFR is escaped the STEREO/EUVI field of view, the eastern MFR shows well visible normal S-shape, which is evident signature for kink-induced process of eruption (Leamon et al. 2003, Kliem et al. 2004, Leka et al. 2005). Moreover, as can see in NAO – Rozhen and SDO/AIA images, at this time the bottom MFR shows well developed kinked loop at the limb. The analysis of the NO)-Rozhen $H\alpha$, SDO/AIA 304 A, and STEREOA/EUVI 304 Å data reveal an interesting case of two neighbor filament segments eruption. One of them (western) actively participates in the eruptive evolution of the large-scale MFR that produce CME (Figure 7). Another one (eastern MFR) shows behavior of confined eruption. The superimposing of the projections of these two MFRs on the sky plane creates the intricate picture of the EP on 7 August 2014 at the limb.

The EP was associated with a large CME, which was registered by LASCO/C2 coronagraph on board on SOHO. The CME first appearance in C2 field of view was in 11:00 UT. The CME was centered in PA of 250 deg, and propagated with average linear speed of 288 km/s.

Acknowledgements

The authors are grateful to SDO/AIA, SOHO/LASCO, and STEREO/EUVI teams for providing the wonderful data.

References

Bi, Y., Jiang, Y., Yang, J., Zheng, R., Hong, J., Li, H., Yang, D., Yang, B.: 2013, *ApJ*, **773**, 162.
Brueckner, G. E., et al.: 1995, *Sol. Phys.*, **162**, 357.
Bruekner, G. E., et al.: 1998,*Geophys. Res. Lett.*, **25**, 3019.
Cheng, X., Zhang, J., Liu, Y., Ding, M. D.: 2011, *ApJL*, **732**, 25.
Cohen, O., Attrill, G. D. R., Schwadron, N. A., et al.: 2010, *JGRA*, **115**, 10104.
Fan, Y., Gibson, S. E.: 2007, *ApJ*, **668**, 1232.
Fan, Y.: 2005, *ApJ*, **630**, 543.

Filippov, B. P., Koutchmy, S.: 2008, *Ann. Geophys.*, **26**, 3025.
Gibson, S. E., Foster, D., Burkepile, J., de Toma, G., Stanger, A.: 2006, *ApJ*, **641**, 590.
Gilbert, H. R, Alexander, D., Liu, R.: 2007, *Sol. Phys.*, **245**, 287.
Gilbert, H. R., Holzer, T. E., Brukerile, J. T., Hundhausen, A. J.: 2000, *ApJ*, **537**, 503.
Gopalswamy, N., Shimojo, M., Lu, W., et al.: 2003, *ApJ*, **586**, 562.
Green, L. M., Kliem, B., Török, T., van Driel-Gesztelyi, L., Attrill, G. D. R.: 2007, *Sol. Phys.*, **246**, 365.
Guo, Y., Schmieder, B., Démoulin, P., et al.: 2010, *ApJ*, **714**, 343.
Hood, A. W., Priest, E. R.: 1981, *Geophys. Astrophys. Fluid Dyn.*, **17**, 297.
Howard, R. A., Moses, J. D., Vourlidas, A., et al.: 2008, *Space Sci. Rev.*, **136**, 67.
Illing, R. M. E., Hundhausen, A. J.: 1983, *JGR*, **88**, 10210.
Ji, H., Wang, H., Schmahl, E. J., Moon, Y. J., Jiang, Y.: 2003, *ApJ*, **695**, L135.
Jiang, Y., Yang, J., Zheng, R., Bi, Y., Yang, X.: 2009, *ApJ*, **693**, 1851.
Jing, J., Yuan, Y., Wiegelmann, T., et al.: 2010, *ApJL*, **719**, 56.
Kaiser, M. L., Kucera, T. A., Davila, J. M., et al.: 2008, *Space Sci. Rev.*, **136**, 5.
Kliem, B., Török, T., Thompson, W. T.: 2012, *Sol. Phys.*, **281**, 137.
Kliem, B., Titov, V. S., Török, T.: 2004,*A&A*, **413**, L23.
Leamon, R. J., Canfield, R. C., Blehm, Z., Pevtsov, A. A.: 2003, *ApJ*, **596**, L255.
Leka, K. D., Fan, Y., Barnes, G.: 2005, *ApJ*, **626**, 1091.
Lemen, J. R., Title, A. M., Akin, D. J., et al.: 2012, *Sol. Phys.*, **275**, 17.
Lemen, J. R., Title, A. M., Akin, D. J. et al.: 2011, *Sol.Phys.*, **172**.
Li, X., Morgan, H., Leonard, D., Jeska, L.: 2012, *ApJ*, **752**, L22.
Liu, C., Lee, J., Karlický, M., Prasad Choudhary, D., Deng, N., Wang, H.: 2009, *ApJ*, **703**, 757.
Liu, R., Alexander, D.: 2009, *ApJ*, **697**, 999.
Martin, S. F.: 2003, *AdSpR*, **32**, 1883.
Panasenco, O., Martin, S., Joshi, A. D., Srivastava, N.: 2011, *JASTP*, **73**, 1129.
Panesar, N. K., Innes, D. E., Tiwari, S. K., Low, B. C.: 2013, *A&A*,**549**, 105.
Pesnell, W. D., Thompson, B. J., Chamberlin, P. C.: 2012, *Sol. Phys.*, **275**, 3.
Riley, P., Lionello, R., Mikić, Z., Linker, J.: 2008, *ApJ*, **672**, 1221.
Rubio da Costa, F., Zuccarello, F., Fletcher, L., Romano, P., Labrosse, N.: 2012, *A&A*, **539**, 27.
Rust, D. M., LaBonte, B. J.: 2005, *ApJ*, **622**, L69.
Sakurai, T.: 1976, *PASJ*, **28**, 177.
Schrijver, C. J., Elmore, C., Kliem, B., Török, T., Trrle, A. M.: 2008, *ApJ*, **674**, 586.
Sterling, A. C., Moore, R. L.: 2005, ApJ, **630**, 1148.
Su, Y. ,Wang, T., Veronig, A., Temmer, M., Gan, W.: 2012, *ApJ*, **756**,41.
Su, Yingna, van Ballegooijen, Adriaan: 2013, *ApJ*, **764**, 91.
Tandberg-Hanssen, E.: 1995, The Nature of Solar Prominences (Dordrecht: Kluwer)
Thompson, W. T.: 2011, *JASTP*, **73**, 1138.
Török, T., Berger, M. A., Kliem, B.: 2010, *A&A*, **516**, 49.
Török, T., Kliem, B.: 2005, *ApJ*, **630**, L97.
Wang, H., Liu, C., Jing, J., Yurchyshyn, V.: 2007, *BAAS*, **38**, 214.
Wedemeyer - Böhm, S., Scullion, E., Steiner, O., Rouppe van der Voort, L., et al.: 2012, *Nature*, **486**, 505.
Wedemeyer, S., Scullion, E., Rouppe van der Voort, Luc, Bosnjak, A., Antolin, P.: 2013, *ApJ*, **774**, 123.
Wuelser, J.-P., Lemen, J. R., Tarbell, T. D, et al.,: 2004, in **SPIE Conf.**, ed. S. Fineschi & M. A. Gummin, **5171**, 111.
Yan, X. L., Pan, G. M., Liu, J. H., Qu, Z. Q., Xue, Z. K., Deng, L. H., Ma, L., Kong, D. F.: 2013, *AJ*, **145**, 153.
Yan, X. L., Xue, Z. K., Liu, J. H., Ma, L., Kong, D. F., Qu, Z. Q., Li, Z.: 2014, *ApJ*, **782**, 67.
Zhang, J., Liu, Y.: 2011, ApJ, **741**, L7.
Zuccarello, F., Romano, P., Farnik, F., Karlický, M., et al.: 2009, *A&A*, **493**, 629.

Proceedings of the IX Bulgarian-Serbian Astronomical Conference: Astroinformatics (IX BSACA) Sofia, Bulgaria, July 2-4, 2014,
Editors: M. K. Tsvetkov, M. S. Dimitrijević, O. Kounchev, D. Jevremović and K. Tsvetkova
Publ. Astron. Soc. "Rudjer Bošković" No 15, 2015, 127-135

ATMOSPHERIC, OCEANIC AND GEOMAGNETIC EXCITATION OF NUTATION

CYRIL RON[1], JAN VONDRÁK[1] and YAVOR CHAPANOV[2]

[1]*Astronomical Institute, Academy of Sciences of the Czech Republic*
Prague, Czech Republic
E-mail: ron@asu.cas.cz, vondrak@ig.cas.cz
[2]*National Institute of Geophysics, Geodesy and Geography,*
Bulgarian Academy of Sciences, Sofia, Bulgaria
E-mail: astro@bas.bg

Abstract. We tested the hypothesis of Malkin (2013), who recently demonstrated that the observed changes of Free Core Nutation parameters (phase, amplitude) occur near the epochs of geomagnetic jerks (rapid changes of the secular variations of geomagnetic field). We found that if the numerical integration of Brzezinski broad-band Liouville equations of atmospheric/oceanic excitations is re-initialized at the epochs of geomagnetic jerks, the agreement between the integrated and observed celestial pole offsets is improved (Vondrák & Ron 2014). Nevertheless, this approach assumes that the influence of geomagnetic jerks leads to a stepwise change in the position of celestial pole, which is physically not acceptable. Therefore we introduce a simple continuous excitation function that hypothetically describes the influence of geomagnetic jerks, and leads to rapid but continuous changes of pole position. The results of numerical integration of atmospheric/oceanic excitations plus this newly introduced excitation are then compared with the observed celestial pole offsets, and prove that the agreement is improved significantly.

1. INTRODUCTION

Atmospheric and oceanic excitations play dominant role in polar motion and rotational velocity of the Earth. As we demonstrated in our paper Vondrák & Ron (2010), thanks to the new precession/nutation model IAU2000/2006 (Matthews et al. 2002; Capitaine et al. 2003) used after 2003, their small but non-negligible effect can be detected also in nutation. The effects of geophysical excitations in nutation, i.e. the quasi-periodic motion of Earth's axis of rotation in space, especially at annual and semi-annual frequencies, are caused by quasi-diurnal changes of angular momentum functions of the atmosphere and oceans, expressed in terrestrial frame. Therefore, high-resolution data are needed. Fortunately, the atmospheric/oceanic data with 6-hour steps are available, from different agencies, which enable these studies to be made. However, this effect was found to be different for different sources

of atmospheric/oceanic angular momentum functions (Ron et al. 2011; Vondrák & Ron 2014). Better agreement with Very Long Baseline Interferometry (VLBI)-based celestial pole offsets (CPO) was achieved for the atmospheric/oceanic data from U.S. agency (NCEP + ECCO) than from the European one (ERA + OMCT). Very recently Malkin (2013) implied that the observed rapid changes of Free Core Nutation (FCN) amplitude and phase were probably related to the epochs of geomagnetic jerks. Therefore we tested this possibility by re-initializing numerical integration at these epochs to see if the agreement between the observed and excited CPO is improved. Preliminary results are presented by Ron et al. (2014) and Vondrák & Ron (2014). The present paper continues in these efforts, namely by applying additional excitations at the geomagnetic jerk epochs. This approach has more physical basement than the simple re-initialization of the numerical integration used in the our last papers.

2. METHOD USED

The excitations of the Earth rotation in the celestial reference frame (nutation) by atmosphere and ocean were studied using Brzezinski (1994) broad-band Liouville equations

$$\begin{aligned} \ddot{P} \quad & -i(\sigma'_C+\sigma'_f)\dot{P}-\sigma'_C\sigma'_f P = -\sigma_C\left\{\sigma'_f(\chi'_p+\chi'_w)+\right. \\ & \left.\sigma'_C(a_p\chi'_p+a_w\chi'_w)+i[(1+a_p)\dot{\chi}'_p+(1+a_w)\dot{\chi}'_w]\right\} \end{aligned} \tag{1}$$

where $P = dX + idY$ is excited motion of Earth's spin axis in celestial frame (CRF), $\sigma'_C = 6.32000 + 0.00237i$, $\sigma'_f = -0.0146011 + 0.0001533i$ (in radians per sidereal day) are the complex Chandler and FCN frequencies in celestial frame, respectively, $\sigma_C = 0.01962 + 0.00237i$ in the complex Chandler frequency in terrestrial frame and $a_p = 9.509 \times 10^{-2}$, $a_w = 5.4809 \times 10^{-4}$ are dimensionless constants. χ'_p and χ'_w are the angular momentum excitation functions (presure and wind) in the celestial frame. To solve the second order differential equation (1) we apply substitutions

$$\begin{aligned} y_1 &= P, \quad \text{and} \\ y_2 &= \dot{P} - i\sigma'_C P, \end{aligned}$$

and get two first-order differential equations

$$\begin{aligned} \dot{y_1} &= i\sigma'_C y_1 + y_2 \\ \dot{y_2} &= i\sigma'_f y_2 - \sigma_C\left\{\sigma'_f(\chi'_p+\chi'_w)+\sigma'_C(a_p\chi'_p+a_w\chi'_w)+\right. \\ &\quad \left.+i[(1+a_p)\dot{\chi}'_p+(1+a_w)\dot{\chi}'_w]\right\} \end{aligned} \tag{2}$$

To be able to integrate the system (2) we set the initial values P_0, $\dot{P}_0$ constrained so that the free Chandlerian term (with quasi-diurnal period in celestial frame) vanishes. The initial values are closely connected to the phase and amplitude of the integrated series. The final choice of P_0 was made by repeating integration with different values P_0 to fit the integrated motion to VLBI observations so that reaches a minimum rms differences, and the numerical integration was performed using the Runge-Kutta 4th order in 6h steps (Press et al. 1992).

In our previous studies Ron et al. (2013) and Vondrák & Ron (2014), we looked for additional excitations to explain the inconsistency in phases of observed CPO and integrated series. The best agreement has been found for the geomagnetic jerks (or secular geomagnetic variation impulse) that are relatively sudden changes in the second time derivative of the Earth's magnetic field. More informations on geomagnetic jerks can be found in Olsen & Mandea (2007).

We found the double ramp function as the closest one. We tested the behaviour of the double ramp function using the integration with simulated schematic excitation, which is shown in Fig. 1.

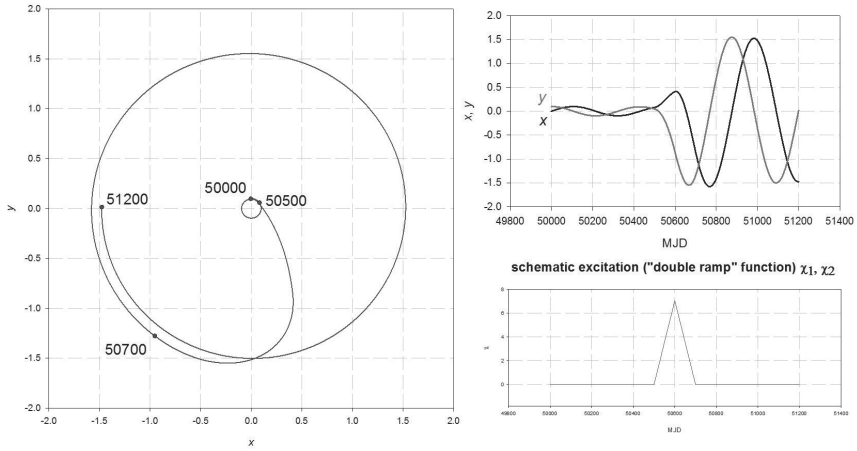

Figure 1: The integration with the simulated schematic excitation function.

We fix the the central epochs of additional excitations around geomagnetic jerks epochs: 1991.0, 1994.0, 1999.0, 2003.5, 2004.7, and 2007.5 taken from Malkin (2014) and take into account that the geomagnetic jerks last typically several months. We fix the length of an excitation to 200 days. The complex amplitudes of the excitations were estimated to lead to the best rms fit to observed celestial pole offsets. We also tested if the excitations is preceeding, delaying or corresponding to the geomagnetic jerk epochs. The values[1] of the rms and correlations are displayed in Tab. 1. The best agreement was found just for the epochs of the geomagnetic jerks.

Table 1. The values of rms of the residuals between observed celestial pole offsets and integrated series of AAM functions with the additional excitations in the epochs preceeding and delaying 100 days the geomagnetic jerk epochs.

epoch of GMJ +	rms [mas]	correlation
−100d	0.211	0.578
0d	0.196	0.632
+100d	0.213	0.570

[1]These values were obtained from slightly shorter interval and do not correspond to the presented solution.

3. DATA USED

3. 1. THE CELESTIAL POLE OFFSETS

There exist many solutions provided by different VLBI analysis centers, but, Malkin (2012) demonstrated that IVS series may be preferable for applications of FCN models. We used the celestial pole offsets from IVS combined solution `ivs13q4X.eops` (Schlüter & Behrend 2007) covering the interval 1989.0-2014.0. The coordinates dX and dY are given in unequally spaced intervals (typically 1-7 days long), sometimes with outliers. We cleaned the data by removing CPO $>$ 1mas. The empirical Sun-synchronous correction has been added to the IAU2000 nutation model (Matthews et al. 2002) to account the influence of atmosphere into the theoretical model. In order the observed CPO can be compared with the atmosheric contribution we added the Sun-synchronous correction $(0.1082 + 0.0104i)e^{il'}$ (in mas), where l' is the mean anomaly of Sun, to the complex CPO values. The data were then filtered (Vondrák 1977) to retain only periods between 60 and 6000 days. Finally the series were interpolated at regular 10-day intervals and both the observed and filtered ones are shown in Fig. 2.

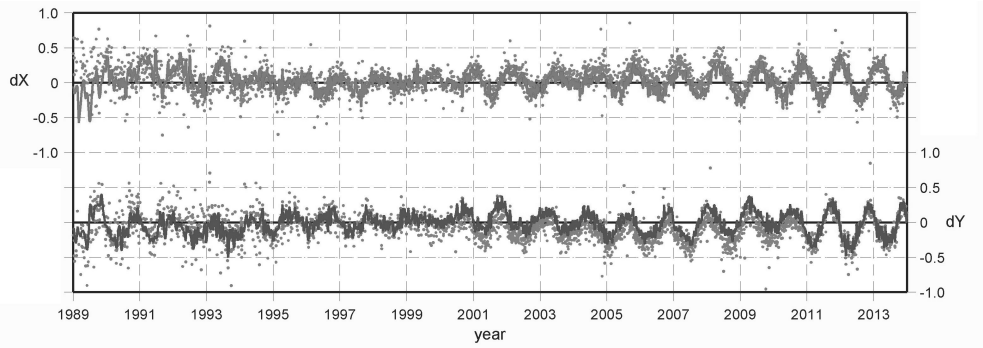

Figure 2: IVS Celestial pole offsets dX (up) and dY (bottom) in mas. The observed values (dots) and then filtered so that the periods are longer than 60d and shorter than 6000d (lines).

3. 2. ATMOSPHERIC ANGULAR MOMENTUM

There are two different series of Atmospheric Angular Momentum (AAM) available on the website of the IERS. First the European Centre for Medium-Range Weather Forecasts (ECMWF) that produced a reanalysis ERA40 on the time interval 1958–2001 and after 2001 is producing solutions ERAInterim, that are provisional solutions before a new global reanalysis. The corresponding oceanic angular momentum based on the model OMCT is produced continuosly by Dobslaw et al. (2010). The second series are produced by Atmospheric and Environmental Research, USA. That are NCEP/NCAR reanalysis prepared yearly in the time interval 1948–present. Unfortunately, there is no model of oceanic angular momentum available for the whole period of our interest (1989–2014). The pressure term of AAM function with the inverted barometer correction, that is provided by NCEP/NCAR Data Center as well, can serve alternatively as a simple model of oceanic response on the pressure changes (Wunsch & Stammer 1997).

Our previous studies based on atmospheric/oceanic angular momemtum function of European meteorological Center ECMWF ERA40 and on the ocean model OMCT showed relatively worse agreement in comparison with the NCEP/NCAR data (Vondrák & Ron, 2014). That is why we only used the NCEP/NCAR data in this study.

The time series of AAM χ (complex values) were transformed from the terrestrial frame to the celestial frame by using the complex decomposition at retrograde diurnal frequency $\chi' = -\chi e^{i\Phi}$, Φ is the Greenwich sidereal time.

Because we are interested in the long-periodic motion that is comparable with nutation, we applied the smoothing (Vondrák 1977) to remove periods shorter than 10 days and at the same time calculated their time derivatives needed for integration. The time series of the NCEP/NCAR atmospheric excitations corrected for inverted barometer after demodulation is displayed in Fig. 3. The dimensionless values of χ_1, χ_2 are given in units of 10^{-8}. The wind terms, which are much larger than pressure term, have in resulting integration lower influence because of two-order smaller value of the constatnt coefficient a_w mentioned above. The pressure term is better seen in Figures 4 and 5.

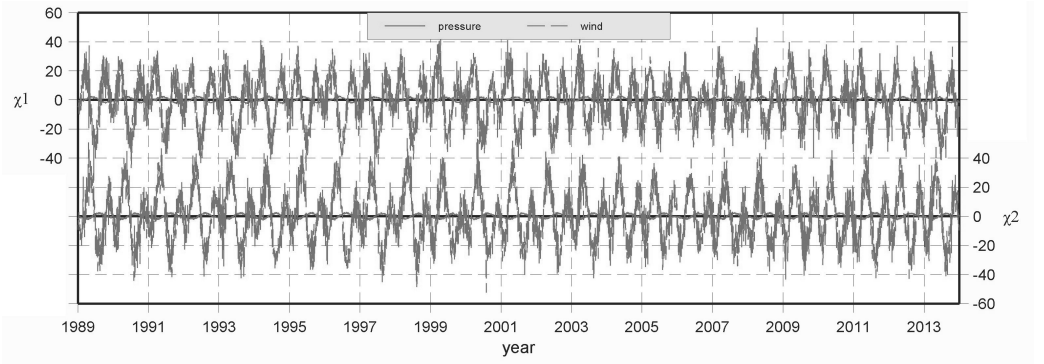

Figure 3: NCEP excitations pressure and wind terms. Pressure with the inverted barometer correction.

4. RESULTS

The IVS solution of CPO corrected for the sun-synchronous correction is compared with geophysically excited motion of celestial pole obtained by numerical integration of Eq. (2). To obtain the best fit to CPO values, the integration was repeated with different initial values for the first interval, i.e., from the beginning of the series in 1989 up to the first epoch of geomagnetic jerk 1991 and then were searched the complex values of the additional excitations for each interval between the successive geomagnetic jerks.

The integrated CPO obtained with NCEP excitations without and with the inverted barometer correction are graphically depicted in Figures 4 and 5, respectively.

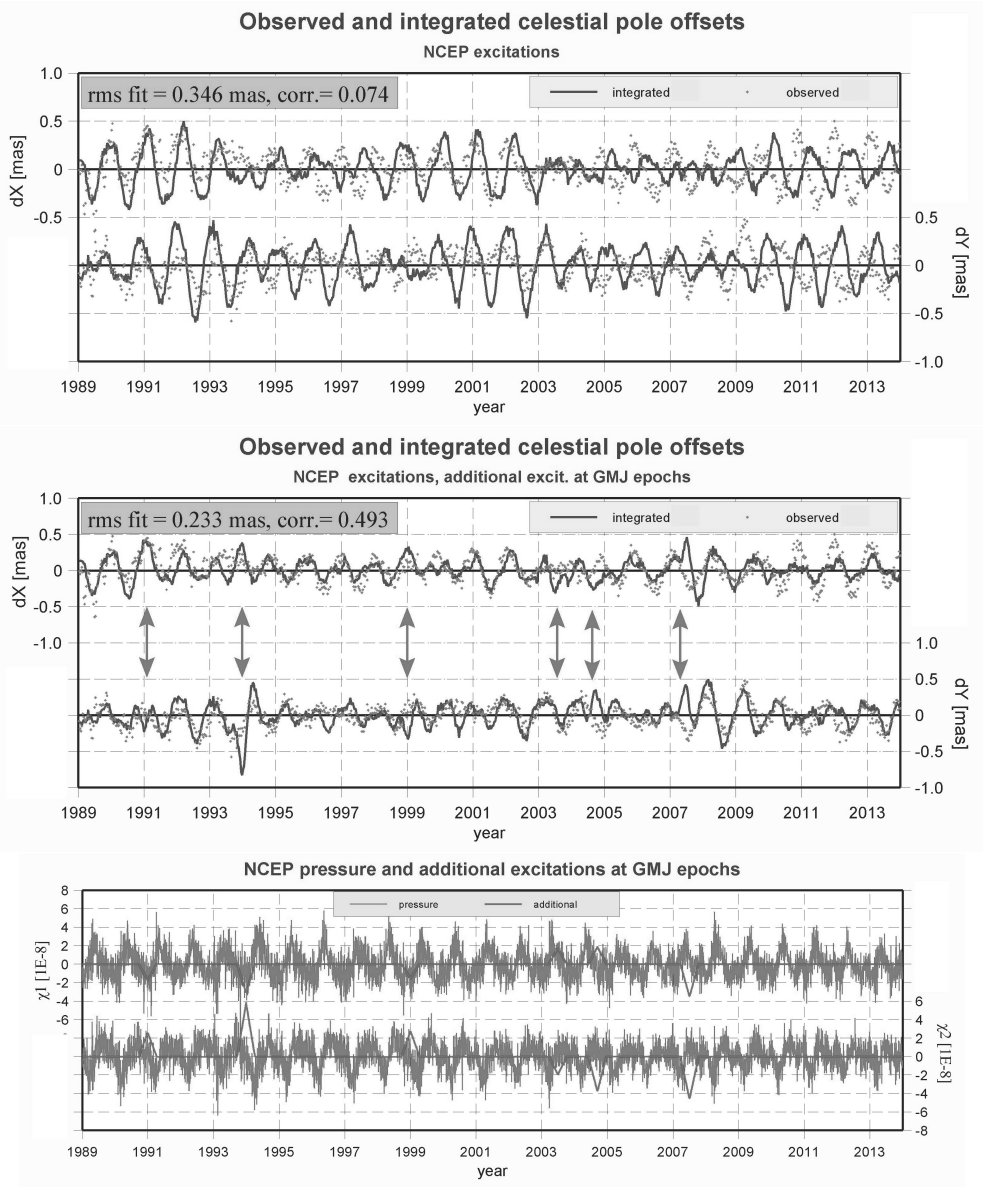

Figure 4: Top: Observed and integrated CPO obtained with NCEP excitations without inverted barometer correction. Middle: the same with the added geomanetic excitations. Bottom: The added geomagnetic exciations together with the pressure term.

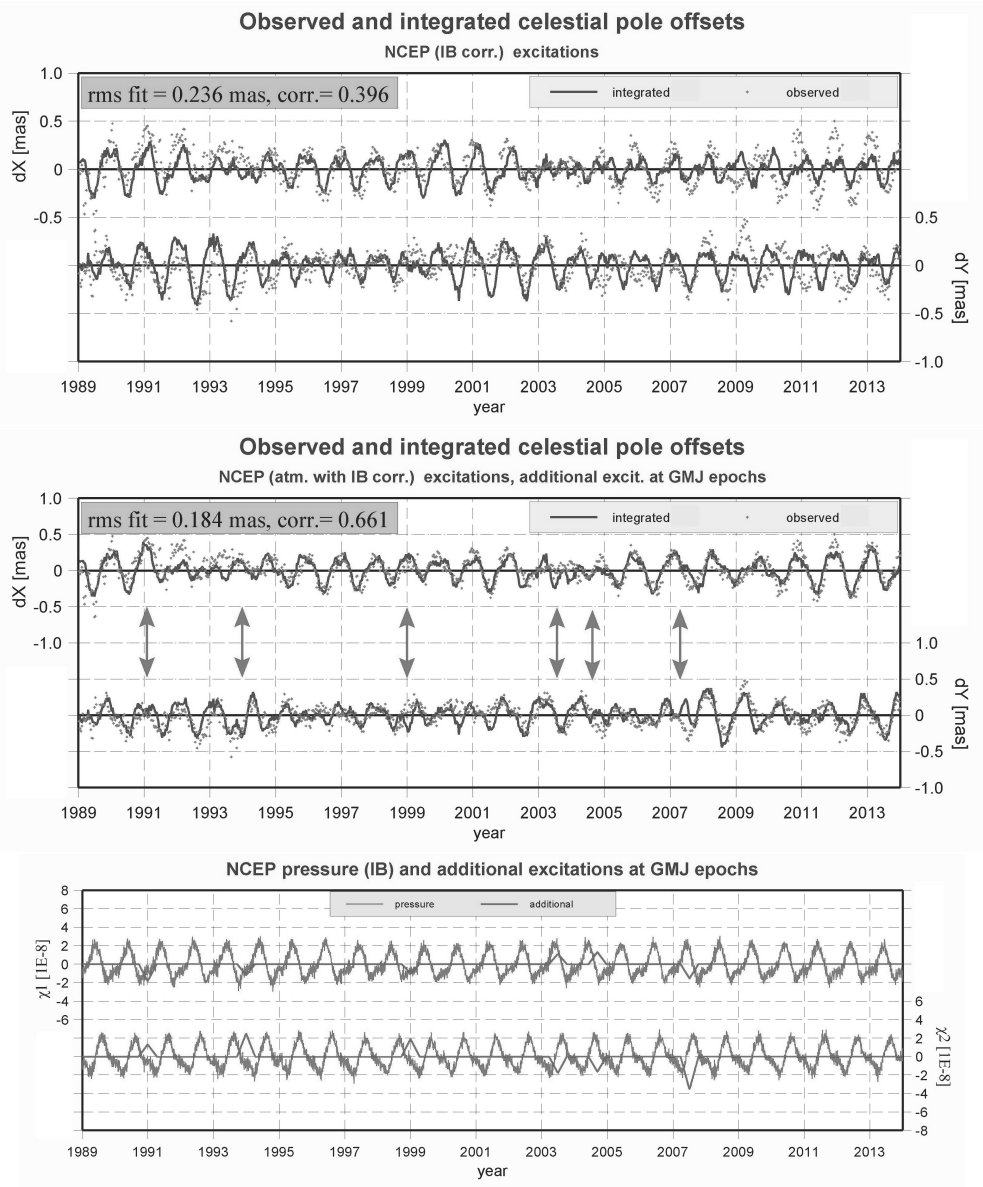

Figure 5: Top: Observed and integrated CPO obtained with NCEP excitations with the inverted barometer correction. Middle: the same with the added geomanetic excitations. Bottom: The added geomagnetic exciations (in blue) together with the pressure term (red).

The application of the additional exitations in the epochs of geomagnetic jerks to the NCEP atmospheric exciation functions with the inverted barometer correction improves the agreement of the integrated CPO with the observed CPO significantly as it is seen from Tab. 2.

Table 2. The rms fits and the correlations between integrated and observed CPO

Series	without		with additional exc	
	rms [mas]	corr.	rms[mas]	corr.
NCEP without IB	0.346	0.074	0.233	0.493
NCEP with IB	0.236	0.396	0.184	0.661

5. CONCLUSIONS

In our previous work (Vondrák & Ron 2014) we detected considerable differences between ERA40 and ERAinterim the wind term in AAM data about 30% relative difference in amplitude of the semi-annual wind term. NCEP solution with the inverted barometer correction leads to better agreement than with the ERA series and therefore we used only the NCEP solution in this study. Geophysical excitations yield significant contribution to nutation, of the order of 0.1mas. The influence of motion (wind) terms is one order of magnitude smaller than that of matter (pressure) terms. The application of the pressure term of AAM function with the inverted barometer correction, that implies a simple ocean model, improved the correlation between the observed and integrated CPO series in relation to the case when the the pressure term of AAM function without the inverted barometer correction is used. The application of schematic additional excitations at geomagnetic jerk epochs improves the agreement of integrated pole position with VLBI observations even more.

Acknowledgements

This research was financially supported by the grant No. 13-15943S "Geophysical excitations in the motion of Earth's axis of rotation", awarded by the Grant Agency of the Czech Republic. The support given to C.R. and J.V. by Bulgarian Academy of Sciences to participate the IX$^{\text{th}}$ Bulgarian-Serbian Astronomical Conference held in Sofia is appreciated.

References

Brzeziński, A.: 1994, Polar motion excitation by variations of the effective angular momentum function: II. Extended Model, *Manuscripta Geodaetica*, **19**, 157.

Capitaine, N., Wallace, P. T. and Chapront, J.: 2003, Expressions for IAU 2000 precession quantities. *Astron. and Astrophys.*, **412**, 567.

Dobslaw, H., Dill, R., Grotzsch, A., Brzeziński, A. and Thomas, M.: 2010, Seasonal polar motion excitation from numerical models of atmosphere, ocean, and continental hydrosphere, *J. Geophys. Res.*, **115**, B10406, doi: 10.1029/2009JB007127.

Malkin, Z.: 2012, Celestial pole offsets: From initial analysis to end user. *Proc. IVS 2012 General Meeting*, 375.

Malkin, Z.: 2013, Free core nutation and geomagnetic jerks, *Journal of Geodynamics*, **72**, 53.

Mathews, P.M., Herring, T.A. and Buffett, B.A.: 2002, Modeling of nutation and precession: New nutation series for nonrigid Earth and insights into the Earths interior, *J. Geophys. Res. (Solid Earth)*, **107(B4)**, doi:10.1029/2001JB000390.

Olsen, N. and Mandea M.: 2007, Investigation of a secular variation impulse using satellite data: The 2003 geomagnetic jerk. *Earth and Planetary Science Letters*, **255**, 94.

Press, W.H., Teukolsky, S.A., Vetterling, W.T and Flannery, B.P.: 1992, "Numerical Recipes in Fortran 77. The Art of Scientific Computing", 2nd Edition, Cambridge University Press, 993 p.

Ron, C., Vondrák, J. and Štefka, V.: 2011, Comparison of the various atmospheric and oceanic angular momentum series, In Proc. Journées 2010 Systèmes de référence spatio-temporels, ed. N. Capitaine, Observatoire de Paris, 221.

Ron, C., Vondrák, J. and Chapanov, Ya.: 2014, Free core nutation – possible causes of changes of its phase and amplitude, In Proc. Journées 2013 Systèmes de référence spatio-temporels, ed. N. Capitaine, Observatoire de Paris, in press.

Schlüter, W. and Behrend, D.: 2007, The International VLBI Service for Geodesy and Astrometry (IVS): Current capabilities and future prospects. *J. Geod.*, **81**, 379.

Vondrák, J.: 1977, Problem of smoothing of observational data II, *Bull. Astron. Inst. Czechosl.*, **28**, 84.

Vondrák, J. and Ron, C.: 2010, Study of atmospheric and oceanic excitations in the motion of Earths spin axis in space. *Acta Geodyn. Geomater.*, **7**, No. 1, 19.

Vondrák, J. and Ron, C.: 2014, Geophysical Excitation of nutation – comparison of different models, *Acta Geodyn. Geomater.*, **11**, No. 3, 193.

Wunsch, C. and Stammer, D.: 1997, Atmospheric loading and the oceanic "inverted barometer" effect. *Reviews of Geophysics*, **35**, 79. doi: 10.1029/96RG03037

Proceedings of the IX Bulgarian-Serbian Astronomical Conference: Astroinformatics (IX BSACA) Sofia, Bulgaria, July 2-4, 2014,
Editors: M. K. Tsvetkov, M. S. Dimitrijević, O. Kounchev, D. Jevremović and K. Tsvetkova
Publ. Astron. Soc. "Rudjer Bošković" No 15, 2015, 137-147

DIFFERENCES IN DETECTION OF D-REGION PERTURBATIONS INDUCED BY THE UV, X AND γ RADIATION FROM OUTER SPACE USING VLF SIGNALS

ALEKSANDRA NINA[1], VLADIMIR M. ČADEŽ[2], LUKA Č. POPOVIĆ[2], VLADIMIR A. SREĆKOVIĆ[1] and SAŠA SIMIĆ[3]

[1]*Institute of Physics, University of Belgrade, Serbia*
E-mail: sandrast@ipb.ac.rs, vlada@ipb.ac.rs
[2]*Astronomical Observatory Belgrade, Serbia*
E-mail: vcadez@aob.rs, lpopovic@aob.rs
[3]*Faculty of Science, Department of Physics, University of Kragujevac*
E-mail: ssimic@kg.ac.rs

Abstract. In this paper we present characteristics of detection of various events occurring in the outer space that perturb the D-region by emission of the UV, X, and γ radiation. The method of our analysis is based on monitoring variations of recorded VLF (very low frequency) radio signals in real time that are reflected from the D-region. We show examples of strong and weak perturbations and present a procedure for detection hydrodynamic waves.

1. INTRODUCTION

The ionosphere, having plasma characteristics, is very sensitive to electromagnetic disturbances whose intensity and variable influences coming from outer space as well as from the terrestrial atmosphere and lithosphere. The non-periodic and sudden events, such as solar flares (Nina et al. 2011, 2012a; Kolarski et al. 2011, 2014, Singh et al. 2014), coronal mass ejections (Bochev and Dimitrova 2003, Balan et al. 2008), solar eclipses (Singh et al. 2012), influences of processes in distant parts of the universe like supernova explosions followed by hard X and γ radiation (Inan et al. 2007), lightnings (Voss et al. 1998, Collier et al., 2011), and some processes in the terrestrial lithosphere like volcanic eruptions and earthquakes (Gousheva et al. 2008, Nenovski et al. 2010), induce temporal, space and time varying ionospheric perturbations. These disturbances cause numerous complex physical, chemical and dynamical phenomena in the ionosphere (Nina et al. 2012a, Nina and Čadež 2013, Jilani et al. 2013, Maurya et al. 2014) and may directly affect human activities, especially in the telecommunications. Besides a pure scientific interest to study the influence of solar activity to the terrestrial atmosphere, the understanding mechanisms and making predictions on resulting consequences in turbulent regions of the

ionosphere has important applications in radio communications, planning networks of mobile communications satellites, high-precision applications of global navigation satellite systems, etc. (Bajčetić et al. submitted paper).

The atmospheric monitoring depends on altitude of considered medium. The location of the low ionosphere lies below the area being studied by satellite observations and above the region where balloon measurements find their application. The low ionospheric monitoring is based on rocket and radar measurements (Strelnikova and Rapp 2010, Chau et al. 2014), and on technology involving on propagation of very low frequency (VLF) radio waves. The advantages of the VLF method come from possibilities to observe a large part of the low ionosphere, to detect local perturbations, and to detect sudden events. All this is enabled by means of numerous transmitters and receivers forming a worldwide international network for continuous signal emission and reception.

The VLF radio signal propagation properties are determined by the wave attenuation and reflection. Changes in the received signal amplitude and phase are primarily consequences of variations in the low ionospheric electron density which enables investigation of this atmospheric layer by the VLF signal technology.

In this paper we show a possibility to detect different astrophysical phenomena by using the VLF method. We consider differences in ways of their detection and we present our procedure developed to detect hydrodynamic waves.

2. EXPERIMENTAL SETUP

The Belgrade VLF station consists of two receivers with one electrical (AbsPAL - Absolute Phase and Amplitude Logger) and two magnetic loop (AWESOME - Atmospheric Weather Electromagnetic System for Observation Modeling and Education) antennas, respectively. They can simultaneously register 6 and 15 signals emitted by different transmitters at fixed frequencies, respectively. The first of them has been operating since 2004, while the second one since 2008. During this period we have collected a large data base containing a written information about numerous low ionospheric responses to different natural and human-induced events. This allows for making statistical analyses of considered phenomena and to detect differences within a long-term period. In our investigations we considered signals whose characteristics are given in Table 1.

3. OBSERVATIONS AND RESULTS

3. 1. DETECTABILITY

As a part of atmosphere, the low ionosphere is under permanent influences of events coming from outer space, and Earth's layers. Here, we consider detections of low ionospheric plasma perturbations due to the radiation coming from outer space. The intensity of plasma reactions in the low ionosphere depends on the incoming radiation flux in atmosphere, absorption in higher layers, and total ionization cross section in the ionospheric D-region. During perturbations, variations in the D-region electron density can be large, but they can also be very small which, consequently, causes large and small changes in VLF signal characteristics.

Table 1: Transmitters characteristics and path length of analyzed VLF/LF signals. The data for transmitters are found in file AWESOME Transmitters.pdf in website `http://nova.stanford.edu/~vlf/IHY_Test/TechDocs/`.

SIGN	LOCATION	FREQUENCY (kHz)	POWER (kW)	LENGTH (km)
DHO	Rhauderfehn Germany	23.4	800	1304
GQD	Anthorn UK	22.1	200	1935
ICV	Isola di Tavolara Italy	20.27	20	976
NRK	Grindavik Island	37.5	800	3230
NAA	Cutler Maine, USA	24.0	1000	6548
NWC	North West Cape Australia	19.8	1000	11974

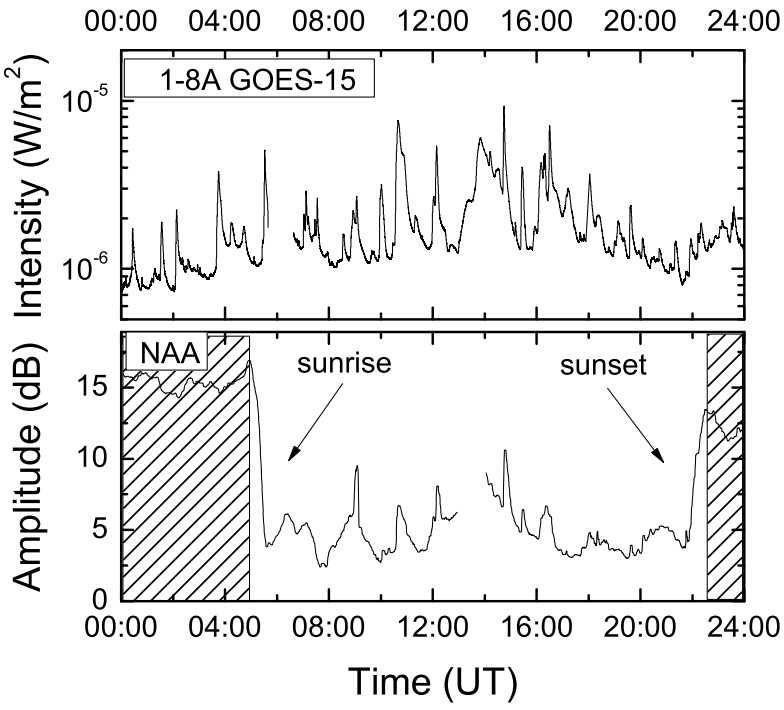

Figure 1: Amplitude variation of the NAA signal emitted from the USA (bottom panel). The shaded domains are related to the signal propagation during the nighttime. The large variations during the daytime are due to the increased radiation induced by the solar X-flare (upper panel).

As investigations showed, dominant roles in the quite D-region plasma ionization have the Lyα radiation coming from the Sun, and cosmic radiation (Swamy 1991). The most important perturber of this area is the X-radiation emitted from the Sun during solar X-flares.

In Fig. 1, we show differences in the NAA signal amplitude at the nighttime and daytime, and its increases as reactions to the rising of the incoming X-radiation in the atmosphere, registered by the GOES-15 satellite during solar X-flares.

The variations shown in Fig. 1 are the evident consequences of considered phenomena. But, in some cases, the reactions to a particular phenomenon are weak and changes in the recorded signal cannot be related to them with certainty. The inability to pinpoint particular weak influences is consequence of numerous events which affect ionospheric plasma. They have time and space dependent intensity at the considered location and cause a signal noise that can be very large during unstable conditions. As illustration, the NAA signal during the period around the time of registration the γ ray burst GRB090726 is given in Fig. 2.

A more quiet state was in the period around the γ ray burst GRB110412A that can be visible from the time evolution of amplitude of five VLF signals as shown in Fig. 3. Here we can see signal changes after starting the GRB detection, but more cases must be considered for a certain confirmation of possibility to detect a ionospheric response to a similar high energy radiation impact (Nina et al. 2013, Nina et al. paper in preparation).

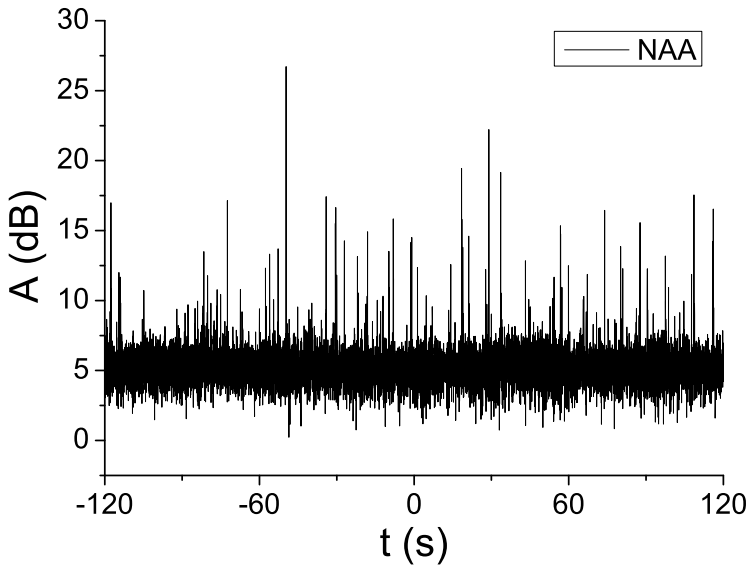

Figure 2: Display of frequent amplitude disturbances of the VLF signal emitted by NAA transmitter located in the United States on July 26, 2009 during the period around the time of registration the γ ray burst GRB090726 whose starting time corresponds to 0 in the graph.

3. 2. DETECTION OF HYDRODYNAMIC WAVES

Hydrodynamic waves in the ionosphere can be induced by different events that relatively strongly perturb a part of the atmosphere. They can be both sudden like sprite and periodical like a solar terminator (ST). In literature, the study of the latter case is related only to altitudes above the D-region. Our intention was to develop a procedure for detection acoustic and gravity waves in the low ionosphere (Nina and Čadež 2013).

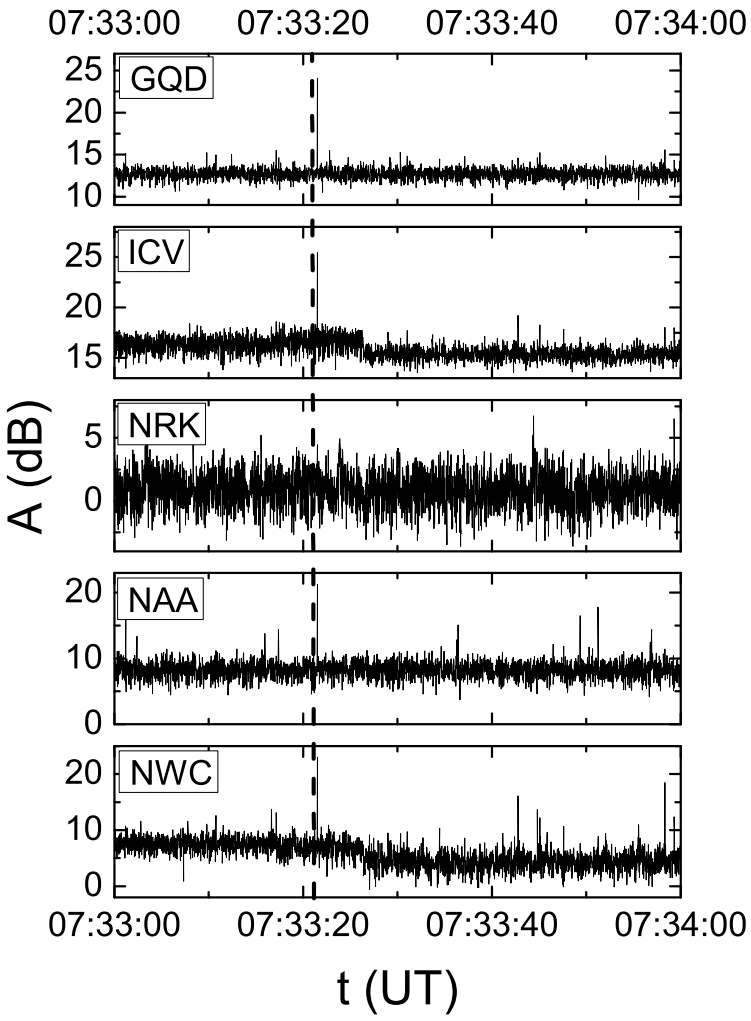

Figure 3: Amplitude variations of signals emitted from different locations (from the top panel: the UK, Italy, Iceland, the USA and Australia) and recorded in Belgrade after the γ ray burst GRB110412A registered on April 12, 2011, with start at 7:33:21.15 UT indicated by vertical line.

In this paper we show our investigation of the sunrise effect on the low ionosphere using the signal registered within the time interval 5:00 UT - 7:00 UT, emitted by the DHO transmitter located in Germany (Fig. 4). Here, the three distinct time sections of 30 min are shaded and labeled by **n**, **sr** and **d**, respectively. They cover periods before (the entire signal path is at the nighttime), during, and after (the entire signal path is at the daytime) the sunrise, respectively.

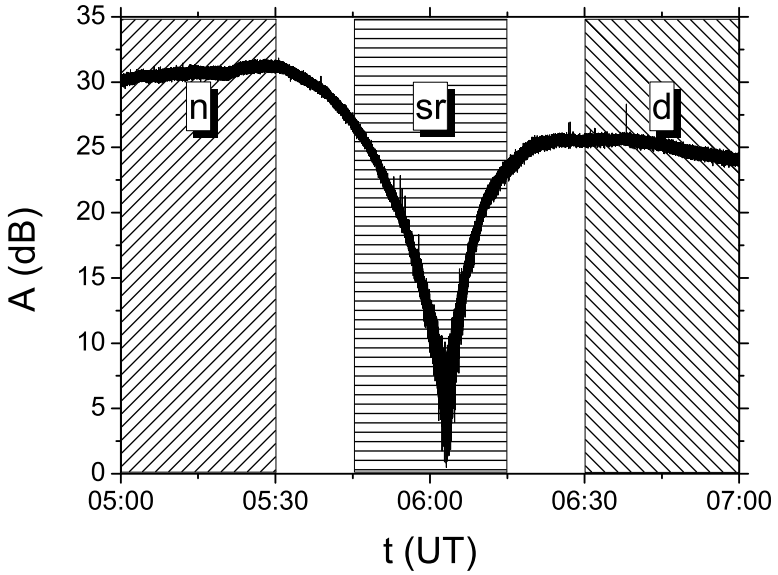

Figure 4: The time evolution of the VLF signal amplitude emitted by the DHO transmitter in Germany and recorded by the AWESOME VLF receiver in Serbia. The shaded domains designate the 30 min time intervals before, during and after the sunrise.

Details of the applied procedure of signal analysis are explained in Nina and Čadež (2013). The procedure consists of two steps. First, the Fourier transform is applied to the recorded amplitudes A(t) during each of the considered time domains. The corresponding oscillation spectrum $A_{\rm F}(\omega)$ follows from the Fourier transform:

$$A_{\rm F}(\omega) = \frac{1}{\sqrt{2\pi}} \int_{-\infty}^{+\infty} {\rm e}^{-i\omega t} A(t) dt,$$

where $\omega \equiv 2\pi/\tau$ and τ are the oscillation frequency and oscillation period, respectively. The obtained values are shown in the Fig. 5 (left panels) for $\tau > 1$ min. Second, Fourier amplitudes $A_{\rm F}$ for relevant domains (as labeled in Fig. 4) are compared by scaling as follows:

$$\alpha_n^{sr}(\tau) \equiv \frac{A_{\rm F}(\tau; sr)}{A_{\rm F}(\tau; n)},\ \alpha_d^{sr}(\tau) \equiv \frac{A_{\rm F}(\tau; sr)}{A_{\rm F}(\tau; d)},\ \alpha_{dn}(\tau) \equiv \frac{A_{\rm F}(\tau; d)}{A_{\rm F}(\tau; n)}.$$

Resulting values are shown in Fig. 5 (right panels).

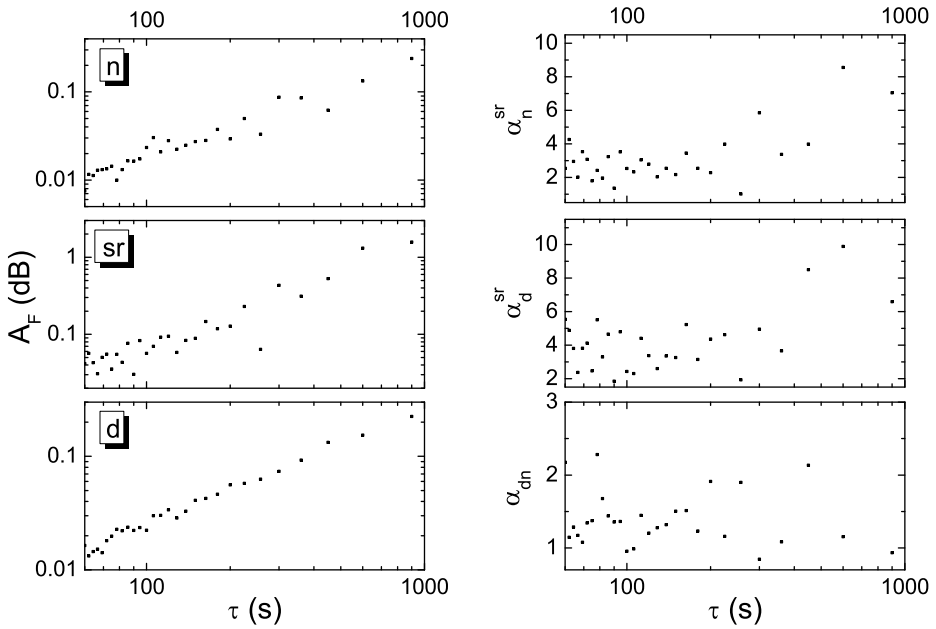

Figure 5: Fourier amplitudes of the VLF signal for domains **n**, **sr** and **d** (upper, middle and bottom left panels, respectively). The right panels show ratios of Fourier amplitudes related to domains **sr** and **n**, **sr** and **d**, and **d** and **n**, respectively.

For investigations of physical conditions in the low ionosphere, the most important information is the relation between signal properties in the **d** and **n** domains with quasi-stationary conditions which allows for detections of AGWs. In Nina and Čadež (2013) the extraction of waves excited by the ST was carried out by considering the following three typical characteristics of the phenomenon:

1. AGW waves are excited during the ST and become attenuated to a certain degree afterwards.

2. These two processes occur both at the sunrise and sunset in spite of different daytime/nighttime conditions of the medium.

3. This repeats itself daily.

The peaks in the bottom right panel show the excitation of the Fourier amplitude of the VLF signal after the sunrise. The obtained peak values at 60 s and 400 s for τ are in a good agreement with results in Nina and Čadež (2013) for the low ionosphere showing an enhanced induction of AGWs by the ST for oscillation periods τ within intervals 60 s - 100 s, 300 s - 400 s, and over 1000 s. Our results for the low ionosphere are very similar to those obtained for higher altitudes (De Keyser and Čadež 2001a, 2001b, Hernandez-Pajares et al. 2006, Afraimovich 2008).

3. 3. VARIATIONS IN PLASMA CHARACTERISTICS

As we said in Introduction, the recorded signal characteristics can be used for diagnostic of the low ionosphere. This can be done by using some numerical models for

simulation of VLF signal propagations. In our investigations the Long-Wave Propagation Capability (LWPC) numerical model (Ferguson, 1998) was used. Here, we point out that the signal characteristics cannot be monotonous functions of electron density. For this reason, the quantitative descriptions in some cases, especially within the periods of solar terminator, cannot be obtained directly from the observed data and it is necessary some additional modeling of the low ionosphere.

To calculate the altitude and time dependencies of the electron density $N(h,t)$, we usually perform the ground based low ionosphere monitoring using the VLF radio signal emitted by the DHO transmitter (Germany). The reason for this is the best quality of the recorded signal owing to the high emission power of 800 kW and a suitable signal frequency for the location of the receiver, and a relatively short signal propagation path. The latter property is significant as it excludes significant variations in the vertical stratification of parameters in the ambient ionospheric plasma. This is important because the low ionospheric characteristics are time and space dependent, variations can be both periodically and sudden, and can be caused by events that induced both global and local perturbations.

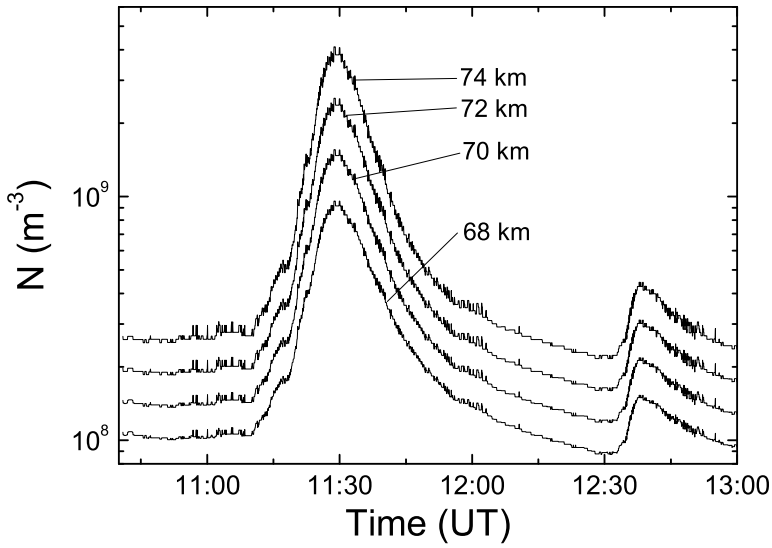

Figure 6: Time evolution of electron density during solar flares occurred on 24. 03. 2011.

The reactions of considered plasma on astrophysical events depend on the state of physical and chemical conditions in the medium. For example, the study published in Nina et all. (2011), has shown that increasing of the Lyα radiation, the most important origin of the quiet D-region plasma photo-ionization, does not have an important influence during presence of the solar X-flare influence. Also, the different geophysical conditions (for example in polar and equatorial zones) and periodical time variations in external influences (for example during the solar cycle, year, and day)

make ionospheric variations space and time dependent. This points to the limited use of data from the literature in specific calculations related to a specific location and in a specified time period. For this reason, the main goal of our investigations of D-region plasma properties is the development of procedures for modeling plasma parameters from experimental data related to the considered time and space defined by transmitter and receiver locations. Thus, in studies of Nina et al. (2012a,b) we have calculated the electron density time and altitude distributions during the influence of two flares. In Fig. 6 we have shown one typical reaction of the D-region plasma to solar X-flares.

In Fig. 7, obtained in Nina and Čadež (2014), we can see variations in the Lyα photo-ionization rate in quiet low ionosphere calculated in periods after large perturbations and their comparison with corresponding results from literature.

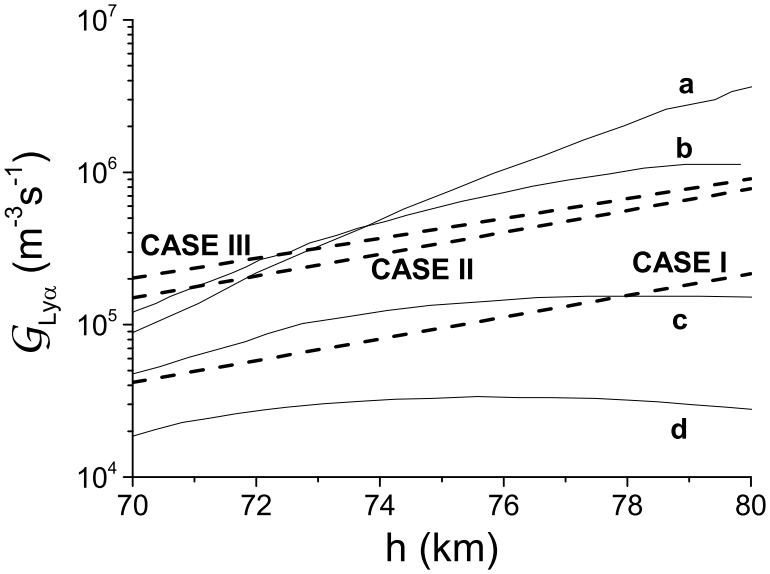

Figure 7: Altitude dependencies of the electron gain rate $\mathcal{G}_{Ly\alpha}$ for Case I, II and III (Nina and Čadež, 2014), and their comparison with data presented in Mitra (1977) (a), Rowe (1972) (b), Aikin et al. (1969) (c) and Bourdeau et al. (1965) (d). Case I, II and III relate to flares occurred on May 5th, 2010, February 18th, 2011, and March 24th, 2011 analyzed in Nina and Čadež, 2014.

4. SUMMARY

In this paper we present analyses and differences in detection of D-region perturbations induced by the UV, X and γ radiation from outer space using VLF signals. We overview our procedures related to detection of hydrodynamic waves and calculations of plasma parameters, which have a universal character in sense that they can be applied to any relatively small part of the D-region during its reactions to different events.

Acknowledgment

The authors would like to thank the Ministry of Education, Science and Technological Development of the Republic of Serbia for the support of this work within the projects III-44002, 176001, 176002 and 176004.

References

Afraimovich, E. L: 2008, First GPS-TEC evidence for the wave structure excited by the solar terminator, *Earth, Planets and Space*, **60**, 895.

Aikin, A. C.: 1969, The ion pair production function of the lower ionosphere, National Aeronautics and Space Administration, Goddard Space Flight Center, Greenbelt, Md.

Bajčetić, J., Kolarski, A., Nina, A, Čadež, V. M., Todorović, B. M.: Solar X-flares and HF radio signal propagation in ionospheric D-region, *Geoscience and Remote Sensing Letters, IEEE*, submitted paper

Balan, N., Alleyne, H., Walker, S., Reme, H., McCrea, I., Aylward, A.: 2008, Magnetosphere-ionosphere coupling during the CME events of 07-12 November 2004, *Journal of Atmospheric and Solar-Terrestrial Physics*, **70**, 2101.

Bochev, A. Z., Dimitrova, I. I. A.: 2003. Magnetic cloud and magnetosphere - ionosphere response to the 6 November 1997 CME, *Advances in Space Research*, **32**, 1981.

Bourdeau, R. E., Aiken, A. C., Donley, J. L.: 1965, The lower ionosphere at solar minimum, Goddard Space Flight Center, NASA, Greenbelt, Md.

Chau, J. L., Röttger, J., Rapp, M.: 2011, PMSE strength during enhanced D region electron densities: Faraday rotation and absorption effects at VHF frequencies, *Journal of Atmospheric and Solar-Terrestrial Physics*, **118**, Part A, 113.

Collier, A. B., Lichtenberger, J., Clilverd, M. A., Rodger, C. J., Steinbach, P.: 2011, Source region for whistlers detected at Rothera, Antarctic, *Journal of Geophysical Research*, **116**, 3219.

De Keyser, J., Čadež, V. M.: 2001a, Excitation of low-frequency fluctuations at the magnetopause by intermittent broadband magnetosheath waves, *Journal of Geophysical Research*, **106**, 29467.

De Keyser, J., Čadež, V. M.: 2001b, Transient development of magnetohydrodynamic wave mode conversion layers, *Journal of Geophysical Research*, **106**, 15609,

Ferguson, J. A.: 1998, Computer programs for assessment of long wavelength radio communications, Version 2.0, Technical document 3030, Space and Naval Warfare Systems Center, San Diego CA.

Gousheva, M. N., Glavcheva, R. P., Danov, D. L., Hristov, P. L., Kirov, B. B., Georgieva K. Y.: 2008, Electric field and ion density anomalies in the mid latitude ionosphere: Possible connection with earthquakes?, *Advances in Space Research*, **42**, 1, 206.

Hernandez-Pajares, M., Juan, J. M., Sanz, J.: 2006, Medium scale traveling ionospheric disturbances affecting GPS measurements: Spatial and temporal analysis, *Journal of Geophysical Research*, **111**, A07S11.

Inan, U. S., Lehtinen, N. G., Moore, R. C., Hurley, K., Boggs, S., Smith, D. M., Fishman, G. J.: 2007. Massive disturbance of the daytime lower ionosphere by the giant γ-ray flare from magnetar SGR 1806-20, *Geophysical Research Letters*, **34**, 8103.

Jilani, K., Mirza A. M., Khan, T. A.: 2013, Ion-acoustic solitons in pair-ion plasma with non-thermal electrons, *Astrophysics and Space Science*, **344**, 135.

Kolarski, A., Grubor, D.,Šulić, D.: 2011, Diagnostics of the solar X-Flare impact on lower ionosphere through seasons based on VLF-NAA signal recordings, *Baltic Astronomy*, **20**, 591.

Kolarski, A., Grubor, D.: 2014, Sensing the earths low ionosphere during solar flares using VLF signals and goes solar X-ray data, *Advances in Space Research*, **53**, 11, 1595.

Maurya, A. K., Phanikumar, D. V., Singh, R., Kumar, S., Veenadhari, B., Kwak, Y. S., Kumar, A., Singh, A. K., Kumar, N. K.: 2014, Low-mid latitude D region ionospheric perturbations associated with 22 july 2009 total solar eclipse: Wave-like signatures inferred from VLF observations, *Journal of Geophysical Research: Space Physics*, **119**, 10, 8512.

Mitra, A. P.: 1977, Ionospheric Effects of Solar Flares, Mir, Moscow.

Nenovski, P., Spassov, C., Pezzopane, M. Villante, U., Vellante, M., Serafimova, M.: 2010, Ionospheric transients observed at mid-latitudes prior to earthquake activity in Central Italy, *Natural Hazards and Earth System Sciences*, **10**, 1197.

Nina, A., Čadež, V. M.: 2013, Detection of acoustic-gravity waves in lower ionosphere by VLF radio waves, *Geophysical Research Letters*, **40**, 18, 4803.

Nina, A., Čadež, V. M.: 2014, Electron production by solar Lyα line radiation in the ionospheric D-region, *Advances in Space Research*, **54**, 7, 1276.

Nina, A., Čadež, V. M., Srećković, V. A., Šulić, D.: 2011, The Influence of solar spectral lines on electron concentration in terrestrial ionosphere, *Baltic Astronomy*, **20**, 609.

Nina, A., Čadež, V. M., Srećković, V. A., Šulić, D.: 2012a, Altitude distribution of electron concentration in ionospheric D-region in presence of time varying solar radiation flux, *Nuclear Instruments and Methods in Physics Research B*, **279**, 110.

Nina, A., Čadež, V. M., Šulić, D., Srećković, V. A., Žigman, V.: 2012b, Effective electron recombination coefficient in ionospheric D-region during the relaxation regime after solar flare from February 18, 2011, *Nuclear Instruments and Methods in Physics Research B*, **279**, 106.

Nina, A., Popović, L. Č., Srećković, V. A., Simić, S.: 2013b, Book of Abstracts of IX SCSLSA, eds L. Č. Popović, M. S. Dimitrijević, Z. Simić and M. Stalevski, 70.

Nina, A., Popović, L. Č., Srećković, V. A., Simić, S.: paper in preparation.

Rowe, J. N.: 1972, Model studies of the lower ionosphere, Sci. Rep.No. 406, Pennsylvania State Univ., Univ. Park, USA.

Singh, Ashutosh K., Singh, Rajesh, Veenadhari, B., Singh, A. K.: 2012, Response of low latitude D-region ionosphere to the total solar eclipse of 22 July 2009 deduced from ELF/VLF analysis, *Advances in Space Research*, **50**, 10, 1352.

Singh, Ashutosh K, Singh, Ashutosh K, Singh, Rajesh, Singh, R. P.: 2014, Solar flare induced D-region ionospheric perturbations evaluated from VLF measurements, *Astrophysics and Space Science*, **350**, 1, 1.

Strelnikova, I., Rapp, M.: 2010, Studies of polar mesosphere summer echoes with the EISCAT VHF and UHF radars: Information contained in the spectral shape, *Advances in Space Research*, **45**, 247.

Swamy, A. C. B.: 1991, A new technique for estimating D-region effective recombination coefficients under different solar flare conditions, *Astrophysics and Space Science*, **185**, 153.

Voss, H. D., Walt, M., Imhof, W. L., Mobilia, J., Inan, U. S.: 1998, Satellite observations of lightning-induced electron precipitation, *Journal of Geophysical Research*, **103**, 11725.

Proceedings of the IX Bulgarian-Serbian Astronomical Conference: Astroinformatics (IX BSACA) Sofia, Bulgaria, July 2-4, 2014,
Editors: M. K. Tsvetkov, M. S. Dimitrijević, O. Kounchev, D. Jevremović and K. Tsvetkova
Publ. Astron. Soc. "Rudjer Bošković" No 15, 2015, 149-158

THE RELATION BETWEEN SOLAR PROTON FLARES AND THE BACKGROUND CONCENTRATIONS OF NITROGEN OXIDES IN THE TROPOSPHERE

BORIS KOMITOV, MOMCHIL DECHEV and PETER DUCHLEV

Institute of Astronomy, Bulgarian Academy of Sciences
E-mail: mdechev@astro.bas.bg

Abstract. The results from the study of daily average values of the background concentrations of nitrogen oxides (NO and NO_2) in the terrestrial atmosphere are presented. The study aim was to reveal some aspects of the relation between the solar flares, as sources of solar energy protons (SEP-Solar Energetic Protons), and the nitrogen oxides formation in the Earth's atmosphere. For this aim, except the time series of the nitrogen oxides for the period Oct 15, 2004 – Sept 1, 2009, the total daily fluxes of the solar protons for the energy diapasons $E \geq 10MeV$ and $E \geq 100MeV$, registered by GOES-11 and GOES-13 satellites, were used. The obtained results suggest that the significant peaks in the time series of the nitrogen oxides should be explained with *volley* effect of NO and NO_2 formation in the middle atmosphere, which pass in the time interval from one month to about one year before the peaks registration. In view of the short period with continuous time series, to give a certain answer of the question whether and how the solar protons affect the NO and NO_2 formation it is necessary to prolong the study in future.

1. INTRODUCTION

The nitrogen oxides NO, NO_2, NO_x, and their derivatives belong to so called "small components" of the terrestrial atmosphere. Because of the toxic properties of the nitrogen oxides, their concentrations in the air are important subjects of ecologic monitoring. Energetic particles (e.g. solar protons and auroral electrons) provide the energy to drive an endothermic reaction: $NO + O_3 \longrightarrow NO_2 + O_2; NO_2 + O \longrightarrow NO + O_2; O_3 + O \longrightarrow O_2 + O_2$. The net result is *odd nitrogen*, a complex of nitrate radicals designated by the symbol NO_x. Some of the NO_x is transported downward to the troposphere, and then it is precipitated to the surface in ~ 6 weeks.

Important agents for the nitrogen oxides formation are solar activity events, such as UV and EUV radiation, solar X-ray (SXR) flares, and solar energetic particles. From a vital importance for the endothermic reactions, which produce NO and NO_2 are solar proton events, whose sources are SXR flares of class $\geq M5$ (see, e.g., Jackman and McPeters, 2011 for a review).

The subject of this study was the relation between the background concentrations of NO, NO_2 and NO_x in the Earth's atmosphere and the SPEs. The main goals were: 1) Statistical significance and rate of the influence of the solar proton flares; 2) The delay (resident time), between SPEs action and the nitrogen oxides enhancement in the Earth's atmosphere. 3) The transfer processes of nitrogen oxides between the middle atmosphere and the terrestrial surface.

2. DATA AND METHODS OF ANALYSIS

The daily average values of the background concentrations $[\mu/m^3]$ of NO, NO_2 and NO_x were registered by the complex background station of the Ministry of Environment and Water, located in the National Astronomical Observatory (NAO) – Rozhen at altitude of 1760 m above the sea. The data time series span the period from 15 October 2004 to 31 December 2012. Because of a lot of gaps in the time series in the period 15 October 2004 – 31 August 2009, the data from 1 September 2009 to the end of 2012 were used.

The data of total daily fluxes [n/day] of the solar energetic protons (SEPs), registered by GOES-11 and GOES-13 geostationary satellites and hosted in Space Weather Center in Boulder, Colorado were also used (http://www.swpc.noaa.gov/Data/index.html#indices). The values of total daily fluxes are considered in two energetic diapasons - $E \geq 10MeV$ and $E \geq 100MeV$. For examination of the nitrogen oxides data, two methods were used: T-R periodogram analysis and cross-correlation analysis (Komitov 1986, 1997).

3. RESULTS

The comparison of the behavior of the NO, NO_2, and NO_x concentrations and the solar proton events presented in Fig. 1, 2, and 3 suggests two features of the SEPs flux behavior.

1. The SEPs flux series contain a quiet component that is characterized with low values and very slow and gradual increasing from October 2004 to September 2008, whereupon the variation tendency changes to gradual decreasing up to December 2012.

2. The SEPs flux series contain consecution of strong and weak flux peaks. The difference between strong and weak flux values vary in the range of several orders.

Fig. 1, 2, and 3 suggest three special features of the relation between the nitrogen oxides concentrations and solar proton events.

1. There is a conformity two types of events – the high values of NO, NO_2, and NO_x concentrations are measured in periods of strong proton flares.

2. The relation between two events is strong delayed by time – the nitrogen oxides concentrations are registered 7-10 months late with respect to the SEPs fluxes peaks.

3. There is second, more expressed tendency of the delaying of the nitrogen oxides in relation to SEPs fluxes – about one month.

The period of low NO, NO_2, and NO_x values between 2007 and 2009 coincides with the deep minimum of solar activity between 11-year solar cycles 23 and 24.

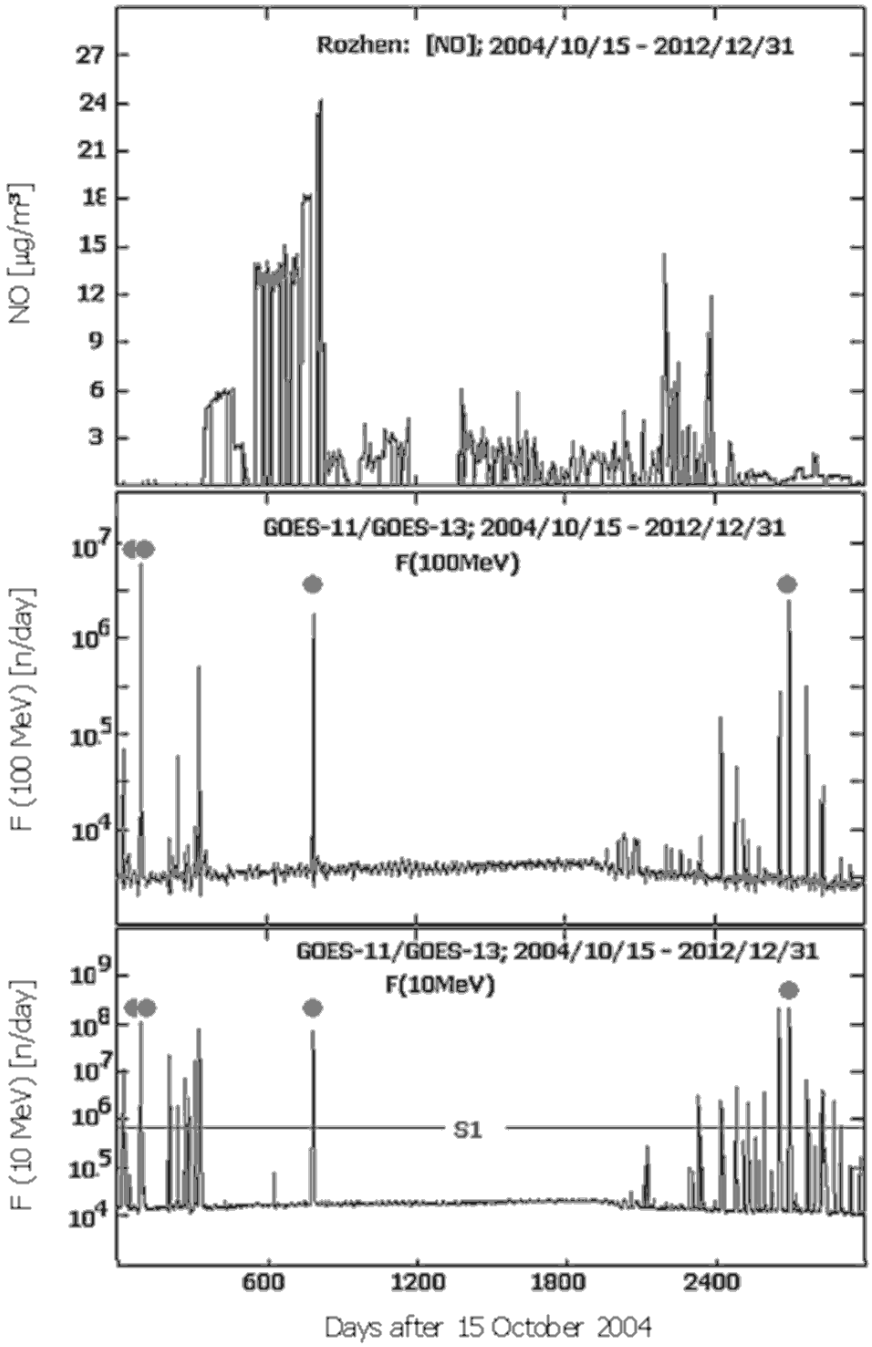

Figure 1: Daily average values of NO concentration and daily total flux (F) of the high energy protons - $F \geq 100MeV$ (middle panels) and low energy protons - $F10 \geq MeV$ (bottom panel).

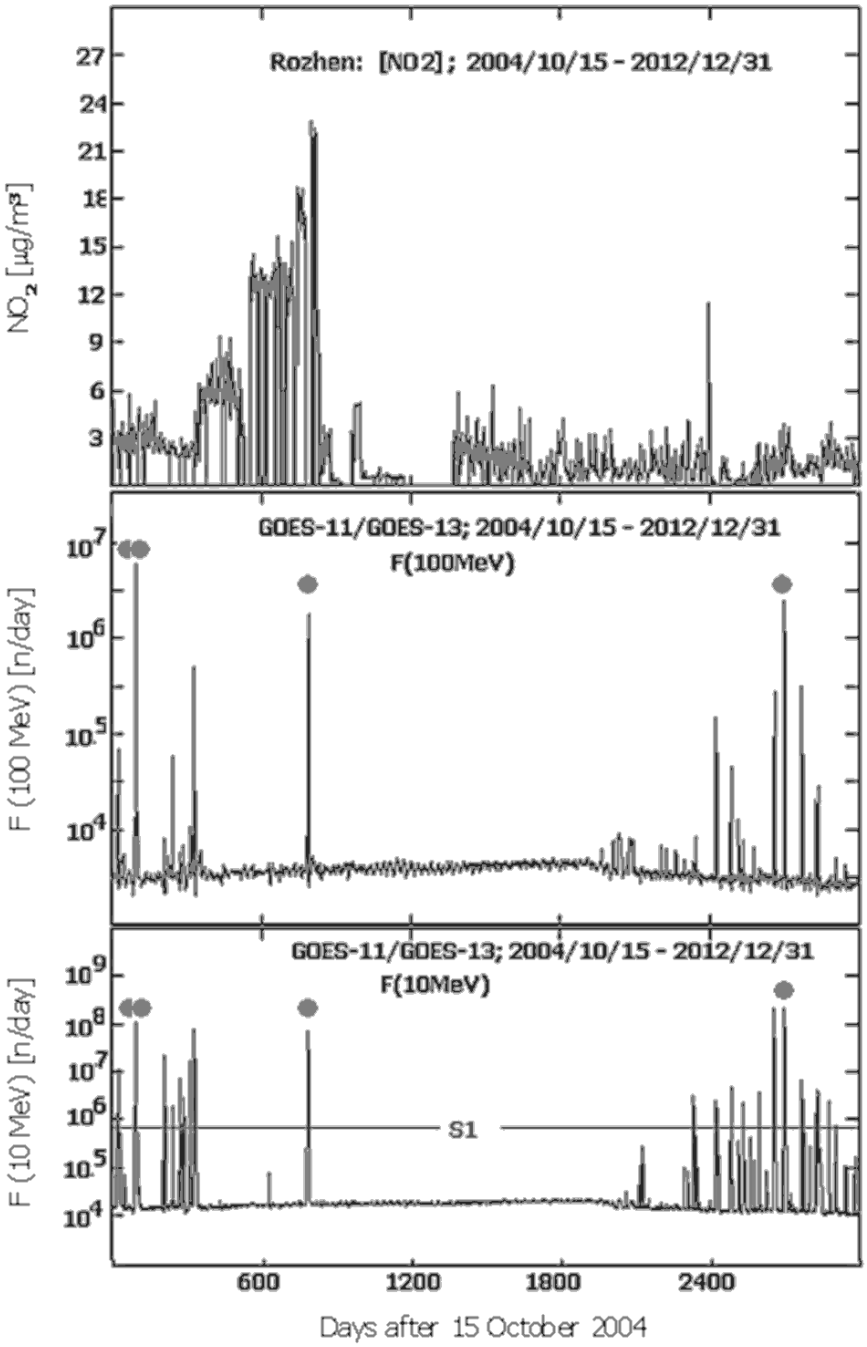

Figure 2: Daily average values of NO_2 concentration and daily total flux of the high energy protons - $F \geq 100MeV$ (middle panel) and low energy protons - $F \geq 10MeV$ (bottom panel).

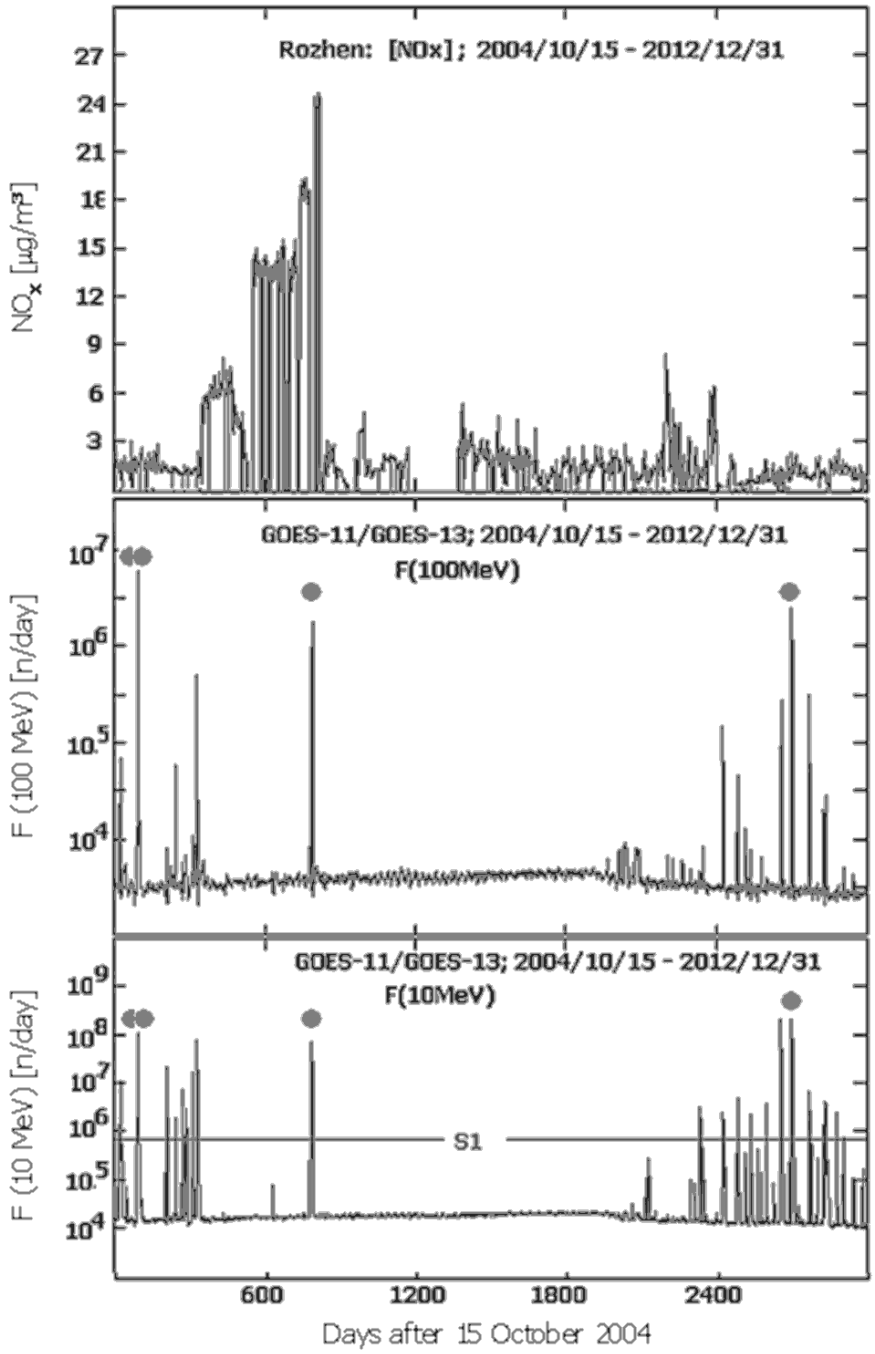

Figure 3: Daily average values of NO_x concentration and daily total flux of the high energy protons - $F \geq 100MeV$ (middle panel) and low energy protons - $F \geq 10MeV$ (bottom panel).

An important question in our analysis of the two types of data series is searching of statistically significant cyclicities in their behaviors. In the first part of data (15 October 2004 – 31 August 2009) the time series have many data gaps and only visual indications for some cyclicities could be found. In the second data part (1 September 2009 – 31 December 2012) the time series are continuous and a quantitative analysis is applicable for them, e.g. T-R periodogram and cross-correlation analysis.

The results from the T-R periodogram analysis are presented in Fig. 4 for the nitrogen oxides data and in Fig. 5 for the SEP data. These analyses of the two events outline three important features.

1. A significant variations with duration of 9-10 months (270–290 days) are outlined in the NO and NO_2 time series (Fig.4).

2. There is a strongly indicative cycle of about 540 days in the $NO-2$ time series, which is resonantly divisible by 180-day one (Fig.4).

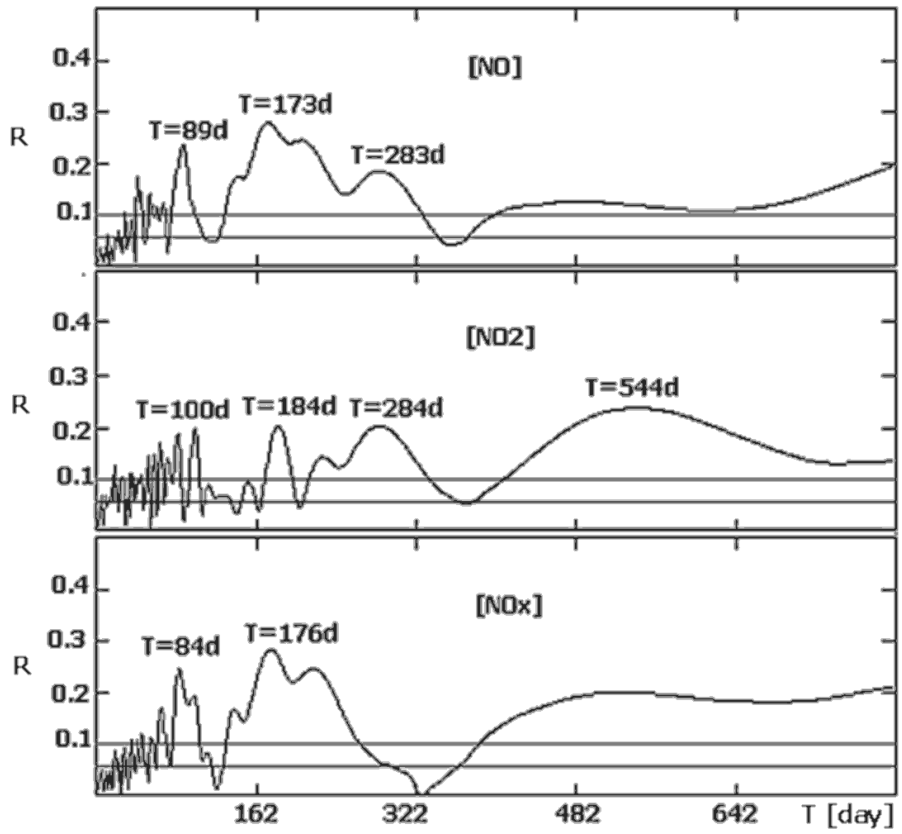

Figure 4: T-R correlagrams of the NO, NO_2, and NO_X time series for the period 1 September 2009 - 31 December 2012.

3. There is a statistically significant cycle with duration of about 180–200 days (T=182 days for F10 MeV and T=204 days for F100 MeV) in the SEP fluxes data. The origin of the quasi 180-day cycle is still uncertain (Fig.5).

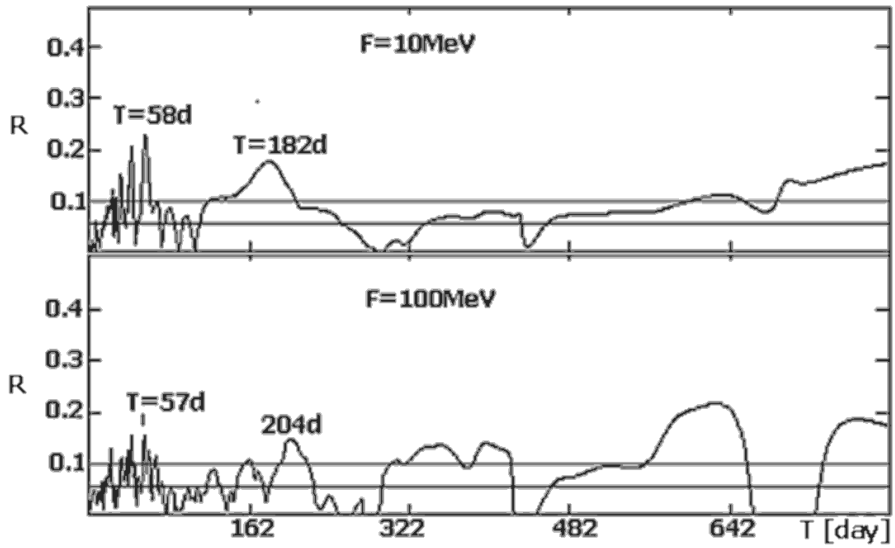

Figure 5: T-R correlagrams of the daily total fluxes time series of the low energy protons $F \geq 10MeV$ (top) and high energy protons $F \geq 100MeV$ (bottom) for the period 1 September 2009 - 31 December 2012.

The cross-correlation analysis was used to reveal some specific features refering to the phase shifting between NO, NO2, and NOx time series and those of the SEPs. The cross-correlation coefficients Rc between nitrogen oxides concentrations and SEP fluxes, presented in Fig. 6 and 7, reveals several important results:

1. There are three significant, positive peaks of Rc at a time lag (t-to) of about 260-280 days ($\sim$ 8-9 months), 305-320 days (10 months), and 430-460 days ($\sim$ 15 months).

2. There are well expressed peaks of Rc at the time lags of 9, 10, and 15 months in the time series of NO and NO_x.

3. For NO_2, a peak at a lag of about one month (30 days) is observed again. Such, but weaker peak at a lag of 28 days is observed for NO_x.

4. It is very interesting that there are two peaks in NO_2 time series at big lags (above one month) - the strong peak at lag of 306 days ($\sim$ 10 months) and another one at lag of 263 days ($\sim$ 9 months).

The results obtained by correlograms (Fig. 6 and 7) suggest that an essential feature of the relationship between SEPs and the nitrogen oxides formation in the atmosphere is its phase shifting in time. Hence, it exists delay time between the SEPs registering at a geostationary orbit, the endothermic reactions responsible for the nitrogen oxides formation in the middle atmosphere, and their registration in the

ground-based station (e.g. in NAO – Rozhen). The presence of more than one peaks for the delay time nitrogen oxides registration could be explained with the different altitudes and geographical positions of their formation, as well as with different processes (diffusion, convection, and wind), which transfer them to the station registering equipment.

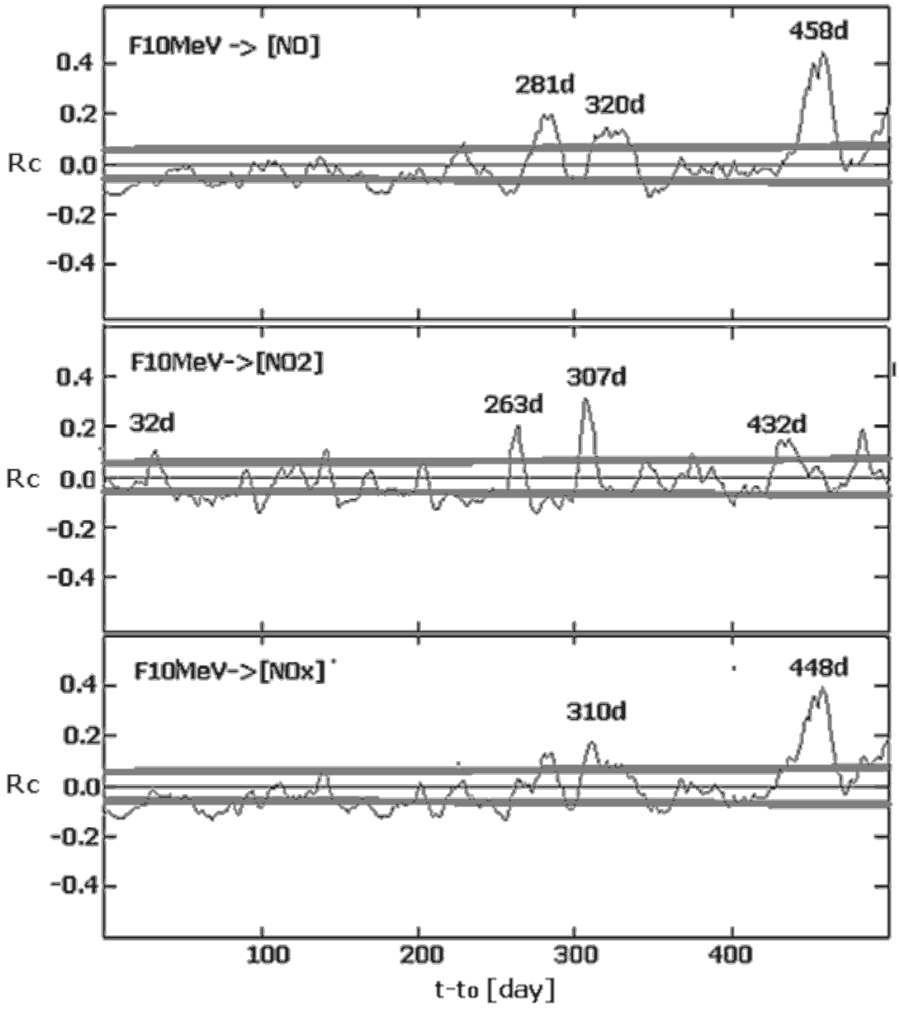

Figure 6: Cross-correlation coefficients Rc between NO, NO_2, and NO_x concentrations and low energy proton flux $F \geq 10MeV$ for the period 1 September 2009 - 31 December 2012.

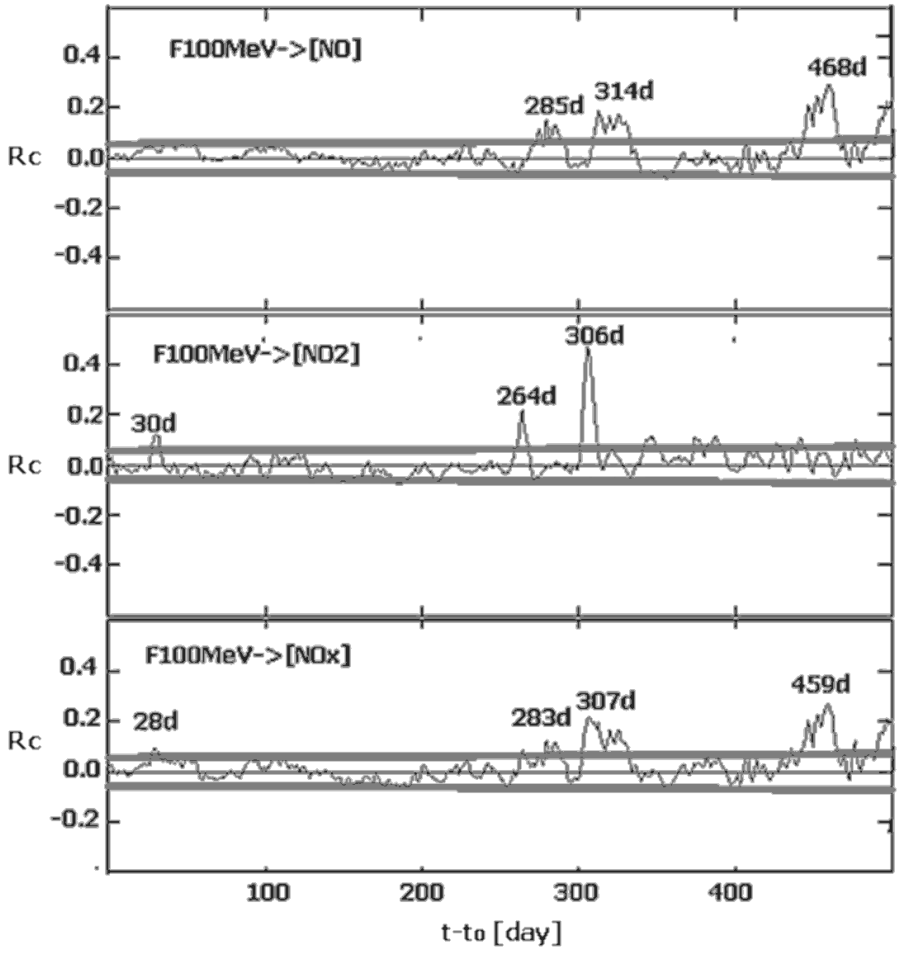

Figure 7: Cross-correlation coefficients Rc between NO, NO_2, and NO_x concentrations and high energy proton flux $F \geq 100MeV$ for the period 1 September 2009 - 31 December 2012.

4. SUMMARY

The obtained results suggest that the significant peaks in the time series of the nitric oxides should be explained with *volley* effect of the NO and NO_2 formation in the middle atmosphere. The formation process pass in the time interval from one month to about one year before the NO and NO_2 peaks registration in the ground-based station, in dependence on their formation altitude, formation geographical position, and the type of the transfer atmospheric processes.

The time series of the nitric oxides span only part of the solar cycle 24 – its increasing phase. Therefore, to give a more certain answer of the question how the solar proton flares affect the NO and NO_2 formation, it is necessary to prolong the

study during next several years, up to the end of the present 24th solar cycle (2018-2019).

The prolongation of these studies could be the base for developing of prognostic models and forecasting of the enhanced NO and NO_2 concentrations in the troposphere.

Acknowledgments

This work is supported by a grant **No. 8785/16.01.2013** of the Enterprise for management of the activities by environment protection, Ministry of Environment and Water, Bulgaria

References

Jackman, C. H., Marsh, D. R., Vitt, F. M., Roble, R. G., Randall, C. E., Bernath, P. F., Funke, B., Lopez-Puertas, M., Versick, S., Stiller, G. P., Tylka, A. J., Fleming, E. L.: 2011, *Atmos. Chem. Phys.*, **11**, 6153-6166.

Komitov B.: 1986, *Soln. Dannye Byull.*, No 5, 73-78.

Komitov B.: 1997, *Bulg. Geoph. J*, **23**, 74-82.

Proceedings of the IX Bulgarian-Serbian Astronomical Conference: Astroinformatics (IX BSACA) Sofia, Bulgaria, July 2-4, 2014,
Editors: M. K. Tsvetkov, M. S. Dimitrijević, O. Kounchev, D. Jevremović and K. Tsvetkova
Publ. Astron. Soc. "Rudjer Bošković" No 15, 2015, 159-163

ON THE STARK BROADENING OF Zr IV IN THE SPECTRA OF DB WHITE DWARFS

ZLATKO MAJLINGER[1], ZORAN SIMIĆ[2] and MILAN S. DIMITRIJEVIĆ[2]

[1]*Faculty of Humanities and Social Sciences, University of Rijeka, 51000 Rijeka, Croatia*
[2]*Astronomical Observatory, Volgina 7, 11060 Belgrade, Serbia*
E-mail: zlatko.majlinger@gmail.com, zsimic@aob.bg.ac.rs, mdimitrijevic@aob.bg.ac.rs

Abstract. The electron-impact widths for four Zr IV spectral lines have been calculated by using the modified semiempirical method. Additionally, by using the obtained results we analized the importance of Stark broadening in the spectra of DB white dwarfs.

1. INTRODUCTION

Zirconium has a significant role in stellar spectroscopy as a member of Sr-Y-Zr triad, important in studying of s-process of nucleosynthesis in HgMn type of so-called chemically peculiar (CP) stars. These stars show great anomalies in their abundances (Lecrone et al, 1993) and provide us a useful informations about stellar evolution. Zirconium is often overabundant in HgMn star spectrum giving thus a better insight in a complex dinamical proccesses occuring in their interior and atmosphere (Heacox, 1979). Also, it is evident (Lecrone et al, 1993, Sikström et al. 1999) that the zirconium abundance determination from weak Zr II optical and from strong Zr III UV spectral lines give significantly different results. This, so-called «zirconium conflict» is still unresolved mistery supposed to be explained as a result of inadequate use of stellar model, e.g. without taking into account of non-LTE effects or diffusion.

The Stark broadening of spectral lines in stellar plasma has already been studied in the case of singly (Zr II) and doubly (Zr III) charged zirconium ions (Popović and Dimitrijević, 1996, 1997, Popović et al. 2001). We hope that new foundings about abundance of triply charged zirconium ions (Zr IV) in stellar spectra get us closer to the solution of «zirconium conflict» mentioned above. Although this problem cannot be solved without the reliable Stark broadening parameters, since it is shown (see for example Popović et al. 2001) that neglecting

the Stark effect influence on line width calculation can cause errors in abundance determination.

2. METHOD OF CALCULATION

Here, we provided Stark full width at half maximum (FWHM) for four transitions of Zr IV, calculated using the modified semiempirical method MSE (Dimitrijević and Konjević 1980) of interest not only for in astrophysics, but also for laboratory, and technological plasmas investigations.

Modified semiempirical method (Dimitrijević and Konjević 1980), for the Stark broadening of isolated, nonhydrogenic ion lines, has been described elsewhere (for example, see Dimitrijević and Popović, 2001). Compared to some other approaches for Stark width and shift calculations, such as semiempirical method of Griem (1968) or semiclassical perturbation method of Sahal-Bréchot (1969a,b), MSE needs less atomic data. If there is no perturbing levels violating the assumed approximations, only energy levels with $\Delta n=0$ and orbital quantum numbers l_i , l_f , $l_i \pm 1$, $l_f \pm 1$ (where l_i and l_f represent initial and final orbital quantum numbers of transition respectively) are needed for a line width calculation. All levels with $\Delta n\neq 0$, needed for semiempirical or semiclassical perturbation methods, are lumped together here and approximately estimated, significantly simplifying calculation technique. The needed matrix elements are obtained within the Coulomb approximation formalism of Bates and Damgaard (1949), while the line and multiplet factors are taken from Shore and Menzel (1968) whenever it is neccesary. MSE approach is tested and confirmed many times, even for complex spectra, mostly with an accuracy not worse then ±50% (Dimitrijević and Konjević 1980, Popović and Dimitrijević, 2001).

3. RESULTS AND DISCUSSION

The Stark width calculations for four Zr IV transitions, 5s $^2S_{1/2}$ - 5p $^2P^o_{1/2}$ λ = 2287.38, 5s $^2S_{1/2}$ - 5p $^2P^o_{3/2}$ λ = 2164.36, 5p $^2P^o_{1/2}$ – 5d $^2D_{3/2}$ λ = 1536.67 and 5p $^2P^o_{3/2}$ – 5d $^2D_{3/2}$ λ = 1607.95 have been performed. The energy levels used to calculate electron-impact FWHM of spectral lines have been taken from Reader and Acquista (1997). The Stark widths are calculated for the electron density of 10^{23} m^{-3} and for temperatures from 10000 K to 500000 K.

Table 1. Stark full widths at half maximum (W_{Mse}) for for the electron density of 10^{23} m^{-3} and for temperatures from 10000 K to 500000 K. W_{Pur}(Å), estimates of Purić and Šćepanović (1999).

	T(K)	W_{Mse}(Å)	W_{Pur}(Å)	W_{Mse}/W_{Pur}
Zr IV λ=2287.38Å $5s\ ^2S_{1/2} - 5p\ ^2P^o_{1/2}$	10000	0.08435	0.06305	1.34
	20000	0.05964	0.04459	1.34
	50000	0.03772	0.02820	1.34
	100000	0.02704	0.01994	1.36
	200000	0.02154	0.01409	1.53
	300000	0.01997	0.01151	1.74
	500000	0.01048	0.00892	1.17

	T(K)	W_{Mse}(Å)	W_{Pur}(Å)	W_{Mse}/W_{Pur}
Zr IV λ=2164.36Å $5s\ ^2S_{1/2} - 5p\ ^2P^o_{3/2}$	10000	0.07681	0.05645	1.36
	20000	0.05431	0.03992	1.36
	50000	0.03435	0.02525	1.36
	100000	0.02457	0.01785	1.38
	200000	0.01959	0.01262	1.55
	300000	0.01811	0.01031	1.76
	500000	0.01702	0.00798	2.13

	T(K)	W_{Mse}(Å)	W_{Pur}(Å)	W_{Mse}/W_{Pur}
Zr IV λ = 1536.67Å $5p\ ^2P^o_{1/2} – 5d\ ^2D_{3/2}$	10000	0.04218	0.05318	0.79
	20000	0.02983	0.03760	0.79
	50000	0.01887	0.02378	0.79
	100000	0.01341	0.01682	0.80
	200000	0.01064	0.01189	0.89
	300000	0.01011	0.00971	1.04
	500000	0.01005	0.00752	1.33

	T(K)	W_{Mse}(Å)	W_{Pur}(Å)	W_{Mse}/W_{Pur}
Zr IV λ = 1607.95Å $5p\ ^2P^o_{3/2} - 5d\ ^2D_{3/2}$	10000	0.04690	0.06058	0.77
	20000	0.03316	0.04284	0.77
	50000	0.02097	0.02709	0.77
	100000	0.01488	0.01916	0.78
	200000	0.01181	0.01355	0.87
	300000	0.01120	0.01106	1.01
	500000	0.01115	0.00857	1.30

We compared our results with estimates of Purić and Šćepanović (1999). The equation obtained from Purić's regression analysis of existing set of Stark broadening data for all ionisation levels of the multiply charged ions and for all elements along the periodic table was adopted for our purpose. After transformation of width from Purić and Šćepanović (1999), which are in angular frequency units, in Å (see for example Dimitrijević and Konjević, 1984) the Stark width is:

$$W_{Pur} = a \cdot Z^{c} \cdot \lambda^{2} \cdot N \cdot T^{-1/2} \cdot (E_{ion}-E_f) - ^{b}$$

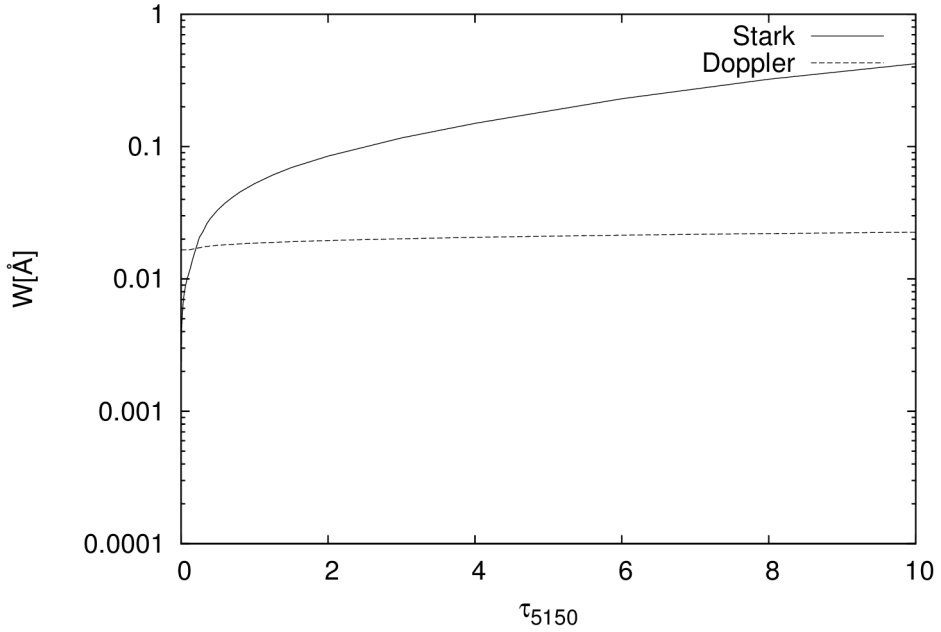

Figure 1. Thermal Doppler and Stark widths for Zr IV 5s $^2S_{1/2}$ - 5p $^2P^o_{1/2}$ λ = 2287.38 Å spectral line for a DB white dwarf atmosphere model with T_{eff} = 15,000 K and log g = 8, as a function of optical depth τ_{5150}.

where W_{Pur} is the estimated width of Purić and Šćepanović (1999) in Å, λ spectral line wavelenght in Å, E_{ion} and E_f energies of ionization and of final level of transition in eV respectively, T temperature in K, Z rest core charge and N electron density in m^{-3}. Coefficients a , b and c are independent of temperature, ionization potential and electron density for a given transition. Coefficients values are $a = 3.27 \cdot 10^{-28}$, $b = 3{,}1$ and $c = 5.2$ (according to Purić and Šćepanović, 1999). The tabulated results show a very good agreement. It is interesting that ratio between calculated and estimated widths remains equal for the temperatures below 100000 K, but above this limit accuracy becomes worst. This phenomenon could be a consequence of approximate use of temperature dependence in the formula of Purić and Šćepanović (1999).

We tested our results in stellar plasma conditions of DB white dwarf atmosphere. White dwarfs have a strong gravity field intensity on their surface causing that the change of particle density being more rapide with the depth then in some other stellar objects. We note also, that Stark width shows linear correlation with the plasma concentration, and Doppler width depends on temperature only. One can see in Fig. 1 that the Stark width is dominant in comparison with Doppler width in DB dwarf stellar spectra, as it has been proved in some recent investigations (see e.g. Simić et al. 2006). For this comparison, the existing stellar model atmosphere for DB white dwarfs published by Wickramasinghe (1972) is taken with $\log g = 8$ and $T_{eff} = 15000$ K.

It is evident from the Figure 1 that the electron-impact width shows the significant dependence on the optical depth in the atmosphere of DB white dwarf, while the thermal width almost remains constant with the optical depth change, and that Stark broadening is dominant in comparison with Doppler broadening.

References

Bates, D. R., Damgaard, A.: 1949, *Phil. Trans. Roy. Soc.* London, Ser. A, **242**, 101.
Dimitrijević, M. S., Konjević, N.: 1980, *JQSRT*, **24**, 451.
Dimitrijević, M. S., Konjević, N.: 1984, *Z. Naturforsch.,* **39A**, 553.
Dimitrijević, M. S., Popović, L. Č.: 2001, *J. Appl. Spectrosc*., **68**, 893.
Griem, H.R.: 1968, Phys. Rew., 165, 258.Heacox, W.D.: 1979, *ApJS*, **41**, 645.
Leckrone, D. S., Wahlgren, G. M., Johansson, S. G. and Adelman, S. J.: 1993, Peculiar Versus Normal Phenomena in A-type and Related Stars, ed. M. Dworetsky, F. Castelli and R.Faraggiana, *ASP Conf. Ser*. **44**, 42.
Sikström, C. M., Lundberg, H., Wahlgren, G. M., et al.: 1999, *A&A*, **343**, 297.
Popović, L. Č., Dimitrijević, M. S.: 1996, *A&AS*, **120**, 373.
Popović, L. Č., Milovanović, N. Dimitrijević, M. S.: 2001, *A&A,* **365**, 656.
Purić, J., Šćepanović M.: 1999, *ApJ*, **521**, 490.
Reader, J., Acquista, N.: 1997, *Phys. Scr*., **55**, 310.
Sahal-Bréchot, S.: 1969a, *A&A*, **1**, 91.
Sahal-Bréchot, S.: 1969b, *A&A*, **2**, 322.
Shore, B. W., Menzel, D. H.: 1968, *ApJ*, **12**, 187.
Simić, Z., Dimitrijević, M. S., Popović L. Č., Dačić, M.: 2006, *New Astronomy*, **12**, 187.
Wickramarsinghe, D. T.: 1972, *Mem.R. Astron.Soc.*, **76**, 129.

Proceedings of the IX Bulgarian-Serbian Astronomical Conference: Astroinformatics (IX BSACA) Sofia, Bulgaria, July 2-4, 2014,
Editors: M. K. Tsvetkov, M. S. Dimitrijević, O. Kounchev, D. Jevremović and K. Tsvetkova
Publ. Astron. Soc. "Rudjer Bošković" No 15, 2015, 165-170

OBSERVATIONS AT THE 60 cm ASV TELESCOPE AND THE LINK GAIA CRF - ICRF

GORAN DAMLJANOVIĆ[1], FRANCOIS TARIS[2], GEORGI LATEV[3] and MILAN STOJANOVIĆ[1]

[1]*Astronomical Observatory, Volgina 7, 11060 Belgrade, Serbia*
[2]*SYRTE, Observatoire de Paris, 61 avenue de l'Observatoire, 75014 Paris, France*
[3]*Institute of Astronomy and NAO Rozhen, Bulgarian Academy of Sciences, 72 Tsarigradsko shosse, BG-1784 Sofia, Bulgaria*
E-mail: gdamljanovic@aob.rs

Abstract. The Gaia mission is a cornerstone of European Space Agency (ESA). It was launched at the end of 2013. The Gaia is the next step (after HIPPARCOS) in development of European pioneering high accuracy astrometry; the main goal is to make a dense QSO-based Gaia Celestial Reference Frame (Gaia CRF). Because of it, it is necessary to link future Gaia CRF and International Celestial Reference Frame (ICRF) with high accuracy. Also, to compare QSOs (or the extragalactic radio sources - ERS) optical and radio positions (VLBI ones), and to search for a relation between optical and radio reference frames. At the other hand, in 2014 one of us (GD) started joint research project "Observations of ICRF radio-sources visible in optical domain", in the frame of bilateral cooperation between Serbian Academy of Sciences and Arts and Bulgarian Academy of Sciences (BAS), which partly deals with Gaia CRF - ICRF link investigation. In mentioned collaboration, we are using the 2 m telescope of NAO Rozhen (Bulgaria) for investigation of morphology of ICRF objects interesting to Gaia astrometry, and the 60 cm telescope of Astronomical Station Vidojevica - ASV (Serbia) for photometry investigation of QSOs. The displacements of the optical photocenter of QSOs could be the result of its astrophysical processes and in line with their positions (astrometry); it is of importance for mentioned link. Some preliminary photometric results of QSOs using the 60 cm ASV are presented here.

1. INTRODUCTION

As a cornerstone of the European Space Agency (ESA), the Gaia space-based mission is the next step of the European pioneering high accuracy astrometry, after the HIPPARCOS one (Kovalevsky et al. 1997). It was launched at December 2013. During its 5-year lifetime, the Gaia is going to map repeatedly over one billion stars. It means, the objects of entire Galaxy with apparent V magnitude between 5.6 and 20, and about 500000 quasars (QSOs) or extragalactic radio sources (ERS); a large amount of astronomical data. So, the Gaia is going to revolutionize our knowledge of the Milky Way.

The main goal of that mission is to make a dense QSO-based Gaia Celestial Reference Frame (Gaia CRF). And it is of importance the relation between optical and radio reference frames via the observations of some ICRF objects (Fey et al. 2009) which are visible in the optical domain. Also, to compare their optical and radio positions (VLBI ones). The other important task is to establish the link between future Gaia CRF and International Celestial Reference Frame (ICRF) with high accuracy (Bourda et al. 2010, 2011; Petrov 2011, 2013; Taris et al. 2013), but for now only about 10% of the ICRF objects are good enough for mentioned link: some sources are not bright enough in optical domain of wavelengths, some objects have significant extended radio emission, etc. So, it is of importance to find and check other sources; they are weak ERS with bright optical counterparts and it is necessary to observe and investigate these objects. At the other hand, the coordinates of sources (it means, astrometry) are in line with the displacements of their optical photocenter as a result of astrophysical processes of objects. And it is necessary to investigate the variations of the light curves of mentioned objects.

For morphology investigation of QSOs we use the CCD observations of ERS made at the RCC telescope[1] of Rozhen National Astronomical Observatory - NAO (Bulgarian Academy of Sciences). For photometry investigation we make the observations of QSOs using the 60 cm telescope at Astronomical Station Vidojevica - ASV (in Fig. 1) of the Astronomical Observatory in Belgrade (AOB), Serbia.

From mid 2013, we did the photometry observations of 47 objects using the 60 cm ASV telescope, and some preliminary photometry results are presented here.

2. DATA AND RESULTS

At the beginning of 2014, GD started joint research project "Observations of ICRF radio-sources visible in optical domain", in the frame of bilateral cooperation between Serbian Academy of Sciences and Arts and Bulgarian Academy of Sciences. That project partly deals with Gaia CRF - ICRF link investigation. And in collaboration with Bulgarian colleagues, we are doing our observations at the Rozhen telescope (D/F=2m/16m) of National Astronomical Observatory, Bulgarian Academy of Sciences (BAS), for investigation of morphology of ICRF objects interested for Gaia astrometry. For photometry investigation, the ASV (in Fig. 1) of AOB telescope (D/F=60cm/600cm) is useful. These telescopes are between other instruments for mentioned subjects; the main information of the 2 m Rozhen and 60 cm ASV telescopes are in Table 1. The information of the first column of Table 1 are: site, telescope and D(cm)/F(cm). In the second column, the geographic coordinates (longitude - λ, latitude - φ) and altitude (h) of site are presented. The field of view (FoV) and some details of CCD cameras are in the third column. In the near future (during next year), a new $D = 1.4$ m telescope will be installed at ASV in the frame of Belissima project (http://belissima.aob.rs).

The 60 cm ASV telescope was used for optical observations of 47 objects, mostly QSOs, and photometry investigation (for the link Gaia CRF - ICRF) since mid-2013. Until now, near all objects were observed, some of them few times. We did it in the

[1]Based on observations with the 2 m RCC telescope of the Rozhen National Astronomical Observatory operated by the Institute of Astronomy, Bulgarian Academy of Sciences.

Figure 1: Telescope Cassegrain 60 cm, ASV.

B, V and R bends (three CCD images per filter). Here, we present some preliminary photometric results of objects QSO 1212+467 (in Fig. 2, the observations were done at June 27^{th} 2014) and BL 1722+119 (in Fig. 3, July 9^{th} 2013). One of our observations with 60 cm ASV is presented in Fig. 2; the exposure time $exp. = 300^s$ in R filter. All exposures were guided.

The standard bias, dark and flat-fielded corrections were done (Berry and Burnell 2002); also, hot/bad pixels were removed. For 1722+119, the comparison stars were used via http://www.lsw.uni-heidelberg.de/projects/extragalactic/charts/; C1, C2,

Table 1: The main information of the ASV 60 cm and Rozhen 2 m telescopes.

Site	longitude - $\lambda(^o)$	CCD camera
Telescope	latitude - $\varphi(^o)$	pixel array and scale ($''$)
$D(cm)/F(cm)$	altitude - h (m)	pixel size (μm) and field of view - FoV ($'$)
ASV (AOB)	21.5	Apogee Alta U42
Cassegrain	43.1	2048x2048, 0.46
60/600	1150	13.5x13.5, 15.8x15.8
Rozhen (NAO BAS)	24.7	VersArray 1300B
Ritchey-Chretien	41.7	1340x1300, 0.26
200/1600	1730	20x20, 5.6x5.6

Table 2: Our photometry results of QSO 1212+467 and BL 1722+119 with st. errors.

type&name of object, filter	catalogue or t	mag. of object	magnitude of star 2,3,4,5
B	SDSS		16.40(0.05);16.56(0.05);17.02(0.05);17.94(0.06)
V	SDSS		15.80(0.03);16.07(0.03);16.43(0.03);17.18(0.04)
R	SDSS		15.45(0.04);15.78(0.04);16.08(0.04);16.73(0.05)
Q1212+467B	836.38924	18.15(0.03)	16.46(0.01);16.54(0.01);16.98(0.02);17.84(0.01)
Q1212+467V	836.39287	17.94(0.03)	15.87(0.01);16.05(0.01);16.36(0.01);17.13(0.01)
Q1212+467R	836.39652	17.78(0.01)	15.54(0.01);15.75(0.01);15.99(0.01);16.66(0.01)
			magnitude of C1,C2,C3,C4
B	SDSS		-;-;-;-
V	SDSS		11.98(0.05);13.21(0.05);14.10(0.05);15.74(0.08)
R	SDSS		10.93(0.05);12.62(0.05);13.64(0.50);15.14(0.08)
L1722+119B	483.48651	-	-;-;-;-
L1722+119V	483.48129	15.32(0.02)	-;13.22(0.01);14.10(0.01);15.67(0.01)
L1722+119B	483.49204	14.87(0.01)	-;12.63(0.01);13.62(0.01);15.15(0.01)

C3 and C4 (see Fig. 3), but C1 was saturated in V and R filters (at our data), and in B filter there is not input magnitude data from mentioned site. We need the calibrated stars around the object or precise (as much as possible) photometric input data during determining the calibrated stars (from some photometric catalogue). And for the object 1212+467, we determined the calibrated stars, which are indicated from 2 to 5 in Fig. 2 (the QSO is indicated as 1), by using SDSS catalogue and transformations (Chonis and Gaskell 2008) to calculate B, V, R magnitudes from u, g, r, i, z ones. The relative photometric method was used. The MaxIm DL Pro 5 image processing package was applied for CCD observations, and all frames were reduced individually. We took into account the calibrated stars with the signal to noise ratio (SNR) which is similar to or better than QSO one. The calculated magnitude (of object or output data for calibrated star) is the average value, from three CCD images, with standard error. Our preliminary photometry data of 1212+467 and 1722+19 are presented in Table 2.

The main columns of Table 2 are: the source type, name of ERS and filter are in the first column (Q – quasar L – BL Lac, A – active galactic nuclei or quasar, G – galaxy), the date t (or the catalogue SDSS which was used for calculation of B,V,R magnitudes of comparison stars via u,g,r,i,z magnitudes) in next column, and then the magnitudes for object and comparison stars (or input B,V,R magnitudes of comparison stars) in next two columns; $t = JD - 2456000$, the JD is Julian Date. The calibrated stars, around the object 1212+467, are marked with circles from 2 to 5, and the QSO with 1. Usually, the ERS is near the central part of the images.

The input photometric data and our photometry results (output) for calibrated stars are in accordance with each other. It means, the input data (of stars C1,C2,C3,C4 for object 1722+119, and stars 2,3,4,5 for object 1212+467) are good enough to calculate the magnitudes of our objects with small standard errors; the standard errors are of the order 0.01 magnitude. Also, the CCD observations using the 60 cm ASV

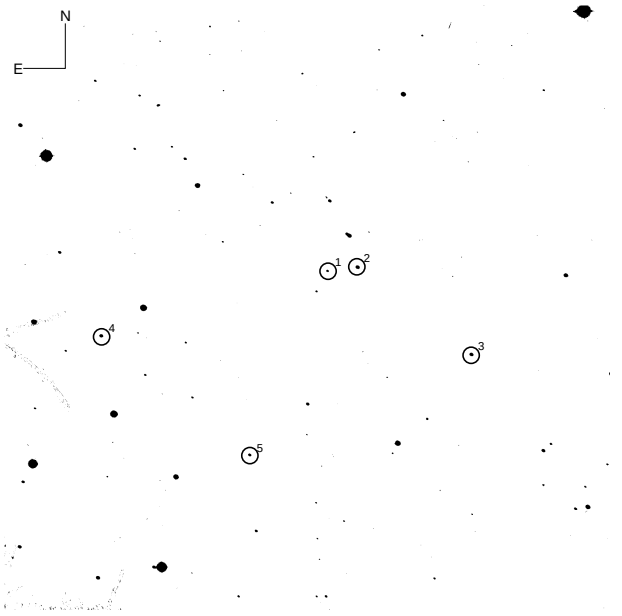

Figure 2: The QSO 1212+467 (1) with calibrated stars (2-5); FoV is 15.′8x15.′8.

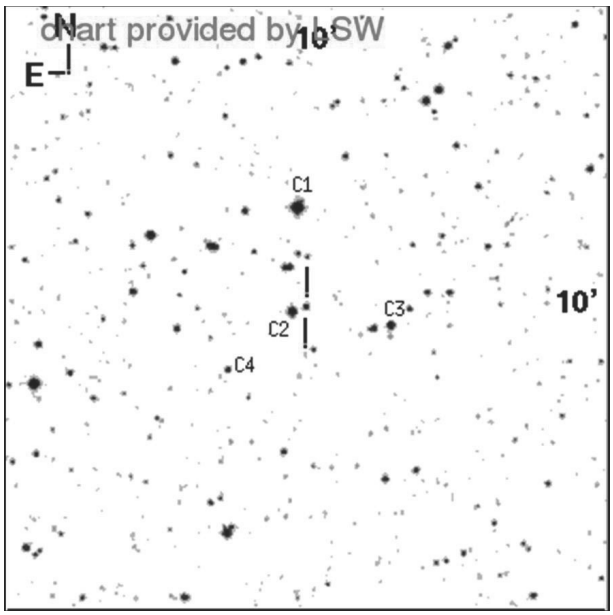

Figure 3: The BL 1722+119 with calibrated stars (C1,C2,C3,C4).

telescope are qualified for precise photometry of QSOs, and mentioned astrometry investigation of QSOs. The standard bias, dark and flat-fielded corrections (with removal of hot/bad pixels) were done to improve photometry results. So, the observations of QSOs using the 60 cm ASV are useful for mentioned link.

3. CONCLUSIONS

Here, we presente our preliminary photometry results of QSOs observations (objects 1212+467 and 1722+119) using the 60 cm ASV telescope. For the object 1722+119, we used the input photometry data of calibrated stars (C1,C2,C3,C4) via site http://www.lsw.uni-heidelberg.de/projects/extragalactic/charts/. For the object 1212+467, we determined calibrated stars around the QSO, and calculated their magnitudes in B,V,R filters using u,g,r,i,z ones (from SDSS catalogue DR7) and transformations (Chonis and Gaskell 2008). All necessary steps for reduction of CCD data (the standard bias, dark and flat-fielded corrections, and removal of hot/bad pixels) were applied. Also, it is of importance for quality data that the average seeing at ASV site is near 1.2 arcsec. So, we can get the magnitudes of our objects (QSOs) with small standard errors which are of the order 0.01 magnitude.

Some problems during calculating of B,V,R magnitudes of QSOs can be caused by: faintness of the optical counterparts to QSOs, atmospheric influences, technical problems, etc. For example, we could improve the quality of ASV data by using star guider (to use the exposures longer than 5 minutes for fain objects).

We conclude that this kind of observations (of QSOs with magnitudes less than about $V = 18.5$) and mentioned investigations are possible with the 60 cm ASV instrument.

Acknowledgements

The authors from the AOB gratefully acknowledge the observing grant support from the Institute of Astronomy and Rozhen National Astronomical Observatory, Bulgarian Academy of Sciences. This research has been supported by the Ministry of Education and Science of Serbia (Project 176011 "Dynamics and kinematics of celestial bodies and systems").

References

Bourda, G., et al.: 2010, *A&A*, **520**, A113.
Bourda, G., et al.: 2011, *A&A*, **526**, A102.
Berry, R., Burnell, J.: 2002, "The Handbook of Astronomical Image Processing, Includes AIP4WIN Software", Willmann-Bell, Inc., Richmond, USA.
Chonis, T. S., Gaskell, C. M.: 2008, *Astron. J.*, **135**, 264.
Fey, A. L., Gordon, D., Jacobs, C. S.: 2009, IERS Technical Note, No. 35.
Kovalevsky, J., Lindegren, L., Perryman, M. A. C., Hemenway, P. D., Johnston, K. J., Kislyuk, V. S., Lestrade, J.-F., Morrison, L. V., Platais, I., Röser, S., Schilbach, E., Tucholke, H.-J., de Vegt, C., Vondrák, J., Arias, F., Gontier, A.-M., Arenou, F., Brosche, P., Florkowski, D. R., Garrington, S. T., Preston, R. A., Ron, C., Rybka, S. P., Scholz,R.-D., Zacharias, N.: 1997, "The Hipparcos Catalogue as a realization of the extragalactic reference system", *A&A*, **323(2)**, 620.
Petrov, L.: 2011, *Astron. J.*, **142**, 105.
Petrov, L.: 2013, *Astron. J.*, **146**, 5.
Taris, F., et al.: 2013, *A&A*, **552**, A198.

Proceedings of the IX Bulgarian-Serbian Astronomical Conference: Astroinformatics (IX BSACA) Sofia, Bulgaria, July 2-4, 2014,
Editors: M. K. Tsvetkov, M. S. Dimitrijević, O. Kounchev, D. Jevremović and K. Tsvetkova
Publ. Astron. Soc. "Rudjer Bošković" No 15, 2015, 171-177

THE MATHEMATICIAN AND THE ASTRONOMER SIMON MARIUS (1573 – 1624)

KATYA TSVETKOVA[1], MILAN S. DIMITRIJEVIĆ[2]
and MILCHO TSVETKOV[1]

[1]*Institute of Mathematics and Informatics, Bulgarian Academy of Sciences*
Acad. Georgi Bonchev Str., Block 8, Sofia 1113, Bulgaria
[2] *Astronomical Observatory, Volgina 7, 11060 Belgrade, Serbia*
E-mail: katya@skyarchive.org, mdimitrijevic@aob.bg.ac.rs,
tsvetkov@skyarchive.org

Abstract. We present the work of Simon Marius - a mathematician and astronomer who discovered in 1610 the four largest satellites of Jupiter with a Belgian made telescope at about the same time as Galileo Galilei, but published his discoveries 4 years later. In 2014 the astronomical community commemorates 400 years since the publishing of Simon Marius' book *Mundus Iovialis* containing his observations done independently by Galilei. Marius' records are even closer to the modern figures than Galilei's ones. Simon Marius noticed also, that the orbital plane of the Jupiter satellites is slightly tilted relative to both the Jupiter equatorial plane and the ecliptic, explaining thus the discrepancies in latitude, which Galilei did not mention. Marius also noticed the change in the satellites brightness and calculated respective tables for the period 1608 - 1630. Simon Marius was a calendar maker and a translator of Euclid from Greek – he published *Die Ersten Sechs Bücher Elementorum Euclidis* (The First Six Books Elementorum Euclidis). Among his observations are the comets of 1596 and 1618, the supernova in the constellation Ophiuchus in 1604 (giving its precise position), observations of Venus, and the sun spots, from whose movement he noticed that the equatorial plane of the sun is tilted relative to the ecliptic and the appearance of sunspots is periodical. Simon Marius first observed with telescope the Andromeda Nebula in December 1612, and gave the first description of this object based on telescopic observation.

The multilingual portal dedicated to Simon Marius (http://www.simon-marius.net/) and prepared by the Nuremberg Astronomical Society, has been opened since February 2014. The portal gives introduction to his biography and scientific achievements, as well as retrievable sources, secondary literature, lectures, news and convenient links.

1. INTRODUCTION

In 2014 the astronomical community commemorates 400 years since the publishing of Simon Marius' book *Mundus Iovialis.* The book (Fig. 1) contains his observations in 1609 - 1610 on the four largest satellites of Jupiter with a Belgian made telescope. Marius's observations had been done at about the same time as Galileo Galilei's discoveries, but published 4 years later than Galilei. Nowadays the first four satellites of Jupiter are known as the Galilean moons, but their own names - Io, Europa, Ganymede, and Callisto, introduced at the beginning of the 20th century, were given by Simon Marius.

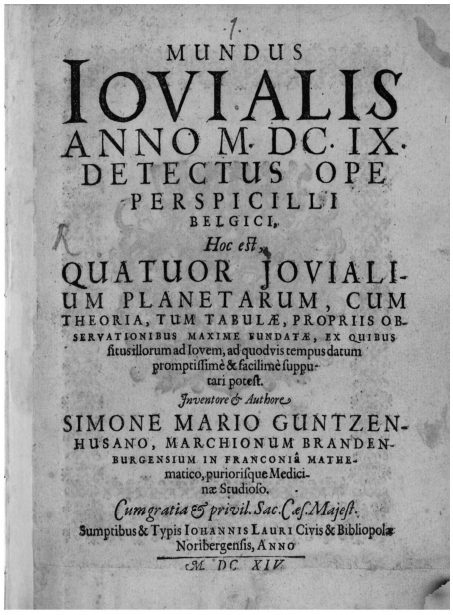
MUNDUS
IOVIALIS
ANNO M. DC. IX.
DETECTUS OPE
PERSPICILLI
BELGICI,
Hoc eſt,
QUATUOR IOVIALIUM PLANETARUM, CUM
THEORIA, TUM TABULÆ, PROPRIIS OBSERVATIONIBUS MAXIMÈ FUNDATÆ, EX QUIBUS
ſitus illorum ad Iovem, ad quodvis tempus datum
promptiſſimè & facilimè ſupputari poteſt.
Inventore & Authore
SIMONE MARIO GUNTZENHUSANO, MARCHIONUM BRANDENBURGENSIUM IN FRANCONIÂ MATHEmatico, purioriſque Medicinæ Studioſo.
Cum gratia & privil. Sac. Cæſ. Majeſt.
Sumptibus & Typis IOHANNIS LAURI Civis & Bibliopolæ
Noribergenſis, ANNO
M. DC. XIV.

Figure 1: Simon Marius' book *Mundus Iovialis* from 1614.

2. SHORT BIOGRAFY

Simon Marius (Fig. 2) was born on January 10, 1573 as Simon Mayr (or Mair) in Gunzenhausen, where his father Reinhard Marius was a mayor in 1576. By chance the local margrave Georg Friedrich overheard the young Simon singing and arranged for him to be enrolled in the Prince school (Fürstenschule) at Heilsbronn. Simon Mayr finished the school in 1601 and being already interested from astronomy went to Prague to meet Tycho Brahe. But unfortunately Brahe died 4 months later, and Simon continued his education in medicine in Padua in the period 1602 – 1605, being even a member of the board of the so-called German Student-Nation in Padua. In the same time (1592 – 1610) Galilei taught geometry, mechanics, and astronomy in the University of Padua. In the period

1606 - 1624 he was a court mathematician to the Margraves in Ansbach, as well as medical practitioner, astronomer and calendar maker. Meanwhile Simon Mayr married Felicitas Lauer – the daughter of his Nuremberg publisher Johann Lauer, and had five sons and five daughters, of whom only the daughters survived their childhood. Simon Mayr died on January 5, 1625.

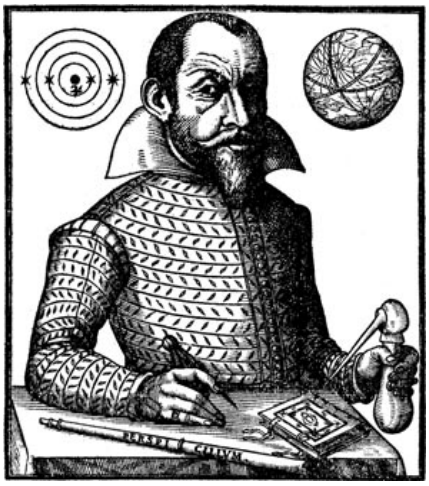

Figure 2: Portrait of Simon Marius from the book *Mundus Iovialis.*

3. RESEARCH ACTIVITY

Simon Mayr published as Simon Marius after the fashion of his times. Still being in the Prince school at Heilbronn in 1594 he began his meteorological records, followed by astronomical observations of the appeared comet in 1596, of the supernova in the constellation Ophiuchus in 1604 (giving the precise positions before the invention of the telescope).

Since summer 1609 Simon Marius had at his disposal a Belgian made telescope, thanks to his mentor Johannes Philipp Fuchs von Bimbach. With this telescope he discovered the four largest satellites of Jupiter – by his own records given according to the Julian calendar on December 29, and therefore just one day after Galileo had discovered them, who dated his observations according to the Gregorian calendar. Simon Marius published his discoveries in the book *Mundus Iovialis* (The World of Jupiter), published by Johann Lauer in Nuremberg in 1614. His observations published in 1614 or 4 years later were done independently by Galilei. Marius‘ records are even closer to the modern figures than Galilei's ones. He noticed also, that the orbital plane of the Jupiter satellites is slightly tilted relative to both the Jupiter equatorial plane and the ecliptic, explaining thus the discrepancies in latitude, which Galilei did not mention.

Marius also noticed the change in the satellites' brightness and calculated respective tables for the period 1608 - 1630.

Marius was also a calendar maker – since 1601 he published yearly the calendars *Prognosticon astrologicum* up to his dead at end of 1624. Johann Lauer continued to publish the prepared calendars up to 1629.

In 1610 Simon Marius published his translation of Euclid from Greek – *Die Ersten Sechs Bücher Elementorum Euclidis* (The First Six Books Elementorum Euclidis) published by Paul Böhem in Ansbach in 1610 and containing, 167 pages (Fig. 3).

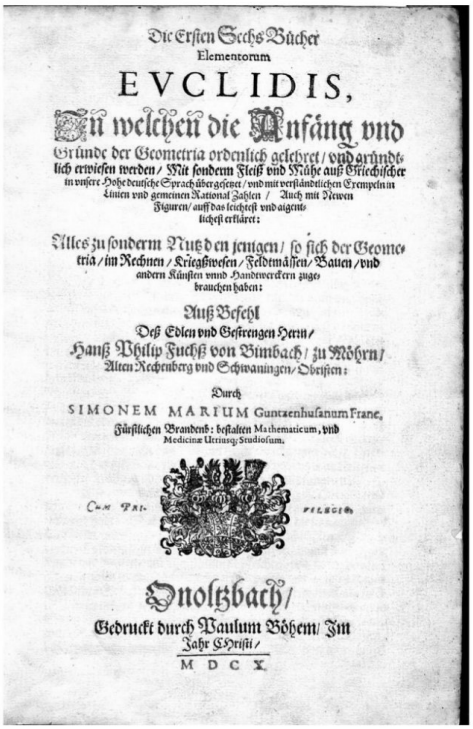
Die Ersten Sechs Bücher
Elementorum
EVCLIDIS,
In welchen die Anfäng vnd
Gründe der Geometria ordentlich gelehret / vnd gründtlich erwiesen werden / Mit sonderm Fleiß vnd Mühe auß Griechischer in vnsere Hohe deutsche Sprach übergesetzet / vnd mit verständlichen Exempeln in Linien vnd gemeinen Rational Zahlen / Auch mit Newen Figuren / auff das leichteste vnd aigentlichest erkläret:
Allen zu sonderm Nutz den jenigen / so sich der Geometriä / im Rechnen / Kriegswesen / Feldtmässen / Bauen / vnd andern Künsten vnnd Handwerckern zugebrauchen haben:
Auß Befehl
Deß Edlen vnd Gestrengen Herrn /
Hanß Philip Fuchß von Bimbach / zu Möhrn / Alten Rechenberg vnd Schwaningen / Obristen:
Durch
SIMONEM MARIUM Guntzenhusanum Franc.
Fürstlichen Brandenb: bestalten Mathematicum, vnd Medicinæ Utriusq; Studiosum.
Onoltzbach /
Gedruckt durch Paulum Böhem / Im Jahr Christi /
M D C X

Figure 3: Simon Marius' *Die Ersten Sechs Bücher Elementorum Euclidis,* published by Paul Böhem in Ansbach in 1610.

In summer 1611 he did observations of Venus, observations of sun spots since August 1611, from whose movement he noticed in November 1611 that the equatorial plane of the sun is tilted relative to the ecliptic. In 1619 he first suggested that the appearance of sunspots was periodical.

Simon Marius was the first observer with telescope of the Andromeda Nebula in December 1612, and gave the first description of this object based on telescopic observation. The Persian astronomer Abd ar-Rahman as-Sufi (Al Sufi) described

the Andromeda galaxy still in 964 according to hand-written parchment. Marius described that this pale gloss observed is not only due of the single stars.

In 1618 Simon Marius observed the third and largest of the three comets of that year.

Although Marius was in the possession of the most important astronomical discoveries of the early 17th century, he opposed the heliocentric world picture and favoured that one of Tycho Brahe after reading Copernicus during the winter of 1595–1596.

To this day, Marius' work is overshadowed by the Gallilei accusation of plagiarism, even though it was proven at the beginning of the 20th century that Marius had conducted his research entirely independently and even his earliest records are closer to the modern figures than those of Galilei - see the paper **Galilee et Marius** (from French: Galilei and Marius) of Oudemans and Boscha (1903), **'Mundus Jovialis' of Simon Marius** - English translation of Mundus Jovialis by Prickard (1916), **Zur Ehrenrettung des Simon Marius** (from German: In Defense of Simon Marius) by E. Zinner (1942).

4. MULTILINGUAL PORTAL

The multilingual portal (in 28 languages) dedicated to Simon Marius (http://www.simon-marius.net/) and prepared by the Nuremberg Astronomical Society, has been opened since February 2014. It is intended to be a guide through the anniversary year of 2014. The portal gives introduction to his biography and scientific achievements, as well as to electronically retrievable sources, secondary literature, lectures, news, convenient links and announcements for various events within the framework of the Simon-Marius-Anniversary 2014. Everybody is invited - from the international research community, as well as all other interested people - to make use of this multilingual portal and also to make your own contributions.

Among 28 languages in this multilingual portal are Bulgarian and Serbian. The corresponding portals are prepared by K. Tsvetkova and M. Tsvetkov for the Bulgarian language and M. S. Dimitrijević for the Serbian language.

5. CONCLUSIONS

The intention of this paper is to make the Bulgarian and Serbian astronomical communities known with the scientific achievements of Simon Marius in the anniversary year of 2014. As a scientific acknowledgment of the astronomical community can be assigned the adoption at the beginning of the 20th century of the names of the four largest Jupiter satellites, which were given by Simon Marius. The names are after the lovers of the Greek god Zeus or his Roman equivalent Jupiter – Io (a nymph who was seduced by Zeus), Europa (a Phoenician woman for whom the continent Europe was named, abducted by Zeus in the form of a white bull), Ganymede (a divine hero whose homeland was Troy, described

by Homer as the most beautiful of mortals, he was the lover of Zeus, abducted by him in the form of an eagle, to serve as cup-bearer in Olympus), and Callisto (as a follower of Artemis, Callisto, who was the daughter of Lycaon, king of Arcadia, took a vow to remain a virgin, as did all the nymphs of Artemis, but to have her, Zeus disguised himself, as Artemis (Diana), in order to lure her into his embrace). The names were suggested to Marius by Kepler during their meeting in Ratisbon (present Regensburg) in 1613.

In 1935 Simon Marius was honoured by the astronomical community by naming a lunar crater in the Oceanus Procellarum, as well as the nearby "Marius Hills" region (see http://www.rimamarius.com/index.php for more details as "Marius Pit", etc.). In 1979, a region of ancient dark terrain on Jupiter's satellite Ganymede was named Marius Regio (how it looks like see at http://www.planetary.org/ multimedia/space-images/jupiter/marius-regio-ganymede .html). Recently, in the end of March 2014, the Minor Planet Center announced the decision of the Committee for Small-Body Nomenclature of the International Astronomical Union to give a name of the asteroid 7984, discovered by the Czech astronomer Zdenka Vavrova, after Simon Marius. The minor planet, moving with an average speed of 7.57 km/s, has an orbit of 4.27 years.

Figure 4: The memorial, commemorating Simon Marius, designed by Friedrich Schelle and placed in Ansbach in 1991.

In 1991 in Ansbach a memorial (Fig. 4), commemorating Simon Marius, was built (it can be seen at http://www.w-volk.de/museum/monum69.htm#bibio00). The memorial, designed by Friedrich Schelle, has a form of a circular flat area with concentric circles, representing the orbits of planet Jupiter and its four largest satellites and an opened book with a telescope separating the two visible pages with a text giving basic information for Simon Marius.

References

Prickard, A. O.: 1916, *The Observatory, A review of astronomy*, 39, 367–381, 403–412, 443–452, 498–503.

Oudemans, J. A. C., Boscha, J.: 1903, *Archives Néerlandaises des Sciences Exactes et Naturelles*, Ser. II, T. VIII, La Haye 115–189 (in French).

Zinner, E.: 1942, *Vierteljahrsschrift der Astronomischen Gesellschaft*, 77, Leipzig, 23–75, (in German).

Proceedings of the IX Bulgarian-Serbian Astronomical Conference: Astroinformatics (IX BSACA) Sofia, Bulgaria, July 2-4, 2014,
Editors: M. K. Tsvetkov, M. S. Dimitrijević, O. Kounchev, D. Jevremović and K. Tsvetkova
Publ. Astron. Soc. "Rudjer Bošković" No 15, 2015, 179-187

MILUTIN MILANKOVIĆ DIGITAL LEGACY

NADA PEJOVIĆ[1], SAŠA MALKOV[1],
NENAD MITIĆ[1] and ŽARKO MIJAJLOVIĆ[2]

[1]*Faculty of Mathematics, University of Belgade, Belgrade, Serbia*
[2]*State University of Novi Pazar, Novi Pazar, Serbia*
E-mail: nada@matf.bg.ac.rs, smalkov@matf.bg.ac.rs, nenad@matf.bg.ac.rs, zarkom@matf.bg.ac.rs

Abstract. The aim of this paper is to present the Digital legacy of Milutin Milanković, the great Serbian astronomer and geoscientist. The Legacy contains various items related to Milanković's life and work: scientific papers, books, manuscripts, photos, letters, diplomas, patents, etc. For this occasion we give more detailed survey of digitized Milankovic's books deposited in the Legacy.

1. INTRODUCTION

There are important collections of books, scientific papers, photos and other documents in printed form related to people from the past who had important contributions to science. These documents at present are an important part not only of the scientific but of the cultural heritage as well. However, this documents are not easily accessible, particularly not to the wider audience. For this reason, we decided to present in digital form the legacies of the most important Serbian scientists from the past who had significant contributions to different areas of mathematical sciences: pure mathematics, mechanics, astronomy, theoretical physics and geosciences. Digitized items are deposited in several digital repositories with open access of the Faculty of Mathematics in Belgrade:

Digital legacy of Serbian mathematicians, http://legati.matf.bg.ac.rs,
Digital archive, http://digitalnilegati.matf.bg.ac.rs and
Virtual library, http://elibrary.matf.bg.ac.rs.

On this occasion, the aim of this paper is to present Digital legacy of scientific works of famous Serbian astronomer, mechanic, climatologist, civil engineer, professor of the Belgrade University and academician Milutin Milanković (1879-1958). The particular value of this collection is that it is the most complete as it contains all published Milanković's books and scientific papers. His curiosity in natural sciences was very broad and this is reflected in his works. However, Milanković's most important contributions were characterization of climate of the planets of the Solar system and the explanation of the Earth's long-term climate changes caused by astronomical phenomena. Besides papers on these topics, the collection contains some his less known papers, such as on the theory of relativity and cosmology and should be of an interest even today. We classified his books and papers thematically and gave short descriptions of the content of each group. We believe that retro-digitization of Milanković's works and free access to them trough Internet, will give the opportunity to the wide audience, scientists, students, but to the general public as well, to read and study directly Milanković's scientific works. In the rest of the paper we shall give a short Milankovic's biography and an overview of his most representative books.

2. MILANKOVIĆ'S BIOGRAPHY

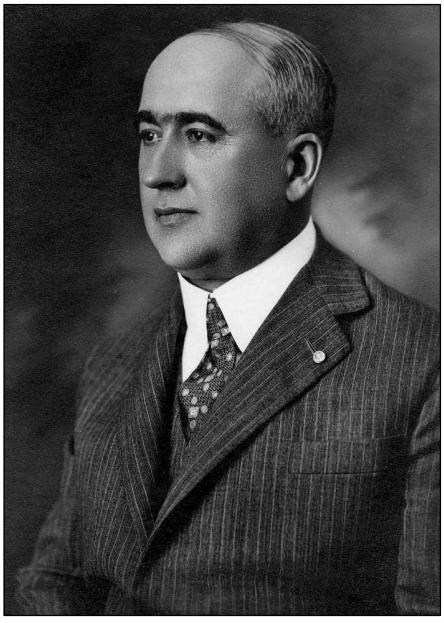

Milutin Milanković

Milutin Milanković was born on May 28, 1879 in Dalj (Slavonia, nowadays part of Republic of Croatia). The real gymnasium he finished in Osijek, to become a student of civil engineering at the Technische Hochschule in Vienna. There he took the first degree in 1903 and the PhD one in 1904. He was the first Serb who acquired the PhD title in engineering.

Following an invitation Milutin Milanković came from Vienna in 1909, after the University of Belgrade had been founded in 1905, to teach applied mathematics at the Faculty of Philosophy of this University. His coming was a merit of Bogdan Gavrilović and Mihailo Petrović Alas who both taught at the University of Belgrade. As a staff member Milanković was at the Belgrade University till his retirement in 1955. He taught applied mathematics (theoretical physics, mechanics and astronomy). He was the first in starting lectures in celestial mechanics. Among other subjects he taught history of astronomy and theory of relativity.

Milanković was a full member, and near the end of his life also Vice President of the Serbian Academy of Sciences, member of Deutsche Akademie der Naturforscher Leopoldina in Halle and corresponding member of a number of other academies and scientific societies in the world. Milanković died on December 12, 1958 in Belgrade. His scientific activity resulted in about ten books and more than hundred papers in mathematics, celestial mechanics, astronomy and geophysics.

Milutin Milanković gave to the world science community his well known theory of glacial ages. The results achieved by him taking into account the complex secular computation of perturbations in planet motions were published in *Théorie mathématique des phénomènes thermiques produits par la radiation solaire* in 1922; the publishers were Yugoslav Academy of Sciences and Arts in Zagreb and publishing house Gauthier Villars, Paris. Due to these results he became well known in the world scientific community, so that great German climatologist W. Köppen invited him to cooperate in building a great work *Handbuch der Klimatologie*. For this purpose a part, which was published in 1930, entitled *Mathematische Klimalehre und Astronomische Theorie der Klimaschwankungen* was written by Milanković. Here his theory of planet heating based on insulation was extended with a special reference to the Earth. By applying this theory to the run of glacial ages it was shown that Milanković had given a very good model of Earth, i. e. that he had created a good and mathematically exact theory of terrestrial climate. This work was translated into Russian in 1939.

Already as a well known scientist he started the cooperation on creation of work *Handbuch der Geophysik* prepared by B. Gutenberg. For this work Milanković wrote four sections where he returned to an old and very difficult problem: that of motion of the terrestrial poles. In these contributions Milanković created a theory of motion of terrestrial poles and succession of glacial ages.

His main work is *Kanon der Erdbestrahlung und seine Anwendung auf das Eiszeitenproblem* the printing of which was finished shortly before the beginning of the Second World War. It should be mentioned that the printed sheets were damaged by a bomb which hit the printing office on April 6, 1941 during the Nazi air raid of Belgrade. Fortunately the original typography of the book was preserved. By using it the book was reprinted during the war on a sufficiently low-quality paper.

During the four war years Milanković could send abroad just a few copies. So this important scientific work was printed at the most unfavorable moment, in war time. Due to this the scientific world community learned about Milanković's theory too late. As a consequence the world recognition arrived only after that. This work appears as a synthesis of his many earlier works which concern his research activity within boundary fields between many natural sciences and mathematics.

Milanković was successful in the field of calendar reform, too. During a Congress devoted to the calendar question organized by the Orthodox Churches in

Constantinople in 1923 he proposed an improvement of the Gregorian time reckoning. The proposal contained in Milanković's calendar-reform project was accepted by the Orthodox Christian Community, but some Churches present at the Congress (for instance, the Serbian one) have not started its application.

Milutin Milanković's Medal

Milanković's contribution to world science is honored in many ways. After Milutin Milanković a minor planet, a lunar crater and a Mars crater have been named. In Belgrade one street and one gymnasium have been named after him. On the banknote of two thousands of Serbian dinars the image of Milutin Milanković is depicted. European Geosciences Union - Division on climate established in 1993 Milutin Milanković's Medal for outstanding research in long term climatic changes and modeling.

Milanković's student and later the academician, Tatomir Anđelić wrote (1979) very detailed biography of Milutin Milanković.

3. MILANKOVIĆ'S BOOKS IN THE LEGACY

All Milanković's books are digitized and deposited in the Virtual Library and Digital Archive of the Faculty of Mathematics in Belgrade. The list of these books together with active links can be found in the supplement of this article. His most important books are commented and presented in more details in the Digital Legacy of the same institution. Therefore, we shall comment here only briefly some of the Milanković's books.

The book "Kanon der Erdbestrahlung" (*The Canon of Insulation*) is by no means Milanković's the most important book and scientific work. This book presents his astronomical theory of climatic changes. Even if the book is published in Serbia by Serbian Academy of Science, it is written in German that was then the main language of science. However, it took almost two decades that his theory was recognized, widely accepted and experimentally proved. But thereafter Milanković's theory was celebrated as the great achievement in geosciences and particularly in the theory of climate changes. Mainly due to this work, NASA experts said that Milanković was one of the world's "fifteen most important geoscientists". Many Serbian and foreign scientists wrote many scholar and good explanatory articles on Milanković's theory of climate changes and so we do not want to enter into explanation of this theory here. However we would like to note the following facts. Milanković was an excellent mathematician and mechanist even if his basic education was in civil engineering. *Canon* reflects this fact, as it presents very well mathematically founded theory of insulation of planets of Solar system. The mathematical apparatus is based on vector calculus and partial

gradients of perturbation functions appearing in descriptions of planetary orbits. The book is in fact the synthesis of his work in this area which he started immediately upon his arrival in Belgrade. For example he published the book *Phenomenes thermiques* in French already in 1920. Astronomy also advanced very rapidly at this time. Solar constant was determined in 1913 and allowed him to develop mathematically founded theory of thermal phenomena. All these leaded him to the development of planetary climates. He succeeded determine the average annual temperature on Mars surface, -17^{o} C and this attracted the worldwide attention. He also found a function which represents secular variations of Earth insulation and using them explained the formation of ice ages. This theory made him later famous. For detailed explanation of Milanković's theory of ace ages the reader may consult for example Grubić's articel (2006).

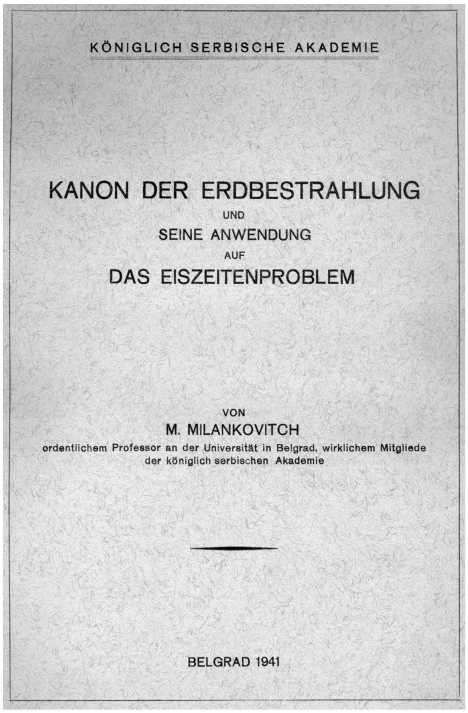
KÖNIGLICH SERBISCHE AKADEMIE

KANON DER ERDBESTRAHLUNG
UND
SEINE ANWENDUNG
AUF
DAS EISZEITENPROBLEM

VON
M. MILANKOVITCH
ordentlichem Professor an der Universität in Belgrad, wirklichem Mitgliede
der königlich serbischen Akademie

BELGRAD 1941

The Canon of Insulation

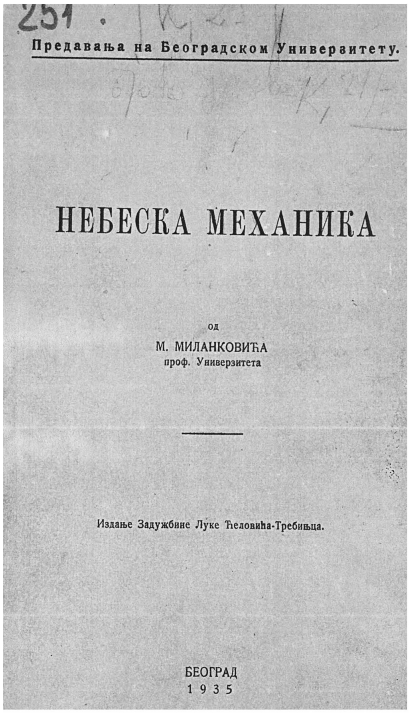
Предавања на Београдском Универзитету.

НЕБЕСКА МЕХАНИКА

од
М. МИЛАНКОВИЋА
проф. Универзитета

Издање Задужбине Луке Ћеловића-Требињца.

БЕОГРАД
1935

Celestial Mechanics

Milanković wrote two versions of his university textbook "Небеска механика" (*Celestial Mechanics*). The book was published thanks to the sponsorship of "Luka Ćelović-Trebinjac" endowment in Belgrade in 1935. The book was based on the lectures on Celestial Mechanics delivered by Milanković at the Belgrade University. At that time already existed several books in Serbian in the field of theoretical mechanics. The main novelty that this book introduced in the Serbian scientific literature is the consistent and systematic use of vector calculus for solving problems of celestial mechanics. Milanković used there the vector-scalar

system of elements of planetary orbits. For this reason connecting his name with this system is fully justified. *Небеска механика* was written on 333 pages with 22 figures in its text. The book is divided into two parts and consist of 15 chapters. The first part *Транслаторно кретање небеских тела* (*Translatory Motion of Celestial Bodies*) contains nine chapters; the second one *Ротационо кретање небеских тела* (*Rotational Motion of Celestial Bodies*) is written on 130 pages containing six chapters. At the end of both parts there is a list of references in foreign languages. The book is presented in details by N. Pejović (2011).

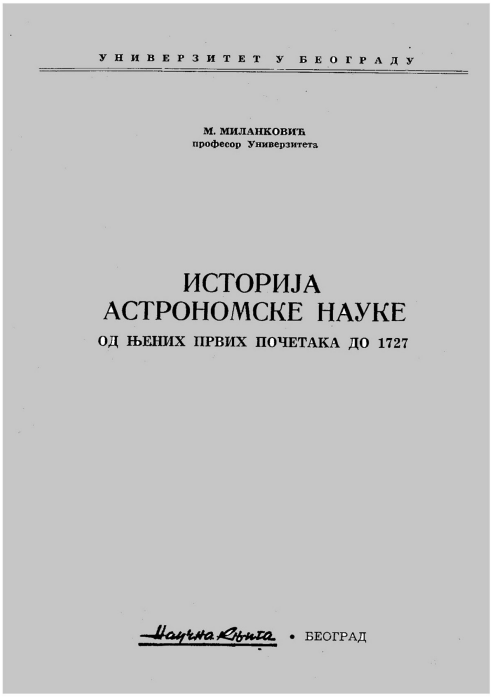

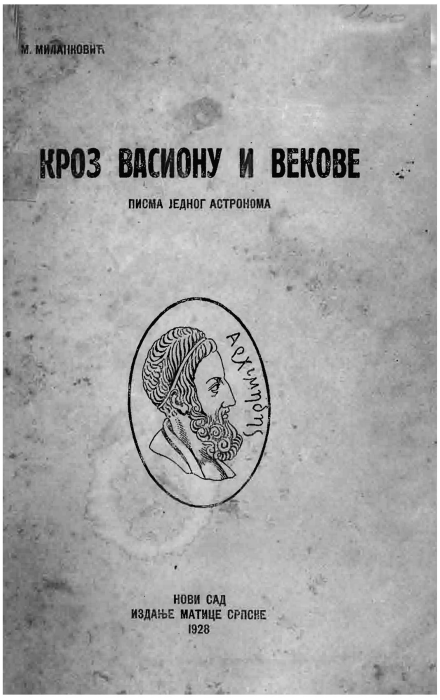

History of Astronomy Through Space and Centuries

Milanković wrote books not only in science but on science as well. The book that is still used in university courses on history of science is his "Istorija astronomske nauke od njenih prvih početaka do 1727" (*History of astronomy since the very beginning untill 1727*). Even if this book is printed after the Second World War, in 1948, Milanković started lecturing history of astronomy immediately upon his arrival in Belgrade, in 1909. We may take that Milanković is the real founder of this course at the Belgrade University. The book arose from his lectures and written notes and so the book, in a sense, is used over a century at the Belgrade University for teaching history of astronomy. The book was not available in bookstores for long time so that for students digital copies from the Virtual Library of the Faculty of Mathematics are very useful. The Milanković's

stand point was that if a student wants to understand the achievements of the contemporary astronomical sciences, he should know the development and evolutions of ideas in astronomy through centuries. So, the first chapters of the book are devoted to astronomy of ancient Greeks and astronomers of this time: Apollonius of Perga, Aristarchus of Samos, Hipparchus, Claudius Ptolemy and some others. However, Milanković considered that Aristarchus had the main role in the foundation of Astronomy as science mainly because he had enough courage to advocate the heliocentric World system in spite of then widespread geocentric perception of the Universe. In the second part of the new astronomy that brought the Renaissance and astronomers of that time: Galileo Galilei, Nicolaus Copernicus, Johannes Kepler, Isaac Newton. Mains achievements, such as Kepler laws of planetary motion and Newton law of universal gravitation.

Milanković highly cherished the written word. After reading his books that popularize science, or on the history of the science, the reader would certainly conclude that Milanković would be a great writer if he did not devoted himself to science. His celebrated book *Through Space and Centuries* without doubt witnesses this opinion. This book fictionalized the development of astronomy through centuries. The novel explains the scientific history of astronomy written as a travelogue prose. It consists of a collection of letters sent by Milanković to the loved one describing the long imaginative journey through the past of millions of years and travel through the deep Universe. Letters represent a treasury of scientific explanations and portraits of famous scientist: Eratosthenes, Ptolemy, Pythagoras, Copernicus, Kepler, Newton, Einstein and Tesla. The book is a collection of records about the cradle of wisdom, scientific knowledge and philosophical views of ancient people of Babylon, China, India, old Greece and Rome up to the modern times. This book of stories about the ancient beauties and thoughts written in the splendid language has become his brand name. Five editions of the book were published in Serbian, one in Slovenian, and two editions in German.

Acknowledgments

This work is supported by a grant of the Serbian Ministry of education, science and technology under the project III 44006.

REFERENCES AND SELECTED LITERATURE ON MILUTIN MILANKOVIĆ

Anđelić, T.: 1979, Biografija Milutina Milankovića, *Galerija SANU*, **36**, 7-34.

Grubić, A.: 2006, The astronomic theory of climatic changes of Milutin Milankovich, *Episodes*, **29**, no. 3, 197-203.

Mijajlović, Ž.: Digitization of scientific and cultural heritage in Serbia, *Scientific Review*, n. s. **S2**, editors K. Hedrih, Ž. Mijajlović, Serb. Sci. Soc., Belgrade, 481-483, (Dedicated to Milutin Milanković [1879-1958]).

Mijajlović, Ž.: 2009 Application of information science in digitization of scientific and cultural heritage, Proc. Conference: Mathematical and Information Technologies - MIT 2009, Kopaonik, Serbia, eds. J. I. Shokin et al., Publ: PMF Univ. Priština (Kos. Mitrovica), Inst. Comput. Technol., Siberian branch RAN, Novosibirsk, Russia, August 5-8, 232-239 (CompSci, http://mit.rs/2009/zbornik.pdf)

Mijajlović, Ž., Malkov, S., Mitić, N.: 2013, Digital legacies, *NCD Review,* **22**,148-152.

Mijajlović, Ž., Ognjanović, Z., Đorđević, N., Zečević, T.: 2004, Virtual Library -- data base of textual data, *NCD Review*, **5**, 42-48 .

Mijajlović, Ž, Ognjanović, Z., Pejović, A.: 2010 Digitization of mathematical editions in Serbia, *Mathematics in Computer Science*, **3**, 251-263.

Mijajlović, Ž., Pejović, N.: 2012, National Serbian digitization project: Its achievements and activities, Proc. VII Bulgarian-Serbian Astronomical Conference, Chepelare, Bulgaria, June 1-4, 2010, eds. M. K. Tsvetkov et al., *Publ. Astron. Soc. "Ruđer Bošković",* **11**, 75-81.

Pantić, N.: 2001, Milutin Milanković, *Lives and work of the Serbian scientists*, **7,** Serbian Acad. of Sciences and Arts, 171-222.

Pejović, N.: 2011, Digitisation of textbook "Небеска маханика" by Milutin Milanković, *NCD Review*, **19**, 63-68.

Pejović, N., Mijajlović, Ž.: 2011, Early astronomical heritage in Virtual Library of Faculty of Mathematics in Belgrade, *NCD Review*, **19**, 11-25.

Pejović, N., Mijajlović, Ž.: 2012, Astronomical books in Virtual Library of Faculty of Mathematics in Belgrade, *Publ. Observ. Astron. Belgrade*, **91**, 267-271.

Pejović, N., Mijajlović, Ž., Valjarević, A., Damljanović, G.: 2012, Serbian astronomical works in the Virtual Library of the Faculty of Mathematics in Belgrade*,* Proc. VII Bulgarian-Serbian Astronomical Conference (VII BSAC), Chepelare, Bulgaria, June 1-4, 2010, eds. M. K. Tsvetkov et al., *Publ. Astron. Soc. "Rudjer Bošković"*, **11**, 311-323.

Spasova, D., Maksimović, S.: 2009, *Milutin Milanković - putnik kroz vasionu i vekove*, publ. Udruženje Milutin Milanković, Beograd.

Stojković, A.: 1979**,** Mesto shvatanja Milutina Milankovića i Pavla Savića među kosmogonijsko-kosmološkim hipotezama XX veka*, Dijalektika*, Beograd.

SUPPLEMENT: BOOKS AND MONOGRAPHS OF MILUTIN MILANKOVIĆ IN VIRTUAL LIBRARY
(with active links in electronic version of this paper)

O primjeni matematičke teorije sprovođenja toplote па probleme kosmičke fizike, Zagreb, 1913.

O pitanju astroпomskih teorija ledenih doba, Dionička Tiskara, Zagreb , 1914.

Phenomenes thermiques, Paris , 1920.

Reforma julijanskog kalendara, Belgrade , 1923.

Nebeska mehanika , Belgrade , 1935.
Kanon der Erdbestrahlung, Serbian Royal Academy, Belgrade , 1941.
Kroz vasionu i vekove - jedna astronomija za svakoga, Belgrade , 1943.
Osnivači prirodnih nauka - Pitagora - Demokritos - Aristoteles - Arhimedes, Belgrade , 1947.
Astronomska teorija klimatskih promena i njena primena u geofizici, Naučna Knjiga, Beograd , 1948.
Kroz carstvo nauka, Naučna Knjiga, Beograd , 1950.
Uspomene doživljaji i saznanja iz godina 1909 do 1944, Naučna Knjiga, Beograd, 1952.
Uspomene doživljaji i saznanja posle 1944 godine, Naučno delo, Beograd, 1957.
Astronomische Theorie der Klimaschwankungen, Belgrade, 1957.
Istorija astronomske nauke - od njenih prvih početaka do 1727, Belgrade , 1979.
Glas SKA CIX - Kalorična godišnja doba, SKA, Belgrade, 1923.
Glas SKA CXVII - Kalendar Zemljine prošlosti, SKA, Belgrade, 1926.
Glas SKA CXX - Ispitivanja o termičkoj konstituciji planetskih atmosfera, SKA, Belgrade, 1926.
Glas SKA CLXXV - Novi rezultati astronomske teorije klimatskih promena, SKA, Belgrade, 1937.

INTERNET LINKS
(All internet sites belong to the Faculty of Mathematics in Belgrade)

Digitalni legati (Digital legacies): http://legati.matf.bg.ac.rs
Digitalna arhiva (Digital Archieves): http://digitalnilegati.matf.bg.ac.rs
Virtuelna biblioteka (Virtual Library): http://elibrary.matf.bg.ac.rs

Proceedings of the IX Bulgarian-Serbian Astronomical Conference: Astroinformatics (IX BSACA) Sofia, Bulgaria, July 2-4, 2014,
Editors: M. K. Tsvetkov, M. S. Dimitrijević, O. Kounchev, D. Jevremović and K. Tsvetkova
Publ. Astron. Soc. "Rudjer Bošković" No 15, 2015, 189-206

SOCIETY OF ASTRONOMERS OF SERBIA 2012-2014

MILAN S. DIMITRIJEVIĆ

Astronomical Observatory, Volgina 7, 11060 Belgrade, Serbia
E-mail: mdimitrijevic@aob.bg.ac.rs

Abstract: The review of activities of the Society of Astronomers of Serbia within the period 2012-2014 is presented.

1. INTRODUCTION

Author of this contribution was the second time elected for president of Society of Astronomers of Serbia on Assembly held in October 2011. The period from 2008 to 2011, during his first term of office has been analyzed in Dimitrijević (2013, 2014). Activities of the Society from October 2011 up to the new Assembly scheduled for 27 septembre 2014 will be analyzed in this contribution. They are:

Olympiads in astronomy;
Mobile planetarium and project "Popularization of astronomy in educational and cultural institutions and schools";
Scientific meetings organized by DAS;
Publishing activity of SAS;
Foreign scientists – guests of Society of Astronomers of Serbia;
Links with the European Astronomical Society;
Links with the International Astronomical Union;

2. OLYMPIADS IN ASTRONOMY

Competitors from Serbia in this period took part in the following international Olympiads covering astronomy and astrophysics:

VI International Olympiad on Astronomy and Astrophysics, Rio de Janeiro, 4-14 August 2012, three competitors, team leaders were Sonja Vidojević and Slobodan Ninković. Luka Bojović won the silver medal, Aleksandar Miladinović bronze, and Predrag Obradović was commended.

VII International Olympiad on Astronomy and Astrophysics, Volos (Greece), from 27 of July to 5 of August 2013, five competitors, team leaders were Sonja Vidojević and Slobodan Ninković. Ivan Tanasijević and Luka Bojović won the gold medal, Aleksandar Miladinović silver, while Predrag Obradović and Uroš Ristivojević were commended.

VIII International Olympiad on Astronomy and Astrophysics, Suceava (Romania), 1-11 August 2014. Team leaders were Sonja Vidojević and Slobodan Ninković. Ivan Tanasijevic won the gold medal, Luka Bojović silver, Predrag Obradović and Djordje Žikelić bronze, and Marko Purić was commended.

In the period 2008-2014, Society of Astronomers of Serbia took part in eleven Olympiads in astronomy, in which participants from Serbia won five gold medals, thirteen silver and fourteen bronze medals, seven participants were commended and one received a special award.

Team leaders were: Slobodan Ninković ten times, Sonja Vidojević four, Ivan Milić three, Ratomirka Miller two and by once Aleksandar Vasiljković and Nikola Božić.

3. PROJECT "POPULARIZATION OF ASTRONOMY IN EDUCATIONAL AND CULTURAL INSTITUTIONS AND SCHOOLS"

For popularization of astronomy using a mobile planetarium, SAS was applied at the Ministry of Science and Technological Development with the project "Popularization of astronomy in educational and cultural institutions and schools" for 2010 and 2011 and at the Center for Promotion of Science for 2012 and 2013. For 2010 as well as for 2011 and 2012, 300 000 RSD for each year was obtained and for 2013, 150 000 RSD. For 2014, the competition is not announced up to now.

Program activities are primarily designed to popularize astronomy in the towns in the interior of Serbia and the Republic Srpska. To this end, the lecturers with the mobile planetarium, obtained in 2009 thanks to the donation of UNESCO, visited particular towns, organizing a day of astronomy, in order to acquaint students, educators and concerned citizens with the phenomena and objects in the night sky and the results and achievements in this science.

Activities achieved during the realization of project in 2012 year are shown here in the table.

Date	*Lecture and Place*	*Attendies*	*Lecturer*
27/03/12	Astronomy of XXI century – Library Mokrin	50	Milan S. Dimitrijević
27/03/12	Mileva Marić Ajnštajn – Library Mokrin	50	Petar Vuca
28/03/12	Astronomy of XXI centu-ry – Primary school «4th October», Vojvoda Stepa	60	Milan S. Dimitrijević

Date	*Lecture and Place*	*Attendies*	*Lecturer*
28/03/12	Mileva Marić Ajnštajn – Primary school «4th October», Vojvoda Stepa	60	Petar Vuca
28/03/12	Astronomy of XXI century – Primary school «Djura Jakšić», Srpska Crnja	50	Milan S. Dimitrijević
28/03/12	Mileva Marić Ajnštajn – Primary school «Djura Jakšić», Srpska Crnja	50	Petar Vuca
30/03/12	Planetarium projection (mobile planetarium) – «Science is not bugbear 4», Electronic Faculty, Niš	300	Goran Pavičić
30/03/12	Milutin Milanković and the secret of ice ages - «Science is not bugbear 4», Electronic Faculty, Niš	70	Milan S. Dimitrijević
31/03/12	Planetarium projection (mobile planetarium) – «Science is not bugbear 4», Electronic Faculty, Niš	300	Goran Pavičić
31/03/12	Supermassive binary black holes - «Science is not bugbear 4», Electronic Faculty, Niš	70	Luka Popović
12/05/11	Planetarium projection (mobile planetarium) – Novi Sad	300	Kristina Savić, Nevena Grubač, Robert Džudžar
13/05/11	Planetarium projection (mobile planetarium) – Novi Sad	300	Kristina Savić, Nevena Grubač, Robert Džudžar
15/05/12	Astronomy of XXI century – Primary school «Dr Boško Vrebalov», Melenci	60	Milan S. Dimitrijević
15/05/12	Mileva Marić Ajnštajn – Primary school «Dr Boško Vrebalov», Melenci	60	Petar Vuca
15/05/12	Astronomy of XXI century – Primary school ”Svetozar Marković – Toza”, Elemir	60	Milan S. Dimitrijević

Date	*Lecture and Place*	*Attendies*	*Lecturer*
15/05/12	Mileva Marić Ajnštajn – Primary school "Svetozar Marković – Toza", Elemir	60	Petar Vuca
17/05/12	Milutin Milanković and the secret of ice ages — Banski Dvori, Banja Luka	70	Milan S. Dimitrijević
18/05/12	Milutin Milanković and the secret of ice ages – People's Library, Doboj	70	Milan S. Dimitrijević
18/05/12	Planetarium projection (mobile planetarium) – Kraljevo	300	Goran Pavičić
19/05/12	Planetarium projection (mobile planetarium) – Kraljevo	300	Goran Pavičić
25/05/12	Astronomy of XXI century – Primary school "Dositej Obradović", Farkaždin	50	Milan S. Dimitrijević
25/05/12	Mileva Marić Ajnštajn – Primary school "Dositej Obradović", Farkaždin	50	Petar Vuca
31/05/12	Astronomy of XXI century – Primary school «Moro Karolj», Sajan	50	Milan S. Dimitrijević
31/05/12	Mileva Marić Ajnštajn – Primary school«Moro Karolj», Sajan	50	Petar Vuca
12/06/12	Astronomy of XXI century – Primary school „Djura Jakšić", Perlez	50	Milan S. Dimitrijević
12/06/12	Mileva Marić Ajnštajnн – Primary school „Djura Jakšić", Perlez	50	Petar Vuca
29/08/12	Astronomy of XXI century – Local Community and Library, Banatska Topola	50	Milan S. Dimitrijević
29/08/12	Mileva Marić Ajnštajn – Local Community and Library, Banatska Topola	50	Petar Vuca
27/09/12	Astronomy of XXI century – Primary school "Petar Kočić", Nakovo	50	Milan S. Dimitrijević

Date	*Lecture and Place*	*Attendies*	*Lecturer*
27/09/12	Mileva Marić Ajnštajn – Primary school "Petar Kočić", Nakovo	50	Petar Vuca
28/09/12	Planetarium projection (mobile planetarium) – Novi Sad	600	Kristina Savić, Robert Džudžar
06/10/12	Milutin Milanković and the secret of ice ages – Eureca Day, Secondary School, Kruševac	60	Milan S. Dimitrijević
06/10/12	Cosmical rains – Eureca Day, Secondary School, Kruševac	60	Jovan Aleksić
06/10/12	The center of our Galaxy - Eureca Day, Secondary School, Kruševac	60	Slobodan Ninković
06/10/12	Planetarium projection (mobile planetarium) – Eureca Day, Secondary School, Kruševac	300	Jovan Aleksić
18/10/12	Astronomy of XXI century – Primary school "Boško Djurić", Jagodina	200	Milan S. Dimitrijević
18/10/12	Planetarium projection (mobile planetarium) – Primary school "Boško Djurić", Jagodina	300	Jovan Aleksić
22/10/12	Astronomy of XXI century – Primary school «Miloš Crnjanski», Itebej	50	Milan S. Dimitrijević
22/10/12	Mileva Marić Ajnštajn – Primary school «Miloš Crnjanski», Itebej	50	Petar Vuca
03/11/12	Recording of TV emission with mobile planetarium – Magic Village, Banja Vrujci	30	Milan S. Dimitrijević, Jovan Aleksić
03/11/12	Good morning Sun - Magic Village, Banja Vrujci	30	Jovan Aleksić

Date	*Lecture and Place*	*Attendies*	*Lecturer*
03/11/12	Planetarium projection (mobile planetarium) – Magic Village, Banja Vrujci	30	Jovan Aleksić
07/11/12	Astronomy of XXI century – Primary school «Dositej Obradović», Bočar	50	Milan S. Dimitrijević
07/11/12	Mileva Marić Ajnštajn – Primary school «Dositej Obradović», Bočar	50	Petar Vuca
08/11/12	Astronomy of XXI century – Primary school «1st October», Bašaid	50	Milan S. Dimitrijević
08/11/12	Mileva Marić Ajnštajn – Primary school «1st October», Bašaid	50	Petar Vuca
21-28/11/12	Planetarium projection (mobile planetarium)- Fair of education ZVONCE	1710	Goran Pavičić, Nemanja Jeftić
14/12/12	Planetarium projection (mobile planetarium)- Zvezdara Festival of Science – VI Belgrade Secondary School	120	Goran Pavičić,
20/12/12	Planetarium projection (mobile planetarium), Trade and Catering School „Toza Dragović, Kragujevac	210	Jovan Aleksić
20/12/12	Astronomy of XXI century – Trade and Catering School „Toza Dragović, Kragujevac	50	Milan S. Dimitrijević
21/12/12	Planetarium projection (mobile planetarium) – Trade and Catering School „Toza Dragović, Kragujevac	210	Jovan Aleksić
21/12/12	Black holes – Faculty of Sciences, Kragujevac	50	Jovan Aleksić
21/12/12	Astronomy of XXI century – Trade and Catering School „Toza Dragović, Kragujevac	50	Milan S. Dimitrijević


МИНИСТАРСТВО ПРОСВЕТЕ РЕПУБЛИКЕ СРБИЈЕ
ОШ „БОШКО ЂУРИЧИЋ“

ДОДЕЉУЈЕ

ЗАХВАЛНИЦУ

Проф. др Милану Димитријевићу

ЗА УСПЕШНУ САРАДЊУ У ОСТВАРИВАЊУ
ШКОЛСКОГ ПРОГРАМА И ПОБОЉШАЊЕ
УСЛОВА РАДА ШКОЛЕ

У ЈАГОДИНИ ДАНА 18.10.2012 ГОДИНЕ

М.П.

Директор школе
Зоран Марковић

Figure 1: Acknowledgement of the Primary school”Boško Djuriić”.

To the above listed activities 7510 listeners were present in 2012. On total of 38 lectures were 2230 listeners, and 176 planetarium projections with lectures, were attended by 5280 listeners (since in a planetarium projection the number of listeners is limited to 30, the total number of listeners during the day is shown in the table).

Such "Days of Astronomy" were organized during 2012 in Mokrin, Vojvoda Stepa, Srpska Crnja, Kragujevac, Doboj, Banja Luka, Belgrade, Novi Sad, Niš, Kruševac, Melenci, Elemir, Kraljevo, Farkaždin, Sajan, Perlez, Banatska Topola, Nakovo, Jagodina, Itebej, Banja Vrujci, Bočar and Bašaid

In the realization of the project were involved Goran Pavičić, Milan S. Dimitrijević, Jovan Aleksić, Luka Č. Popović, Darko Jevremović, Petar Vuca, Kristina Savić, Kristina Kaćanski, Nevena Grubač, Robert Džudžar, Nemanja Jeftić, Slobodan Ninković.

Activities achieved during the realization of project in 2013 year are shown here in the table.

Date	*Lecture and Place*	*Attendies*	*Lecturer*
1-2/04/13	Planetarium projection (mobile planetarium) – Festival of Science, Leskovac	350	Jovan Aleksić, Milan S. Dimitrijević, Darko Jevremović
1/04/13	Milutin Milanković and the secret of ice ages – Festival of Science, Leskovac	80	Milan S. Dimitrijević
2/04/13	Astronomy of XXI century – Festival of Science, Leskovac	80	Milan S. Dimitrijević
3/04/13	Planetarium projection (mobile planetarium) — Primary school «Vuk Karadžić», Leskovac	300	Jovan Aleksić, Milan S. Dimitrijević, Darko Jevremović
3/04/13	Astronomy of XXI century – Primary school «Vuk Karadžić», Leskovac	50	Milan S. Dimitrijević
19-20/04/13	Planetarium projection (mobile planetarium) – DKC „Majdan“, Festival „Propeler“, Belgrade	400	Aleksandar Otašević, Nataša Stanić, Jovan Aleksić
11-12/05/13	Planetarium projection (mobile planetarium) – Festival of Science, Novi Sad	1300	Aleksandar Otašević, Nataša Stanić, Jovan Aleksić

Date	*Lecture and Place*	*Attendies*	*Lecturer*
14-15/05/13	Planetarium projection (mobile planetarium) — Primary school «Trajko Stamenković» Leskovac	400	Aleksandar Otašević, Nataša Stanić
17/05/13	Planetarium projection (mobile planetarium) — Primary school «Stevan Sremac», Belgrade	60	Aleksandar Otašević, Nataša Stanić
21/05/13	Planetarium projection (mobile planetarium) — Primary school «King Aleksandar I», Požarevac	550	Jovan Aleksić, Milan S. Dimitrijević, Zoran Simić
23/05/13	Planetarium projection (mobile planetarium) - Primary school „Desanka Maksimović“, Prijedor	450	Jovan Aleksić, Milan S. Dimitrijević, Luka Popović
23/05/13	Where are they? Fermi paradox or big silence of Universe – Medical School, Prijedor	60	Milan S. Dimitrijević
24/05/13	Planetarium projection (mobile planetarium) - House of Youth, Banjaluka	150	Jovan Aleksić, Milan S. Dimitrijević, Luka Popović
24/05/13	Nobel prizes for Physics from the domain of Astronomy in XXI century – Banski dvori, Banjaluka	80	Milan S. Dimitrijević
27-28/05/13	Planetarium projection (mobile planetarium) – Primary school “Knez Sima Marković”, Barajevo	500	Aleksandar Otašević, Nataša Stanić
24/06/13	Planetarium projection (mobile planetarium) – Game room “Minicity”, Belgrade	Promotive projection for Game room menagement 2	Aleksandar Otašević, Nataša Stanić, Ana Zlatanović

Date	*Lecture and Place*	*Attendies*	*Lecturer*
6-7/07/13	Planetarium projection (mobile planetarium) – Festival "Way of Sciences" - Senta (The First Prize for the most interesting content)	220	Jovan Aleksić, Aleksandar Otašević
12/07/13	Planetarium projection (mobile planetarium) – Game room "Minicity", Belgrade	20	Aleksandar Otašević
17/08/13	Planetarium projection (mobile planetarium) – Days of Mensa, Belgrade	60	Jovan Aleksić
14/09/13	Planetarium projection (mobile planetarium) – Primary school "Djura Jakšić", Kovin	258	Aleksandar Otašević, Nataša Stanić
20/09/13	Planetarium projection (mobile planetarium) - Secondary School, „Barajevo", Barajevo	128	Aleksandar Otašević, Nataša Stanić
26/09/13	Planetarium projection (mobile planetarium) – Primary school „Djuro Strugar", Belgrade	165	Aleksandar Otašević, Nataša Stanić
27/09/13	Planetarium projection (mobile planetarium) – „Night of researchers", Banjaluka	240	Branko Simonović, Aleksandar Otašević
1/10/13	Planetarium projection (mobile planetarium) – Primary school „Stevan Sremac", Belgrade	190	Aleksandar Otašević, Nataša Stanić
3/10/13	Planetarium projection (mobile planetarium) – Primary school „Servo Mihalj", Zrenjanin	350	Aleksandar Otašević, Nataša Stanić
8/10/13	Planetarium projection (mobile planetarium) – „Science Festival of Zmaj and sports days", Srbobran	500	Aleksandar Otašević, Nataša Stanić

Date	*Lecture and Place*	*Attendies*	*Lecturer*
10/10/13	Planetarium projection (mobile planetarium) – Primary school „King Petar I“, Belgrade	220	Aleksandar Otašević, Nataša Stanić
12/10/13	Chat with astronomers – Magic Village, Vrujci	20	Jovan Aleksić, Milan S. Dimitrijević, Sonja Vidojević, Zoran Simić
15/10/13	Planetarium projection (mobile planetarium) – Primary school „Djura Daničić“, Belgrade	280	Aleksandar Otašević, Nataša Stanić
17/10/13	Planetarium projection (mobile planetarium)– Primary school „Rade Drainac“, Belgrade	375	Aleksandar Otašević, Nataša Stanić
18/10/13	Astronomy of XXI century – Primary school «Jovan Popović», Kruševac	50	Milan S. Dimitrijević
18/10/13	Planetarium projection (mobile planetarium) – Primary school «Jovan Popović», Kruševac	350	Jovan Aleksić, Milan S. Dimitrijević, Darko Jevremović
19/10/13	Planetarium projection (mobile planetarium) – Eureca Day, Secondary School, Kruševac	350	Jovan Aleksić, Milan S. Dimitrijević, Darko Jevremović
19/10/13	How were created our calendars – Eureca Day, Secondary School, Kruševac	60	Milan S. Dimitrijević
19/10/13	Habitable worlds – Eureca Day, Secondary School, Kruševac	60	Jovan Aleksić
25/10/13	Planetarium projection (mobile planetarium) – Primary school «Vuk Karadžić», Surčin	359	Aleksandar Otašević, Nataša Stanić

Date	*Lecture and Place*	*Attendies*	*Lecturer*
29/10/13	Planetarium projection (mobile planetarium) – Primary school „20th October“, Belgrade	290	Nataša Stanić, Srdjan Djukić
1/11/13	Planetarium projection (mobile planetarium) – Conference on Educational Tourism, Secondary School, Mionica	120	Jovan Aleksić, Sonja Vidojević, Milan S. Dimitrijević, Zoran Simić
2/11/13	Planetarium projection (mobile planetarium) – Conference on Educational Tourism, Primary school ”Milan Rakić”, Vrujci	100	Jovan Aleksić, Sonja Vidojević, Milan S. Dimitrijević, Zoran Simić
2/11/13	How was created Calendar — Magic Village, Vrujci	20	Milan S. Dimitrijević
2/11/13	Chat with Astronomers — Magic Village, Vrujci	20	Sonja Vidojević, Jovan Aleksić, Milan S. Dimitrijević
7/11/13	Habitable worlds – Festival of Science, Banjaluka	30	Jovan Aleksić

Figure 2: Poster for the lecture in Banjaluka.

Figure 3: Jovan Aleksić in Banjaluka 7. November 2013.

In 2013, "Days of Astronomy" are organized in Leskovac, Novi Sad, Banjaluka, Požarevac, Prijedor, Barajevo, Senta, Kovin, Zrenjanin, Srbobran, Banja Vrujci, Kruševac, Belgrade, Surčin and Mionica.

To the above listed activities 9647 listeners were present in 2013. On total of 11 lectures were 610 listeners, and 312 planetarium projections with lectures, were attended by 9617 listeners.

In the realization of the project were involved Milan S. Dimitrijević, Luka Č. Popović, Darko Jevremović, Jovan Aleksić, Nataša Stanić, Aleksandar Otašević, Zoran Simić, Sonja Vidojević, Srdjan Djukić, Branko Simonović and Ana Zlatanović.

Unfortunately in 2014, The Center for the Promotion of Science has not yet announced a new competition so that SAS is not performed any action. Movable planetarium was used by fellows of Astronomical Society "Rudjer Bošković" Jovan Aleksić, Nataša Stanić and Aleksandar Otašević.

4. SCIENTIFIC CONFERENCES ORGANIZED BY SAS

Within the considered period from 2012 to 2014, SAS organized four scientific conferences.

II Workshop on Active Galactic Nuclei and gravitational lensing, Andrevlje (Fruška Gora) 24-28 April 2012. The meeting was conceived, as the previous from this series, as a workshop, so in the morning were lectures, and in the afternoon, participants worked in groups on specific topics or mini projects.

Regional Workshop on Atomic and Molecular Data, with introductory tutorial for Virtual Atomic and Molecular Data Center (VAMDC), which atended sixty participants from Serbia, Bulgaria, Slovenia, Italia, Bangladesh, Republic of Srpska, Austria, England, Germany, France and Croatia.

II Workshop on Astrophysical Spectroscopy, Vrujci, 9-13. October 2013, organized by the same principle as the workshop in Andrevlje.

III Workshop on Active Galactic Nuclei and gravitational lensing, Končarevo (Jagodina), 7-11 October 2014, organized by the same principle as the previous one.

In addition, SAS was co-organizer of international conferences VIII Serbian – Bulgarian Astronomical Conference, Leskovac, 8-12 May 2012 and IX Serbian Conference on Spectral Line Shapes in Astrophysics, Banja Koviljača, 13-17 May 2013, as well as of the National Conference with international participation "Development of astronomy among Serbs VIII", Belgrade, 22-26 April 2014.

5. PUBLISHING ACTIVITY

Within the considered period, SAS published the following bibliographic items: Proceedings of the Seventh Bulgarian-Serbian Astronomical Conference (with the Astronomical Society "Rudjer Bošković"), Book of Abstracts of the Eight Serbian-Bulgarian Astronomical Conference (with Astronomical Observatory) and eight electronic optical DVD discs (four were published together with the Astronomical observatory, three with the Astronomical Society "Rudjer Bošković" and one with Serbian Academy of Sciences and Arts – Branch in Novi Sad and Astronomical Observatory).

Published bibliographic units are:

1. PROCEEDINGS OF THE VII BULGARIAN – SERBIAN ASTRONOMICAL CONFERENCE, Chepelare, 1-4 June 2010, eds. M. Tsvetkov, M. S. Dimitrijević, K. Tsvetkova, O. Kounchev, Ž. Mijajlović, Publ. Astron. Soc. »Rudjer Bošković«, No. 11, Belgrade, 2012.

2. VII BULGARIAN – SERBIAN ASTRONOMICAL CONFERENCE, ASTROINFORMATICS, Chepelare, 1-4 June 2010, eds. M. Tsvetkov, M. S. Dimitrijević, K. Tsvetkova, O. Kounchev, Ž. Mijajlović, organized by the Institute of Astronomy and National Astronomical Observatory of the Bulgarian Academy of Sciences and Belgrade Astronomical Observatory. DVD prepared by Milan S. Dimitrijević and Tatjana Milovanov - Belgrade: Astronomical Society “Rudjer Bošković”: Serbian Astronomical Society, 2012 (Belgrade: Astronomical Society “Rudjer Bošković”). - 1. Electronic optical disc (DVD).

3. II Workshop on Active Galactic Nuclei and Gravitational Lensing, April 24 - 28, 2012, Andrevlje, Abstracts, Presentations and Photos [Electronic source], eds. Luka Č. Popović, Wolfram Kollatschny and Milan S. Dimitrijević, DVD prepared by Milan S. Dimitrijević and Tatjana Milovanov. – Belgrade: Astronomical Observatory and Serbian Astronomical Society, 2012, Electronic optical disc (DVD).

4. Conference "Djordje Stanojević, – Life and work", Novi Sad, 10-11 October 2008, Proceedings with Photos [Electronic source], eds. Milan S. Dimitrijević, Borivoje Mirosavljević, Vojislav Marić. DVD prepared by Milan S. Dimitrijević, Miodrag Dačić and Tatjana Milovanov. - Belgrade: Serbian Astronomical Society, Serbian Academy of Sciences and Arts – Branch in Novi Sad and Astronomical Observatory 2012, Electronic optical disc (CD ROM).

5. Book of Abstracts, VIII Serbian-Bulgarian Astronomical Conference, May 8-12, 2012, Leskovac, Serbia, eds. Milan S. Dimitrijević and Milcho K. Tsvetkov, Serbian Astronomical Society, Astronomical Observatory, Belgrade, 2012.

6. Regional workshop on Atomic and Molecular Data, June 14-16, 2012, Belgrade, Serbia, Abstracts, Presentations and Photos [Electronic source], ed. Milan S. Dimitrijević, DVD prepared by Milan S. Dimitrijević, Vladimir Čadež and Tatjana Milovanov. - Belgrade: Astronomical Observatory and Society of Astronomers of Serbia, 2013, Electronic optical disc (DVD).

7-8. VIII Serbian-Bulgarian Astronomical Conference, May 8-12, 2012, Leskovac, Serbia [Electronic source], Discs 1-2, eds. Milan S. Dimitrijević and Milcho K. Tsvetkov, DVD prepared by Milan S. Dimitrijević, Miodrag Dačić and Tatjana Milovanov. - Belgrade: Astronomical Society "Rudjer Bošković" and Serbian Astronomical Society, 2013, Electronic optical discs (DVD).

9. IX Serbian Conference on Spectral Line Shapes in Astrophysics, May 13-17, 2013, Banja Koviljača, Serbia, Abstracts, Presentations and Photos [Electronic source], eds. Milan S. Dimitrijević, Luka Č. Popović and Zoran Simić, DVD prepared by Milan S. Dimitrijević, Miodrag Dačić and Tatjana Milovanov. - Belgrade: Serbian Astronomical Society and Astronomical Observatory, 2014, Electronic optical disc (DVD).
10. II Workshop on Astrophysical Spectroscopy, October 9-13, 2013, Vrujci, Serbia, Abstracts, Program and Photos [Electronic source], eds. by Milan S. Dimitrijević and Zoran Simić, DVD prepared by Milan S. Dimitrijević, Miodrag Dačić and Tatjana Milovanov. - Belgrade: Astronomical Observatory and Society of Astronomers of Serbia, 2014, Electronic optical disc (DVD).

6. FOREIGN SCIENTISTS – GUESTS OF SOCIETY OF ASTRONOMERS OF SERBIA

Within the 2012-2014 period, Society of astronomers of Serbia had fifteen stays of foreign guests, not taking into account the Workshop in October 2014 in Končarevo. Guests Scientists from abroad who stayed in Serbia as guests of SAS were:

Viktor Afanasjev, Russia
Emannouil Danezis, Greece,
Wolfram Kollatschny, Germany
Giovanni La Mura, Italy,
Evaggelia Lyratzi, Greece
Piero Rafanelli, Italy,
Galina Semenovna Afanasjeva, Russia

They have been guests of II Workshop on Active Galactic Nuclei and gravitational lensing, Andrevlje (Fruška Gora) 24-28 April 2012. On the Regional Workshop on Atomic and Molecular Data the official guests of SAS, for which was applied for fees to the Ministry, were:

Dejan Vinković, Croatia
Magdalena Christova, Bulgaria,
Kiril Blagoev, Bulgaria,
Sylvie Sahal-Bréchot, France.

On the II Workshop on Astrophysical Spectroscopy, Vrujci, 9-13 October 2013, the guests of SAS were:

Magdalena Christova, Bulgaria,
Giovanni La Mura, Italy,
Nemanja Rakić, Republic of Srpska,
Alla I. Shapovalova, Russia.

7. OTHER ACTIVITIES

7.1. Links with the European Astronomical Society

Directional Board of SAS regularly collected and paid annual dues for the European Astronomical Society, for those members who wanted to.

On general Assembly of EAS and other meetings on "European Week of Astronomy and Space Science" (EWASS) 2012, Rome, 1-6 July, Andjelka Kovačević, Luka Č. Popović (who was a member of Scientific Committee), Darko Jevremović and Milan S. Dimitrijević have been present. On EWASS 2013, Turku

(Finland), 8-12 July, the representative of SAS was Luka Č. Popović, who had an invited lecture, and on EWASS 2014, Geneva, 30 June – 4 July, SAS had not a representative.

Until the General Assembly of EAS in Rome 2012, Dimitrijević was councelor of EAS and participated in activities and meetings of the Governing Board. Additionally, he represented SAS on meetings of affiliated Societies in Rolle (Switzerland) 1-2 February 2012 and 24-25 January 2013. There, he presented SAS and its activities and the corresponding presentations are on the web site of EAS:

http://eas.unige.ch/meetings/rolle_2012/presentations/Dimitrijevic_Serbia.pdf
http://eas.unige.ch/meetings/rolle_2013/presentations/Dimitrijevic_Serbia.pdf

7.2. Links with the International Astronomical Union

Links with the International Astronomical Union (IAU) were held from one side through the National Committee for Astronomy, whose president within the period considered was Milan Ćirković.

8. CONCLUSION

We can conclude that within the period 2012 to 2014, Society of Astronomers of Serbia successfully organized the preparation and participation of our competitors at three International Olympiad in Astronomy. The Center for the promotion of science accepted the project "Popularization of astronomy in education, educational institutions and schools." During its realization a series of popular lectures and planetarium projections were organized in different places in Serbia and Republic Srpska. Only during 2012, to the activities covered by this project, within which was organized "Day of astronomy" in different places, attended 7510 listeners. Within the considered period, SAS organized four scientific conferences and was co-organizer of three, has published a Conference Proceedings, a book of abstracts and eight electronic optical discs. DAS organized 15 stays of foreign visitors and also maintained and developed links with the European Astronomical Society and the International Astronomical Union

References

Dimitrijević, M. S.: 2013, *Society of Astronomers of Serbia 2008-2011*, Proceedings of the VIII Serbian-Bulgarian Astronomical Conference, Leskovac, Serbia, May 8-12, 2012, eds. M. S. Dimitrijević, M. K. Tsvetkov, *Publ. Astron. Soc. »Rudjer Bošković«*, **12**, 153.

Димитријевић, Милан С.: 2014, *Друштво астронома Србије 2008-2011*, Зборник радова конференције “Развој астрономије код Срба VII”, Београд, 18-22. април 2012, уредник М. С. Димитријевић, *Публ. Астр. друш. “Руђер Бошковић”*, **13**, 421.

AUTHORS' INDEX

Aleksić J. 37
Antipin S. V. 67
Boeva S. 99
Boneva D. 93
Čadež V. M. 137
Chapanov Y. 127
Cvetković Z. 99
Damljanović G. 165
Dechev M. 117, 149
Dimitrijević M. S. 23, 49, 63, 159, 171, 189
Duchlev P. 117, 149
Gamero A. 63
Garcia M. C. 63
Ilić D. 83
Jevremović D. 7, 37
Kalaglarsky D. 55
Kirov N. 43
Kolesnikova D. M. 67
Kolev A. A. 13
Koleva K. 117
Komitov B. 149
Kovačević A. 83
Latev G. 99, 165
Majlinger Z. 159
Malkov S. 179
Mijajlović Ž. 179
Mitić N. 179
Moreau N. 23
Nina A. 137
Ninković S. 99
Pavlović R. 99
Pejović N. 179
Petrov N. 117
Popović L. Č. 49, 75, 83, 137
Ron C. 127
Sahal-Bréchot S. 23
Samus N. N. 67
Shapovalova A. I. 83
Simić S. 75, 137
Simić Z. 49, 159
Sokolovsky K. V. 67
Sola A. 63
Srećković V. A. 137
Stojanović M. 165
Taris F. 165
Tsvetkov M. 43, 55, 171
Tsvetkova K. 29, 43, 55, 171
Vondrák J. 127
Vujčić V. 37
Yankova K. 107
Yubero C. 63
Zubareva A. M. 67

CIP - Каталогизација у публикацији - Народна библиотека Србије, Београд

520/524:007(082)

BULGARIAN-Serbian Astronomical Conference (9 ; 2015 ; Sofia)
Proceedings of the IX Bulgarian-Serbian Astronomical Conference: Astroinformatics, Sofia, Bulgaria, July 2-4, 2014 / eds. Milcho K. Tsvetkov ... [et al.]. - Belgrade : Astronomical Society "Rudjer Bošković", 2015 (Beograd : Solution+). - 207 str. : ilustr. ; 24 cm. - (Publikacije Astronomskog društva "Ruđer Bošković" = Publications of the Astronomical Society "Rudjer Bošković" ; sv. 15)

Tiraž 100. - Bibliografija uz svaki rad. - Registar.

ISBN 978-86-89035-06-3

a) Астрономија - Информатика - Зборници b) Астрофизика - Информатика - Зборници

COBISS.SR-ID 217599756